

HIV integrase: Inhibition, dolutegravir resistance  
pathways and subtype variability

Peter Kojo Quashie

Division of Experimental Medicine

McGill University

Montreal, Quebec, Canada

July, 2015

A thesis submitted to the Faculty of Graduate Studies and Research in  
partial fulfillment of the requirements for the degree of  
Doctor of Philosophy.

©Copyright Peter Kojo Quashie 2015 All rights reserved.

## DEDICATION

This thesis is dedicated firstly to:

The Almighty God of Abraham, Isaac and Jacob,  
who gives me the strength and willingness to go on,

and secondly to:

the memory of my father,

Ing. Alexius Allen Bonso Quashie (1944-2014)

who was my idol, teacher and judge in my childhood and became my chief  
advisor, supporter, fan and motivator in my young adulthood.

Daddy, I miss you dearly.

## ACKNOWLEDGMENTS

These last four and a half years have included the happiest, most successful, proudest, saddest, weakest and strongest times of my life, thus far. Thus, as I look forward to more positive points in the future, I have a great many people to appreciate for helping me to reach this great height.

I firstly sincerely thank Dr. Mark Arnold Wainberg for accepting me into his lab and for his exceptional mentorship during my Ph.D. program. I thank him for his prodding and restraint at the right instances and his impatience and patience at important junctures of this journey. He has been exactly the mentor I hoped he would be and more. Thanks to him, I have achieved more during my Ph.D. program far beyond my most lofty expectations. Additionally, had I never joined his lab, I might never have met one of the most gracious and elegant Nobel Prize winners of the modern era (in my somewhat biased opinion), Dr. Françoise Barré-Sinoussi on, not one, but two occasions.

I thank my committee members during these years, Drs. Lorraine Chalifour, Chen Liang, Nicole Bernard, and Andrew Mouland who provided challenging critique and guidance during my progress. I also thank Dr. Hugo Soudeyns for joining my committee as an external

examiner brought new perspectives to my comprehensive examination. I would like to thank Dr. Bluma Brenner for her collaborations and perspective.

I would like to thank all the associations and institutes that provided scholarships and fellowships during my academic studies, especially the Quebec Black Medical Association, whose late founder and former president, Dr. Elrie Clifford Tucker (1932-2015), I regarded as a mentor and a great man. I thank his widow, Dr. Penelope Tucker for always welcoming us into their home and for supporting his ability to touch as many lives as he did, through the QBMA and through his larger than life personality. I made most of my non-classmate friends through associations with the QBMA and I still count many of them as my friends, such as Ms. Neressa Noel and Ms. Damika Sonja Lue.

I wish to thank my family for helping me to be the person I am today. I owe a lot of my success, to my father, and the people he surrounded me with throughout my life. As a child I felt my father was invincible; I wanted to be like him, be a successful sought-after engineer (initially) like him. He wanted us to be more successful than him, and less flawed. I am sincerely grateful to him for pushing us to be the very best we could be; I am grateful for always having to read ahead of the class and spell more words

than necessary and for learning what a rhombus was two years before I needed to. He expected more from us, and that led us to expect more of ourselves. I am grateful to my mother Mrs. Patience Oduro for being there for me, for her support and for her enduring love. I thank her for constantly writing and calling even when I was too lazy to reciprocate. I am grateful for my uncles Mr. Nana Karikari and Mr. Mike Asomaning, who have provided me with advice and support since I arrived in Canada, almost ten years ago. I would like to thank my siblings, Alexius, Anthony, Precious, Anne and Alix for always being there for me. I thank my brothers and sisters-in-laws for being true to my siblings and embracing our family wholeheartedly. My family has always been my bedrock, my ground zero where I feel most at peace and at ease; I owe that to my siblings, the loyalty we have for one another and the frank honesty we have always expected of each other. The love, friendship and competitiveness of my siblings has held me together, been my refuge and source of motivation; I am never happier than when we are all together. I thank my "other father" and "uncle", Alhaji Dramani Yakubu Esq. (1941-2012) and his widow, my other mummy, Mrs. Justice Ivy Naa-Nyardu Ashong-Yakubu, who together loved me as a son, were always being in my court. They were my support system through my years at Legon, and from both of whom I learnt the

importance of tolerance, perspective, prudence and diplomacy as well as a greater appreciation for the practice and intricacies of law. I would like to thank my "other other father" and the right hand of my father since childhood, Uncle Edward Sam (1945-2014), who was a strong proponent for my move to Canada and who was always a source of unbiased advice and perspective and his widow, Aunty Sarbeh for her quiet support and words over the years especially whilst I was in Ghana.

I would like to thank my wife's family for their love and support especially my father-in-law and mother-in-law, Mr and Mrs Koupaki, Alain and Tantie Dr. Isabelle Choki, Tonton and Tantie Dr. Edouard Kouassi and Dr. Angele Grimaud (to whom I can finally answer, yes it is finished). I thank all our friends who have become part of my social group and network; some of who even made the twenty-some hour trip to Ghana for my recent nuptials; Steve and Bintou, Fatou and Ina Toure, Akwasi Yeboah and Mr. Gerald Arhin.

I would like to thank all my Concordia brethren and friends including Kayode Nwanze and Dwight Best, and especially my classmates and friends with whom I share a similar career paths such as Dr. Francis McManus, Dr. Nicholas Sitaras, Mr. (pharmacist-to-be) Abbas Ghazi, Dr. Christopher Gregg, and my former Turnbull lab colleague- current

Wainberg lab colleague Said Hassounah. It is easy to set lofty standards for yourself, when you are in contact with people with equally lofty expectations of themselves. I especially thank Abbas for those discussions during the dark early days of zero results and troubleshooting. I would like to thank all the members of the Wainberg lab over the years, some of whom I consider to be my friends, especially but not limited to, Dr. Tamara Bar-Magen (from whom I inherited the integrase work and the G118R project), Dr. Richard Sloan (my initial project advisor), Dr. Hongtao Xu (who taught me the gel-based assays, my first collaboration and who, had I been able to keep up with him, would have provided numerous more collaborations), Dr. Thibault Mesplède (my long time project advisor), Dr. Aaron Donahue, Mr. (Dr-to-be) Victor Kramer, Dr. Susan Schader (the very first lab member I met, and on whose collaborative paper I did some of my best modeling and docking work), Ms. (Dr-to-be) Diane Singhroy (my often verbal sparring partner whose advocacy work is very needed in this disease-ridden world), Mr. Cesar Collasos, Ms. Melissa Wares, Dr. Ying-Shan Han (my friend and man of the world), Dr. Yudong Quan, Dr. Eugene Asahchop, Mrs. Bonnie Spira, Rabbi Shalom Spira, Ms. Estrella Moyal (my saviour on several occasions and birthday-mate), Ms. Maureen Oliviera (whose selection skills were absolutely

essential for the success of this thesis), Ms. Illinca Rubanescu, Mrs. Daniela Moisi, Mrs. Susan Germinario Olga Golubkov and Mr. Frederic Ohnona. I thank all my students over the years, including but not limited to, Ms. Tamar Veres (my best and most productive student thus far- a truly Good person), Ms. Olivia Varseneaux (one of the most unashamedly ambitious people I have ever met), Mr. Nathan Osman, Ms. Arrielle Sabbah, Mr. David Arbegel, Ms. Hannah Koubi and Alexandria Crandall. I have enjoyed the company of the new crop of Wainberg lab members such as Kaitlin and Vincent, and I wish them all the best moving forward.

Last, but definitely not least of all, I would like to thank the love of my life, my loving wife of ~0.7, 1.5, or ~2.5 years (depending which ceremony you count), and partner of ~5.8 years, Mrs. Olivia Roseline Ayekemi Koupaki for her tireless support during this long and trying time; your belief in me and my ability is sometimes more than I can comprehend. My wife is Lois Lane to my Clark Kent, sometimes my saviour, other times; she believes I can be Superman.



# TABLE OF CONTENTS

DEDICATION .....	ii
TABLE OF CONTENTS .....	ix
LIST OF TABLES .....	xiv
LIST OF FIGURES.....	xv
Preface .....	xvii
Chapter 1 .....	32
Introduction .....	32
1.1 Part I: A brief history of HIV and AIDS .....	33
1.1.1 Acquired immune-deficiency syndrome .....	33
1.1.2 Early reports .....	33
1.1.3 Human immunodeficiency virus is the cause of AIDS.....	34
1.1.4 Likely origins, types and subtypes of HIV .....	35
1.1.5 Molecular features of HIV and its replication.....	42
1.1.5.1 HIV genomic organisation.....	45
1.1.5.2 Steps in HIV replication.....	47
1.1.6 Circulating recombinant forms.....	51
1.1.7 Anti- Retroviral Therapy .....	53
1.1. 8 The global picture of HIV/AIDS today and future prospects .....	56
1.1. 8.1 Expanded ARV access .....	56
1.1. 8.2 Fusion, entry and integration .....	57
1.1. 8.3 Vaccine initiatives .....	62
1.1. 8.4 Preexposure prophylaxes of ARVs .....	63
1.1. 8.5 Cure Initiatives .....	64
1.2 Part II: Therapeutic targeting of HIV integrase .....	65
1.2.1 HIV integrase function and structure .....	65
1.2.2 Host-factor proteins interacting with HIV IN .....	67
1.2.2.1 INI1.....	67
1.2.2.2 BAF .....	68
1.2.2.3 LEDGF/p75 .....	69
1.2.2.4 KAP1 .....	72
1.2.2.5 Transportin-3 and RANBP2 .....	73
1.2.2.6 Importin- $\alpha$ .....	74
1.2.2.7 NUP153 and NUP160.....	74
1.2.2.8 Ku70.....	75
1.2.3 Integrase Inhibitors .....	75

1.2.3.1 Early integrase inhibitors.....	76
1.2.3.2 First generation integrase inhibitors.....	78
1.2.3.3 Second generation integrase inhibitors .....	89
1.2.4 Advances aiding integrase inhibitor discovery .....	96
1.2.4.1 Crystallization of full-length integrase .....	96
1.2.4.2 Quantitative structure-property and -activity relationships.....	98
1.2.5 Next-generation strand transfer inhibitors in preclinical development .....	99
1.2.5.1 MK-0536.....	99
1.2.5.2 LEDGINS and BI 224436 .....	100
1.2.5.3 Dual acting RT/IN inhibitors .....	102
1.2.6 HIV diversity and integrase inhibitors .....	102
1.3 Conclusions .....	103
1.4 Rationale for this thesis .....	104
1.5 Objectives of this thesis .....	105
1.5.1 Specific Objective 1 .....	105
1.5.2 Specific Objective 2 .....	105
1.5.4 Specific Objective 3 .....	106
1.5.5 Specific Objective 4 .....	106
1.6 References .....	<b>Error! Bookmark not defined.</b>
Chapter 2 .....	107
Structural modeling of HIV-1 integrase proteins and screening of potential integrase inhibitors .....	107
2.1 Abstract.....	108
2.2 Introduction .....	109
2.2 Materials and Methods .....	111
2.2.1 Generation of the monomeric IN model .....	111
2.2.2 Verification of model quality and creation of model 7.....	113
2.2.3 Creation of a dimeric IN model.....	115
2.2.4 Compound library docking.....	116
2.2.5 Antiviral activity of HDS1 measured by RT activity and quantitative PCR....	116
2.2.6 Biochemical evaluation of the impact of HDS1 on IN. ....	116
2.3 Results and discussion .....	117
2.3.1 Homology modeling.....	117
2.3.2 Docking simulations .....	123
2.3.3 Characterization of the inhibitory impact of HDS1 .....	133
2.4 Conclusions .....	137
2.5 References .....	<b>Error! Bookmark not defined.</b>

Chapter 3 .....	151
Characterization of the R263K mutational pathway in HIV-1 integrase that confers resistance to the second-generation integrase strand transfer inhibitor Dolutegravir ....	151
3.1 ABSTRACT.....	153
3.2 INTRODUCTION .....	155
3.3 MATERIALS AND METHODS.....	158
3.3.1 Cells and antiviral compounds. ....	158
3.3.2 Serial passage experiments. ....	158
3.3.3 Generation of replication-competent genetically homogeneous HIV-1.....	159
3.3.4 Replication capacity in TZM-bl cells. ....	160
3.3.5 Q-PCR for reverse transcripts and integrated viral DNA.....	160
3.3.6 Protein Expression and Purification. ....	161
3.3.7 Protein concentration and identity. ....	161
3.3.8 DNA substrates for <i>in vitro</i> assays. ....	162
3.3.9 Strand transfer activity.....	162
3.3.10 3' processing activity. ....	164
3.3.11 Microplate-based assay for IN-DNA binding. ....	164
3.3.12 Monogram Biosciences PhenoSense replication capacity and phenotyping assays.....	165
3.3.13 Data processing.....	165
3.3.14 Homology modeling.....	166
3.4 RESULTS .....	167
3.4.1 Isolation of R263K mutant viruses with DTG .....	167
3.4.2 R263K confers resistance against DTG <i>in vitro</i> . ....	168
3.4.3 Characterization of R263K in cell-based assays.....	170
3.4.4 Expression and purification of IN <sub>R263K</sub> . ....	172
3.4.5 Strand transfer and 3'-processing activities of IN <sub>R263K</sub> . ....	173
3.4.6 Effects of the R263K mutation on susceptibility to INSTIs <i>in vitro</i> . ....	177
3.4.7 Addition of H51Y to R263K .....	180
3.4.8 <i>In silico</i> studies of R263K and H51Y/R263K mutant integrase. ....	181
3.4.9 R263K impairs IN-DNA binding <i>in vitro</i> . ....	184
3.5 DISCUSSION .....	186
3.6 REFERENCES .....	<b>Error! Bookmark not defined.</b>
Chapter 4 .....	191
Biochemical analysis of the role of G118R-linked dolutegravir drug resistance substitutions in HIV-1 integrase .....	191
4.1 Abstract.....	192

4.2 Introduction .....	194
4.3 Materials and Methods .....	198
4.3.1 Antiviral compounds .....	198
4.3.2 Site-directed mutagenesis .....	198
4.3.3 Protein expression, purification and quantification .....	199
4.3.4 DNA substrates for <i>in vitro</i> assays .....	199
4.3.5 Preparation of pre-processed LTR-coated plates for strand transfer activity	200
4.3.6 Protein calibration for strand transfer activity .....	201
4.3.7 Time-phase strand transfer activity assay .....	202
4.3.8 Fixed [LTR]- variable [target] strand transfer activity assay .....	202
4.3.9 Variable [LTR]- variable [target] strand transfer activity assay .....	203
4.3.10 LTR-DNA binding assay .....	204
4.3.11 3' processing assay .....	205
4.3.12 Competitive inhibition of strand transfer inhibition by DTG, RAL and EVG	206
4.3.13 Homology modeling .....	207
4.4 Results .....	209
4.4.1 Generation of recombinant integrase proteins and calibration of enzyme activity .....	209
4.4.2 G118R causes a deficit in integrase strand transfer activity .....	210
4.4.3 Addition of H51Y and E138K to G118R regulates the formation of integrase- LTR complexes .....	213
4.4.4 G118R reduces 3' processing activity yet G118R/H51Y and G118R/E138K are fully active .....	215
4.4.5 H51Y and E138K partially rescue G118R activity by enhancing LTR-DNA binding .....	217
4.4.6 The H51Y and E138K double mutants do not show increased resistance to DTG, RAL and EVG .....	219
4.4.7 Structural analysis of the impact of G118R, E138K, and H51Y on the integrase active site .....	221
4.5 DISCUSSION .....	225
4.6 REFERENCES .....	<b>Error! Bookmark not defined.</b>
Chapter 5 .....	232
Differential effects of the G118R, H51Y and E138K resistance substitutions in HIV integrase of different subtypes .....	232
5.1 ABSTRACT .....	233
5.2 INTRODUCTION .....	234
5.3 MATERIALS AND METHODS .....	236

5.3.1 Cells and antiviral compounds. ....	236
5.3.2 Plasmids and site-directed mutagenesis.....	236
5.3.3 Protein expression, purification and quantification.....	238
5.3.4 DNA substrates for <i>in vitro</i> assays .....	239
5.3.5 Preparation of pre-processed LTR-coated plates for strand transfer activity	239
5.3.6 Protein calibration for strand transfer activity .....	240
5.3.7 Strand transfer activity assay .....	241
5.3.8 3' processing activity assay .....	242
5.3.9 Confirmation of the impact of G118R and E138K on subtype C integrase inhibition by MK-2048 .....	243
5.3.10 Competitive inhibition of strand transfer by DTG, RAL and EVG.....	244
5.3.11 Monogram biosciences PhenoSense replication capacity and phenotyping assays.....	245
5.3.12 Data processing.....	246
5.3.13 Homology modeling and active site analysis. ....	246
5.4 RESULTS .....	247
5.4.1 Generation of recombinant HIV subtype C and CRF02_AG integrase enzymes	247
5.4.2 Effect of the G118R on integrase strand transfer efficiency when alone or in combination with H51Y or E138K.....	248
5.4.3 Impact of the G118R, H51Y, and E138K substitutions on 3' processing ability	251
5.4.4 The effect of G118R, and E138K on subtype C integrase protein resistance to MK-2048 .....	253
5.4.5 Effect of G118R on susceptibility to DTG, RAL and EVG .....	255
5.4.6 Amino acid sequences differ at key positions between the three subtypes..	261
5.5 DISCUSSION .....	264
5.6 References .....	<b>Error! Bookmark not defined.</b>
Chapter 6 .....	275
General Discussion.....	275
6.1 Important considerations in homology modeling of HIV-1 integrase structures ...	275
6.2 Comparing G118R and R263K and their associated secondary substitutions ....	277
6.3 How does our work agree with current literature?.....	282
6.4 Conclusions .....	283
6.5 References .....	284

## LIST OF TABLES

Table 1.1: Food and Drug Administration Approved Antiretroviral Drugs .....	58
Table 1.2: Main resistance pathways for currently approved INSTIs expressed in fold-change (FC) susceptibility relative to wild-type viruses (331).....	85
Table 1.3: Alternative resistance pathways for current INSTIs expressed in fold change (FC) susceptibility relative to wild-type viruses (331).....	88
Table 1.4: Clinically relevant INI compound structures.....	101
Table 2.1 Best-docked compounds to the dimeric CRF02_A/G IN model .Error! Bookmark not defined.	
Table 3.1 Serial passage experiments with CBMCs infected with subtype B, A/G and C HIV-1 viruses in the presence of increasing concentrations of DTG. Baseline polymorphisms and acquired substitutions are indicated. ....	169
Table 3.2 R263K susceptibility to DTG and EVG. ....	170
Table 3.3 Effects of R263K mutation on half-inhibitory concentrations (IC <sub>50</sub> , nM) and 95% confidence intervals (nM) for various INSTIs.....	179
Table 3.4: H51Y increases resistance of R263K containing virus to DTG and EVG but drastically reduces viral replication. ....	181
Table 4.1: Strand transfer activity parameters for purified integrase proteins .....	211
Table 4.2: Susceptibilities of purified integrase proteins to DTG, RAL and EVG .....	220
Table 5.1: Selection of substitutions in cell-culture by MK-2048 and DTG. ....	248
Table 5.2: Enzymatic and virological parameters of variant HIV-1 integrase protein and viruses in CRF02_AG and subtypes B and C.....	258
Table 5.3: Comparative analysis of biochemical and virology data.....	259

## LIST OF FIGURES

Figure 1.1: Evolutionary relationships of HIV and SIV lineages by neighbour-joining phylogenetic analysis of partial Pol sequences (54).....	39
Figure 1.2: Suspected sources and localisation of origin of HIV-1 viral groups (54).....	40
Figure 1.3: Suspected sources and localisation of origin of HIV-1 viral groups (54).....	42
Figure 1.4: Key genomic similarities and differences between complex and simple retroviruses (77).....	44
Figure 1.5: HIV-1 genomic and structural organisation (83).....	46
Figure 1.6: Main steps in the HIV-1 replication cycle (113).....	51
Figure 1.7: Geographical localisation of HIV-1 subtypes and key CRFs (78).....	52
Figure 1.8: Genomic structure and subtype make-up of common CRFs (56).....	53
Figure 1.9: Steps of HIV integration (243).....	67
Figure 1.10: Domain organisation of Ldgf and HIV-1 IN showing key motifs and residues. ....	70
Figure 1.11 Proposed mechanism of TNPO3 and RANBP2 in nuclear import. ....	73
Figure 1.12 Circumvention of transportin pathway by the N74D capsid mutant virus (263). ....	74
Figure 1.13: Prototype foamy virus (PFV) IN active site showing bound RAL (a), EVG (b), and DTG (c) (331).....	98
Figure 2.1: Automated modeling of CRF02_A/G IN.....	122
Figure 2.2: Modeling of CRF02_A/G IN based on the top 10 structural and sequence homologues.....	Error! Bookmark not defined.
Figure 2.3: HHpred alignment used to create model 3 with key features highlighted. Error! Bookmark not defined.	
Figure 2.4: Analysis of model 6 and creation of dimeric model 7 HIV-1 CRF02_AG IN structure. ....	Error! Bookmark not defined.
Figure 2.5: Ramachandran plot analysis of models 6 and 7 compared to the two lead templates.....	Error! Bookmark not defined.
Figure 2.6: Location of docking grid box and docking of FZ41 to IN dimer. ....	Error! Bookmark not defined.
Figure 2.7: Screening of compounds for interaction with dimeric CRF02_AG IN in the absence of DNA ligands. ....	Error! Bookmark not defined.
Figure 2.8: Inhibition of HIV-1 in culture by HDS1. ....	Error! Bookmark not defined.
Figure 2.9: Biochemical characterisation of HDS1 on purified HIV-1 IN enzyme.....	Error! Bookmark not defined.
Figure 3.1: The R263K mutation specifically decreases HIV-1 integration. ....	171

Figure 3.2: Strand transfer activity of purified recombinant wild-type (IN) and R263K (IN <sub>R263K</sub> ) integrase proteins. ....	174
Figure 3.3: 3'-processing activity of purified recombinant wild-type (IN) and R263K (IN <sub>R263K</sub> ) integrase proteins. ....	176
Figure 3.4: H51Y reduces viral infectivity of integrase R263K virus by reducing integration. ....	180
Figure 3.5: <i>In silico</i> studies of the wild-type and R263K integrase proteins. ....	182
Figure 3.6: Effect of residues at position 51 and 263 on local side-chain electrostatic interactions and side-chain mobility in IN CTD. ....	185
Figure 3.7: DNA-binding activity of purified recombinant wild-type (IN) and R263K (IN <sub>R263K</sub> ) integrase proteins. ....	186
Figure 4.1: Generation and quantitation of drug resistant HIV-1 integrase proteins. ....	210
Figure 4.2: Strand transfer activities of purified recombinant integrase proteins at target saturation. ....	212
Figure 4.3: LTR binding experiments using purified integrase proteins. ....	214
Figure 4.4: Measurements of the 3' processing activities of integrase. ....	216
Figure 4.5: Measurements of the strand transfer activities of integrase with bisubstrate variation. ....	218
Figure 4.6: Competitive inhibition of strand transfer by DTG, RAL and EVG. Strand transfer reactions were carried out in the presence of 300 nM integrase. ....	220
Figure 4.7: Modeling of the HIV integrase active site. ....	223
Figure 4.8: The G118R mutation in the context of INSTI drug resistance. ....	229
Figure 5.1: Comparative strand transfer activities of purified HIV-1 WT and variant integrase proteins of CRF02_AG, subtype C and subtype B (A-C) origin. ....	250
Figure 5.2: Comparative 3' processing activities of purified HIV-1 WT and variant integrase proteins of CRF02_AG, subtype C and subtype B (A-E) origin. ....	252
Figure 5.3: Confirmation of the role of G118R and E138K substitutions in conferring resistance to MK-2048 in subtype C integrase. ....	254
Figure 5.4: Subtype-specific susceptibility of WT and variant integrase proteins to clinically relevant INSTIs. ....	257
Figure 5.5: Multiple sequence alignment of subtype B, subtype C and CRF02_AG integrase sequences from the plasmids pNL4_3, pINdieC and p97, respectively, performed using ClustalW (1.8). ....	263
Figure 5.6: Modeled HIV-1 WT and G118R target capture complexes show differential impact of G118R in the active sites of the three integrase subtypes. ....	268
Figure 5.7: Active site modeling of DTG-bound integrase. ....	271





## Preface

This thesis was written in accordance with McGill University's "Guidelines for thesis Preparation." The format of this thesis conforms to the "Manuscript-based (Article-based) Thesis" option, which states: "As an alternative to the traditional thesis format, the thesis research may be presented as a collection of scholarly papers of which the student is the author or co-author; that is, it can include the text of one or more manuscripts, submitted or to be submitted for publication, and/or published articles reformatted according to thesis requirements as described below...The thesis is expected to be a more detailed, scholarly work than manuscripts for publication in journals, and must conform to general thesis requirements. Note: These papers cannot alone constitute the thesis;

the thesis must contain additional text that will connect them, producing a cohesive, unitary focus, and documenting a single program of research. A Manuscript- (or Article-) based thesis will be judged by the examiners as a unified, logically-coherent document in the same way a traditional thesis is judged. "

The following manuscripts are included in this thesis:

Chapter 1

- Quashie PK, Sloan RD, Wainberg MA. Novel therapeutic strategies targeting HIV integrase. *BMC Med.* 2012 Apr 12;10:34. doi: 10.1186/1741-7015-10-34. Review.
- Quashie PK, Mesplède T, Wainberg MA. Evolution of HIV integrase resistance mutations. *Curr Opin Infect Dis.* 2013 Feb;26(1):43-9. doi: 10.1097/QCO.0b013e32835ba81c. Review.
- Quashie PK, Mesplède T, Wainberg MA. HIV Drug Resistance and the Advent of Integrase Inhibitors. *Curr Infect Dis Rep.* 2013 Feb;15(1):85-100. doi: 10.1007/s11908-012-0305-1. Review.

## Chapter 2

- Quashie PK\*, Han Y\*, Hassounah S, Mesplède T and Wainberg MA. **Structural studies of the HIV-1 CRF02\_AG integrase protein: Compound screening and characterization of a DNA-binding inhibitor.** *PLoS One.* 2015 Jun 5;10(6):e0128310. doi: 10.1371/journal.pone.0128310. eCollection 2015.

## Chapter 3

- Quashie PK, Mesplède T, Han Y, Oliveira M, Singhroy DN, Fujiwara T, Underwood MR, Wainberg MA. **Characterization of the R263K mutation in HIV-1 integrase that confers low-level resistance**

to the second-generation integrase strand transfer inhibitor **Dolutegravir**. *J Virol*. 2012 Mar;86(5):2696-705. Epub 2011 Dec 28.

- Mesplède T, Quashie PK, Osman N, Han Y, Singhroy DN, Lie Y, Petropoulos CJ, Huang W, Wainberg MA. **Viral fitness cost prevents HIV-1 from evading dolutegravir drug pressure**. *Retrovirology*. 2013 Feb 22;10:22. doi: 10.1186/1742-4690-10-22

#### Chapter 4

- Quashie PK, Mesplède T, Han YS, Veres T, Osman N, Hassounah S, Sloan R, Xu HT, Wainberg MA. **Biochemical analysis of the role of G118R-linked dolutegravir drug resistance substitutions in HIV-1 integrase**. *Antimicrob Agents Chemother*. 2013 Dec;57(12):6223-35. doi: 10.1128/AAC.01835-13. Epub 2013 Sep 30.

#### Chapter 5

- Quashie PK, Oliviera M, Veres T, Osman N, Han YS, Hassounah S, Lie Y, Huang W, Mesplède T, Wainberg MA. **Differential effects of the G118R, H51Y and E138K resistance substitutions in HIV integrase of different subtypes**. *J Virol*. 2015 Mar 15;89(6):3163-75. doi: 10.1128/JVI.03353-14. Epub 2014 Dec 31.

The author of this thesis is the first or co-first author on all the manuscripts listed above, save one, and where necessary, has the permission of co-

authors to use the manuscripts in this thesis. All the manuscripts listed above will only be included in this thesis and none other. In each manuscript-based chapter, the contributions of individual co-authors of each manuscript is clearly outlined.

Fully published co-authored manuscripts not explicitly used in this thesis

1. Quashie, Peter K\*; Mesplède, Thibault\*; Hassounah, Said; Osman, Nathan; Han, Yingshan; Liang, Jiaming; Singhroy, Diane N.; Wainberg, Mark A. **The R263K substitution in HIV-1 subtype C confers resistance against dolutegravir and decreases integrase enzymatic function and viral replication** *AIDS* (Post Acceptance: June 19, 2015 doi: 10.1097/QAD.0000000000000752).
2. Depatureaux A, Mesplède T, Quashie P, Oliveira M, Moisi D, Plantier JC, Brenner B, Wainberg MA. **HIV-1 group O resistance against integrase inhibitors.** *J Acquir Immune Defic Syndr.* 2015 May 21. [Epub ahead of print].
3. Xu HT, Colby-Germinario SP, Quashie PK, Bethell R, Wainberg MA. **Subtype-specific analysis of the K65R substitution in HIV-1 that confers hypersusceptibility to a novel nucleotide-competing reverse transcriptase inhibitor.** *Antimicrob Agents Chemother.* 2015

Jun;59(6):3189-96. doi: 10.1128/AAC.00315-15. Epub 2015 Mar 16.

4. Han YS, Quashie PK, Mesplède T, Xu H, Quan Y, Jaeger W, Szekeres T, Wainberg MA. **A resveratrol analog termed 3,3',4,4',5,5'-hexahydroxy-trans-stilbene is a potent HIV-1 inhibitor.** *J Med Virol.* 2015 May 18. doi: 10.1002/jmv.24271. [Epub ahead of print].
5. Depatureaux A, Quashie PK, Mesplède T, Han Y, Koubi H, Plantier JC, Oliveira M, Moisi D, Brenner B, Wainberg MA. **HIV-1 Group O Integrase Displays Lower Enzymatic Efficiency and Higher Susceptibility to Raltegravir than HIV-1 Group M Subtype B Integrase.** *Antimicrob Agents Chemother.* 2014 Dec;58(12):7141-50. doi: 10.1128/AAC.03819-14. Epub 2014 Sep 15.
6. Hardy I, Brenner B, Quashie P, Thomas R, Petropoulos C, Huang W, Moisi D, Wainberg MA, Roger M. **Evolution of a novel pathway leading to dolutegravir resistance in a patient harboring N155H and multiclass drug resistance.** *J Antimicrob Chemother.* 2015 Feb;70(2):405-11. doi: 10.1093/jac/dku387. Epub 2014 Oct 3.
7. Hassounah SA, Mesplède T, Quashie PK, Oliveira M, Sandstrom PA, Wainberg MA. **Effect of HIV-1 integrase resistance mutations**

- when introduced into SIVmac239 on susceptibility to integrase strand transfer inhibitors. *J Virol.* 2014 Sep 1;88(17):9683-92. doi: 10.1128/JVI.00947-14. Epub 2014 Jun 11.
8. Mesplède T, Osman N, Wares M, Quashie PK, Hassounah S, Anstett K, Han Y, Singhroy DN, Wainberg MA. **Addition of E138K to R263K in HIV integrase increases resistance to dolutegravir, but fails to restore activity of the HIV integrase enzyme and viral replication capacity.** *J Antimicrob Chemother.* 2014 Oct;69(10):2733-40. doi: 10.1093/jac/dku199. Epub 2014 Jun 10.
9. Mesplède T, Quashie PK, Zanichelli V, Wainberg MA. **Integrase strand transfer inhibitors in the management of HIV-positive individuals.** *Ann Med.* 2014 May;46(3):123-9. doi: 10.3109/07853890.2014.883169. Epub 2014 Mar 3.
10. Oliveira M, Mesplède T, Quashie PK, Moïsi D, Wainberg MA. **Resistance mutations against dolutegravir in HIV integrase impair the emergence of resistance against reverse transcriptase inhibitors.** *AIDS.* 2014 Mar 27;28(6):813-9. doi: 10.1097/QAD.0000000000000199.
11. Wares M, Mesplède T, Quashie PK, Osman N, Han Y, Wainberg MA. **The M50I polymorphic substitution in association with the**

**R263K mutation in HIV-1 subtype B integrase increases drug resistance but does not restore viral replicative fitness.**

*Retrovirology*. 2014 Jan 17;11:7. doi: 10.1186/1742-4690-11-7.

12. Singhroy DN, Mesplède T, Sabbah A, Quashie PK, Falguyret JP, Wainberg MA. **Automethylation of protein arginine methyltransferase 6 (PRMT6) regulates its stability and its anti-HIV-1 activity.** *Retrovirology*. 2013 Jul 17;10:73. doi: 10.1186/1742-4690-10-73.

13. Han YS, Xiao WL, Quashie PK, Mesplède T, Xu H, Deprez E, Delelis O, Pu JX, Sun HD, Wainberg MA. **Development of a fluorescence-based HIV-1 integrase DNA binding assay for identification of novel HIV-1 integrase inhibitors.** *Antiviral Res*. 2013 Apr 9. doi:pil: S0166-3542(13)00087-9.

14. Asahchop EL, Oliveira M, Quashie PK, Moisi D, Martinez-Cajas JL, Brenner BG, Tremblay CL, Wainberg MA. **In vitro and structural evaluation of PL-100 as a potential second-generation HIV-1 protease inhibitor.** *J Antimicrob Chemother*. Jan;68(1):105-12. doi: 10.1093/jac/dks342. Epub 2012 Sep 3.

15. Wainberg, M.A., Quashie, P.K., Mesplède, T. **Dolutegravir.** *Drugs Fut*. 2012, 37(10): 697. Review.



16. Xu HT, Oliveira M, Asahchop EL, McCallum M, Quashie PK, Han Y, Quan Y, Wainberg MA. **Molecular mechanism of antagonism between the Y181C and E138K mutations in HIV-1 reverse transcriptase.** *J Virol.* 2012 Dec;86(23):12983-90. doi: 10.1128/JVI.02005-12. Epub 2012 Sep 19.
17. Wainberg MA, Mesplède T, Quashie PK. **The development of novel HIV integrase inhibitors and the problem of drug resistance.** *Curr Opin Virol.* 2012 Oct;2(5):656-62. doi: 10.1016/j.coviro.2012.08.007. Epub 2012 Sep 16. Review.
18. Han YS, Quashie P, Mesplede T, Xu H, Mekhssian K, Fenwick C, Wainberg MA. **A high-throughput assay for HIV-1 3' processing activity using time-resolved fluorescence.** *J Virol Methods.* 2012 Sep;184(1-2):34-40. Epub 2012 May 11.
19. Mesplède T, Quashie PK, Wainberg MA. **Resistance to HIV integrase inhibitors.** *Curr Opin HIV AIDS.* 2012 Sep;7(5):401-8. doi: 10.1097/COH.0b013e328356db89. Review.
20. Schader SM, Colby-Germinario SP, Quashie PK, Oliveira M, Ibanescu RI, Moisi D, Mesplède T, Wainberg MA. **HIV gp120 H375 is unique to HIV-1 subtype CRF01\_AE and confers strong resistance to the entry inhibitor BMS-599793, a candidate**

**microbicide drug.** *Antimicrob Agents Chemother.* 2012 Aug;56(8):4257-67. Epub 2012 May 21.

21. Xu HT, Oliveira M, Quashie PK, McCallum M, Han Y, Quan Y, Brenner BG, Wainberg MA. **Subunit-selective mutational analysis and tissue culture evaluations of the interactions of the E138K and M184I mutations in HIV-1 reverse transcriptase.** *J Virol.* 2012 Aug;86(16):8422-31. Epub 2012 May 23.

22. Xu HT, Asahchop EL, Oliveira M, Quashie PK, Quan Y, Brenner BG, Wainberg MA. **Interactions of E138K and M184I/V mutations in HIV-1 reverse transcriptase restore enzyme processivity and viral replication capacity.** *J Virol.* 2011 Nov;85(21):11300-8. Epub 2011 Aug 17.

## ABSTRACT

The integrase protein of the Human Immunodeficiency Virus, HIV, is necessary for the insertion of the viral genome into the host chromosomal DNA. It is therefore an important therapeutic target. Though highly potent, first-generation integrase strand transfer inhibitors, raltegravir and elvitegravir, have only a modest genetic barrier to resistance development, and there are several overlapping mutational pathways for viral escape. Rationally designed second-generation integrase strand transfer inhibitors, such as dolutegravir exhibit a high resistance barrier and to date, drug resistance substitutions have not been described for dolutegravir in treatment-naive patients.

This thesis, through a combination of structural biology, biochemistry and virology methods, seeks to understand the mechanisms involved in integrase inhibition, resistance development and the effect of subtype on substitution with a major focus on pathways of resistance development against second generation integrase strand transfer inhibitors, exemplified by dolutegravir. Understanding HIV integrase and its inhibition is complicated by the lack of clinically viable full-length structures. In lieu of this, in Chapter 2, we generated homology structural models of HIV integrase, based jointly on partial-HIV crystal structures and

substrate/ligand-bound crystal structures of prototype human foamy virus integrase protein. These models were useful in screening potential modulators of integrase dimerization and DNA binding. The homology modeling facilitated the identification of putative binding sites of a novel integrase inhibitor, HDS1, and subsequent biochemical and virological characterization of its mode of inhibition. We next used the protocol to model different amino acid substitutions in dolutegravir resistance pathway analyses in the subsequent chapters. We performed *in vitro* dolutegravir resistance selection experiments using HIV subtype B, C and circulating recombinant form A/G. Two main resistance pathways were observed; R263K was selected in subtypes B and AG, while G118R was selected in subtype C and AG. A common secondary substitution to both R263K and G118R was H51Y. The G118R had previously been selected in our lab, in subtype C virus, with the second generation integrase strand transfer inhibitor MK-2048. The secondary substitution to G118R in that instance, E138K, was one of the secondary substitutions observed with R263K in subtype B under dolutegravir pressure. It was therefore evident that the positions 263, 118, 51 and 138 might be involved in overlapping resistance mechanisms towards second generation integrase inhibitors such as dolutegravir. Chapter 3 focused on the tissue culture selections

with dolutegravir and the subsequent structural, biochemical and virological characterization of R263K and H51Y/R263K variant integrase proteins and viruses. We then characterized the impact of the G118R substitution, alone or in combination with either H51Y or E138K on integrase function, viral fitness and resistance to the three approved drugs, dolutegravir, raltegravir and elvitegravir. In Chapter 4 we sought to understand the lack of G118R appearance in a subtype B background and Chapter 5 compared the impact of G118R, H51Y and E138K on fitness and drug susceptibility of integrase proteins and viruses of the three subtypes.

This thesis establishes that R263K and G118R substitution represent potential avenues for resistance against dolutegravir. For both pathways, secondary substitutions can lead to either diminished integrase activity or increased integrase strand transfer inhibitor susceptibility but the effect of secondary substitutions will likely be modulated by the subtype and/or sequence of the particular virus. While R263K will likely predominate in the clinic, its effect may be easier to predict and more innocuous than G118R, which causes changes in drug susceptibility that can vary wildly between subtypes.

## ABRÉGÉ

L'intégrase du virus de l'immunodéficience humaine, VIH, est nécessaire pour l'insertion du génome viral dans l'ADN chromosomique de l'hôte. Il est donc une cible thérapeutique importante. Bien qu'efficace, les inhibiteurs de l'intégrase de première génération, le raltégravir et l'elvitégravir, n'ont qu'une barrière génétique modeste contre le développement de la résistance. Les inhibiteurs de l'intégrase de deuxième génération, dont le dolutégravir, présentent une barrière de résistance élevée. À ce jour, aucune substitution de résistance n'a été décrite contre le dolutégravir chez les patients naïfs de traitement. Cette thèse, à travers une combinaison de méthodes biologiques, biochimiques et de virologie structurale, a étudié les mécanismes impliqués dans l'inhibition de l'intégrase, le développement de la résistance et l'effet des sous-types sur ces processus avec un accent majeur sur le dolutégravir. La compréhension de l'intégrase du VIH et de son inhibition est compliquée par l'absence de structure cristalline. Dans le chapitre 2, nous avons produit des modèles de l'intégrase du VIH par homologie avec les structures cristallines partielles de l'intégrase du VIH et les structures cristallines de l'intégrase du virus mousseux prototype (PFV) avec les inhibiteurs liés. Ces modèles ont été utiles pour l'identification d'inhibiteurs potentiels de la dimérisation et de la liaison à l'ADN de l'intégrase ainsi que l'identification des sites de liaison putatifs d'un nouvel inhibiteur, HDS1, et la caractérisation

biochimique et virologique de son mode d'inhibition. Dans les chapitres suivants, nous avons utilisé le protocole de modélisation moléculaire pour analyser le rôle de différentes substitutions de résistance contre le dolutégravir. Nous avons réalisé des expériences de sélection *in vitro* avec le dolutégravir et les sous-types B, C et la forme circulante recombinante A/G du VIH. Deux principales voies de résistance ont été observées : R263K dans le sous-type B et A/G, et G118R dans le sous-type C et A/G. Une substitution secondaire commune à R263K et à G118R était H51Y. Le G118R avait déjà été sélectionné à partir d'un sous-type C dans notre laboratoire avec l'inhibiteur de seconde-génération MK-2048. La substitution secondaire à G118R dans ce cas, E138K, était l'une des substitutions secondaires observées en association avec R263K dans le sous-type B traité avec le dolutégravir. Il était donc évident que les positions 263, 118, 51 et 138 sont impliquées dans les mécanismes de résistance contre les inhibiteurs de l'intégrase de deuxième génération tels que le dolutégravir. Le chapitre 3 est axé sur les sélections de résistance avec le dolutégravir et la caractérisation structurale, biochimique et virologique de R263K et H51Y/R263K au niveau protéique et viral. Nous avons caractérisé l'effet de G118R, seul ou en combinaison avec H51Y ou E138K sur la fonction de l'intégrase, la capacité répliquative et la résistance contre le dolutégravir, le raltégravir et l'elvitégravir. Dans le chapitre 4, nous avons cherché à comprendre l'absence de G118R dans

le sous-type B et dans le chapitre 5 nous avons comparé l'impact de G118R, H51Y et E138K sur la capacité répliquative et la sensibilité aux médicaments des protéines et des virus des trois sous-types étudiés.



# Chapter 1

## Introduction

Some sections of this chapter have been previously published in the three invited literature review articles listed below:

- Quashie PK, Sloan RD, Wainberg MA. **Novel therapeutic strategies targeting HIV integrase**. *BMC Medicine* 2012 Apr 12;10:34. Copyright© 2012 Quashie et al; licensee BioMed Central Ltd.

Contributions: PKQ researched the material, generated the figure and wrote ~95% of the review with additional writing and editing by RDS and MAW.

- Quashie PK, Mesplède T, Wainberg MA. **Evolution of HIV integrase resistance mutations**. *Current Opinion in Infectious Diseases* 2013 Feb;26(1):43-9. Copyright© 2013 Lippincott Williams & Wilkins, Inc.

Contributions: PKQ researched the material, generated the figures and wrote ~95% of the review with additional writing and editing by TM and MAW.

- Quashie PK, Mesplède T, Wainberg MA. **HIV Drug Resistance and the Advent of Integrase Inhibitors**. *Curr Infect Dis Rep*. 2013 Feb;15(1):85-100. doi: 10.1007/s11908-012-0305-1. Copyright© Springer Science+Business Media New York 2012.

Contributions: PKQ researched the material, generated the figures and wrote ~75% of the review with additional writing and editing by TM and MAW.

## 1.1 Part I: A brief history of HIV and AIDS

### 1.1.1 Acquired immune-deficiency syndrome

During a Washington meeting on July 27, 1982 between officials of the Center for Disease Control (CDC), federal bureaucrats and gay community leaders, the term 'Acquired Immune Deficiency Syndrome (AIDS)' was coined [1-4]. This term was the first to comprehensively describe the disease characterised by the loss of cell-mediated immunity with ~60% 1-year post diagnosis mortality in 1982 [5].

### 1.1.2 Early reports

The first confirmed report of AIDS dates back to 1959 [6] and was retroactively diagnosed in blood samples collected by researchers studying the links between glucose-6-phosphatase deficiency, malaria and sickle cell disease [6]. There is also a less accepted case of a British apprentice printer living in Manchester England dying of an AIDS-like illness which he may have contracted in 1957 [7].

Though there is evidence that HIV existed in the United States (US) prior to the 1980s [8], the HIV epidemic in the US was only followed closely by the CDC after 1981. Previously healthy gay men in New York, Los Angeles and San Francisco started to die from combinations of new infections of previously rare diseases such as *Pneumocystis carinii* pneumonia (PCP), cytomegalovirus (CMV), and Kaposi's Sarcoma [5, 9-11]. These patients all had evidence of

severe immune deficiency, making them vulnerable to opportunistic infections [5, 10-15]. The reports gradually started spreading across the country but were largely known only in the gay and haemophiliac communities [5, 10-15]. The US public was awakened to the scourge of AIDS by the sudden death of the celebrity Rock Hudson in 1985 [1, 2, 16, 17]. In 1984, Canada started antibody testing for then-called human T-lymphotropic virus type III (HTLV III) at the Laboratory Centre for Disease Control in Ottawa [18]. By 1985, over 25000 serum samples from high risk groups (patients with AIDS or "pre-AIDS", haemophiliac patients, symptomatic homosexual men and cohabitants of AIDS-diagnosed patients) had been tested in Canada with high prevalence rates in these samples. It was estimated then that rates in certain populations of asymptomatic homosexual men in Canada could be as high as 21% [18].

### **1.1.3 Human immunodeficiency virus is the cause of AIDS**

In 2008, the "Nobel Prize in Medicine or Physiology" was shared by scientists of the Institut Pasteur in Paris, Luc Montagnier and his former trainee, Françoise Barré-Sinoussi [19, 20]. They had published in 1983 on the isolation of a T-lymphotropic virus taken from the lymph nodes of a patient who appeared to be in the early stages of AIDS [21]. They called this virus lymphadenopathy associated virus (LAV) to differentiate it from the human T-cell lymphotropic virus I (HTLV I) previously discovered by Robert Gallo of the US National

Institutes of Health (NIH) [22]. The award was also shared by Harald zur Hausen, who had discovered that human papilloma virus infection caused cervical and related cancers [23, 24]. Conspicuously missing from the recipients was Robert Gallo [20], whose lab had published in 1984 the identification of a seemingly different virus termed HTLV III as the etiological cause of AIDS [25]. It was established later that HTLV III and LAV were the same virus, subsequently renamed HIV [8, 26-28]. Despite Gallo not being the initial discoverer of HIV, his lab established key protocols for the laboratory propagation of HIV and provided evidence that HIV, not other AIDS-associated viruses, was the causative organism of AIDS [3, 4, 25, 29-31].

#### **1.1.4 Likely origins, types and subtypes of HIV**

The suspected origin of the HIV/AIDS pandemic is a highly controversial topic with a mixture of diverging and converging theories [8, 32-41]. One key fact is that HIV is related to simian immunodeficiency virus (SIV) that is found in certain species of African monkeys, chimpanzees and gorillas [8, 38-43] (Figure 1.1). A hint that SIV could be an ancestral precursor to HIV became clear when a different virus in West African AIDS cases was found to more closely related to the SIV endemic in sooty mangabeys living in the same region as the patients [41, 43-46]. This SIV was related to viruses which had caused immunodeficiency in captive macaques in research facilities [38, 39]. The new HIV was termed

human immunodeficiency virus type 2 (HIV-2) to differentiate it from the initial virus, which was termed as human immunodeficiency virus type 1 (HIV-1).

There is evidence in West Africa of continuous cross-infection of humans with endemic SIV viruses; these viruses are largely thought to result in transmission incompetent infections since they are never detected in more than one or two individuals (41,43,46) supporting the hypothesis that SIV must have crossed over into humans multiple times prior to the start of the current pandemic. Phylogenetic studies have shown that the SIV and HIV lineages may have diverged as far back as the late nineteenth century or the early twentieth century [8, 38, 40, 41, 47]. HIV-1 (particularly subtypes A, B and C) appears to have originated and spread world-wide from the Central African countries of Democratic Republic of Congo (then French Equatorial Africa), Equatorial Guinea and Cameroon [8, 38-41, 47] (Figure 1.1), whereas HIV-2 originated from and has remained largely confined in West Africa [8, 38, 40, 41, 44, 45, 47-55], with reportedly lower prevalence, pathogenicity and transmissibility compared to HIV-1 [38, 44, 46, 48, 50, 56]. This implies that a particular event or series of events occurred between the early 1900s, when the separate cross-species transmissions might have occurred, and the 1970s, when HIV had probably already been well dispersed, but not detected [8, 57], sparking the rapid transformation of SIV<sub>cpz</sub> from a weakly pathogenic and poorly transmissible virus

in humans to the highly pathogenic, transmissible and devastating HIV-1, which results in AIDS [8, 35, 38-40, 45, 54, 58, 59].

As mentioned above, a multitude of views abound on what those events, mostly believed to be anthropogenic, were. The most widely accepted hypothesis is also the most plausible. Western and Equatorial Africa had a multitude of diseases that plagued the region and decimated the populations of locals and European settlers. In the beginning of the twentieth century, multiple mass vaccination campaigns were organized to vaccinate the local populations [8, 37, 38, 54, 57, 58]. During these campaigns, the reuse of needles was common due to their high cost; this practise was only partially curtailed in the 1950s when disposable needles became available [54, 58]. Still, due to the cost savings, needle reuse has remained common in Africa and elsewhere even up into the 2000s [37, 60-64]. Needle sharing, which has been documented to increase the likelihood of HIV transmission several fold [59, 60, 62-68] is also suspected to have fast-tracked the adaptation of HIV to human hosts. The hypothesis referred to as 'serial passage/transmission' [54] implies that a person, possibly a chimpanzee hunter or butcher, became infected with SIV. This person then went to receive a vaccination and the virus was transferred to another human host when the needle was reused. This means that the virus would have different pressures driving its evolution. Supposing this second person went and received another

set of vaccinations with a different needle, and that needle was used on yet another person, the transmitted viral population would evolve yet again in rapid succession [8, 54, 58]. Though unsterile vaccination practises had previously been considered [21, 40, 41, 47, 69, 70], along with a multitude of reasons, as a contributing factor to the spread of HIV, it was Preston Marx and colleagues in 2001 who placed a greater emphasis on the possible role of these practises in accelerating the evolution of SIV to HIV to mere decades [54, 58]. Several groups were able to show in captive monkeys that SIV was able to quickly adapt to a new species after being serially passaged through 3-4 monkeys [71, 72]. Due to the low probability of serial passaging, Marx postulated that the SIV-HIV species jump may have occurred when vaccinations were at their peak, i.e. 1950s [8, 54, 58], and that the strong selection pressure placed on the viral populations drove divergence into the different subtypes. Sexually transmitted ulcer-causing diseases such as syphilis are also known to increase HIV transmissibility; syphilis was reportedly common in colonial cities, particularly Kinshasa, due to the high number of prostitutes [8] and likely also played a part in the early dissemination of the virus. Other factors such as the poor working conditions and health of the local populace of French Equatorial Africa may have created the perfect melting pot to overcome the epidemiological threshold [73, 74]. The current driving forces of the pandemic are somewhat different. In much

of Africa, India and South America [51, 75], it is thought that heterosexual sex drives much of the epidemic there, whilst in Europe and North America, homosexual sex and injection drugs appear to be the main drivers. A mixture of commercial sex trade and injection drug use is likely the key driving force behind the epidemics in South East Asia [76, 77].

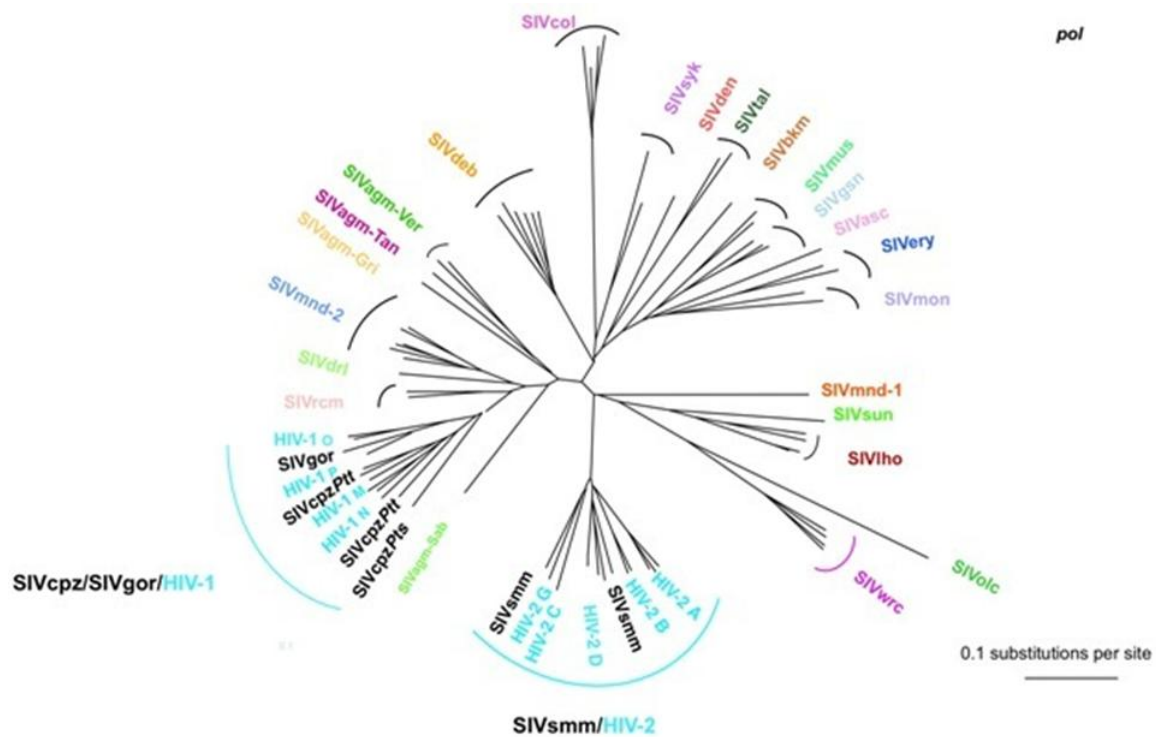


Figure 1.1: Evolutionary relationships of HIV and SIV lineages by neighbour-joining phylogenetic analysis of partial pol coding sequences [55].

Currently there are four known groups of HIV type 1, Groups M, O, N and P [51-53, 78] (Figure 1.2). Each of these groups are thought to be the result of an independent transmission event and the resulting subtypes/clades are the result



of evolutionary pressure and adaptation [8, 52, 53, 57, 79, 80]. The largest group, Group M (group major), derived from a SIV<sub>cpz</sub> transmission, is responsible for greater than 90% of all HIV/AIDS cases and has ~11 suspected or confirmed subtypes (A-K). Of these, subtypes A, B and C form the bulk of infections. HIV subtypes have a tendency to recombine and form recombinant forms; when these forms are transmissible, they are referred as circulating recombinant forms. Subtypes E and G have never been identified as pure non-recombinant viruses, but as part of recombinant A/E and A/G viruses respectively [51, 52].

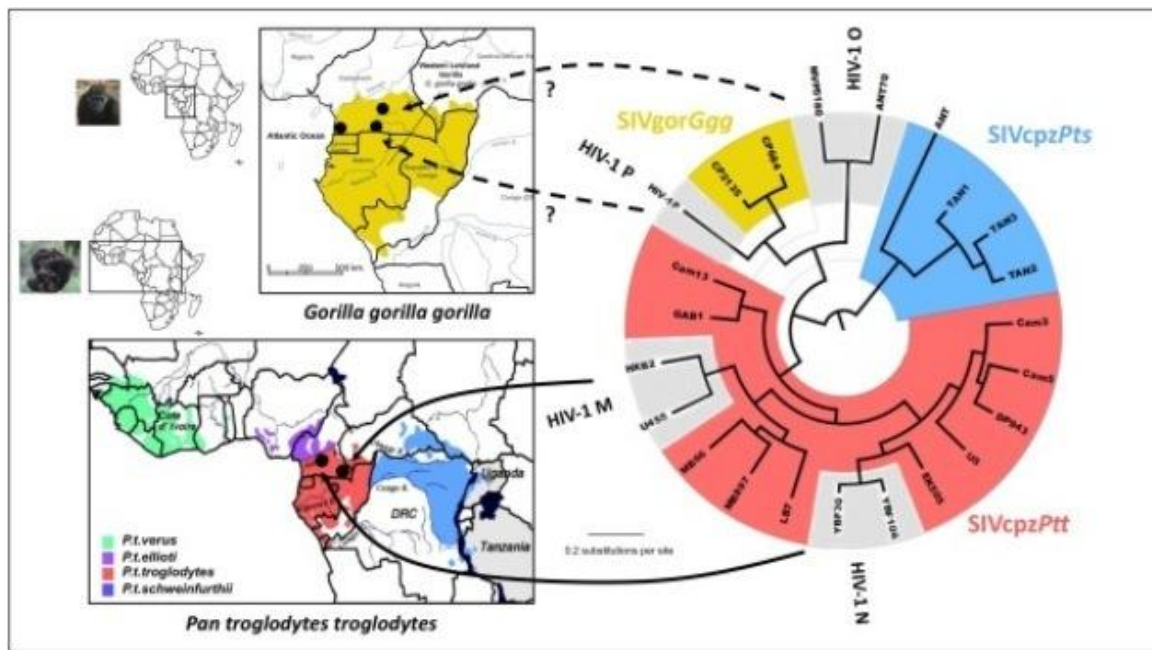
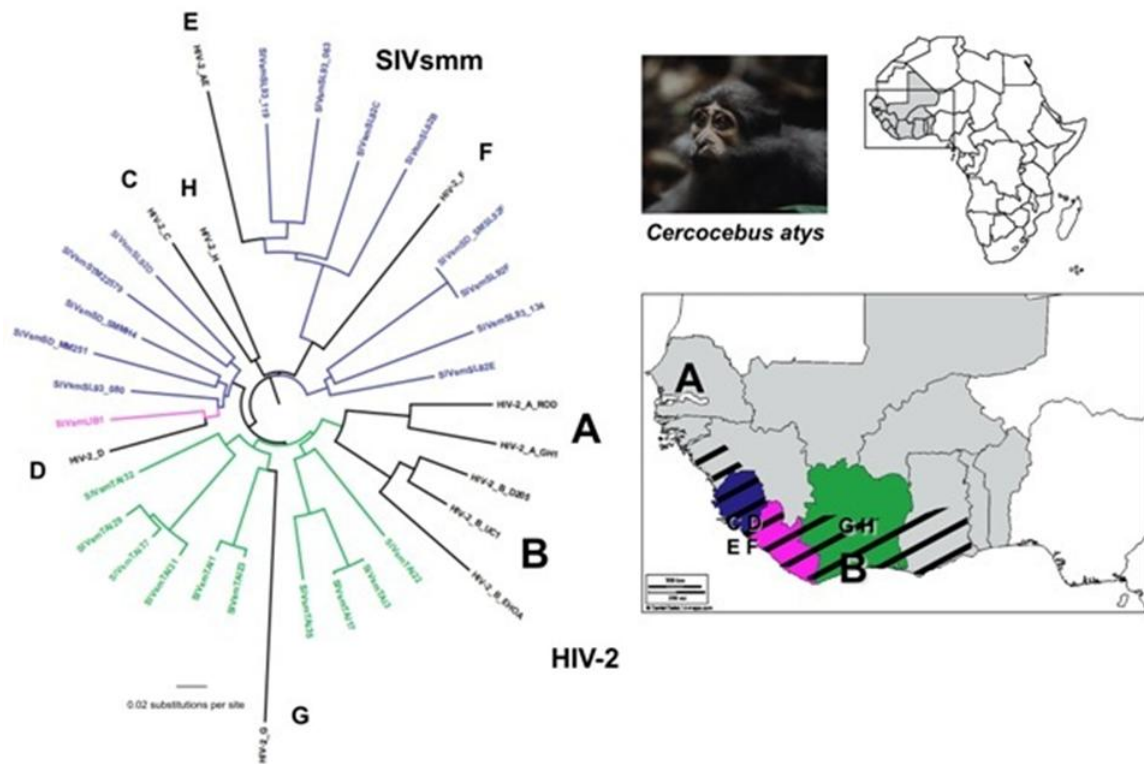


Figure 1.2: Suspected sources and localisation of origin of HIV-1 viral groups [55].

Interestingly, non-M HIV-1 has mostly been identified in and remains endemic only in Cameroon, Gabon and Equatorial Guinea [8]. The SIV strain closely

related to subtype O, SIV<sub>gor</sub>, affects gorillas living in Cameroon and surrounding areas. In fact, despite groups N, O and P being sometimes classified as CPZ transmissions (Figure 1.1), only N appears to be a transmission from a chimpanzee [80]. This was thus termed the outlier (O) group. Group O infections are mostly contained within Cameroon, Gabon and Equatorial Guinea and comprise about 2% of national infections [51-53]. Group N (non-M, non-O) HIV-1 infections are also confined within Cameroon and account for less than 0.1% of the total disease burden in that country. The rarest group is Group P (pending identification of further human cases/putative), also identified in Cameroon [51-53, 57].



**Figure 1.3: Suspected sources and localisation of origin of HIV-1 viral groups [55].**

Like the non-M groups of HIV-1, HIV-2 is mostly confined within its locus of origin, West Africa [8, 38, 41, 45, 78] (Figure 1.3). The HIV-2 epidemic has its epicentre in and around Guinea, Sierra Leone and Ivory Coast [8, 38, 41, 45, 78]. It is closely related to the SIV species SIV<sub>smm</sub> infecting sooty mangabeys in the region [44-46, 48]. There are eight known groups of HIV-2 (A-H) (Figure 1.3), with only A and B being widely disseminated within West Africa. Like the non-M HIV-1 viruses, HIV-2 does not appear as virulent as HIV-1 group M and the progression to AIDS is prolonged [50].

### **1.1.5 Molecular features of HIV and its replication**

HIV, belongs to the family *Retroviridae* [78, 81]. Two main defining hallmarks of retroviral infection are reverse transcription and integration [78, 81]. Viral genomic material is found on plus sense RNA; this RNA is then reverse transcribed into complementary DNA (cDNA) once the virus infects a cell. The cDNA then is inserted into the host genome, forming what is termed proviral DNA, a template for transcription of viral RNA. Virion proteins are translated from this transcribed RNA which is also incorporated into newly formed virions. This family of viruses is important because the establishment of proviral DNA inside

the host genome means that the viral genome will be replicated whenever cellular division takes place and will persist in the host even in the absence of active viral replication. It also means the possibility of vertical germline transmission of viral genomes [78]. Additionally, the ability of retroviruses to form DNA from RNA was an affront to the established molecular dogma of DNA $\Rightarrow$ RNA $\Rightarrow$ Protein [78]. That also made it a relatively predictable process to therapeutic target since it was a process undiscovered in mammals. Retroviruses are implicated in cancers due to their ability for semi-random insertion into host genomes and are probably the most studied viruses to date. The discovery of reverse-transcription has also revolutionised the field of medicine and biochemistry and is one of the most important recent discoveries in science and medicine [3, 78].

Retroviruses are classified based on structural features of the virion, genomic content and organisation as well as the location of virion assembly [78] (Figure 1.4). Simple retroviruses encode only key gene products : Gag, Pol and Env (These will be described in more detail below) ; a typical example is the alpharetrovirus avian leukosis sarcoma virus (ASLV) [78]. Two other simple retroviruses are the betaretroviruses (e.g. Mason-Pfizer monkey virus) and gammaretroviruses (e.g. murine leukemia virus-MLV) [78] (Figure 1.4). Complex retroviruses encode the key gene products as well as additional features and

gene products with varying functions (Figure 1.4). The genetic material is relatively compact and complex retroviruses have multiple reading frames [78]. Viral genera considered as complex retroviruses include deltaretroviruses (e.g. HTLV) (Figure 1.4), epsilonretroviruses (e.g. the fish infection, walleye dermal sarcoma virus), lentiviruses (e.g. HIV and SIV) (Figure 1.4) and spumaviruses (e.g. prototype human foamy virus-PFV) [78, 81].

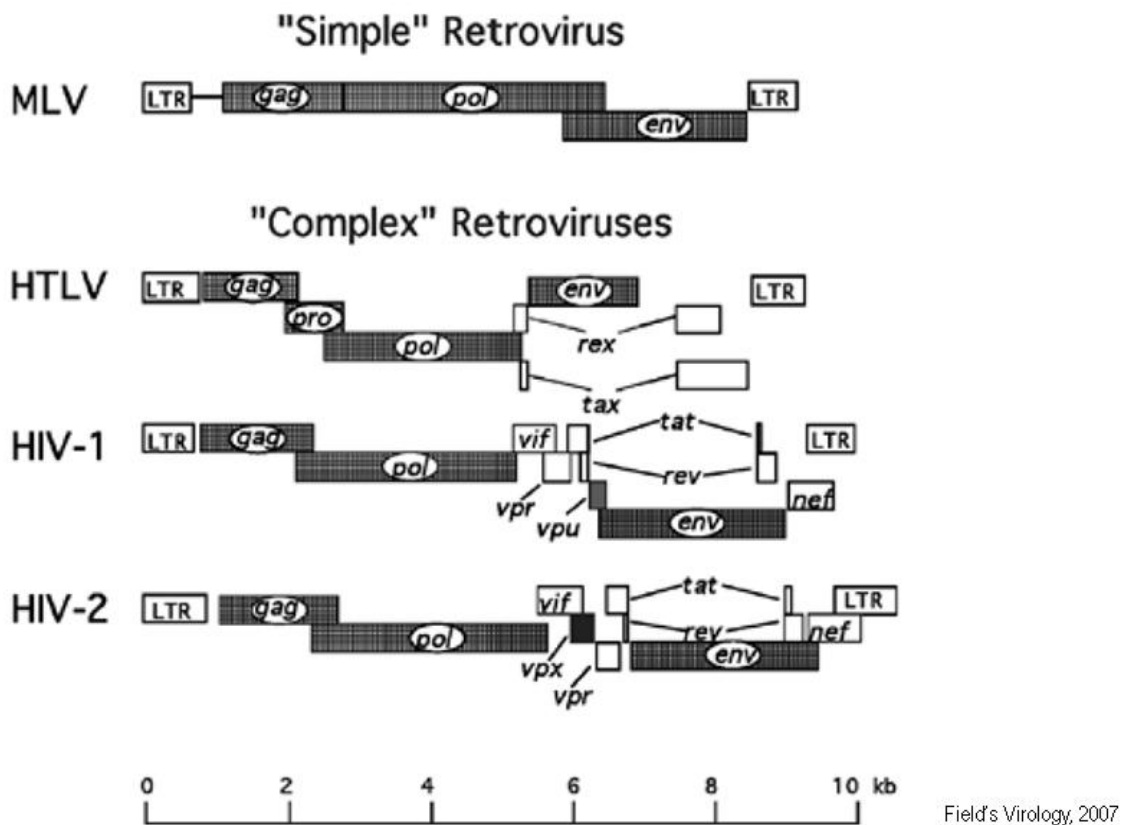


Figure 1.4: Key genomic similarities and differences between complex and simple retroviruses [78].

Lentiviral genomes are contained within a cylindrical or conical core and genomes of this genus encode Gag, Pol and Env expression. The prototypical

lentivirus, HIV-1 also contains several accessory genes; *vif*, *vpr*, *vpu*, *tat*, *rev* and *nef* [78, 81] (Figure 1.4). The putative and confirmed roles of the various HIV genes and gene products in the viral replication cycle are described in brief below.

#### 1.1.5.1 HIV genomic organisation

HIV is an enveloped spherical retrovirus with its genomic material consisting of two copies of plus strand ribonucleic acid (RNA) molecules encapsulated within a conical capsid core [78, 81-83] (Figure 1.5). The compact genome of HIV is approximately 9.7 Kb (Figure 1.4; 1.5), is flanked on either end by the 5' and 3' untranslated regions (UTR), both of which contain the long terminal repeats (LTR). The LTR contains the promoter regions as well as several cis-acting elements [78, 83, 84].

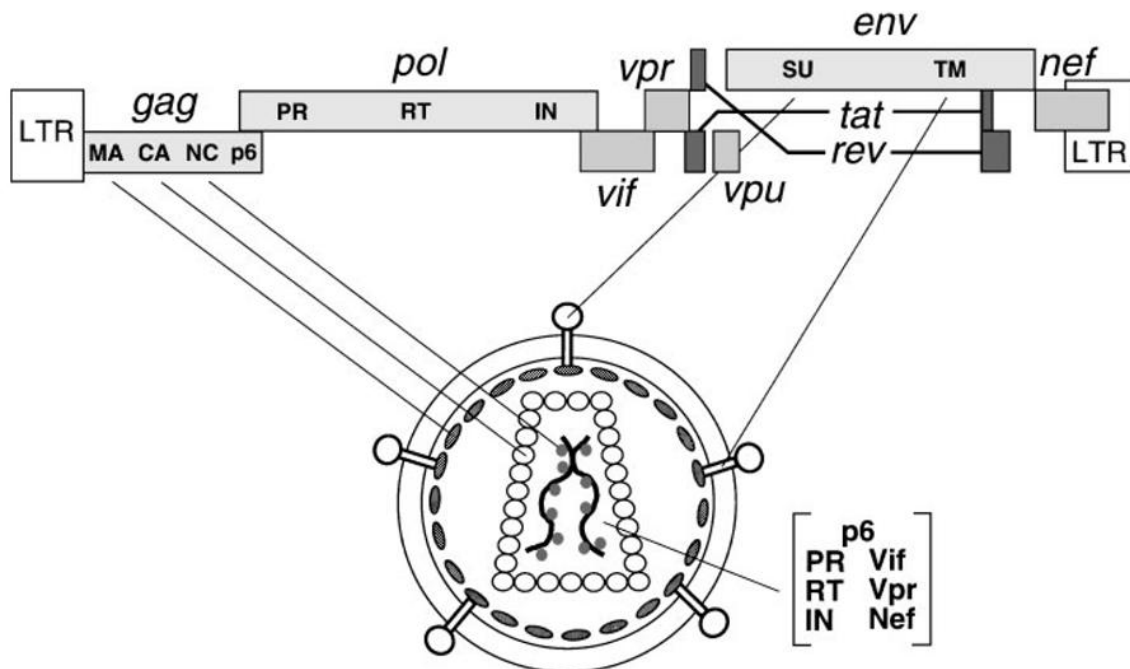


**Figure 1.5: HIV-1 genomic and structural organisation [84].**

The remaining genome consists of nine open reading frames (ORF), and encodes fifteen different proteins [78, 81-83] (Figure 1.5). Three of these ORFs are responsible for the translation of the Gag, Gag-Pol and Env polyproteins [78, 83, 84]. Maturation of the Gag and Gag-Pol polypeptides begins during budding or shortly after [85]. Autocatalysis of the Gag-Pol polyprotein yields the protease, reverse transcriptase (RT) and integrase (IN) proteins [78, 83, 84]. Proteolysis of the Gag polyprotein by protease yields the matrix (MA), capsid (CA), nucleocapsid (NC) and p6 proteins. The viral infectivity factor (Vif), viral protein R (Vpr), regulator of viral expression (Rev), negative regulatory factor (Nef), viral protein unique (Vpu) and transactivator of transcription (Tat) proteins are all

separately translated from spliced HIV mRNA [78, 83, 84]. One key difference between HIV-1 and HIV-2 is that HIV-2, like most SIVs, has the virion-associated protein (Vpx) while HIV-1 has Vpu [48, 84, 86, 87]. This difference has key impacts on HIV disease progression and pathogenesis [48, 86, 87].

#### **1.1.5.2 Steps in HIV replication**

The steps in viral replication are briefly elucidated below in steps (i)-(xvi) (Figure 1.6). (i) Infection begins with engagement of a viral gp120 protein with the human cellular receptor CD4, present on the cell surface of T-lymphocytes, amongst other cells [78, 81-83, 88, 89]. (ii) The interaction of gp120 with CD4 exposes an interaction interface on gp120, which allows the binding of co-receptor molecules present on the cell surface. Common co-receptors are the chemokine receptors CCR5 and CXCR4 [78, 81-83, 88, 89], though several others such as CCR2b, and CCR3 have been known to be used, albeit rarely [90-93]. The major co-receptor used in primary infection is CCR5 and mutations within its encoding gene has major implications for HIV infection and disease progression [83, 94]. (iii) Once the co-receptor has been recruited to the gp120-CD4 complex, a conformation change in the viral gp41 results in the viral membrane and cellular membrane being brought close together, and subsequently (iv) fusing [78, 81-83, 88, 89]. Uncoating of the viral capsid begins almost immediately upon fusing with the aid of the viral proteins MA, Nef, Vif, and cellular factors [83, 84]. (v) Reverse



transcription occurs after uncoating, beginning with the binding of the tRNA<sup>Lys3</sup> to the primer binding site (pbs) of the 5' LTR of the HIV RNA [78, 83, 84]; NC facilitates primer binding by unwinding the tRNA<sup>Lys3</sup> and pbs and by packaging tRNA<sup>Lys3</sup> molecules into newly synthesized virions [78]. Reverse transcriptase lacks a proof-reading mechanism and is thus highly error-prone [78, 83, 84, 95, 96]. It is also able to use either HIV RNA as a template during reverse transcription [78, 83, 84, 95, 96]. This increases the number of potential genetic variants produced during reverse transcription and it is a major driving force of HIV diversity [78, 83, 84, 95], immune system evasion [97] and drug resistance [96, 98-101]. The host apolipoprotein B mRNA-editing, enzyme catalytic, polypeptide-like 3G protein (APOBEC 3G), increases the inherent low fidelity of RT, and thus restricts HIV infection [78]. The expression of this protein and its subsequent packaging into progeny virions is however counteracted by the HIV Vif protein [83, 84]; HIV is therefore heavily restricted in APOBEC 3G containing cells in the absence of Vif [83]. There is evidence that IN is associated with RT during reverse transcription [102, 103], however its main role in the replication cycle is the (vi) integration of the proviral DNA into the cellular DNA. Failure of the virus to integrate will result in an accumulation of circular episomal viral DNA designated as 1-LTR, or 2-LTR circles, based on the presence of 1 or 2 LTR portions in the unintegrated DNA [104, 105]. In this case, despite several

accessory proteins being made, structural proteins are not synthesized and the infection is non-productive [104]. Once HIV is successfully integrated into the host genome, (vii) transcription of the viral genome is initiated from the 5' LTR by the host RNA polymerase II [83, 84]. The Tat protein binds to the transactivating response element (TAR) found in the 5'LTR and enhances both initiation of and rate of transcription [83, 84, 106, 107]. (viii) The viral mRNA transcripts are spliced under regulation by Rev within the nucleus by the host spliceosome machinery and (ix) then exported to the cytoplasm, for translation and viral packaging to occur [78, 83, 84]; Rev binds to the Rev response element (RRE) of mRNA and prevents double splicing by exporting these elements out of the nucleus; double splicing only yields accessory protein mRNAs and no structural mRNAs [78, 83, 84]. (x) Translation of the Gag and Gag-Pol polyproteins takes place in the cytoplasm and (xi) assembly of the core particle from Gag and Gag-Pol polypeptides begins at the plasma membrane, driven by the MA and NC proteins. (xii) The Env polypeptide is translated and glycosylated in the endoplasmic reticulum (ER) where it is often co-expressed with CD4 [78, 83, 84]. Vpu promotes the ubiquitination and subsequent degradation of CD4 and allows (xiii) Env to be released from the ER in order for Env to be processed into gp41 and gp120 in the Golgi apparatus. The cleaved Env proteins are then targeted to and inserted into the plasma membrane surrounding the budding

virion [78, 83, 84]. In order to prevent CD4 interactions with newly synthesized Env, cell surface CD4 is gradually down-regulated by the actions of Nef and Vpu as the infection progresses [78, 83, 84]. Nef also prevents detection of the viral infection by the immune system, by causing the endocytosis and degradation of the antigen presenting complexes, major histocompatibility complex I and II (MHCI, MHCII) [78, 83, 84, 108, 109]. Vpu also antagonizes the viral restriction factor tetherin[110]. The primary function of NC protein is to bind the packaging signal and (xiv) incorporate two full-length molecules of HIV RNA into the core of the budding virion [84]. NC coats the viral RNA within the virion core. Several cellular proteins and factors such as tRNA<sup>Lys3</sup>, cyclophilin A [111, 112], ubiquitin [112], and other proteins are required for various stages of budding or viral infectivity and are thus incorporated into the virion [78, 83, 84, 111-115]. (xv) During budding, (xvi) maturation of the Gag and Gag-Pol polypeptides begins with autoproteolysis of Gag-Pol to release protease, which completes cleavage of the viral polyproteins. The mature virion (Figure 1.5; 1.6) is then able to infect another cell [78, 83, 84].

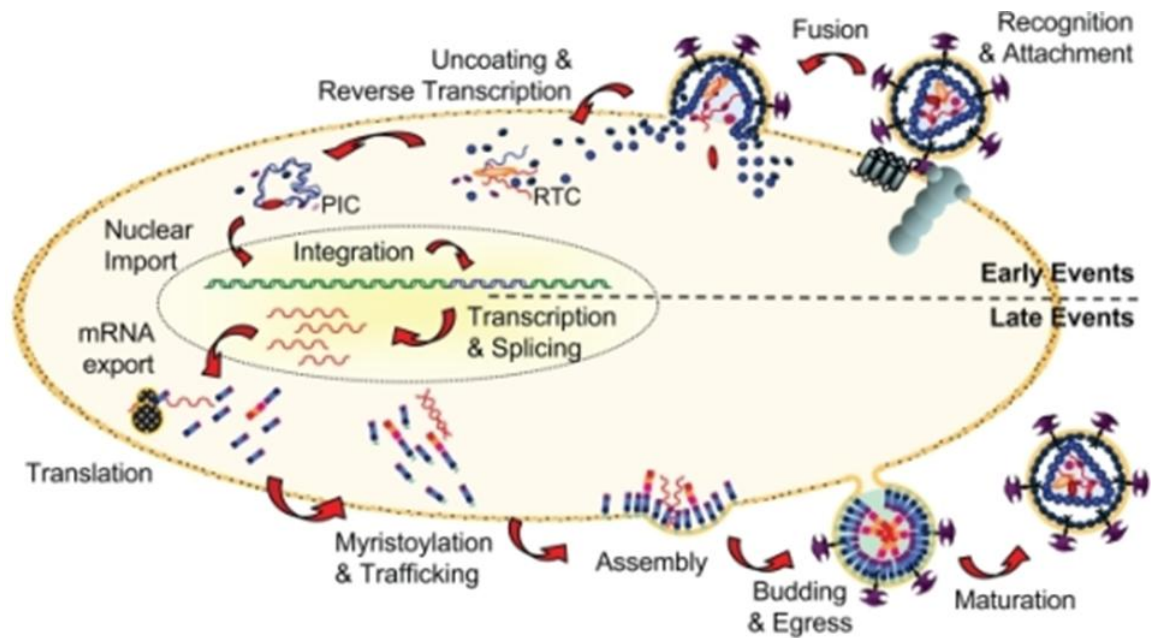
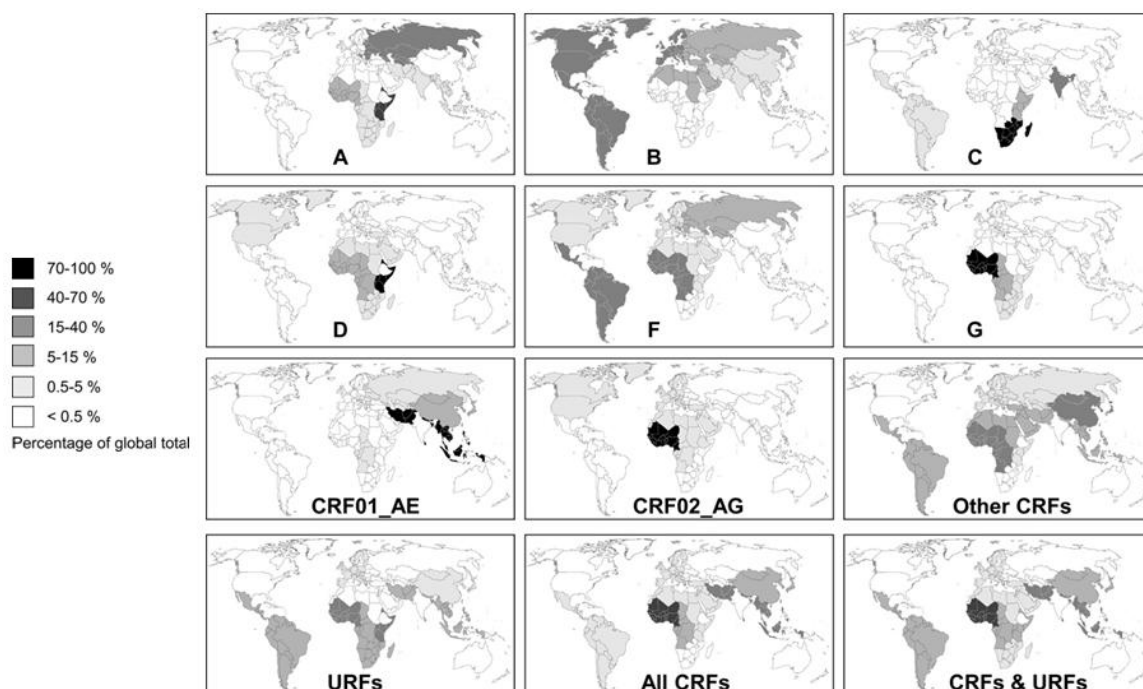


Figure 1.6: Main steps in the HIV-1 replication cycle [116].

### 1.1.6 Circulating recombinant forms

There is a relatively high template switching rate of RT during the strand transfer step of reverse transcription [57, 96]. This coupled with the possibility of simultaneous or subsequent infection with other HIV strains [51, 117-121] creates the possibility of viral recombination, leading to circulating and transmissible HIVs which are recombinants of more than one strain [51-53, 57, 79]. These viruses are termed circulating recombinant forms (CRFs) (Figures 1.7; 1.8) and numbered 55 in December 2012 [51]; less prevalent recombinants are termed unique recombinant forms (URFs) [51, 122].



**Figure 1.7: Geographical localisation of HIV-1 subtypes and key CRFs [79].**

CRFs are estimated to be responsible for ~20-% of the world-wide current infections [57, 79] and ~88 percent of Indian and Asian epidemics [57]. The first recombinant form, CRF\_02AE was discovered in central Africa but is now prevalent in Asia [51]. The majority of circulating recombinant forms are inter-group recombinants of HIV-1 group M [51]. Based on recently published analysis of sequences present in the Los Alamos HIV Database [123], recombinants of subtype B are currently leading all subtypes with 19% contribution [51, 123] followed by subtype G (12%) and subtype A (11%). Interestingly the same analysis shows CRF01\_AE, CRF02\_AG and CRF06\_cpx, which are numbered in order of official identification, respectively contributing to further recombination at frequencies of 9%, 3% and 1% [51]. This study highlights the increasing subtype

B content in CRFs and URFs and is in line with other recent reports [57, 79] .  
 Importantly, the number of CRFs are climbing world-wide, and the use of broadly targeting antiviral therapy may have even more importance moving forward.

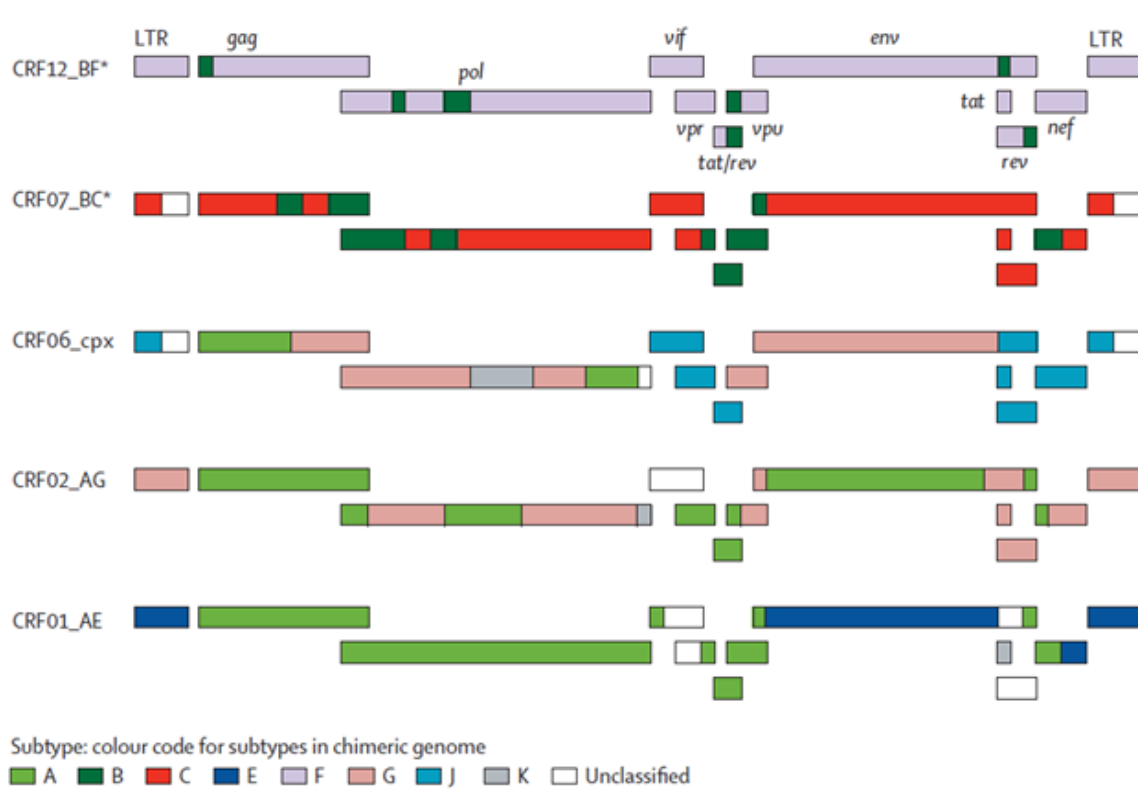


Figure 1.8: Genomic structure and subtype make-up of common CRFs [57].

### 1.1.7 Anti- Retroviral Therapy

In the early days of the various AIDS epidemics, treatment options were limited, and treatments focussed on reductions in symptomatic/opportunistic infection rather than the viral cause of the disease [3, 5, 8, 35, 124-129]. Once the causative agent of AIDS was identified [21, 130], drug discovery efforts intensified and a compound, azidothymidine (AZT), previously synthesized to combat cancer [131], showed promise in 1986 for AIDS therapy and was

approved for clinical use in 1987 [132, 133]. This compound was the first member of the nucleoside reverse transcriptase inhibitors (NRTI), and targets the RT of HIV by mimicking and competing with nucleosides; incorporation of an NRTI into the DNA chain leads to termination of reverse transcription. The use of AZT led to reduced progression to AIDS in treated patients, but resistance to AZT was reported almost immediately [98, 101, 134-136], highlighting the need for additional compounds. Several other NRTIs were discovered or repurposed for HIV therapy in the early 1990s, including 2'-deoxy-3'-cytidine (3TC-lamivudine®) [137], which exhibited lower toxicity than AZT and maintained suppression of known AZT-resistant HIV clinical isolates [137]. Other NRTIs such as 2',3'-dideoxyinosine (ddI- didanosine®) [138], 2',3'-dideoxycytidine (ddC-zalcitabine) [136, 139-142] and 2',3'-didehydro-3'-dideoxythymidine (d4T-stavudine®) [139, 143-145] had either significant cross resistance with AZT or significant toxicity [98, 136, 144, 146-149]. Zalcitabine has been discontinued in most countries due to excessive mitochondrial toxicity [150-152]. Improvements in therapeutic potency and delayed resistance was achieved initially by combinations of NRTIs compared to the previous monotherapy. Of particular importance were clinical data that AZT and 3TC had synergistic reductions in viral load and T-cell rebound [153]. The clinical additions of non-nucleotide reverse transcriptase inhibitors (nNRTIs) [154-157] and protease inhibitors (PIs)

[158-161] yielded new options for combination therapy. The success of combination therapy [153, 158, 160-162] and computer modelling suggested that successful viral suppression required therapeutic agents which required the virus to develop three or more different mutations to develop significant resistance. This new data along with the development of protease inhibitors ushered in the era of highly active antiretroviral therapy (HAART) [163-167]. There was strong initial belief that HAART would be sufficient to fully suppress viral replication [168-170], yet almost immediately after HAART initiation, data showed that both viral replication and transmission occurred in patients who were responsive to HAART [169-174]. HAART has however been credited with 60-80% decreases in progression to AIDS and AIDS-related mortality [168, 171, 175]. According to 2013 WHO recommendations, effective first-line ARV therapy make-up should include a backbone of two NRTIs and one NNRTI [176]. Whilst the initiation of HAART reduced mortalities and resulted in fewer cases of AIDS in resource-rich settings, the high cost of medication meant that the bulk of HIV infected people in Africa, South America and Asia had no access to life saving medications [177-181]. In 2000, the 13th international Conference on AIDS was held in Durban, South Africa with over twelve thousand people in attendance. The theme of the conference was "Breaking the Silence", and placed enormous pressure on pharmaceutical companies to allow equal treatment and access to medicine for



people living with HIV/AIDS in Africa (PLWHA) [182, 183]. At this conference, a call was made by the Chairman of the WHO Commission on Macroeconomics and Health, Dr. Jeffrey Sachs, for the set-up of a global fund to fight AIDS [182]. This conference provided concrete evidence that HIV caused AIDS and helped reduce AIDS denialism [32, 33, 182].

## **1.1. 8 The global picture of HIV/AIDS today and future prospects**

### **1.1. 8.1 Expanded ARV access**

Prior to, and following the Durban AIDS conference, several African governments had angered pharmaceutical companies by engaging companies in India to produce generic versions of ARVs. Following the conference, and especially after the patenting of the CD4 receptor [184], the pressure to provide affordable drugs for poor nations grew [184-187]. In 2003, The Foods and Drugs Administration (FDA) of the US granted the first licence for production of generic ARVs in Africa, under the Clinton Foundation [188, 189]. The company, whose main aim was to provide ARVs for less than \$1/day, and was initially approved to produce d4T, followed by AZT, 3TC, and nevirapine (NVP), followed by combinations of the above drugs [188, 189]. Though effective in the early decades of HIV therapy, D4T has been recently disrecommended for first line therapy due to significant toxicity [176]. For perhaps the first time since the recognition of the AIDS epidemic in the 1980s, there was a glimmer of hope in Africa. Due to the

prevention efforts and expanded access to ARVs and global initiatives by UNAIDS [190-193], the Gates Foundation [194-196], Clinton Foundation [189, 197-199], Global Fund [200-204], donor nations and various partners, there has been a 40-fold increase in antiretroviral access between 2002-2012 [190]. This has resulted in several milestones in the fight against HIV/AIDS [190]. In the snapshot year 2013, there was a 33% decrease in new HIV infections compared with 2000, a 29% decrease in AIDS-related deaths since 2005 and a 52% decrease in new HIV infections in children since 2001 [190]. Currently ~9.7 million people in low-middle income countries have access to ARV therapy at a cost of ~US\$140 per person/ year (compared with ~US\$10000/person/year in 1990) [190]. New drugs and promising developments in vaccine and 'cure' research promises an even brighter outlook for HIV therapy, even in the face of rising costs. This may be aided by the advent of generic ARVs to the US market and the global war on patents [201, 205-207], which appears to be encouraging competition amongst makers of generic ARVs and driving down prices [201].

#### **1.1. 8.2 Fusion, entry and integration**

The addition of the fusion inhibitor enfuvirtide (T20) in 2003 [208, 209] to HAART drugs expanded the ARV classes, which had hitherto been limited to NRTIs, NNRTIs and PIs [208]. This allowed more options for patients failing first and second line therapies. Enfuvirtide, which is a modified peptide complementary to

the gp41 protein of HIV, had to be administered subcutaneously, and had significant toxicities [208, 210]. It was never tested in first-line patients due to its high cost and mode of administration. It is therefore not recommended for first-line therapy.

In 2007, two new drugs representing two new classes of ARV were granted FDA approval in the United States; Maraviroc (MVC) and Raltegravir (RAL) [211].

A new class of HIV entry inhibitors was created with MVC. MVC binds to the cellular co-receptor CCR5 and allosterically inhibits the entry of HIV into host cells. It was also the first ARV for HIV therapy that specifically targeted a host protein. Apart from the controversies this created, patients in the MVC MOTIVATE trials showed artificially increased levels of viral RNA, and this led to difficulties in interpreting the data. This increase was later shown to be due to the repulsion of bound virions by the cells upon MVC therapy. The development of RAL and the class of integrase inhibitors will be discussed later in the introduction. The advent of these three new classes of ARVS has greatly improved treatment outcomes, and PLWHA have much improved health outcomes [124, 190, 200, 212]. Table 1.1 summarizes all FDA approved drugs for HIV therapy.

**Table 1.1: Food and Drug Administration Approved Antiretroviral Drugs**

<b>Brand Name (Manufacturer; contraction)</b>	<b>Generic Name (Abbreviation)</b>	<b>FDA Approval Year</b>	<b>Notes</b>
<b>Nucleoside Reverse Transcriptase Inhibitors (nRTIs)</b>			
Retrovir (GlaxoSmithKline, GSK)	zidovudine, azidothymidine (AZT, ZDV)	1987	
Videx (BristolMyers- Squibb, BMS)	didanosine, dideoxyinosine (ddl)	1991	
Hivid (Hoffman-La Roche)	zalcitabine, dideoxycytidine (ddC)	1992	Discontinued
Zerit (BMS)	Stavudine (d4T)	1994	
Epivir (GSK)	Lamivudine (3TC)	1995	
Combivir (GSK)	AZT+3TC	1997	First approved multi- drug ARV
Ziagen (GSK)	Abacavir sulfate (ABC)	1998	
Videx EC (BMS)	Enteric coated didanosine (ddl EC)	2000	
Trizivir (GSK)	ABC+AZT+3TC	2000	
Viread (Gilead Sciences, Gilead)	Tenofovir disproxil fumarate (TDF)	2001	
Emtriva (Gilead)	Emcitricitabine (FTC)	2003	Not Available in Canada
Epzicom (GSK)	ABC+3TC	2004	Kivexa in Canada
Truvada (Gilead)	TDF+FTC	2004	
<b>Non-Nucleoside Reverse Transcriptase Inhibitors</b>			
Viramune	Nevirapine (NVP)	1996	Immediate release

<b>Brand Name (Manufacturer; contraction)</b>	<b>Generic Name (Abbreviation)</b>	<b>FDA Approval Year</b>	<b>Notes</b>
(Boehringer Ingelheim, BI)			
Rescriptor (Pfizer)	Delavirdine (DLV)	1997	
Sustiva (BMS)	Efavirenz (EFV)	1998	
Intelence (Tibotec Therapeutics, Tibotec)	Etravirine (ETV)	2008	
Viramune XR (BI)	NVP	2011	Extended release
Edurant (Tibotec)	Rilpivirine (RPV)	2011	
<b>Protease Inhibitors</b>			
Invirase (Hoffman- La Roche)	Saquinavir mesylate (SQV)	1995	Discontinued
Norvir (Abbott Laboratories, Abbott)	Ritonavir (RTV)	1996	
Crixivan (Merck)	Indinavir (IDV)	1996	
Viracept (Agouron Pharmaceuticals)	Nelfinavir mesylate (NFV)	1997	
Fortovase (Hoffman- La Roche)	Saquinavir (SQV)	1997	Discontinued in US, Available in Canada
Agenerase (GSK)	Amprenavir (APV)	1999	Discontinued
Kaletra (Abbott)	Lopinavir (LPV) and ritonavir (RTV)	2000	
Reyataz (BMS)	Atazanavir sulfate (ATV)	2003	
Lexiva (GSK)	Fosamprenavir	2003	Telzir in Canada

<b>Brand Name (Manufacturer; contraction)</b>	<b>Generic Name (Abbreviation)</b>	<b>FDA Approval Year</b>	<b>Notes</b>
	calcium (FOS-APV)		
Aptivus (BI)	Tiprinavir (TPV)	2005	
Prezista (Tibotec Inc.)	Duranavir (DRV)	2006	
<b>Fusion Inhibitors</b>			
Fuzeon (Hoffman La Roche and Trimeris)	Enfurvitide (T-20)	2003	
<b>Entry Inhibitors- CCR5 co-receptor</b>			
Selzentry (Pfizer)	Maraviroc (MVC)	2007	Celsentri in Canada
<b>Integrase strand transfer inhibitors</b>			
ISENTRESS (Merck & Co. Inc)	Raltegravir (RAL)	2007	
Tivicay (GSK/Shinogi)	Dolutegravir (DTG)	2013	
Vitekta (Gilead)	Elvitegravir EVG	2014	Needs to be boosted
<b>Multiclass Single Pill formulations</b>			
Atripla (BMS and Gilead)	EFV+FTC+TDF	2006	Previous gold standard of care
Complera (Gilead)	RPV+FTC+TDF	2011	
Stribild (Gilead)	Elvitegravir (EVG) + Cobicistat (COBI) + FTC + TDF	2012	
Triumeq (ViiV Healthcare)	DTG+3TC+ABC	2014	Patients need to be screened for genetic ABC hypersensitivity
Evotaz (BMS)	ATV+ COBI	2015	

Brand Name (Manufacturer; contraction)	Generic Name (Abbreviation)	FDA Approval Year	Notes
Prezcobix (Janssen Therapeutics)	DRV+ COBI	2015	By Health Canada, not FDA

### 1.1. 8.3 Vaccine initiatives

In the early days of the AIDS epidemic, riding the wave of successful vaccination programs, the US Health and Human Services Secretary declared that a vaccine would be available in two years [8]. The short-sightedness of this boast is made more apparent with each passing year, as there is still no HIV vaccine and the most promising candidates have flopped [97, 213-222]. Barriers to HIV vaccines were numerous. Unlike other viral vaccines, once infected, a person could not get rid of integrated viral DNA, so a vaccine could not work in the traditional sense [223]. HIV possesses a plethora of immune evasion strategies, and researchers have increasingly had to rethink standard strategies for every aspect of HIV research [57, 97, 224]. Recently, however there have been some promising gains in HIV vaccine research [79, 225, 226], as a result of a huge focus of governments and funding initiatives [227, 228] on vaccine development. Currently clinical trials are underway to test the use of therapeutic DNA vaccines in HIV-positive individuals. This approach aims at augmenting ARV therapy by

stimulating production of antibodies by the immune system [227, 228]. However, concrete gains are still at least 'two years' away.

#### **1.1. 8.4 Preexposure prophylaxes of ARVs**

The advent of successful viral suppression on ARV therapy introduced the concept of pre-exposure prophylaxis (PrEP). The idea was that the presence of active ARVs in the blood or mucosal membranes of an uninfected person may prevent acquisition of HIV despite repeated exposure. PrEP was tested in several instances, as oral administration or as anally/ vaginally applied topical microbicides with variable results [229]. Recently the use of a dual formulation of TDF/FTC was approved for use as orally administered PrEP in sexually active HIV-negative adults at risk of HIV infection [230]. Three landmark clinical trials informed the decision. The iPrEx study found that men who have sex with men (MSM) had 44% reduction in HIV acquisition and those with detectable levels of drug in their blood had greater than 90% reduction in HIV acquisition risk [231, 232]. This was in close agreement with the results of the Partners PrEP study, which followed 4758 serodiscordant couples in Kenya [233]. The results showed that the application of TDF or TDF/FTC led to 63% and 73% fewer HIV transmissions respectively, compared to the placebo control patients. When the patients had detectable levels of drugs in their blood, the reduction in HIV acquisition was greater than 90% [233]. In the Bangkok Tenofovir Study (BTS)



[234], the main target group was injection drug users. At the end of the study period, there was a reduction of 48.9% incidence in the TDF/FTC treated versus placebo arms [234]. When patients had detectable drug in their blood, there was a 95% reduction in HIV incidence in the treated group [234].

### **1.1. 8.5 Cure Initiatives**

The difference between suppressive ARV therapy and a successful HIV cure is that once cured, there would be no need to maintain ARV therapy and the cured person would be able to live a normal productive life without need for additional therapy. There are two ways to cure the body of HIV; a sterilizing cure would purge the body and cells of all integrated HIV DNA whilst a functional cure would successfully incapacitate archived HIV enough to prevent reactivation and subsequent infection of uninfected cells [235-239]. Several cure initiatives are underway. Some of these methods seek to deplete the viral reservoir by cycles of latent virus reactivation and ARV therapy [238, 240]. These efforts have had mixed results with some issues of toxicity.

Other approaches aim to apply what was learned from the first confirmed cured HIV infection (Tim Brown), who was cured by immune cell depletion and bone marrow transplantation with cells from a CCR5  $\Delta$ 32 carrying individual [239, 241, 242]. Due to the high risks and costs associated with such a procedure, it is likely to never become common practice.

## 1.2 Part II: Therapeutic targeting of HIV integrase

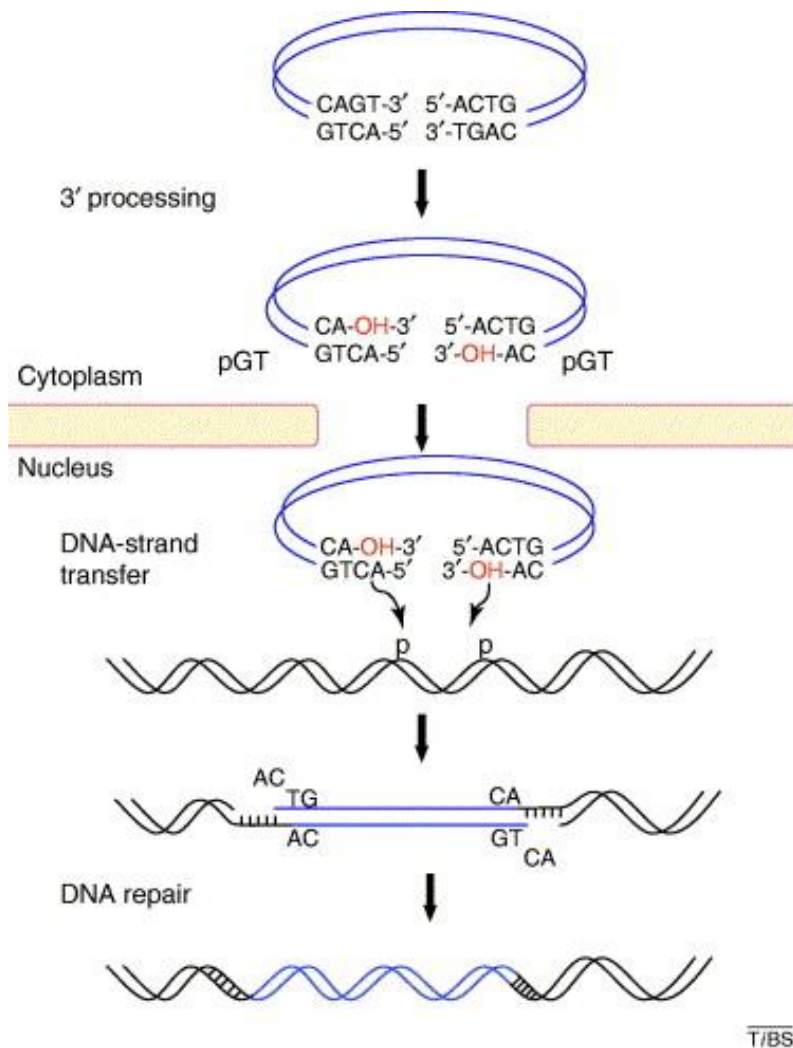
### 1.2.1 HIV integrase function and structure

One of the hallmarks of retroviral infection, integration is also the step responsible for the establishment of viral persistence in host DNA [235].

Immediately after fusion, uncoating and viral entry into the cell, reverse transcriptase retro-transcribes the viral RNA into linear viral DNA flanked at either end by the 5' and 3' LTRs. Viral integrase protein forms on both LTR regions and recruits additional proteins to form the pre-integration complex (PIC), which become transported to the nucleus. In the nucleus, linear viral DNA is integrated into the host DNA (Figure 1.9) [243, 244]. There are three main steps in this process; the phosphodiester cleavage of two terminal nucleotides downstream of a conserved CA dinucleotide sequence in both viral LTR to reveal reactive 3' hydroxyl ends [245]. This is followed a trans-esterification reaction initiated by the phosphodiester cleavage of host DNA by the exposed hydroxyl groups which leads to the formation of a phosphodiester linkage between viral LTR and host DNA. The final step of integration is termed gap repair and entails the cleavage of the unpaired 5' dinucleotides from the viral LTR followed by the joining of the remaining ends of the viral LTR to host DNA. The entire process is referred to as integration and it is critical to the viral life cycle. The viral enzyme integrase, which is present in the infectious virion, and which belongs to the retrotransposon

family of proteins, catalyses the integration step. This enzyme has been shown to be the only viral or host enzyme necessary and sufficient to carry out in vitro 3' processing and strand transfer in an LTR dependent manner. There is yet to no reliable evidence that integrase can catalyze in vitro gap-repair, even though an assay termed as disintegration has been advanced to show this.

Being a viral protein present in the infectious virus particle, and being the only viral protein necessary for the integration of viral DNA into host DNA (Figure 1.2), integrase IN is pivotal in the viral replication cycle and in the establishment of latency.



T/BS

Figure 1.9: Steps of HIV integration [246].

## 1.2.2 Host-factor proteins interacting with HIV IN

### 1.2.2.1 INI1

The first integrase interacting protein, aptly named integrase interactor 1 (INI1), was identified through a yeast two-hybrid screen and it was found to cause an increase in IN-DNA interactions [247]. INI1 was found to be homologous to the yeast chromatin remodeling factor SWF5 [247] part of human SWI/SNF. A portion of INI1 repeat 2 (rpt2) was shown to be necessary and sufficient for

interaction with IN [247]. This region was also found to have a masked nuclear import signal and the S6 fragment of INI1 (minimal IN interaction region) also shown to be a trans-dominant inhibitor of late replication steps when over-expressed in the cell, hinting that integrase was part of the Gag-Pol complex, well known. INI1, when expressed in INI1 deficient cells, caused a clear increase in infectivity and INI1 was detected to localize to the cytoplasm soon after infection. Additionally, INI1 had been detected in infectious virions, and had been shown to be associated with HIV-1 during its nuclear import but there existed no strong evidence establishing INI1 as a factor necessary for *in vivo* retroviral integration or replication [246]. This protein discussed above has now been confirmed as mediating functional coupling of IN-to the SWI/SNF complex, leading to the efficient integration of IN into stable nucleosomes. Without this linkage to the chromatin remodeling complex, IN would not be able to integrate into stable nucleosomes [248].

#### **1.2.2.2 BAF**

The barrier to autointegration (BAF) was first identified as a component of moloney murine leukemia virus (MoMLV) PICs [249] and was found to prevent autointegration of viral LTR into viral DNA, thus preventing viral suicide. It was also found to restore the activity of salt-stripped HIV-1 PICs. Using  $\alpha$ -BAF antibodies and co-immunoprecipitation, the presence of BAF was confirmed in

HIV-1 PICs. BAF was however not found to stimulate the activity of recombinant IN. A two-hybrid screen showed an association of BAF with the lamina-associated polypeptide LAP-2 $\alpha$ . Early work focused on the relationship between BAF and LAP-2 $\alpha$ ; in MoMLV, LAP-2 $\alpha$ , appeared to help in recruitment of BAF to PICs [250] but specific roles of BAF and by extension LAP-2 $\alpha$  had not been properly elucidated until recently.

### **1.2.2.3 LEDGF/p75**

Currently the most researched IN interaction partner, the lens epithelium-derived growth factor (LEDGF/p75) was identified as an IN binding partner by coimmunoprecipitation of HIV-1 complexes present in human nuclei of cells stably over expressing IN [251]. Two separate groups, those of Engelman and Benarous, confirmed the identity of this IN interactor, respectively using coimmunoprecipitation [252] and yeast two-hybrid [253, 254], and naming the protein p75 (based on molecular weight) and lens epithelium derived growth factor (LEDGF) (based on its isolation in lens epithelium and the presumption of it being a growth factor). In fact LEDGF is a commonly expressed protein and is a stringency factor that protects against stress-induced cell death. The cellular role of LEDGF means a strong association with DNA, heat shock proteins, transcriptional activators and other anti-apoptotic proteins [246]. LEDGF has been shown to be cleaved by caspases -3 and -7 [246]. The resulting fragments

abrogate the protective role of LEDGF, implicating LEDGF as a key regulator of cellular survival. Extensive research showed that ~80 residues (148-156) of the 530 aa protein was responsible for interaction with HIV-1 integrase and as such this region was termed the integrase binding domain (IBD) (Figure 1.10) [246]. It was shown by crystallography that the stoichiometry of IN: LEDGF was most likely 2:1 [246, 252]. Several residues of LEDGF within this region were shown to be critical for IN-LEDGF interaction and mutation of these residues was shown to be sufficient for the abrogation of IN-LEDGF interaction [246].

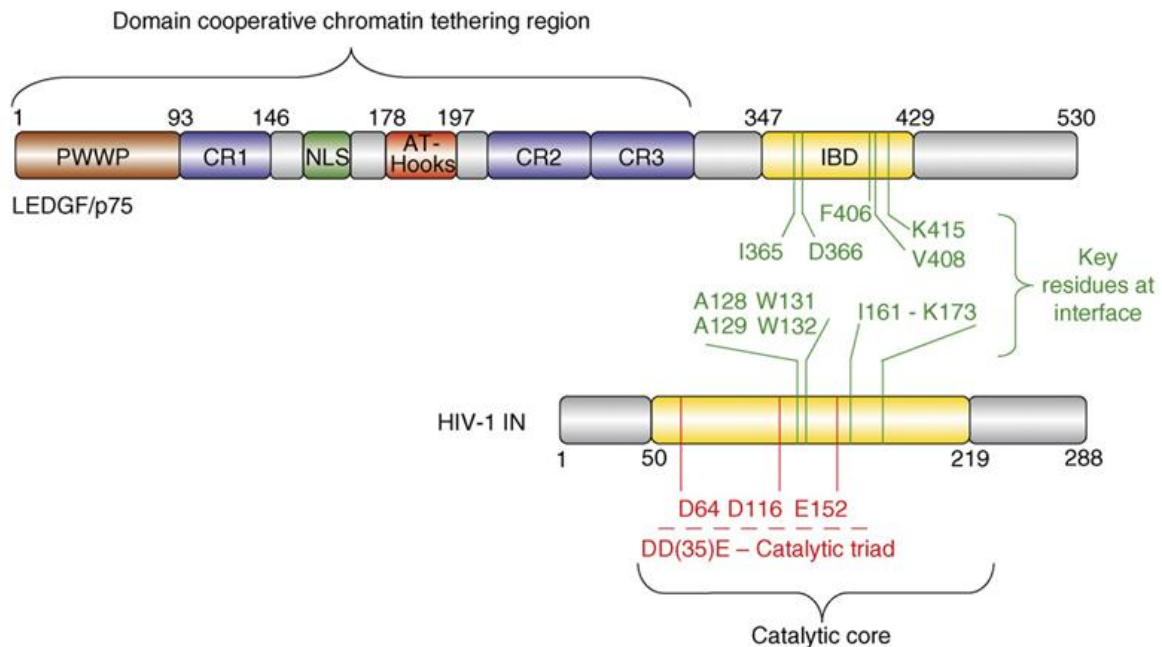


**Figure 1.10: Domain organisation of Ledgef and HIV-1 IN showing key motifs and residues. Adapted from [244].**

Initial studies showed that LEDGF and HIV-1 IN co-localized perfectly by fluorescence studies and suggested a role of LEDGF in nuclear localization of HIV-1 PICs [255]; siRNA knock down of LEDGF resulted in extreme reduction in lentiviral replication. Pull-down assays established that LEDGF interacted with lentiviral IN but not feline immunodeficiency retrovirus. The role of LEDGF on lentiviral integration was the subject of many independent assays. After a substantial volume of conflicting reports [246], it was hypothesized that LEDGF had a role in tethering of HIV-1 IN to host chromatin [246]. The mechanism of nuclear transport was still unknown. Fluorescence-correlation spectroscopy (FCS)-based DNA-binding assay was then proposed as a platform for the identification of inhibitors of the IN-LEDGF interaction [246].

Currently, the most promising inhibitors targeting IN-host interactions disrupt interaction between IN and LEDGF/p75; the latter is a host protein that has been shown to be essential for tethering the IN PIC to host chromatin and also for the recruitment of other cellular factors to the PIC, thereby facilitating effective integration [256, 257]. Integration cannot occur in the absence of LEDGF/p75 and inhibition of the LEDGF/p75-IN interaction can block viral replication [256, 258]. This is supported by the finding that polymorphisms in the PSIP-1 gene which codes for LEDGF/p75 can affect rates of HIV disease advancement [259].



#### 1.2.2.4 KAP1

One of the initial labs to propose a role of p300 in acetylation of HIV-1 IN was the Ceresato group, identifying lysine IN residues, 264, 266 and 273 as the modified residues [260]. Since acetylation has an effect on the propensity of proteins to bind their target DNA, Ceresato and colleagues investigated host proteins that preferentially bound acetylated IN in the hope of discovering additional host regulators of HIV-1 IN [261, 262]. Infection assays done in Hela cells and 293T cells with silenced KAP1 expression showed increased HIV-1 infectivity; KAP1 over-expression led to decreases in viral infectivity. This suggested a role of KAP1 in restricting HIV-1 infection and this was found to be specific for IN integration based on measurements of 2-LTR circles by real-time quantitative PCR (RT-QPCR) [262]. They found that the restriction of viral infection was directly proportional to the increase in 2-LTR circle, thus suggesting IN as the target of restriction. They showed by co-immunoprecipitation that KAP1 likely inhibited IN activity by recruiting its previously known interacting partner histone deacetylase1 (HDAC1). HDAC1 was shown to deacetylate IN. HDAC1 knock-down cell showed increased integration efficiency and subsequently increased viral infectivity. Their finding point to a role of KAP1 in recruiting HDAC1 to acetylated IN and thereby having a restrictive phenotype on HIV-1 replication [262].

### 1.2.2.5 Transportin-3 and RANBP2

Genome-wide siRNA screens identified the nuclear import proteins, transportin-3 (TNPO3) and RanBP2 as being essential for nuclear import of PICs [263]. Bushman and colleagues used RNAi to investigate these effects further [263] and showed a direct role of nuclear import to integration targeting (Figure 1.11). The manuscript also hinted at higher gene densities near nuclear pore complexes [264, 265].

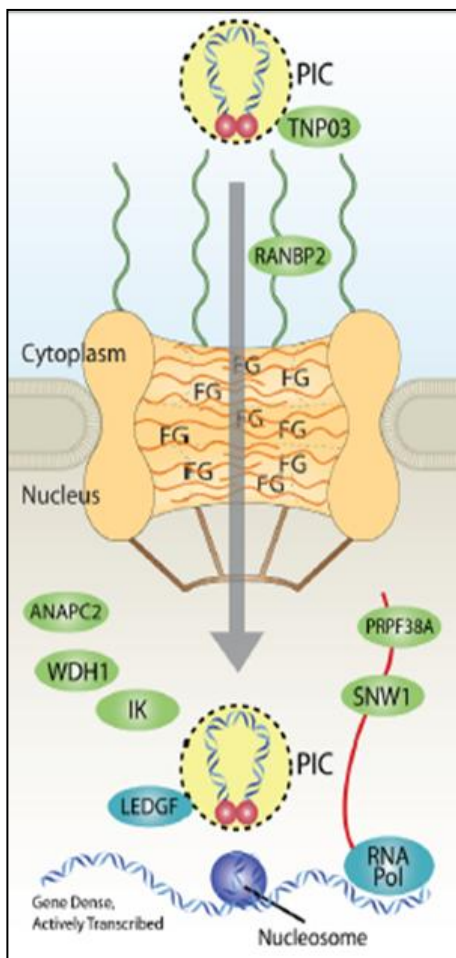


**Figure 1.11 Proposed mechanism of TNPO3 and RANBP2 in nuclear import.**

1: Passage of PIC through nuclear pore to gene dense regions. 2: Targeting of integration to transcription start sites by LEDGF tethering [263].

### 1.2.2.6 Importin- $\alpha$

Importin- $\alpha$  has been recognized as a host protein that can facilitate nuclear import of HIV-1 PICs upon the down-regulation of TNPO3, thus suggesting an alternate route to the nucleus and a synergistic effect of importin and TNPO3 on HIV-1 nuclear import [266]. Loyter and colleagues recently showed that importin- $\alpha$  is the preferred route during transfections whereas TNPO3 is preferred during actual infection. This is still a developing field and seems to support the growing evidence that HIV adapts to find multiple ways to enter the nucleus [265-268].

### 1.2.2.7 NUP153 and NUP160

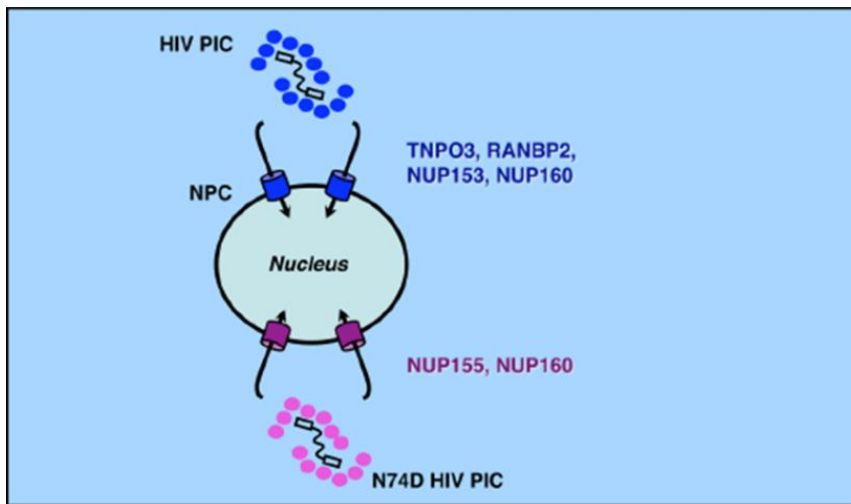


Figure 1.12 Circumvention of transportin pathway by the N74D capsid variant virus [265]. N74D viral PICs enter the nucleus through NUP155/160 pores while non-mutated virus uses the nuclear pore complex proteins NUP153/160 mediated by TNPO3 and RANBP2.

Nup153 and Nup160 are nuclear-pore complexes shown to be involved in transportin regulated nuclear import of HIV-1 PICs. Recent work by the group of Engelman has shown that the requirement of Nup153 for HIV-1 nuclear import is regulated by HIV-1Gag and capsid proteins (Figure 1.12) [265]. This may mean that targeting HIV-1 nuclear import for drug therapy may have to be a multi-factorial approach since other proteins apart from IN are involved.

#### **1.2.2.8 Ku70**

Yao and colleagues at the University of Manitoba recently identified a host protein Ku70, that directly binds to and protects HIV-1 IN from proteasomal degradation [269]. They demonstrated the Ku70 which non-specifically decreases cellular ubiquitination levels, bound specifically to IN, prevented its ubiquitination and thus provided protection from the proteasome machinery. They also showed that depletion of cellular Ku70 resulted in undetectable levels of HIV-1 RNA and 2-LTR circles, hinting at a that Ku70 is necessary to protect IN in the cytosol and allow for nuclear import. They also detected levels of Ku70 in progeny virions [262]. This host factor may yet be a valuable interaction to exploit in our search for newer and more effective therapeutic treatments for HIV-1 integrase.

#### **1.2.3 Integrase Inhibitors**

### 1.2.3.1 Early integrase inhibitors

This unique process has always been considered a viable drug target, which several early studies attempted to exploit [270]. Early integrase inhibitors (INIs) included peptides [271, 272], nucleotides [273] and DNA complexes [274] as well as small molecules derived either from natural products [273] or by rational drug design strategies [272, 275]. Even though some of these compounds advanced into preclinical trials, further clinical development was always curtailed due to *in vivo* toxicity and/or non-specific off-target effects.

For any inhibitor to be considered useful as an antiviral in combination therapy for HIV, selectivity (such as for IN) that is distinct from effects on other targets (such as RT and protease) needs to be proven. The 4-aryl-2,4-diketobutanoic acid inhibitors containing a distinct diketo acid moiety (DKA) were identified in 2000 by Merck investigators from a screen of 250,000 compounds, and for a time were the only biologically validated INIs [276]. Their antiviral activity in cell culture was mitigated by the development of resistance mutations in the IN protein, thereby confirming their mode of action [276]. These compounds, exemplified by L-731988 [277], were found to inhibit strand transfer with much higher potency (half-inhibitory concentration ( $IC_{50}$ )= 80 nM) than 3' prime processing (6  $\mu$ M) [276], and they were thus referred to as integrase strand transfer inhibitors (INSTIs). IN, like most nucleotidyltransferase enzymes, requires two divalent

cations bound at the active site for activity;  $Mg^{2+}$  is likely used *in vivo*, although  $Mn^{2+}$  is used in some *in vitro* assays [278]. Most INSTIs that have been described, including DKA compounds, inhibit IN by chelation of bound cations in a concentration-dependent manner [279]. The crystal structure [280] of IN bound to the prototype DKA, 1-(5-chloroindol-3-yl)-3-hydroxy-3-(2H-tetrazol-5-yl)-propanone (5-CITEP), provided structural evidence for DKA-IN binding interactions. The compound termed 5-CITEP was found to bind in proximity to the evolutionarily conserved D64 D116 E152 motif of IN, also providing valuable structural confirmation of the IN active site [280]. Subsequent variations of DKAs based on the 5-CITEP backbone led to increased potency, specificity, tolerability and bioavailability. This, in turn, led to the first clinically tested INI (S-1360). Despite an initially good pharmacological and pharmacokinetic profile in animal models, S-1360 in initial human trials was found to be rapidly cleared through glucuronidation [281] and its development was curtailed.

Recent resolution of the structure of the prototype foamy virus PFV intasome has been broadly used to explore the mechanisms of action of INSTIs and their resistance mutations [282-286]. INSTIs bind to the catalytic core domain of integrase and compete with host DNA binding [287]. These drugs contain a halogenated phenyl group that invades the catalytic pocket and displaces the 3' viral end [283, 288] and three coplanar oxygen atoms that chelate the divalent

ions within the catalytic pocket, thus inhibiting the activity of the catalytic DDE triad [285, 289-293]. Although coordination of these ions by the triad is also necessary for 3' processing, INSTIs are specific for strand transfer and only poorly inhibit 3' processing [287, 294]. This is due to an allosteric hindrance between the halogenated phenyl group and the 3' dinucleotide cleaved during 3' processing that prevents efficient binding of INSTIs before 3' processing occurs [283, 288].

### **1.2.3.2 First generation integrase inhibitors**

#### **1.2.3.2.1 Raltegravir**

Optimization of lead compounds including L-31988 and L-870812 by Merck pharmaceuticals led to the development of raltegravir (RAL; Isentress®), which in 2007 became the first INI approved for treatment in both antiretroviral (ARV) naïve and treatment-experienced patients [295]. RAL was shown in multiple trials, such as BENCHMRK, to achieve efficient viral load suppression in ARV-experienced patients when included in an optimized background ARV regimen [296]. In the BENCHMRK trials, 57% of patients achieved plasma levels of HIV-1 RNA <50 copies/mL after 97 weeks of therapy, whereas only 26% of the placebo group, treated with optimized background regimen (OBR) drugs, achieved viral suppression. The efficacy of RAL relative to other ARVs has been modeled in cell culture and has been shown to be owing to the activity of INIs at later stages

in the viral replication cycle than either viral entry or reverse transcription inhibitors: they are therefore able to inhibit replication in a larger proportion of productively infected cells [297]. In another study of patients with multidrug-resistant viruses with a median ARV treatment experience of 9 years, a RAL-containing regimen yielded higher viral load suppression than a regimen containing placebo when combined with OBR [298]. RAL has a favorable toxicity profile and does not appear to have a high propensity for clinically relevant drug-drug interactions [278], except for minor induction of the glucuronidation enzyme UGT1A1 responsible for RAL elimination [299]. Interactions with drugs such as rifampin may lead to modest decreases in RAL half-life and blood concentration after 12 hours (C<sub>12hr</sub>). Predictably, other UGT1A1 inhibitors, such as atazanavir, have been shown to exert a modest but not clinically relevant increase of C<sub>12hr</sub> levels for RAL. RAL has been shown to have high bioavailability and is dosed twice daily at 400 mg due to its C<sub>12hr</sub> of 142 nM. Studies to simplify RAL dosage to 800 mg once daily, boosted or unboosted by the UGT1A1 inhibitor atazanavir, did not yield significant promise [300-302].

Despite the high effectiveness of RAL for first-line and salvage therapy, resistance mutations can reduce the susceptibility of the virus to INIs. The occurrence of single point mutations that confer high-level resistance (fold change (FC) >5) to INIs have shown that RAL has a modest genetic barrier to



resistance development. To date, three major resistance pathways involving non-polymorphic residues have been extensively described and characterized for RAL; E92QV/N155H, T97A/Y143C/H/R and G140CS/Q148H/K/R [303, 304]. Although these three pathways have been shown to arise separately, some recent reports suggest that they may be linked. The G140S/C and E92Q/V mutations by themselves impart greater than five- to ten-fold resistance to RAL [305], but usually appear only after the N155H and Q148H/K/R mutations [306], leading to a FC >100 for the combined mutations. In addition to these major resistance mutations, several polymorphic and non-polymorphic residues have been identified that impart a greater than five-fold resistance to RAL. Some of these, such as T66I/L, have been shown to act synergistically with pre-existing major resistance mutations [307]. All major INI resistance mutations have a major impact on both IN activity and viral replication capacity [308]. The result is a swift reversion to wild-type virus in patients soon after therapy with INIs is withdrawn [309].

It has been suggested that patients without a history of nucleoside reverse transcriptase inhibitor (NRTI)-associated resistance may have an increased barrier for the occurrence of resistance to RAL compared with patients with resistance to non-NRTIs, such as nevirapine and efavirenz (EFV) [310]. Most reported virologic failures due to RAL-resistance mutations have occurred in

patients harboring NRTI-resistant viruses or in patients at increased risk of virologic failure [311]. This was highlighted in the SWITCHMRK1 and 2 phase III trials in patients undergoing salvage therapy with lopinavir, a protease inhibitor, and who switched from lopinavir (LPV) to RAL, despite having undetectable viremia. The results showed that 84.4% of those who switched to RAL (n = 353) maintained undetectable levels of viremia compared to >90% in the treatment group who did not switch (n = 354). Thus, this study failed to establish non-inferiority of RAL to LPV in the treatment of ARV-experienced individuals with HIV with undetectable viremia [311]. Of the 11 patients who experienced virologic failure with HIV-1 RNA levels >400 copies/mL, eight harbored RAL-resistance mutations [312]. The evolution of DRMs during selections with RAL and during therapy has been elucidated with the advent of new-generation sequencing methods [313-318]. In a comprehensive study to better define primary resistance variations in patients during continued RAL therapy, characterization of 200 RAL-resistant viruses was carried out. These specimens were derived from patients in the SCOPE cohort, RAL BENCHMRK phase III studies, as well as from patient samples submitted to the Monogram Clinical Reference Library for routine INI testing, with clonal analysis performed for select patient virus isolates [313]. They found that variants with Y143R or Q148H/R tended to have larger susceptibility fold changes than N155H containing viruses in line with previous studies [311,

314, 315, 319-321]. There were also temporal shifts in subpopulation proportions of N155H, Y143R, and Q148H DRMs within the same patient. By using molecular clones from different patients, isolated at different time-points, they showed that N155H, under continued RAL therapy, is gradually replaced with Y143R or Q148HR, and that the pathway that eventually becomes the predominant species is determined by a specific amino acid substitution at residue 148 as well as by a secondary mutation in addition to Y143R [313]. In one patient, N155H was the first mutation to appear at week 8, and was then supplanted by the Y143R mutation that first appeared at week 16 and remained the dominant species at week 24; the maximum fold changes measured in this patient was 54. Another patient had all three primary mutations present as subpopulations at week 11 (11% E92Q/Y143R; 21% wt; 21% E92Q/N155H; 56% G140S/Q148R), despite the fact that none of these mutations was detected at baseline. Y143R was present in all clones by week 28 (5% Y143R/E92Q; 5% Y143R; 90% Y143R/T97A). The fold changes in this patient was greater than 150 at week 11 and remained high with only slight decreases in replicative capacity compared to baseline. In another patient harboring all three primary mutations at week 11 (5% N155H; 23% Q148H/G140S), the N155H mutation was lost by week 16 (15% Y143R; 85% Q148H/G140S) with Q148H/G140S being present in all viruses by week 24. Thus, the 148 pathway dominated when

the mutation was Q148H/G140S and the Y143 pathway became dominant in a mixture of N155H and Y143R mutations in these three patients. In an individual in whom a mixture of all three primary mutations was present, the dominance of the 148 pathway was offset only when Y143R occurred in combination with E92Q [313].

An earlier study analyzed resistance in 23 patients who began a salvage therapy containing RAL. Despite an absence of the 143, 148, and 155 mutations at baseline (frequency <1%), the Y143R, Q148H, and N155H mutations appeared at virological failure under RAL therapy with increased resistance and viral fitness [322]. The presence of secondary resistance mutations such as T97A, V151I, and G163R, despite being detected at very low levels, did not have any effect on the development of resistant variants at failure [322], suggesting that patterns of resistance development did not appear to be significantly affected by baseline mutations, though other baseline mutations in integrase and other proteins such as protease and reverse transcriptase may have an effect on levels of susceptibility even for variants with identical resistance profiles [305, 317, 323].

#### 1.2.3.2.2 Elvitegravir

Elvitegravir (EVG) (GS-9137) is not a DKA but a monoketo acid resulting from early modification of the DKA motif by the Japan Tobacco Company (Table 1.4) [324]. This work resulted in a group of 4-quinolone-3-glyoxylic acids, all of which

had a single pair of coplanar ketone and carboxylic groups and retained high specificity for and efficacy against the strand transfer reaction similar to DKA compounds [325]. EVG, which was subsequently licensed and developed by Gilead Sciences, has been shown to have an *in vitro* IC<sub>50</sub> of 7 nM against IN and an antiviral 90% effective concentration (EC<sub>90</sub>) of 1.7 nM when assayed in the presence of normal human serum [326]. EVG displayed approximately 30% bioavailability in dogs and rats with maximal plasma concentrations being achieved 0.5 to 1 hour post dose [326]. In clinical trials, EVG was found to be well tolerated and efficacious [327]. Pharmacokinetic boosting with ritonavir (RTV) was found to result in higher concentrations and improved virologic response [328]. Stribild®, a single pill formulation consisting of EVG, COBI, TDF and FTC was approved in 2012 for clinical use [329, 330] and singly formulated EVG (Vitekta®) in 2014 [331].

The cytochrome p450 enzyme CYP3A4/5 is the primary metabolizing enzyme for EVG, followed by glucuronidation by UGT1A1/3 [328]. Thus, the bioavailability and clearance of EVG was found to be favored when EVG was dosed in combination with CYP3A4/5 inhibitors [278, 328, 332]. The CYP3A4/5 inhibitor, RTV, was found to cause an approximate 20-fold increase in the area under the curve and to extend elimination half-life from three to ten hours [333]. In a phase II trial of ARV-naïve patients (n = 48) starting initial therapy on an OBR of

tenofovir/emtricitabine (TDF/FTC), the co-administration of EVG with a novel pharmacokinetic booster, cobicistat (COBI), in a single tablet formulation, QUAD, resulted in undetectable viremia in 90% of patients after 48 weeks compared with 83% of patients who received TDF/FTC/EFV [334]. In a Phase IIb study, RTV-boosted EVG was non-inferior to the RTV-boosted protease inhibitors darunavir and tipranavir when used in combination with other drugs [335].

**Table 1.2: Main resistance pathways for currently approved INSTIs expressed in fold-change (FC) susceptibility relative to wild-type viruses [336].**

Resistance pathways	Fold resistance		
	RAL	EVG	DTG
<b>Y143 pathway</b>			
Y143C	<10	<2	<2
Y143R	<50	<2	<2
T97A/Y143C	>100	<2	<2
T97A/Y143R	>100	<2	<2
L74M/T97A/Y143G	<50	ND	<2
L74M/T97A/E138A/Y143C	<20	ND	<2
<b>N155 pathway</b>			
N155H	<50	<50	<2
E92Q/N155H	<100	>100	<10
L74M/N155H	<50	<50	<2
<b>Q148 pathway</b>			
Q148H	<20	<10	<2
Q148K	<100	<100	<2
Q148R	<50	<100	<2
E138K/Q148H	<10	<20	<2
E138K/Q148K	>100	>100	<20

E138K/Q148R	>100	>100	<10
G140S/Q148H	>100	>100	<20
G140S/Q148K	<10	<100	<2
G140S/Q148R	>100	>100	<10
E138A/G140S/Y143H/Q148H	>100	ND	<50

A major drawback to the clinical uptake of EVG, despite it being a once-daily drug, may be that it shares a moderate genetic barrier to INI resistance with RAL and that extensive cross-resistance exists between the two compounds (Table 1.2). The RAL signature mutations N155H, Q148H/R/K and G140A/C/S, as well as associated accessory mutations, were selected by EVG in culture [337] and in patients [311, 338] (Table 1.2). This precludes the use of EVG to treat most RAL-resistant viruses. The only major RAL-associated mutations not selected by EVG were Y143C/H/R and subsequent studies showed that viruses containing Y143C/H/R remained susceptible to EVG [339]. In addition to RAL-associated resistance mutations, EVG selected for other mutational pathways (Table 1.3). T66I did not confer high-level resistance to RAL [337], but conferred a >10-fold resistance to EVG, while a T66R mutation conferred >10-fold resistance to RAL and >80-fold resistance to EVG [340, 341]. The T66I mutation is associated with a series of accessory mutations, including F121Y, S153Y and R263K; the latter two have not been associated with RAL-resistance [342]. F121Y mutation has been selected with RAL and confers high-level resistance to this compound, but

has not yet been identified in the clinic [340]. Other clinically selected EVG mutations are S147G, which confers >eight-fold resistance to EVG but does not affect susceptibility to RAL [340]. Other *in vitro* EVG selections resulted in several high resistance mutations that have yet to be clinically validated, such as P145S, Q146P and V151A/L [340]. The V151L mutation confers an approximate eight-fold cross-resistance to RAL and has been identified in a single patient treated with RAL [343].

Treatment of patients with EVG has the potential to select for EVG resistance mutations, many with demonstrated cross-resistance to RAL [317, 337, 344]. Both the 148 and 155 resistance pathways cause a high fold change for EVG [311, 323, 337, 345]. Mutations at position 143 do not affect the susceptibility of EVG [339], but EVG is associated with additional primary mutations at position 66 in conjunction with mutations that select for high resistance (fold changes >150) (Table 2). Additionally, the RAL secondary mutation E92Q is a primary resistance mutation for EVG [317, 346]. In 10 patients, treated with EVG over 2 weeks, primary resistance mutations selected were T66A/K, E92Q, Q148R, and N155H [323]. After 48 weeks of treatment, there was more resistance mutational diversity in the EVG-treated patients, with the most common double DRM combinations being G140CS/Q148H/K/R, E138AK/Q148H/K/R, S147G/Q148H/K/R, and E92Q/N155H, with a triple DRM combination



E138K/S147G/Q148R being present in three patients. Despite having sequenced multiple clones at multiple time-points in the EVG-treated patients, primary DRMs were not detected at baseline. Moreover, the DRMs E138AK, G140C/S, and S147G were never identified alone and combinations of N155H/S together with S147G or G140C/S were not seen. In the RAL-treated arm, the most common combinations identified were G140S/Q148H, sometimes in conjunction with E138A or Y143C [323].

**Table 1.3: Alternative resistance pathways for current INSTIs expressed in fold change (FC) susceptibility relative to wild-type viruses [336].**

Resistance pathways	Fold resistance		
	RAL	EVG	DTG
<b>T66 pathway</b>			
T66I	<2	<10	<2
T66A	<2	<10	<2
T66K	<10	<100	<50
T66I/L74M	<10	<50	<2
T66K/L74M	<50	>100	<10
T66I/R263K	<2	>100	ND
R263K	<10	<10	<50
<b>E92Q pathway</b>			
E92Q	<10	<50	<10
E92Q/S147G	<10	>100	ND
S147G	<2	<10	ND
<b>G118R pathway</b>			
G118R	<10	<2	<10

G118R/E138K	<10	<2	<10
L74M/G118R	<50	<10	ND
E138K	<10	<10	<10
<b>S153 mutations</b>			
S153F	<2	<10	<2
S153Y	<2	<10	<10

### 1.2.3.3 Second generation integrase inhibitors

#### 1.2.3.3.1 MK-2048

The discovery of a low-to-moderate genetic barrier of resistance with first generation INIs led to efforts to produce second generation INSTIs with activity against RAL-resistant viruses. Optimization of tricyclic 10-hydroxy-7,8-dihydropyrazinopyrrolopyrazine-1,9-dione compounds led to the development of MK-2048 [347] (Table 1.4), which demonstrates a  $EC_{95} < 50$  nM when assayed in 50% human serum and possesses a favorable pharmacokinetic profile in dogs and rats [348]. MK-2048 was subsequently shown in tissue culture and biochemical assays to be effective against RAL- and EVG- resistant viruses [347-351], with only slightly diminished effectiveness against viruses containing at least two of the following mutations: E138K, G140S and Q148R [347-351]. Selection studies in culture with MK-2048 did not select for previously recognized mutations but instead selected a novel substitution at position G118R that, in concert with E138K, conferred approximately eight-fold resistance to MK-2048 [352]. Despite its favorable resistance profile, MK-2048 has a poor pharmacokinetic profile and

its clinical development has been arrested. However, it has potential as a candidate microbicide for prevention of HIV infection [353]. It continues to be studied as a prototype second generation INI and has also recently shown effectiveness in the treatment of human T-lymphotropic virus type 1 in culture without causing significant toxicity in target cells [354].

#### 1.2.3.3.2 Dolutegravir

Dolutegravir (DTG) (S/GSK 1349572) has recently been approved for clinical use under the trade name Tivicay® [355] and as part of a triply formulated once daily pill Triumeq® [356]. It was discovered at Shionogi Pharmaceuticals in Japan and developed by a Shionogi-ViiV Healthcare-GlaxoSmithKline joint venture [357, 358]. DTG is a promising HIV INI candidate that specifically inhibits the strand transfer reaction with recombinant purified integrase [358]. Inhibition of the integrase strand transfer reaction by DTG has been confirmed in studies with live virus, which demonstrated an accumulation of 2-long terminal repeat (2-LTR) circles in treated cells at DTG concentrations <1,000-fold of those that caused cell toxicity [104, 359]. DTG also demonstrated efficacy against most viral clones resistant to RAL and EVG and against clinical isolates of HIV-1 and HIV-2, although some viruses containing E138K, G140S or R148H mutations possessed diminished susceptibility to DTG [321, 358, 360, 361]. Double mutants containing combinations of E138K, G140S and R148H had a FC >10 for

DTG, but this was favorable when compared to EVG and RAL, which yielded a FC of >330 and >140, respectively. *In vitro* combination antiviral studies showed that DTG did not increase toxicity when used in combination, but had a synergistic effect with each of EFV, nevirapine, stavudine, abacavir, LPV, amprenavir and enfuvirtide as well as an additive effect in combination with maraviroc. The hepatitis B virus drug adefovir and the hepatitis C virus drug ribavirin had no effect on the efficacy of DTG [361], allowing for its potential use in treating co-infections.

The pharmacokinetic profile of DTG allows once-daily dosing without pharmacokinetic boosting. This is based on a long unboosted half-life (13 to 15 hours) with trough levels of DTG being much higher than the *in vitro* IC<sub>90</sub> [362]. The side-effects of DTG in volunteers with HIV infection were similar to those of placebo in phase I clinical trials [362].

Phase IIa randomized double blind trials provided vital evidence of the anti-HIV effect and potency of DTG [363, 364]. Notably, 35 ARV-experienced INI-naïve patients, who were not receiving therapy, and whose plasma HIV-1 RNA levels ranged from 3.85 to 5.54 log copies/mL, received once-daily doses of 2 mg, 10 mg or 50 mg DTG or placebo for 10 days. More than 90% of patients who received DTG, irrespective of dose, had a decline in viral load to <400 copies/mL while 70% of patients in the 50 mg arm achieved undetectable viremia. In

contrast, the placebo group showed an average increase in viremia. No serious adverse effects were reported in this trial, with headaches and pharyngolaryngeal pain being the most commonly reported consequence [363].

In the SPRING-1 double blind dose-ranging phase II trials, 205 ARV-naïve patients with HIV, with CD4<sup>+</sup> cells >200 cells/mm<sup>3</sup> and HIV-1 RNA >1,000 copies/mL, were treated once daily with DTG (n = 155) at 10 mg, 25 mg or 50 mg doses or 600 mg EFV (n = 50) combined with background therapy of TDF/FTC or ABC/3TC [365]. More than 90% of all participants in the DTG arm had undetectable viremia after 24 weeks of treatment, establishing the non-inferiority of DTG to EFV in an NRTI background and also showing that DTG was at least as safe as EFV.

No primary INI resistance mutations have yet been reported for DTG either in culture or in the clinic (in treatment naive patients) [154, 366]. Tissue culture selection studies over 112 weeks identified, in order of appearance, viruses harboring T124S/S153F, T124A/S153Y, L101I/T124A/S153F and S153Y by week 84. Although these mutations persisted throughout serial passaging, they did not confer high-level resistance to DTG [361]. Position 124 of IN is modestly polymorphic and S153F/Y had previously been described in EVG selection studies [345]. Despite an apparently high genetic barrier for resistance, selection,

recent tissue culture and biochemical studies report that a R263K mutation in IN may confer modest resistance to DTG [367].

It has been suggested that DTG enjoys a high barrier for resistance due to a tighter binding of DTG to IN compared to RAL and EVG [368]. Assays also showed that DTG exhibited tighter binding and had a longer dissociative half-life from IN than either RAL or EVG [369].

In this model, a direct relationship existed between the half-life of binding and the inhibitory potential of INIs when the binding half-life ( $t_{1/2}$ ) was below 4 hours. A >3 FC in regard to drug resistance, relative to the wild-type, was observed when the  $t_{1/2}$  dropped below 1 hour [368]. In assays with wild-type enzymes, the  $t_{1/2}$  of DTG, RAL and EVG were 71, 8.8 and 2.7 hours, respectively. The fact that RAL and EVG have a shorter  $t_{1/2}$  than DTG suggests that resistance mutations that affect binding of RAL and EVG might also be more likely to compromise antiviral potency. As an example, the Y143C/H/R mutations have been shown to compromise interactions between IN and RAL but not those between IN and DTG or between IN and EVG [370]. This is further supported by data on mutations that have been shown to significantly reduce  $t_{1/2}$ , E92Q/N155H, E138K/Q148R and G140S/Q148R, and significantly reduce antiviral potency [368]. This hypothesis had been previously suggested for MK-2048, which also

has a relatively high barrier for resistance, as it also has a slower off-rate ( $t_{1/2} = 32$  hours) for IN compared to RAL ( $t_{1/2} \geq 7.3$  hours) [369].

The use of DTG in INI-salvage therapy is being investigated in an ongoing study called VIKING. The latter is a phase II single arm study investigating the feasibility of replacing RAL with DTG in patients experiencing failure due to RAL-resistant viruses [357]. Participants ( $n = 27$ ) were switched from their previous RAL-containing regimens to receive DTG 50 mg once daily for 10 days and were then prescribed other active drugs over a period of 23 weeks. Eighteen of the study participants had INI-resistant viruses belonging to the Y143, Q148 and N155 pathways prior to initiation of the study. After 10 days of DTG monotherapy, all participants harboring viruses in the Y143 and N155 pathways attained a mean HIV-1 RNA decrease of approximately 1.8 log copies/mL compared with approximately 0.7 log copies/mL for viruses harboring G140S/Q148HRK double mutations. None of the viruses harboring Q148HRK plus two or more additional mutations experienced a decrease of  $\geq 0.7$  log copies/mL, indicating a degree of resistance on the part of Q148HRK viruses to DTG. This trial nonetheless provided proof-of-principle for the use of DTG in RAL-experienced patients infected by subtype-B viruses harboring position Y143 and N155 mutations.

In order to model the effects of DTG in RAL-experienced patients, several serial passaging studies have been carried out and shown that the presence of the N155H and Y143C/H/R resistance did not lead to development of additional resistance mutations under DTG pressure nor to a substantial decrease in DTG susceptibility [62,64]. In contrast, the presence of Q148HRK mutations did lead to further mutations and >100 FC for DTG susceptibility relative to wild-type in subtype B viruses [321, 361]. Interestingly, Q148HRK mutations did not affect susceptibility to DTG in HIV-1 subtype C and HIV-2 isolates [361, 371, 372]. The ongoing trial termed SPRING-2 is evaluating the use of once-daily DTG versus twice-daily RAL in treatment-naïve patients. Recent week 48 reports of SPRING 2 [154] and week 24 data of the VIKING 2 [373] and VIKING 3 [163] all trend to a superiority of DTG over all other previously studied anti-HIV drugs to date, those the appropriate superiority trials need to be carried out to validate that.

#### 1.2.3.3.3 S/GSK-1265744

Another second generation INSTI called S/GSK-1265744 (Table 1.4), which was originally a back-up drug to DTG, was tested in double blind randomized placebo-controlled trials and showed promising efficacy, an excellent pharmacokinetic profile and good tolerability in patients with HIV [374]. This INSTI, which only differs marginally from dolutegravir has exceptional long term residency and it has recently shown promise as a long-acting integrase inhibitor



[375]. Recent studies in macaques have shown an ability of S/GSK-1265744 to protect macaques from infection by an engineered simian-trophic HIV (sHIV) [375]. None of the macaques intramuscularly inoculated with S/GSK-1265744 developed SHIV infection 8 weeks post inoculation even after repeated SHIV exposures [375]. This has appeal for pre-exposure prophylaxis but has even more potential as a monthly/quarterly dosed regimen for HIV infection. The main challenge for dosing of S/GSK-1265744 would be to find similarly long acting compounds for combination therapy.

#### **1.2.4 Advances aiding integrase inhibitor discovery**

##### **1.2.4.1 Crystallization of full-length integrase**

Due to the low solubility of HIV-1 IN [376, 377], elucidation of the full-length IN structure has never been accomplished. The first IN partial-structure was published in 1994 [378]; however, despite the insights afforded by this and subsequent structures, including the first partial IN structure complexed with an inhibitor [280], none of these structures gave a proper depiction of inhibitor drug interactions, IN-DNA interactions or functional IN quaternary structures. Co-crystal structures of integrase from the lentivirus Maedi-Visna with human LEDGF [379] suggested that the functional IN protein might be tetrameric, consisting of a dimer of dimers, and this further showed the necessity of obtaining full-length crystal structure for proper elucidation of IN structure,

function and inhibition. In 2010, the full-length structures of IN from the prototype foamy virus (PFV) in complex with LTR mimetics were published [380]. This paper provided the first glimpse into interactions between IN and viral DNA and also established the binding mode of the INSTIs RAL (Figure 1.13A) and EVG (Figure 1.13B). A follow-up publication [381] provided excellent structural explanations for the impact of mutations at positions 92, 140, 148 and 155 on RAL and EVG susceptibility. Thus, despite the fact that PFV is a spumavirus, only having significant sequence identity with HIV-1 IN in the catalytic core domain (CCD) domain, PFV IN structures could guide construction of reliable homology models of HIV-1 IN with accurate prediction of interactions between IN and INSTI [382]. Later crystallization efforts by the same group yielded IN-DNA strand transfer complexes in the presence and absence of inhibitors [245], again providing new structural data, a better understanding of the strand transfer process and information on new INI discovery initiatives. Co-crystallization studies have attributed the observed efficacy of DTG (Figure 1.13C) against RAL- and EVG-resistant viruses to the flexibility of DTG and its ability to bind to IN, even in the presence of major INI resistance mutations [370]. It remains to be seen whether PFV structures can aid in the elucidation of non-catalytic site INIs, given major differences that may exist distal from the IN active site. For instance,

PFV integrase does not interact with LEDGF [383]; as such, models based on PFV may not be able to help in the design of IN-LEDGF inhibitors.

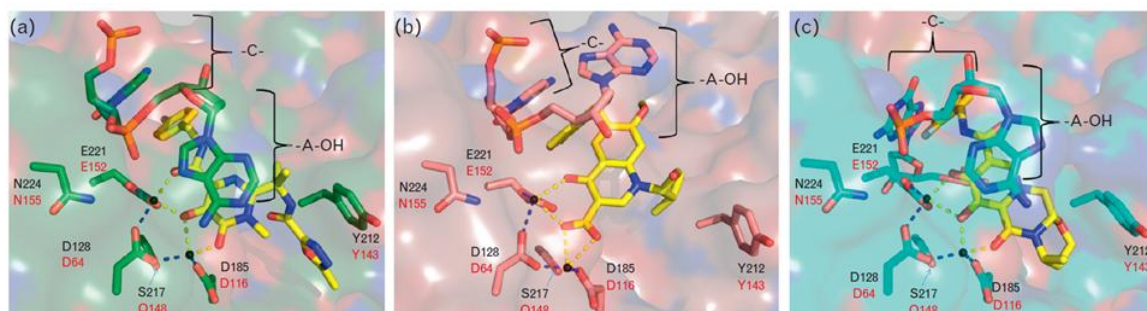


**Figure 1.13: Prototype foamy virus (PFV) IN active site showing bound RAL (a), EVG (b), and DTG (c) [336].**

#### 1.2.4.2 Quantitative structure-property and -activity relationships

The recent elucidation of the full-length PFV intasome and strand transfer complexes have allowed for the generation of homology models of HIV-IN that can be used to ‘train’ and score drug prototypes. There are multiple quantitative structure-property relationships (QSPR) and quantitative structure-activity relationships (QSAR) protocols and programs. Some of these require advanced programming and mathematical skills, but several stand-alone and online programs offer semi-automated drug docking and scoring capabilities with moderate to high accuracy. The main aim of these approaches is to allow *in silico* validation and testing of prototype molecules in order to lower the costs associated with large-scale synthesis of non-validated compounds [384]. Typical QSPR and QSAR protocols use a given set of conditions that train and/or test the

structures and a set of validity parameters that are then used to score the data. Structures can then be selected for subsequent synthesis and experimental validation [385]. Typical input takes into account the physicochemical properties of individual moieties on the compound, bond-length, flexibility, lipophilicity and/or hydrophilicity, information on the target and three-dimensional binding space. This can generate theoretical estimations of  $IC_{50}$ , binding affinity, bioavailability, hepatic clearance and other parameters. Recent work has used a molecular dynamics approach to accurately predict potency of INSTIs based on models derived from the PFV structure [386]. A summary of computer-based approaches for design of novel INIs that target 3' processing, IN multimerization, strand transfer complex assembly and IN-host protein interactions has recently been published [387]. Despite these advances, it is difficult to accurately model drug toxicity, bioavailability and safety prior to the synthesis and study of novel compounds.

### **1.2.5 Next-generation strand transfer inhibitors in preclinical development**

#### **1.2.5.1 MK-0536**

The design of MK-0536 by Merck & Co., Inc. was based on QSPR and QSAR that took into account the optimum minimum structure necessary for activity and generated a set of potential structures that could be synthesized and screened. MK-0536 has shown low hepatocyte clearance values [388] and generally good

inhibition of wild-type IN and RAL-resistant IN [388, 389] but its current level of clinical development is unclear. Other classes of compounds that block strand transfer with high specificity at sub-nanomolar  $EC_{50}$ s and low toxicities are catechol-based [390], pyrimidone-based [391-394], dihydroxypyrido-pyrazine-1,6-diones [395] and quinolones [396, 397].

#### **1.2.5.2 LEDGINS and BI 224436**

LEDGINS were designed as specific small molecular inhibitors of the LEDGF/p75 interaction. 2-(quinolin-3-yl) acetic acid derivatives have been co-crystallized with LEDGF/p75-IN and optimized structures within this group were shown to inhibit the LEDGF/p75-IN interaction at sub  $\mu$ M concentrations [256, 258]. Peptides mimicking the IN-binding domain (IBD) of LEDGF/p75 exhibit potent inhibition of IN [398, 399].

The compound BI224436 is a novel INI [400] with a distinct mode of action from more established INSTIs. It is a non-catalytic site integrase inhibitor (NCINI) (Table 1.4) which interferes with the interaction between IN and the chromatin targeting the LEDGF/p75 protein, yielding low nM inhibition of 3' processing and viruses [400, 401]. The profile of this compound appears favorable and it also appears to be specific since it did not exhibit reduced activity against any INSTI-resistant IN enzymes [400, 401]. This compound has now entered phase Ia clinical trials to evaluate dosing and safety in healthy individuals. Initial reports

indicate high bioavailability with good tolerability at single doses ranging up to 200 mg.

**Table 1.4: Clinically relevant INI compound structures**

Drug candidate	Chemical structure	Activity Targeted	Phase of development
RAL	<p>The structure shows a central pyrimidopyrimidine core with a hydroxyl group at the 2-position and a methyl group at the 4-position. It is substituted with a (4-fluorophenyl)methylamino group at the 6-position and a (1-methyl-1H-tetrazol-5-yl)methylamino group at the 8-position.</p>	Strand Transfer	Approved by FDA in 2007
EVG	<p>The structure features a central pyrimidopyrimidine core with a hydroxyl group at the 2-position and a methyl group at the 4-position. It is substituted with a (4-chloro-2-fluorophenyl)methylamino group at the 6-position and a (1-hydroxyethyl)amino group at the 8-position.</p>	Strand Transfer	Approved by FDA in 2012
DTG	<p>The structure shows a central pyrimidopyrimidine core with a hydroxyl group at the 2-position and a methyl group at the 4-position. It is substituted with a (2,4-difluorophenyl)methylamino group at the 6-position and a (1-methyl-2,3-dihydro-1H-benzoxepin-4-yl)methylamino group at the 8-position.</p>	Strand Transfer	Approved by FDA in 2013
MK-2048	<p>The structure features a central pyrimidopyrimidine core with a hydroxyl group at the 2-position and a methyl group at the 4-position. It is substituted with a (2-chloro-4-fluorophenyl)methylamino group at the 6-position and a (1-ethyl-2-methyl-2,3-dihydro-1H-benzoxepin-4-yl)methylamino group at the 8-position.</p>	Strand Transfer	Phase 2b/ PREP microbicide
S/GSK-1265744	<p>The structure shows a central pyrimidopyrimidine core with a hydroxyl group at the 2-position and a methyl group at the 4-position. It is substituted with a (2,4-difluorophenyl)methylamino group at the 6-position and a (1-methyl-2,3-dihydro-1H-benzoxepin-4-yl)methylamino group at the 8-position.</p>	Strand Transfer	Phase IIb/ PrEP
BI 224436	<p>The structure features a central pyrimidopyrimidine core with a hydroxyl group at the 2-position and a methyl group at the 4-position. It is substituted with a (2-phenylphenyl)methylamino group at the 6-position and a (1-methyl-2,3-dihydro-1H-benzoxepin-4-yl)methylamino group at the 8-position.</p>	3' Processing	Phase Ia

BI 224436 also exhibited good pharmacokinetics when given as a single-dose of 100 mg, and plasma levels appeared adequate to achieve benefit [400].

Recent reports show that the impact of BI 224436, LEDGINS and related compounds, in addition to inhibiting the catalytic activities of integrase, more importantly promote multimerization and aggregation of integrase both *in vitro* and *in vivo* [402, 403]. The *in vivo* aggregation of integrase leads to a block in a post-integration stage of viral replication, possibly maturation [402, 403]. These findings further highlight the importance of integrase in the viral life cycle though additional roles have not yet been fully elucidated for integrase.

#### **1.2.5.3 Dual acting RT/IN inhibitors**

Structural and functional similarities between HIV-1 IN and the RNAse-H domain of HIV-1 RT suggest the possibility of specific yet dual targeting inhibitors of both enzymes. Several early compounds that have been found to target both enzymes are diketo acids (DKA) [404, 405].

#### **1.2.6 HIV diversity and integrase inhibitors**

Recent reports indicate that subtype differences may exist with regard to the development of resistance to IN inhibitors, a phenomenon that also exists with RT inhibitors [305, 406, 407]. Despite the fact that HIV-1 subtype B and C wild-type IN enzymes are similarly susceptible to clinically validated INIs [359], the presence of resistance mutations may differentially affect susceptibility to specific

INSTIs [305]. Recent reports suggest that the G118R mutation, which was previously reported to confer slight resistance to MK-2048, imparts a 25-fold resistance to RAL when present together with the polymorphic mutation L74M in CRF-AG cloned patient isolates [408]. Additionally, it is well documented that the INI Y143C/H/R resistance mutations, which affect susceptibility to DTG in HIV-1 subtype B, may not affect the susceptibility of either HIV-1 subtype C or HIV-2 enzymes to DTG [368].

### **1.3 Conclusions**

The development of integrase inhibitors has resulted in a new drug class in the anti-HIV armamentarium with the clinical licensure of three different INSTI compounds. The continued clinical development of non-INSTI integrase inhibitors remains promising. Integrase inhibitors have the potential to be the most significant development in HIV therapy since the advent of HAART. The high potency and improved resistance profiles of clinically relevant second generation INSTIs such as MK-2048, dolutegravir and S/GSK-1265744 makes the study of inhibition and resistance to second generation INSTIs highly desirable and clinically important. It is also important to investigate the impact of HIV subtype on resistance development and resistance pathways.



#### 1.4 Rationale for this thesis

As the first clinically approved INSTI, RAL has been shown to have a low genetic barrier to development of resistance, and many RAL-resistant mutants show cross-resistance to EVG [311]. Both of these drugs have shown subtype-specific variation in their resistance profiles [305]. The second generation INSTIs, DTG and MK-2048, have been shown to inhibit strand transfer, as with RAL/ EVG, with a significantly higher genetic cost for resistance emergence [352, 409]. Our lab previously selected in HIV sub-type C the resistance substitution G118R in combination with E138K in culture using the integrase strand transfer inhibitor (INSTI) MK-2048, despite that G118R was never selected by either RAL or EVG [305]. The integrase (IN) mutation G118R was subsequently reported in a patient harboring CRF02-AG HIV-1 virus and conferred resistance to RAL [410]. The substitutions G118C/A/R had previously been observed in cell culture with non-B HIV, causing resistance to the experimental INSTI S-1360 [411]. These developments have hinted at differences in resistance mutation acquisition between first generation and second generation INSTIs and have also indicated that HIV subtype may be an important factor in the level of resistance imparted by a specific mutation.

## **1.5 Objectives of this thesis**

This purpose of this thesis was to investigate the inhibitory mechanism(s) of second generation INSTIs, exemplified by DTG and MK-2048, their possible resistance pathways and the impact of subtype on INSTI potency and resistance. All resistance substitutions identified were checked for cross-resistance with the first generation drugs. Cell culture techniques, biochemical analysis and *in silico* bioinformatics' methods were used in the execution of this study.

### **1.5.1 Specific Objective 1**

To develop, based on the published prototype foamy virus structures and partial HIV structures, homology models of full-length HIV integrase to aid in drug discovery and analysis of the structural impact of drug resistance substitutions. This portion of the thesis has been published, is presented in Chapter 2, and its application is evident in the latter chapters.

### **1.5.2 Specific Objective 2**

We wished to identify amino acid substitutions that lead to DTG resistance development, and evaluate their cross-resistance with other INSTIs and their impact on integrase protein structure and activity as well as viral replication and infectivity. This portion of the thesis is presented in Chapter 3 which is the synthesis of two separate published manuscripts. A third manuscript related to

this objective but not presented in this thesis has recently been accepted for publication.

#### **1.5.4 Specific Objective 3**

To investigate reasons for the lack of acquisition of the G118R drug resistance substitution in subtype B in drug selection studies. This portion of the thesis has been published and is presented in Chapter 4.

#### **1.5.5 Specific Objective 4**

Evaluation of the impact of the resistance associated substitution G118R in subtype C and CRF02\_AG HIV integrase proteins and/or viruses. This portion of the thesis has been published and is presented in Chapter 5.

## Chapter 2

### Structural modeling of HIV-1 integrase proteins and screening of potential integrase inhibitors

A majority of the work presented in this chapter will be submitted for publication as follows:

Quashie PK\*, Han Y\*, Hassounah S, Mesplède T and Wainberg MA. Structural studies of the HIV-1 CRF02\_AG integrase protein: **Compound screening and characterization of a DNA-binding inhibitor.** *PLoS One.* 2015 Jun 5;10(6):e0128310. doi: 10.1371/journal.pone.0128310. eCollection 2015.

PKQ and YH contributed equally to this manuscript. PKQ designed the study, performed most of the modeling and simulations, and wrote the manuscript. SH performed some *in silico* simulations. YH designed and performed biochemistry and cell culture experiments. All authors contributed to study design and manuscript preparation.

## 2.1 Abstract

Understanding the HIV integrase protein and mechanisms of resistance to HIV integrase inhibitors is complicated by the lack of a full length HIV integrase crystal structure. Moreover, a lentiviral integrase structure with co-crystallised DNA has not been described. For these reasons, we have developed a structural method that utilizes free software to create quaternary HIV integrase homology models, based partially on available full-length prototype foamy virus integrase structures as well as several structures of truncated HIV integrase. We have tested the utility of these models in screening of small anti-integrase compounds using randomly selected molecules from the ZINC database as well as a well characterized IN:DNA binding inhibitor, FZ41, and a putative IN:DNA binding inhibitor, HDS1. Docking studies showed that the ZINC compounds that had the best binding energies bound at the IN:IN dimer interface and that the FZ41 and HDS1 compounds docked at approximately the same location in integrase, ie behind the DNA binding domain, although there is some overlap with the IN:IN dimer interface to which the ZINC compounds bind. Thus, we have revealed two possible locations in integrase that could potentially be targeted by allosteric integrase inhibitors, that are distinct from the binding sites of other allosteric molecules such as LEDGF inhibitors. Virological and biochemical studies confirmed that HDS1 and FZ41 share a similar activity profile and that both can

inhibit each of integrase and reverse transcriptase activities. The inhibitory mechanism of HDS1 for HIV integrase seems to be at the DNA binding step and not at either of the strand transfer or 3' processing steps of the integrase reaction. Furthermore, HDS1 does not directly interact with DNA. The modeling and docking methodology described here will be useful for future screening of integrase inhibitors as well as for the generation of models for the study of integrase drug resistance.

## 2.2 Introduction

HIV-1 integrase (IN) is a multi-domain protein that is activated after cleavage from the HIV Gag-Pol poly-protein by HIV protease during viral maturation. HIV IN has three well characterised domains (Figure 2.1A); an N-terminal dimerization domain (NTD) that has a conserved HCCH Zn<sup>2+</sup>-binding motif, a central RNase H-like catalytic core domain (CCD), and a C-terminal domain (CTD) that plays a role in IN DNA binding [377, 378, 412]. Each of these domains has been purified, crystallised and characterized, either individually, in complex with other proteins, or as double-domain partial structures [377, 378, 412, 413].

However, crystallization of the full-length HIV-1 IN structure has been elusive and none of the HIV-1 double-domain partial structures has been crystallized together with DNA. Due to high structural flexibility of IN, the available partial crystal structures are unreliable predictors of HIV-IN inter-monomer interactions and IN-DNA interactions [414]. The coordination of divalent  $Mg^{2+}/Mn^{2+}$  ions by the  $D_{64}D_{116}E_{152}$  residues is critical for IN activity [105] and this has led to the development of the cation-chelating diketoacid derivative compounds [276, 289] that are currently used as IN strand transfer inhibitors (INSTIs), such as raltegravir (RAL) [211] and elvitegravir (EVG) [415]. Additional structural knowledge was gained through the elucidation of drug resistance mutations for RAL and EVG in tissue culture [337, 341] and clinical trials [311]. However, it was really the successful crystallization of the prototype foamy virus (PFV) IN protein [245, 370, 380, 416] that provided an understanding of the correct binding mode of INSTIs and resistance to them.

Unlike crystal structures, homology models are not usually deposited into online servers for universal use so different groups have had to generate their own model(s) [382, 383, 417] and validate them, often using molecular dynamics approaches which are beyond the computing abilities of most research groups. Therefore, we have developed a protocol for generation of situation-specific HIV IN models for compound screening or investigation of drug resistance substitutions using free online modeling servers and free software. We have previously used this methodology to model IN proteins of HIV-1 subtype B [177, 418-420], subtype C, and circulation recombinant form number 2 AG (CRF02\_AG).

Here, HIV-1 circulating recombinant form number 2 A/G (CRF02\_AG) IN was modeled and used to screen for possible inhibitors of IN dimerization or DNA binding.

## **2.2 Materials and Methods**

### **2.2.1 Generation of the monomeric IN model**



Due to the incomplete nature of HIV-1 structures in the PDB, the generation of the initial HIV monomer had to be done by multiple template modeling (MTM) [421]. The sequence of CRF02\_AG IN was submitted to three servers for sequence alignment and homology modeling, HHpred [422], PHYRE2 [423] and I-TASSER [424]. HHpred (hidden homology prediction) is a free online server from the Max-Planck Institute for Biotechnology (<http://toolkit.tuebingen.mpg.de/HHpred>). It uses comparative hidden Markov statistical models (HMM) [425] to assess amino acid sequence homology and predict protein structure [426] by scanning the query sequence against protein sequence alignment databases such as Pfam (Protein family) [427] and SMART (Simple Modular Architecture Research Tool) [428, 429] (Supplementary file 1 - S1). PHYRE2 (Protein Homology/analogy Recognition Engine v2.0) is an online server developed and maintained by the structural bioinformatics group at Imperial College, London (<http://www.sbg.bio.ic.ac.uk/phyre2/html/page.cgi?id=index>) [423]. PHYRE2 identifies the structural folding patterns of a query protein by scanning it against a library of known protein structures from the Structural Classification of Proteins Database (SCOP) [430] and the Protein Data Bank (PDB) [431]. I-TASSER (Iterative Threading ASSEmbly Refinement) is an advanced protein homology algorithm which is available as an online server through the ZhangLab server at

the University of Michigan (<http://zhanglab.ccmb.med.umich.edu/I-TASSER/>) [424, 432, 433]. I-TASSER uses multiple individual programs and steps as well as molecular dynamics to create protein structural models of a submitted protein sequence [432]. I-TASSER has been consistently ranked as the best server for online protein structure prediction in the last five competitions of the community-wide experiment Critical Assessment of techniques for protein Structural Prediction (CASP7-CASP11) [433]. CASP rankings are considered the most important metric of method/program confidence in structural biology.

Homology models were created using HHpred by three methods. For model 1, fully automated use of HHpred was used to select templates and construct a structure using MODELLER [434]. In model 2, the HIV-1 template 1EX4 [435] and the PFV template 3OY9 [380] were chosen as templates for modeling by MODELLER. For model 3, the alignment between CRF02\_A/G and 3OY9 was used to drive the modeling. PHYRE2 was used in intensive mode and two additional models were thereby derived, i.e. a consensus model (model 5) as well as model 5 that was built by direct alignment with the PFV crystal structure 3OY9 (14). Finally for I-TASSER, the 3OY9 hybrid was used as a lead template to create a final test model (Model 6).

### **2.2.2 Verification of model quality and creation of model 7**

Main-chain atoms of the models created by the three methods were structurally evaluated using Verify3D [436] and ANOLEA [437]. Briefly, Verify3D compares a three dimensional structure against its own sequence and scores the likelihood of each residue being in its structural class (helix, fold, turn, beta strand, loop, etc), based on the intrinsic properties of that particular amino acid. Good structures have very high scores and improbable structures have low scores [438]. ANOLEA (Atomic Non-Local Environment Assessment), measures the energy for each heavy atom in the structure and performs a pair-wise comparison to the energy of the same heavy atom when present in a non-local environment [439]. Ramachandran analysis was performed using the RAMPAGE server (<http://mordred.bioc.cam.ac.uk/~rapper/rampage.php>). Ramachandran plots analyse the stereochemistry of amino acid side-chains around a peptide bond and each amino acid side-chain is scored based on angular orientation around the PSI ( $\Psi$  -torsion angle of  $\beta$ -carbon and main-chain nitrogen around the  $\alpha$ -carbon) and PHI ( $\Phi$ - torsion angle between  $\beta$ -carbon and main-chain carbonyl carbon) [440]. Since there are a limited number of favourable orientations that can occur for each amino acid, structures can be assessed quickly [440].

When necessary, sequence alignments were edited in an effort to increase the accuracy of modeling. The individual monomers were also aligned with the template structures to verify their structural deviation from the original templates

as well as their similarity to the PFV template. One final model was used as a lead template for subsequent models. The ProtMod server (<http://ffas.burnham.org/protmod-cgi/protModHome.pl>) was used to minimize stochastic error between individual models and remove any sampling errors that may have been introduced by the multi-template modeling method [421] of I-TASSER. Where necessary, side-chain orientations were optimized [441]. Briefly, single template: query (WT: WT/variant) alignments were performed using the alignment program SCWRL [442]. The program MODELLER [434] was then used to create monomeric homology models of each IN based on the SCWRL sequence alignment and the WT I-TASSER structure. Model quality was assessed by Ramachandran analysis and based on root mean square deviation (RMSD) of the global homology structure from the PFV lead template using the RCSB PDB Protein Comparison Tool [443]

### **2.2.3 Creation of a dimeric IN model**

A dimeric model of CRF02\_A/G IN was created by aligning a second monomer to the B chain of The PFV structure PDB ID: 3OY9. All non-aligned residues were deleted to yield only a partially resolved outer monomer as observed in PFV IN dimeric and tetrameric structures [380, 382].  $Mn^{2+}$  and  $Zn^{2+}$  ions from PFV were

retained in the dimeric structure of the CRF02\_A/G IN to aid in docking if needed.

PyMOL [444] was used for most protein visualizations.

#### **2.2.4 Compound library docking**

Thirty randomly selected compounds from the ZINC database were screened as possible IN inhibitors [445] primarily targeting IN:DNA binding and IN:IN dimerization interfaces. The preparation of receptor and ligand residues as well as docking simulations were performed using the PyRx [446] implementation of AUTODOCK Vina [447]. The top 5 hits based on calculated binding energies were further analyzed based on their binding interface, strength and similarity to published INIs for potential future biochemical validation. Docking was also performed using the well characterized IN DNA binding inhibitor, FZ41 (CID 5481653) and a putative IN DNA binding inhibitor, HDS1 (CID 10814237-nigranoic acid). The compound HDS1 was investigated further.

#### **2.2.5 Antiviral activity of HDS1 measured by RT activity and quantitative PCR**

The effect of HDS1 on reverse transcriptase activity present in culture supernatants was measured using a tritiated thymidine triphosphate based assay as previously described [448]. The effect of HDS1 on production of HIV-1 early and late reverse transcripts were measured by qPCR as previously described [449], with RAL and zidovudine (AZT) as comparative controls.

#### **2.2.6 Biochemical evaluation of the impact of HDS1 on IN.**

The inhibitory impact of HDS1 on IN protein was assessed by three discrete reactions; strand transfer, 3' processing and LTR-DNA binding. The Strand transfer assay was performed with fixed enzyme and substrate quantities in the presence of dose-ranging concentrations of HDS1. All assay conditions were as previously described [418]. The 3' processing assay was performed as previously described [450] in the presence of dose ranging concentrations of HDS1. The effect of dose-ranging concentrations of HDS1 on binding of LTR DNA to IN protein was assessed as previously described [451]. To test if HDS1 has intercalative DNA-binding activity, an ethidium bromide (EtBr) displacement assay was carried out as reported previously [452]. Briefly, a solution of EtBr at 1.26  $\mu\text{M}$  was pre-incubated for 10 min at room temperature with a plasmid DNA or target DNA (1  $\mu\text{M}$ ) in a reaction buffer (2 mM HEPES, 10  $\mu\text{M}$  EDTA, 9.4 mM NaCl, pH 7.0). After the incubation, test compound was added into the DNA–EtBr mixture at different concentrations ranging from 0.01–1000  $\mu\text{M}$ . The fluorescence intensity of each mixture was measured (ex. at 544 nm, em. at 590 nm) by a FLUOStar Optima plate reader (BMG Labtech).

## **2.3 Results and discussion**

### **2.3.1 Homology modeling**

In this study, we created several models of HIV IN using available free software and optimised and created a template model of HIV-1 CRF02\_AG IN that could be used for drug screening and/or variant protein modeling.

Models 1-5 were created utilising HHpred (Models 1-3) (S1 - S4 Figs.) and PHYRE2 (Models 4 and 5) (S5 and S6 Figs.). Some of these models are shown in the supplementary material. Models 1-3 did not have good 3-dimensional scores by either Verify3D and or ANOLEA (S1- S3 Figs.). Models 4 and 5 were based primarily on HIV partial structures (Model 4) or PFV structures, respectively (Model 5). These models aligned primarily with the template HIV or PFV IN protein but not vice-versa (S4) and were therefore not further studied, highlighting the importance of selecting the right program for modeling of HIV proteins. The databases and methods used by these two programs differed slightly from I-TASSER which scanned the protein database (PDB) as well as allowed a certain level of user control. HHpred, for example, primarily scans pFam databases, but the classification of IN proteins across species, especially

for PFV IN, is incomplete in most cases and, accordingly, PFV structures were mostly ignored in multiple sequence threading alignments.

The final IN MTM model (model 6) (Figure 2.1B) was created by multi-template threading utilizing the I-TASSER server [453] with the PFV lead template 3OY9.

This allowed not only for the creation of a global model based primarily on the structure of PFV IN, but also allowed the folding of sequence fragments to be driven primarily by the multiple structural fragments of available HIV IN in the PDB, leading to a more representative structure. PFV IN structures are the only full-length IN structures that have bound DNA and are also the only structures that have bound drug. However, HIV structures should not be ignored because HIV IN has only ~20% sequence homology with PFV IN. Model 6, like the PFV template, has a mainly helical CCD domain with a largely disordered CTD domain and an elongated NTD domain. The domain orientation in the models was similar to that of the PFV crystal structure [380] and previously modelled HIV integrase models [382, 417].



Alignment of Model 6 with either of 1EX4 and 3OY9 yielded very good RMSD scores for the aligned regions and the CTD of the model followed a similar trajectory to that of PFV (Figure 2.1B). Verify3D plots indicate that the CCD-CTD portion of model 6 mostly have good 3-D structure with the NTD being poor to fair (Figure 2.1C). This is probably the major reason for an underwhelming score of 60.93, that is nonetheless higher than those of all the previous models studied with the exception of model 4 (89.8). The score of model 4 was even higher than its lead template, 1EX4 (73.02).

Comparing the Ramachandran plots of the two crystal structures 1EX4 and 3OY9 to model 6, it is evident that model 6 and 1EX4 have fewer residues in favored regions, with more in allowed and disallowed regions (84.8, 9.4, 6.3 and 80.8, 14.4, 4.8, respectively) than 3OY9 (96.7, 3.3, 0.0) (S7). Side-chains of residues in disallowed regions have steric clashes with other residues and are not likely in a steady state orientation. This points to more general disorder in HIV-1 IN relative to PFV and also implies that the lower structural confidence

scores for model 6 are due to the HIV templates rather than the PFV templates.

Model 6 was used as a template to create model 7 by single template threading

utilizing the ProtMod server ([http://ffas.burnham.org/protmod-](http://ffas.burnham.org/protmod-cgi/protModHome.pl)

[cgi/protModHome.pl](http://ffas.burnham.org/protmod-cgi/protModHome.pl)). This resulted in a structurally improved model that had

94.7% of peptide bonds in favoured regions, 4.1% in allowed regions and 1.2%

in outlier regions (S7). Monomer B of CRF02\_A/G IN was created as described in

the methodology (Figure 2.1D) and an overlay of dimeric HIV-1 CRF02\_A/G IN

with the PFV structure 3OY9 is shown (Figure 2.1E).

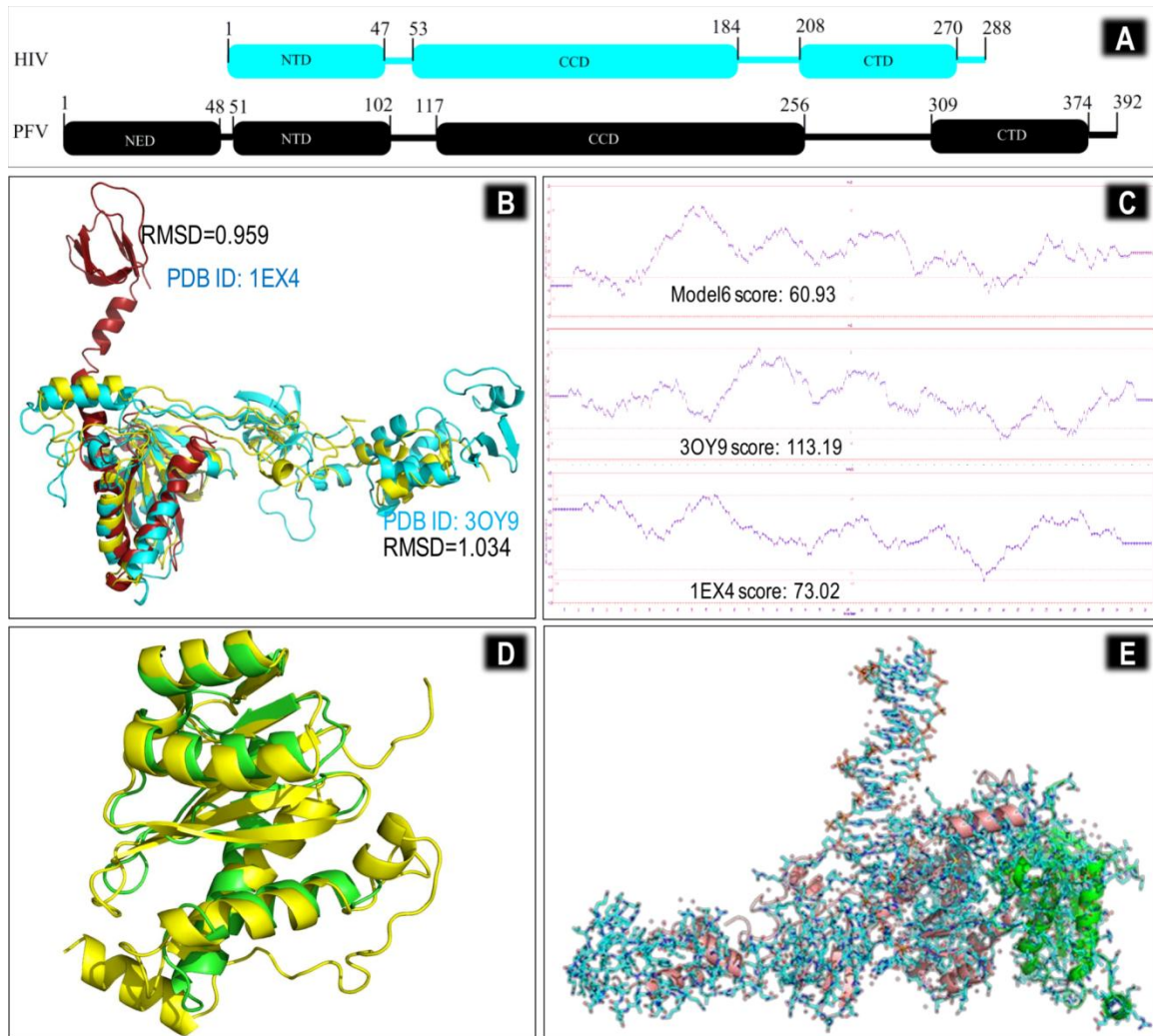


**Figure 2.14: Analysis of model 6 and creation of the dimeric model 7 HIV-1 CRF02\_AG IN structure.** (A) Domain organization of HIV-1 and PFV IN domains showing regions of structural and sequence overlap as well as structural gaps. (B) Structural alignment of modeled chain A (yellow) aligned with templates 3OY9 (cyan) and 1EX4 (dark green); (C) Comparative Verify3D analysis of the two templates with model 6; (D) Modeled Chain B (yellow) is aligned to PFV chain B (light green) and non-overlapping segments have been removed; (E)

Dimeric CRF02\_AG IN structure (pink and green cartoon) overlays well with the dimeric PFV structure (shown as sticks) with a global RMSD  $<1.5\text{\AA}$ . With the exception of carbon atoms, all coloration of the PFV stick structure is based on the Corey-Pauling-Koltun (CPK) coloration scheme [454]; white for hydrogen, blue for nitrogen, and red for oxygen.

### 2.3.2 Docking simulations

Similar to most DNA binding proteins and especially those that have to undergo considerable modification upon substrate binding, IN has large solvent-accessible pockets; hence, there are potential binding pockets for inhibitory compounds. The program PyRx [446] was used for docking simulations with a  $50\text{\AA} \times 50\text{\AA} \times 50\text{\AA}$  grid box that encompassed the active site as well as the DNA binding and dimerization interfaces (Figure 2.2A). Thirty randomly chosen compounds from the ZINC database were utilised as ligands (S8). Compounds that docked near the blue arrow (Figure 2.2B) were considered to bind at the IN-DNA interface while compounds that docked near or around the red arrow were deemed to be dimerization modulators (Figure 2.2B). As has been previously published for PFV [382] and other HIV homology models, a CCD:CCD interaction defines the dimer interface (Figure 2.2C) while bound viral DNA contacts all three domains (Figure 2.2A).

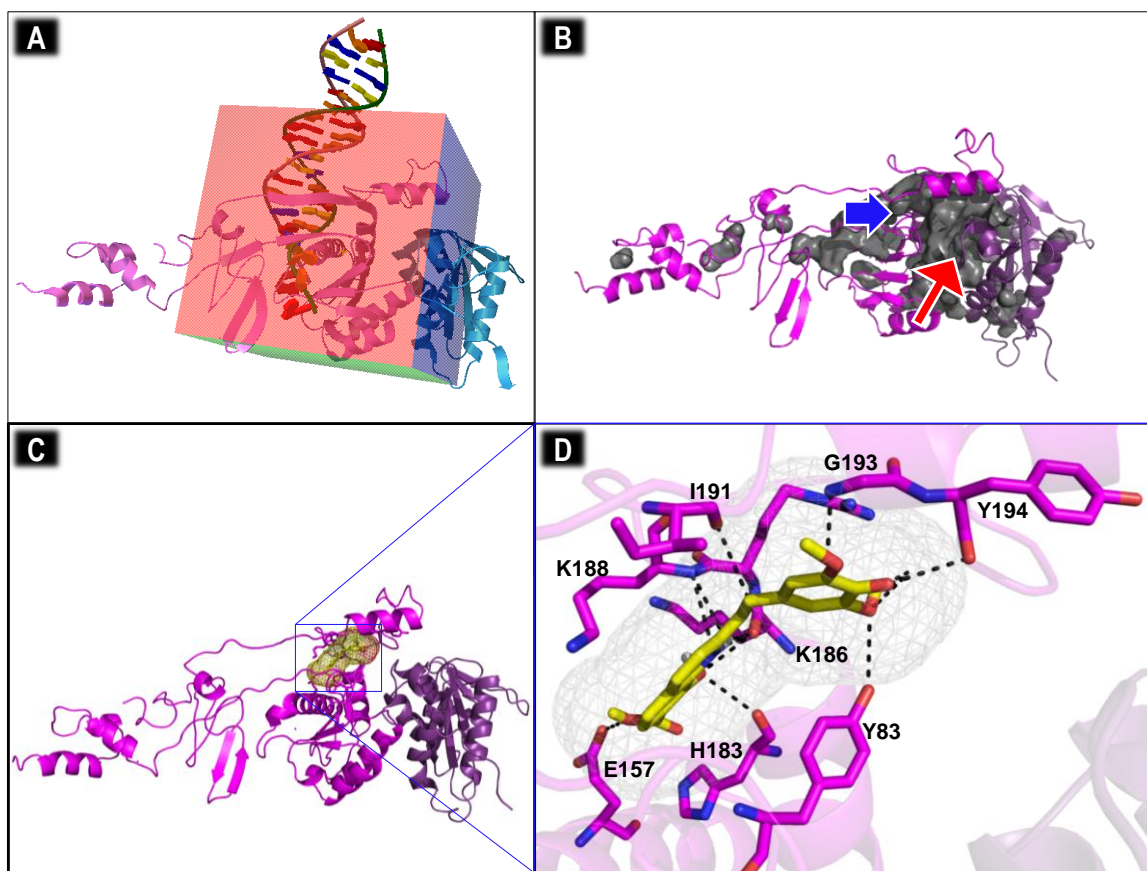


**Figure 2.2: Location of docking grid box and docking of FZ41 to the IN dimer. (A)**

Grid box size and coordinates overlapped with the DNA binding domain as well as the dimerization interface. (B) Pockets within the dimeric model at the DNA interface (blue arrow) and at the dimer interface (red arrow). (C) FZ41 (yellow stick structure within grey mesh) binds within the DNA binding domain. Domains spanning regions corresponding to NTD, CCD, CTD for monomer A and CCD\* for monomer B are indicated. (D) Interactions of FZ41 with IN residues. Docking

simulations were performed utilizing AutoDock Vina [447] on a PyRx platform [446]. All image processing was done using PyMOL [455]. Solvent accessible pockets with a radius larger than 5Å are shown and colored grey. In the figure, the two monomers of the dimer are represented by different shades of magenta. CPK standard coloration is used for stick structural representations. Putative interacting atoms are indicated by a black dashed line.

The ZINC compounds screened and the apparent affinity calculations of the top 100 docked poses are shown in S8. The highest binding energy calculated was -8.4 kcal/mol, calculated for ZINC00337691 (CID 821042). The apparent binding affinity for top poses of FZ41 and HDS-1 were -9.1 kcal/mol and -8.7 kcal/mol, respectively (Figure 2.3), while the apparent affinity for the 100th best docked ZINC compound orientation was -4.5 kcal/mol (S1). The chemical structures of the top five ZINC hits are presented (Figure 2.3).

Published reports of FZ41 implied that this inhibitor acted at a post-RT to early-integration stage of the viral cycle [456]. We recently confirmed that this molecule

inhibited viral replication and integration by decreasing IN binding to viral DNA [451]. In accordance with this result, FZ41 docked within the IN-DNA interface (Figure 2.2C-D) and formed hydrophilic interactions in this pocket with residues Y83, Y194, G193, I191, K188, E157 and H183. Of these residues, both K188 and H183 have been shown to be involved in viral DNA binding [435]; the charge at K188 has been shown as being critical for maintaining IN structural integrity and HIV infectivity in cell culture [457]. Residue G193 has also been shown to affect viral LTR specificity [458]. The location of FZ41 may also mean that it can have a modulating effect on IN quaternary structure, in addition to inhibition of DNA binding, since it also has an inhibitory effect on nuclear import [459]. The putative FZ41 binding domain overlaps with that previously described for a group of putative allosteric inhibitors of HIV IN [460].

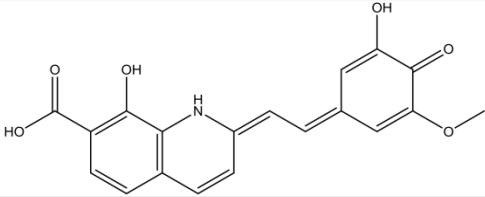
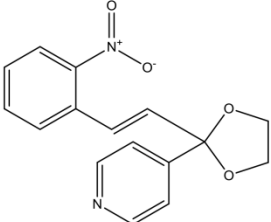
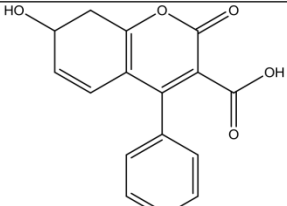
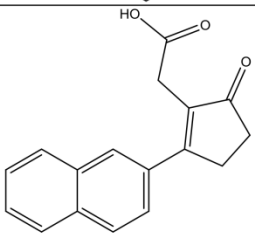
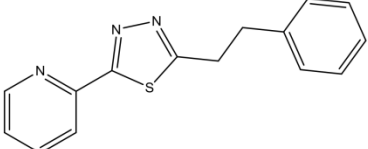
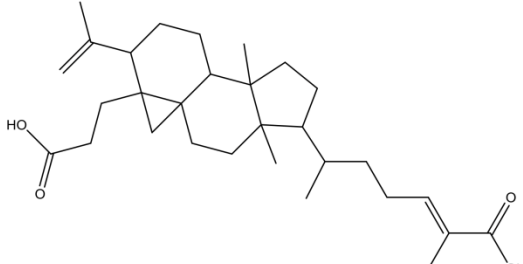
Compound	Structure from ZINC Database	Max Apparent Affinity kcal/mol
FZ41 CID 5481653		-9.1
ZINC00337691 CID 821042		-8.4
ZINC05004388 CID 271624		-8.2
ZINC01703953 CID 97293		-7.9
ZINC04689544 CID 4554474		-7.9
HDS1 CID 10814237		-8.7

Figure 2.3: Best-docked compounds to the dimeric CRF02\_A/G IN model



The compound ZINC00337691 (CID 821042) docks into the IN:IN dimer-interface (Figure 2.4A). ZINC00337691 (4-[2-[(E)-2-(2-nitrophenyl)ethenyl]-1,3-dioxolan-2-yl]pyridine) may act to stabilize the dimeric complex, since it has interactions with both monomers. It also has hydrophilic interactions with the main chain carbonyls of G106, R107 and I84 as well as with the side chains of N184 of chain A. Residue W108 of both subunits forms both hydrophobic stacking interactions and electrostatic interactions with the nitrophenyl portion of the compound. The binding pocket is framed by the hydrophobic contributions from the aliphatic portions of the R107, E85, and V180 residues and the hydrophobic stacking interactions with the two W108 residues. The stabilization of IN dimeric structure has previously been reported for a small group of IN allosteric inhibitors called LEDGINS [414, 458]; even though ZINC00337691 does not appear to bind at the same location, it might stabilize the dimer as well as prevent movement of the protein structure and might therefore be active as a cross-sectional inhibitor in a similar manner as IN allosteric inhibitors [458]. Residues E85 and N184 seem to

also coincide at least partially with the Rev binding interface and thus this compound may also affect Rev regulation of IN nuclear import [266].

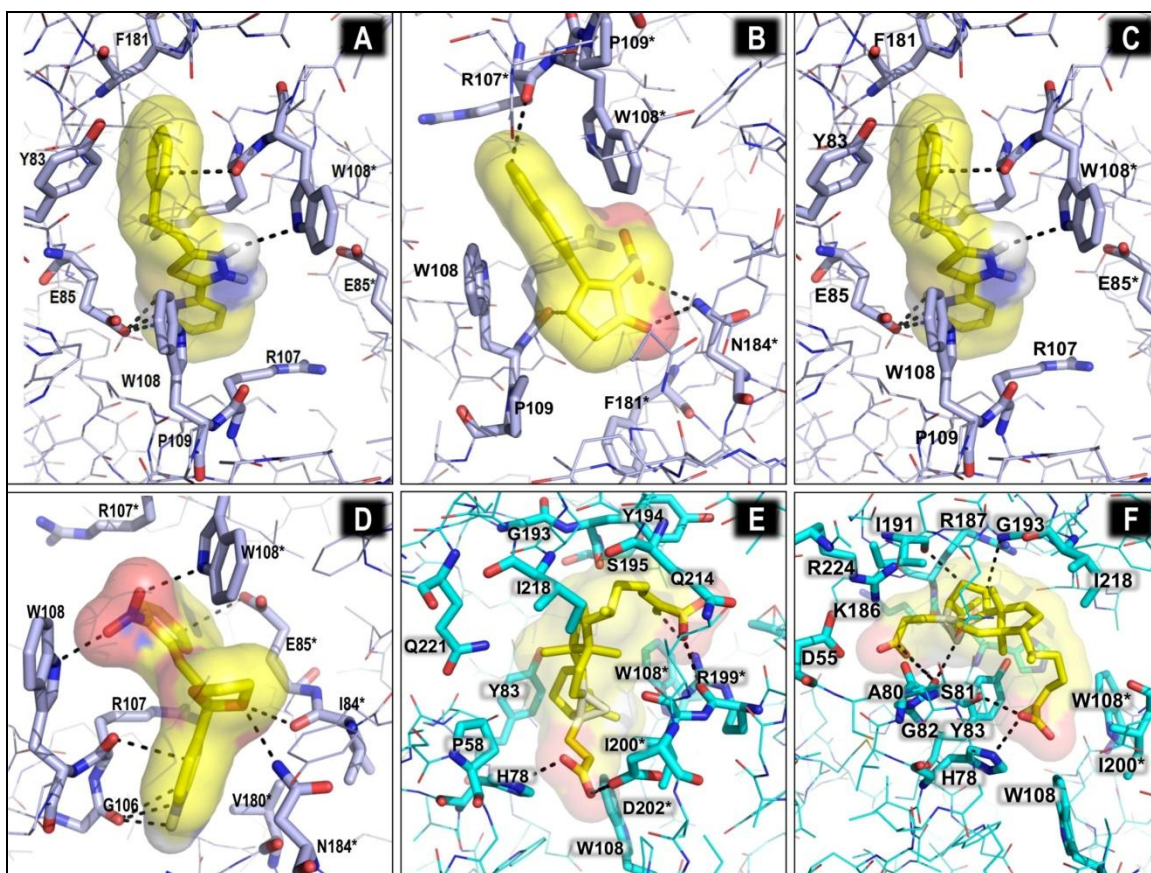


Figure 2.4: Screening of compounds for interaction with dimeric CRF02\_AG IN in the absence of DNA ligands. Interactions of ZINC00337691 (A), ZINC01703953 (B), and ZINC04689544 (C) with residues at the dimer interface. (D) The binding interface of HDS1 spans the dimer (red oval) and DNA binding (blue oval) interfaces. (E) Binding of HDS1 at the dimer interface and (F) DNA interface. In all panels above, the docked compound is represented by yellow main-chain sticks, while the global structure is represented by lines or cartoons and interacting residues are shown as cyan stick structures. Standard CPK coloration

is used for stick and line structures. Putative interacting atoms are indicated by a black dashed line.

Docking of ZINC01703953 (2-(2-naphthalen-2-yl-5-oxocyclopenten-1-yl)acetic acid) (CID 97293) was into the same general location as that of ZINC00337691 at the dimer-interface (Figure 2.4B) but with a somewhat snugger fit. Binding of this compound appeared to be driven mostly by van der Waals interactions and shape complementarity because there were limited hydrogen bonding interactions. ZINC01703953 interacted with R107, W108, P109, F181 and N184 of monomer A and R107, W108 and P109 of monomer B. These residues are all implicated in Rev and distal DNA binding effects. ZINC01703953 also has a diketocarboxylic acid moiety and may possibly exhibit some strand transfer activity under appropriate circumstances. Another compound that docks into the inter-monomer interface, ZINC04689544 (2-(2-phenylethyl)-5-pyridin-2-yl-1,3,4-thiadiazole) (CID 4554474), is more elongated (Figure 2.4C), forming extensive van der Waals contacts with Y83, E85, R107, W108, P109 and F181 of monomer A and E85 and W108 of monomer B. There are also some hydrogen-bonding

interactions with W108 and a salt-bridge with E85 of IN subunit A. The salt-bridge is likely a key driving force for these binding interactions. Additionally, the elongated hydrophobic nature of this molecule may cause it to occupy more space at the interface and it might be a potent modulator of IN activity.

The docking footprint of HDS1 (CID 10814237) on the dimer spanned both the DNA-interaction interface as well as the IN:IN dimer interface (Figure 2.4D).

Three of the best five orientations docked closer to the dimer interface (Figure 2.4E) while two docked in a similar location to FZ41. These HDS1 docking interactions appeared to be driven by van der Waals interactions and shape complementarity with best docked affinity calculations of -8.7 kcal/mol and -8.2 kcal/mol, respectively.

### **2.3.3 Characterization of the inhibitory impact of HDS1**

Although HDS1 inhibits IN DNA binding activity, its effect on viral replication, reverse transcription and/or integration has not been evaluated. Here we show in MT2 cell culture inhibition assays that HDS1 inhibited viral replication as

measured by RT activity in cell culture with an half-effective concentration ( $EC_{50}$ ) of 20.5  $\mu$ M (Figure 2.5A). When quantitative PCR (qPCR) was used to measure the effect of HIV inhibitors, zidovudine (AZT) fully suppressed production of late reverse transcripts, due to its role as a reverse transcription inhibitor, while RAL permitted a build-up of late RT transcripts, due to its role as a post-RT inhibitor. HDS1 also permitted a build-up of late RT transcripts but only to a level of 50% of that associated with RAL (Figure 2.5B). This is also consistent with the reported activity of HDS1 as a weak RT inhibitor [461].

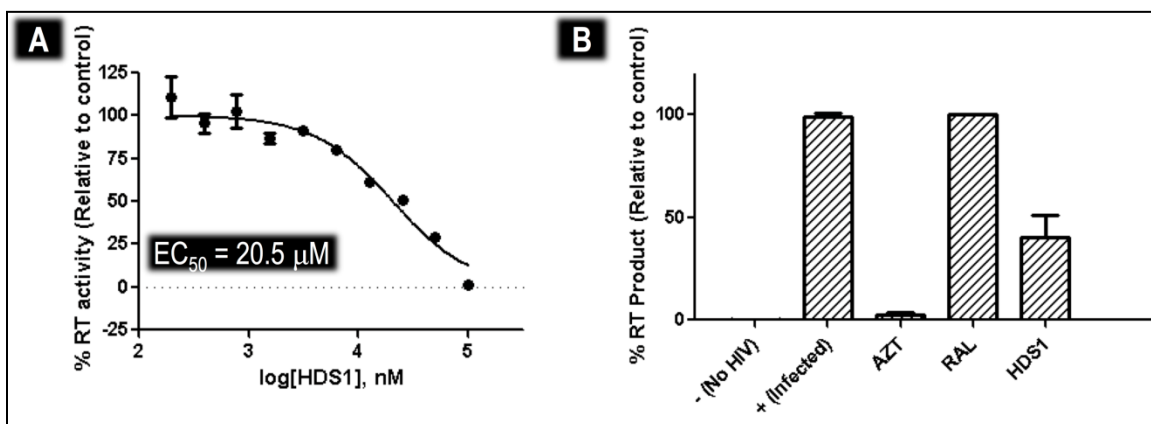


**Figure 2.5: Inhibition of HIV-1 in MT-4 cell cultures by HDS1.** (A) Concentration-dependent inhibition of HIV-1 replication in cell cultures by HDS1. HIV-1 reverse transcriptase activity in cell culture fluids was measured using a tritiated thymidine triphosphate based assay as previously described [448]. (B) Effect of AZT (1 μM), RAL(0.5 μM) and HDS1 (20 μM) on production of late HIV-1 reverse transcripts as measured by qPCR.

Biochemical analysis of the effect of HDS1 on integration confirmed that it impacted DNA binding. The individual IC<sub>50</sub>s for inhibition of strand transfer (Figure 2.6A), 3' processing (Figure 2.6B) and integrase-DNA binding (Figure



2.6C) of HDS1 were 2.9  $\mu\text{M}$ , 2.7  $\mu\text{M}$  and 2.9  $\mu\text{M}$ , respectively. Given that both 3' processing and strand transfer require DNA binding to take place and given that the  $\text{IC}_{50}$ s for inhibition of these reactions were neither additive nor synergistic with inhibition of DNA binding, we conclude that HDS1 blocks integration primarily by inhibition of DNA binding.

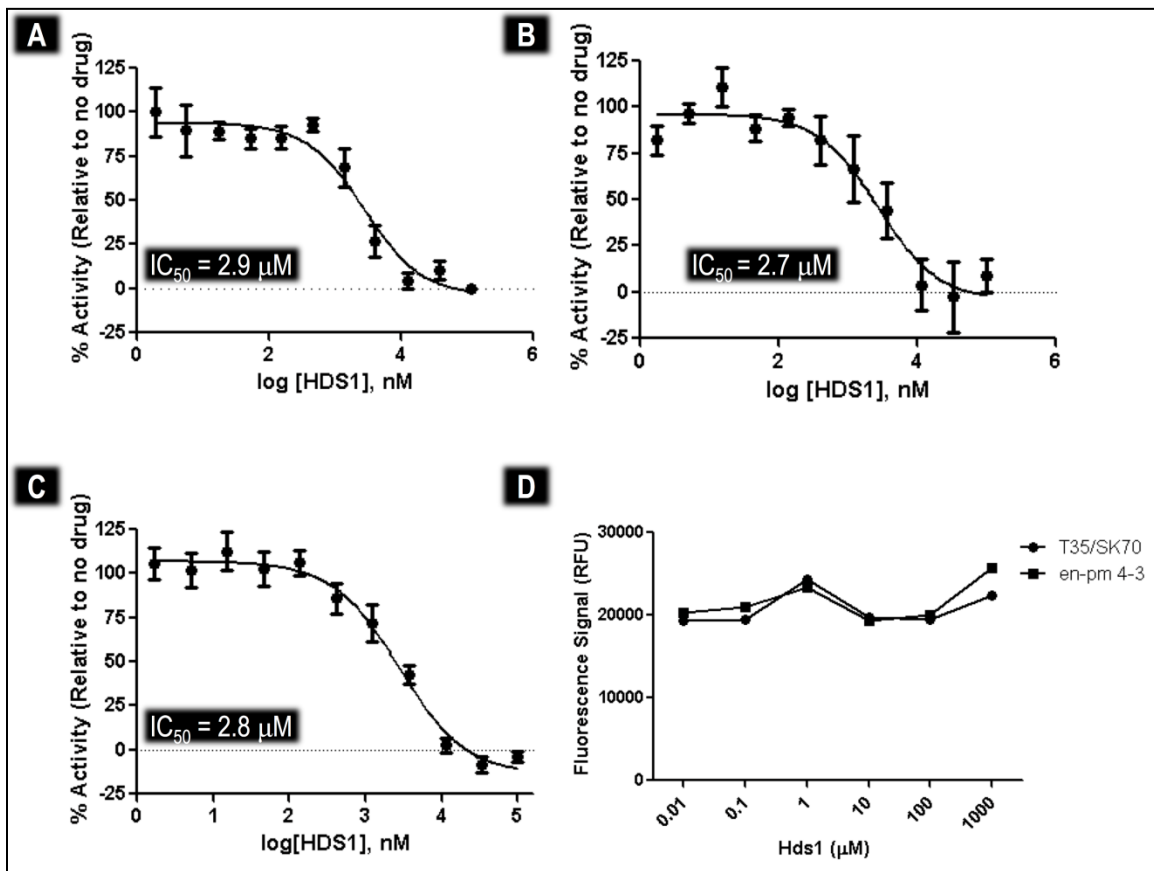


Figure 2.6: Biochemical Characterisation of HDS1 on purified HIV-1 IN enzyme.

(A) Inhibition of the strand transfer reaction. (B) Inhibition of the 3' processing

reaction. (C) Inhibition of the DNA binding activity of HIV integrase. (D) Test for the ability of HDS1 to bind to DNA.

However, our docking studies on HDS1 (Figure 2.4C-E) did not show a direct interaction of HDS1 with DNA in the DNA binding trough, as one would expect in the case of a DNA binding antagonist. We therefore investigated whether HDS1 could affect the ability of ethidium bromide (EtBr) to bind to double-stranded DNA (Figure 2.6D). An EtBr displacement assay showed that the addition of HDS1 did not result in decrease in fluorescence intensity, suggesting that it was unable to displace EtBr. These results demonstrate that HDS1 did not directly interact with DNA.

## **2.4 Conclusions**

We have presented a comprehensive method for creation of viable HIV IN models based on the partial HIV crystal structures as well as full-length PFV IN structures. These models were in good agreement with the PFV crystal structures as well as two published HIV integrase models [382, 417]. They also

did not deviate from DNA:IN architecture as proposed by Kessl and colleagues [383], despite the fact that this group studied DNA-bound tetramers in the presence and absence of the integrase ligand LEDGF/p75 and showed alternate quaternary assembled structures. We have previously utilized these models to investigate the binding of INSTIs to IN and the impact of resistance mutations on enzyme function [418, 462]. Here, we investigated the ability of the models to screen for compounds that bind at the viral LTR interaction domain or at the IN:IN dimerization domain. Given that multiple partial structures of HIV IN have variable structural conformations [413] and different observed dimerization phases, we preferred the quaternary arrangement that is most probable in the active PIC, based on the available structures of PFV IN [245, 370, 380, 382, 416]. By utilizing freely available software and screening the ZINC database, we demonstrated the utility of IN models to screen for novel inhibitors using compound databases.

The compound ZINC05004388 (7-hydroxy-2-oxo-4-phenyl-7,8-dihydrochromene-3-carboxylic acid) (CID 271624) (Figure 2.3) had structural similarity to a class of IN inhibitors that show clinical potential, i.e. non catalytic site IN inhibitors (NCINIs) or LEDGINs, named for their ability to block interaction of IN with its cellular tethering factor LEDGF [463]. Although our models might not have selected LEDGIN-type molecules [256], ZINC05004388 (CID 271624) binds at the same general location as does ZINC01703953 (not shown). Given that LEDGINs have been reported to inhibit IN at multiple steps of the integration process and viral life cycle, this may be an indication of the ability of these compounds to bind at more than one site within IN or to act at different steps of integration and the viral life cycle [402, 464]. Similar to most selected allosteric inhibitors of IN, the ZINC compounds that had the highest affinity calculations were hydrophobic and possessed significant ring structures joined by flexible linkers with isolated hydrophilic/charged moieties.

Our dimeric IN models confirmed that a compound that we previously selected using a DNA-binding screen, i.e. HDS1, binds at a similar location to a well characterized DNA binding inhibitor, FZ41 (Figure 2.7). This region of the IN dimer is important for DNA binding and activity (Figure 2.4D) but is not the target of any approved drug. Virological and biochemical characterization of HDS1 further confirmed that it exhibits a similar activity profile as FZ41 [456]. The binding of either of these compounds to this site most likely inhibits DNA binding through direct steric inhibition and/or altered inter-residue interactions. The elucidation of this unexploited pocket in HIV IN may potentially yield new antiviral compounds in the future.

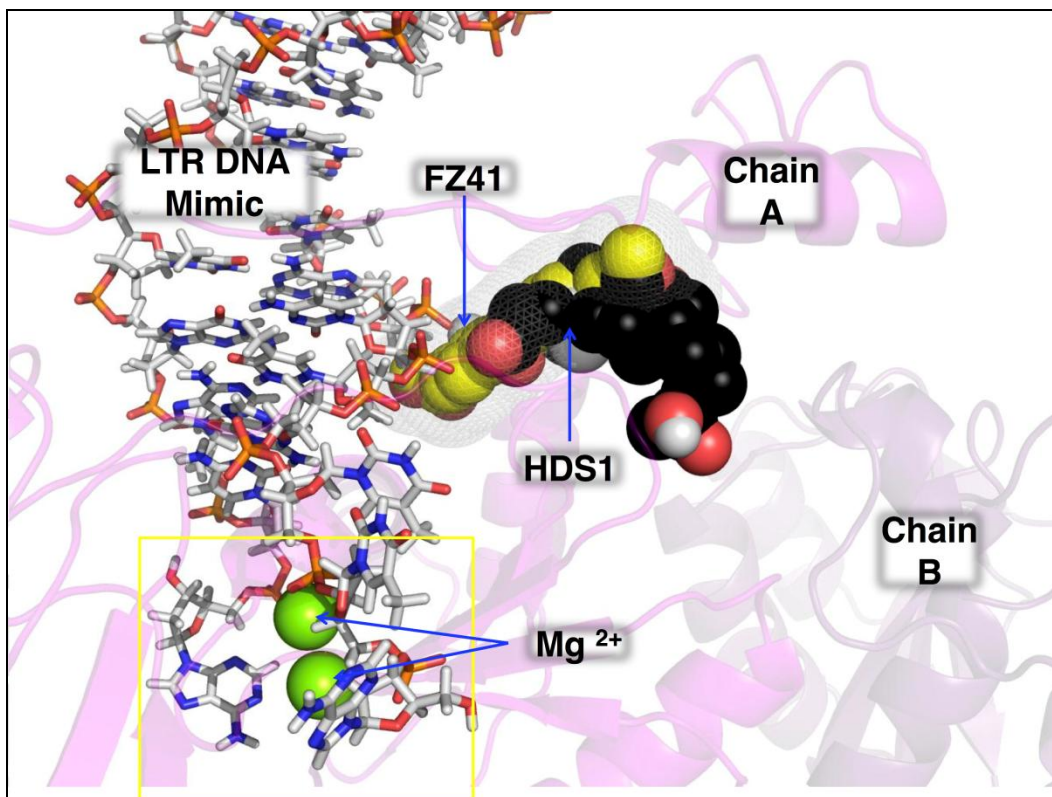


Figure 2.7: FZ41 and HDS1 may directly inhibit DNA binding to integrase. The HDS1 docked structure (shown as a spherical structure with black carbon atoms) (Figure 2.4F) was overlaid onto the FZ41 structure (shown as a spherical structure with yellow carbon atoms) in Figure 2.2D together with DNA (stick structure with white carbon atoms) coordinates from the PFV 3OY9 structure. The active site is indicated by a yellow rectangle. The two monomers of the dimer are represented by different shades of magenta. All other coloration is based on the CPK standard [454].

## 2.5 Appendix

PDB ID	Species and Domain	% identity
3f9k	HIV-2 NTD-CCD	59
3hph	Maedi Visna Virus NTD-CCD	31
1ex4	HIV-1 CCD-CTD	89
1k6y	HIV-1 NTD-CCD	88
3oym	PFV N224H mutant full-length intasome	17
3av9	HIV-1 CCD	86
1c0m	Rous Sarcoma Virus CCD-CTD	23
2x78	PFV CCD	18
1c6v	SIV integrase CCD-CTD	60

CLUSTAL W (1.93) multiple sequence alignment

```

AGWT      FLDGIDKAGEIHERYHNWRAMA---NDFNLPPIVAKEIVASGDKQCQKLRGAIHGQVDC
3f9k_A    ---KIEPAGEIHERYHNVRKELS---HKFGIPNIVARQIVNRCACQQRKREAIHGQVNA
3hph_A    ---NIIFLAEKIHRRWHLRAVGLLI---LEFLGIPRTAEDIVGQID-----V
1ex4_A    -----S
1k6y_A    FLDGIDKAGEIHERYHNWRAMA---SDFNLPPIVVAKEIVASGDKQCQKLRGAIHGQVDC
3oym_A    ---KIVLQGHRLAHRGREATLLKIDALYRW---PDRKIVAKLGRGQQ---LITNAINKA
3av9_A    -----S
1c0m_A    -----G
2x78_A    -----G
1c6v_A    -----NS

          H2                                C2

AGWT      SPGIWQIDPTTHLEGG-----KIIVAVHIVASGYLEAEVIPSSTUQETA-
3f9k_A    ELGTWQMDPTTHLEGG-----KIIVAVHIVASGFLAEVIPSSTUQETA-
3hph_A    CIIHWQVDPPTTHLEGG-----KIIIVWVETNSGLVYAEVIPSSTUQETI-
1ex4_A    SPGIWQIDPTTHLEGG-----KVIIVAVHIVASGYLEAEVIPSSTUQETA-
1k6y_A    SPGIWQIDPTTHLEGG-----KVIIVAVHIVASGYLEAEVIPSSTUQETA-
3oym_A    SPGLLWQIDPTTHLEGG-----KVIIVAVHIVASGYLEAEVIPSSTUQETA-
3av9_A    SPGIWQIDPTTHLEGG-----KVIIVAVHIVASGYLEAEVIPSSTUQETA-
1c0m_A    ELQIWQIDPTTHLEGG-----MAPRGLAVVVTQASDAIVVTHGIGVTV
2x78_A    -----D
1c6v_A    DLGTRWQIDPTTHLEGG-----DKFFFDYIGPLPSPQGYLVVAVVVDGRTGFTHLYPTGISTEATV-

          D

AGWT      ----YFLLKLAGRWIPVKTTHLHLEKSNFTSAAVKAKWMTNVTQRGKLNINPQKGVVREK
3f9k_A    ----YFLLKLAGRWIPVKTTHLHLEKSNFTSAAVKAKWMTNVTQRGKLNINPQKGVVREK
3hph_A    ----VQTRKQYAMFAPKSLQKQNGPAPVAESTQLLMKYLGLRHTTCLHINPQKGVVREK
1ex4_A    ----YFLLKLAGRWIPVKTTHLHLEKSNFTSAAVKAKWMTNVTQRGKLNINPQKGVVREK
1k6y_A    ----YFLLKLAGRWIPVKTTHLHLEKSNFTSAAVKAKWMTNVTQRGKLNINPQKGVVREK
3oym_A    ----KSLNVLTSIAIPKVIHLEKSNFTSAAVKAKWMTNVTQRGKLNINPQKGVVREK
3av9_A    ----YFLLKLAGRWIPVKTTHLHLEKSNFTSAAVKAKWMTNVTQRGKLNINPQKGVVREK
1c0m_A    AVQHHRWALAVLGRFKALEKSNFTSAAVKAKWMTNVTQRGKLNINPQKGVVREK
2x78_A    ----KSLNVLTSIAIPKVIHLEKSNFTSAAVKAKWMTNVTQRGKLNINPQKGVVREK
1c6v_A    ----YFLLKLAGRWIPVKTTHLHLEKSNFTSAAVKAKWMTNVTQRGKLNINPQKGVVREK

          D                                E

AGWT      NRELKCIIGQIRDAQRIHLECTA-----VQMAVFIHNIRKRGKIGGYGAGERIIVDIAT
3f9k_A    NRELKCIIGQIRDAQRIHLECTA-----VQMAVFIHNIRKRGKIGGYGAGERIIVDIAT
3hph_A    NRELKCIIGQIRDAQRIHLECTA-----VQMAVFIHNIRKRGKIGGYGAGERIIVDIAT
1ex4_A    NRELKCIIGQIRDAQRIHLECTA-----VQMAVFIHNIRKRGKIGGYGAGERIIVDIAT
1k6y_A    NRELKCIIGQIRDAQRIHLECTA-----VQMAVFIHNIRKRGKIGGYGAGERIIVDIAT
3oym_A    NRELKCIIGQIRDAQRIHLECTA-----VQMAVFIHNIRKRGKIGGYGAGERIIVDIAT
3av9_A    NRELKCIIGQIRDAQRIHLECTA-----VQMAVFIHNIRKRGKIGGYGAGERIIVDIAT
1c0m_A    NRELKCIIGQIRDAQRIHLECTA-----VQMAVFIHNIRKRGKIGGYGAGERIIVDIAT
2x78_A    NRELKCIIGQIRDAQRIHLECTA-----VQMAVFIHNIRKRGKIGGYGAGERIIVDIAT
1c6v_A    NRELKCIIGQIRDAQRIHLECTA-----VQMAVFIHNIRKRGKIGGYGAGERIIVDIAT

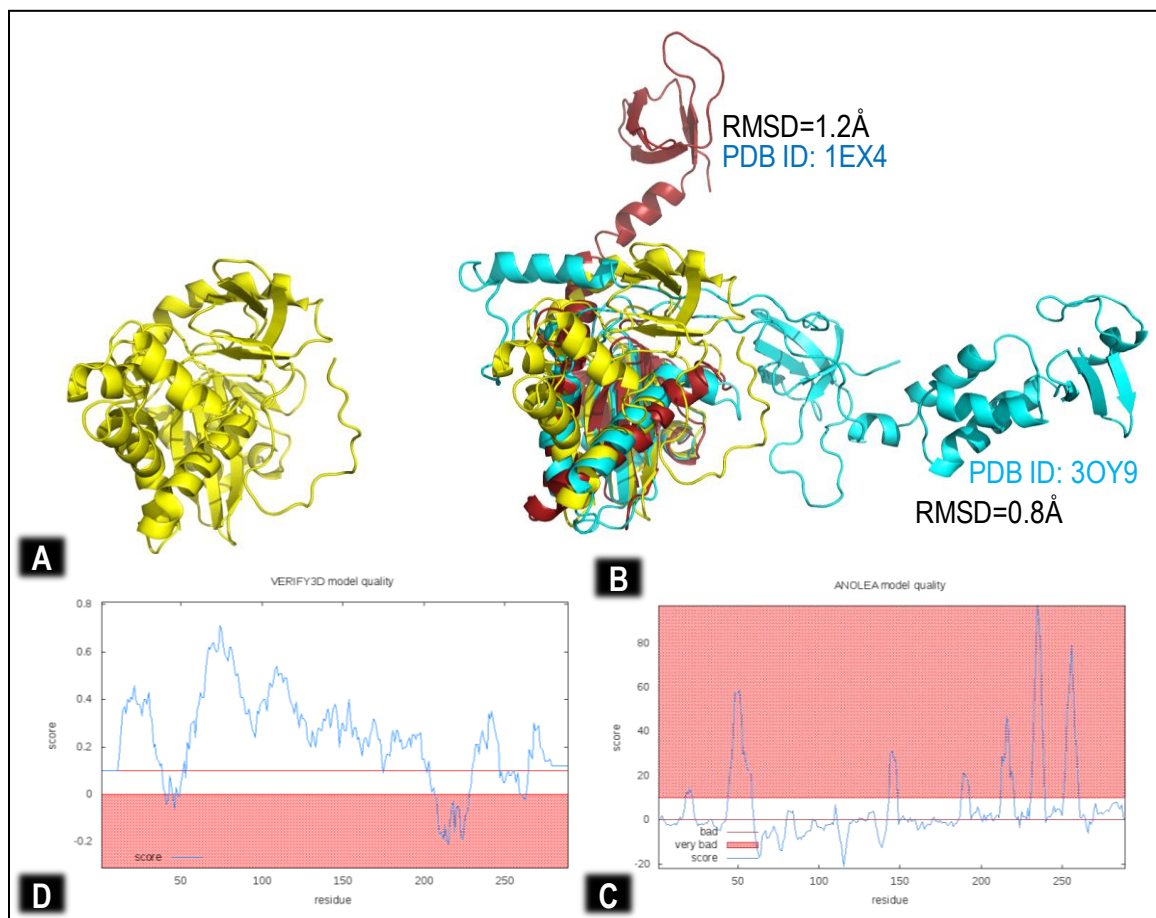
AGWT      DIQTRELQKQIIRKIQNF-----RVVYRDSRDP
3f9k_A    E-----
3hph_A    E-----
1ex4_A    DIQTRELQKQIIRKIQNF-----RVVYRDSRDP
1k6y_A    DIQTRELQKQIIRKIQNF-----RVVYRDSRDP
3oym_A    TTFANQDTLDTREKEELSLQEIIRTSLYHPSTPPASSRWSFVVGQLVQEVVARPALSIP
3av9_A    DIQ-----
1c0m_A    E-----
2x78_A    E-----
1c6v_A    EQEI---QFQ-----

AGWT      LWKGPAKLL--WRGEGAVVIGDNSDIE--VVPRKAKIIRDYGRKMGDDVSAERQDED
3f9k_A    LWKGPAKLL--WRGEGAVVIGDNSDIE--VVPRKAKIIRDYGRKMGDDVSAERQDED
3hph_A    LWKGPAKLL--WRGEGAVVIGDNSDIE--VVPRKAKIIRDYGRKMGDDVSAERQDED
1ex4_A    LWKGPAKLL--WRGEGAVVIGDNSDIE--VVPRKAKIIRDYGRKMGDDVSAERQDED
1k6y_A    RWKHPSTVLKVLNPRVTVVLDLHGNRR--TVPRKAKIIRDYGRKMGDDVSAERQDED
3oym_A    RWKHPSTVLKVLNPRVTVVLDLHGNRR--TVPRKAKIIRDYGRKMGDDVSAERQDED
3av9_A    RWKHPSTVLKVLNPRVTVVLDLHGNRR--TVPRKAKIIRDYGRKMGDDVSAERQDED
1c0m_A    RWKHPSTVLKVLNPRVTVVLDLHGNRR--TVPRKAKIIRDYGRKMGDDVSAERQDED
2x78_A    RWKHPSTVLKVLNPRVTVVLDLHGNRR--TVPRKAKIIRDYGRKMGDDVSAERQDED
1c6v_A    RWKHPSTVLKVLNPRVTVVLDLHGNRR--TVPRKAKIIRDYGRKMGDDVSAERQDED

```

S1. Ten of the major 15 structural homologues of CRF02\_A/G integrase identified by HHpred and aligned using T-COFFEE [465]. In alignment, key structural and functional features are indicated in highlighted regions; Zn<sup>2+</sup> binding domains are indicated by green rectangles and labeled H<sub>2</sub> and C<sub>2</sub> for relevant portions of the H<sub>2</sub>C<sub>2</sub> motif. CCD catalytic residues are boxed in blue

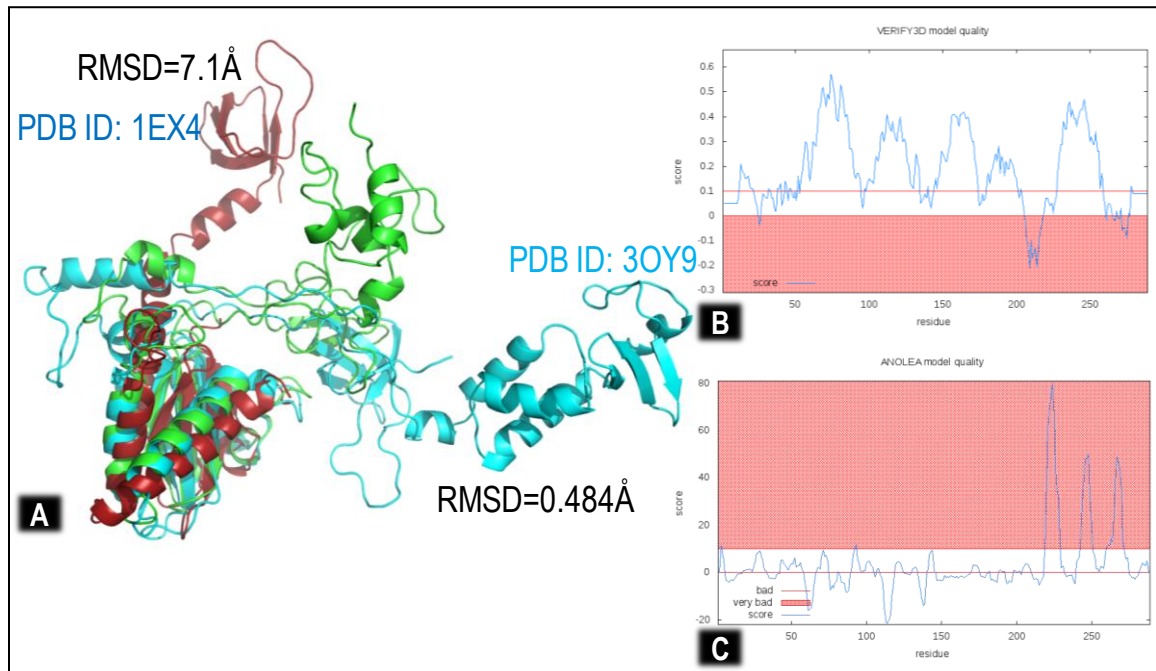
and labeled D,D and E as appropriate. Key residues involved in INSTI drug resistance are highlighted in red boxes reflecting positions 92, 118, 140, 143, 148, 155 and 263, respectively, based on previously published data [317, 346].



**S2. Automated modeling of CRF02\_AG IN.** (Figure A) The globular model 1 that was generated and (Figure B) the alignment of the model with the 'best' two possible templates, HIV (dark green) and PFV (cyan) using HHpred. RMSD



values are indicated for the structurally aligned portions only. The quality of the model was evaluated using (Figure C) VERIFY 3D and (Figure D) ANOLEA algorithms.



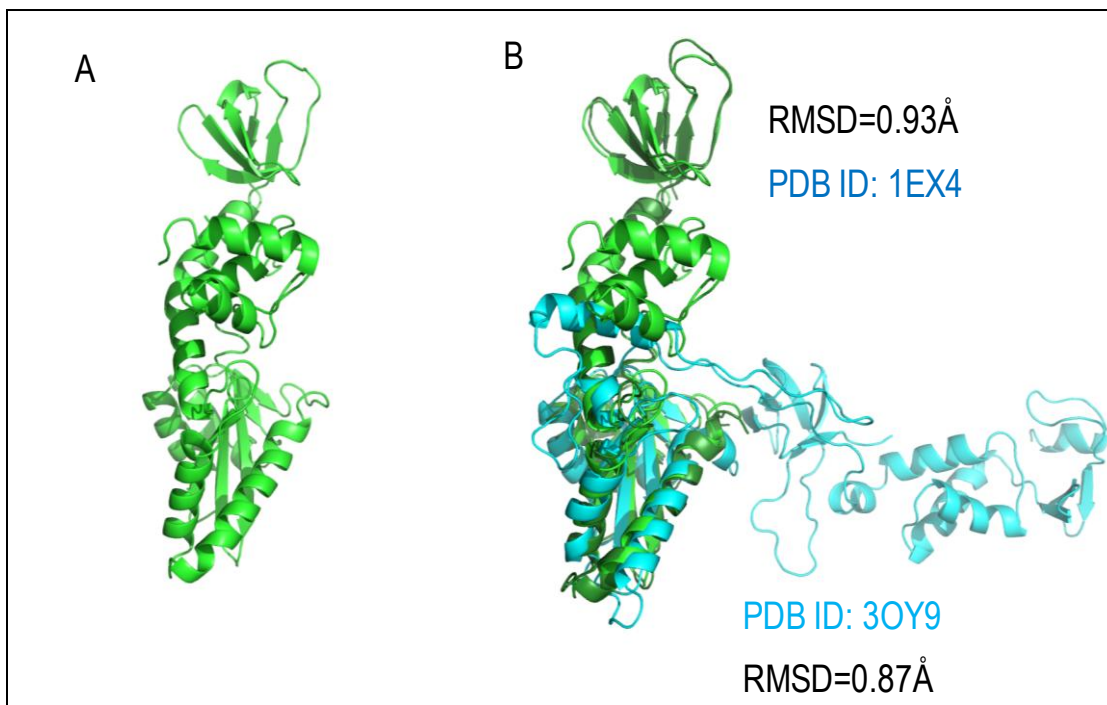
**S3. Modeling of CRF02\_AG IN based on the major 10 structural and sequence homologues.** (Figure A) Alignment of model 2 (green) with the 'best' two possible templates, HIV (dark green) and PFV (cyan). RMSD values are indicated for the structurally aligned portions only. The quality of model 2 was verified by (Figure B) Verify3D and (Figure C) ANOLEA.



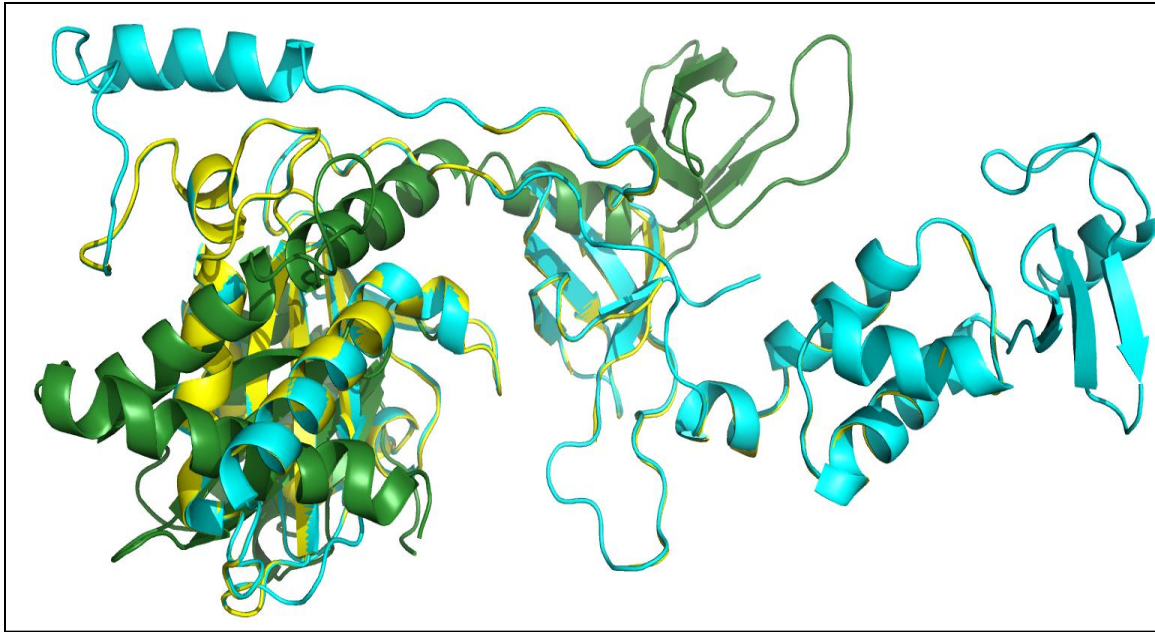
structure of the template (T ss\_pred) and the actual secondary structure of the template (T ss\_dssp; "H" denotes helices, "C" coils, "E" extended  $\beta$ -strand ).

Sequence conservation between the two sequences is shown in two manners; any consensus residues between the template and query sequences are linked by a "|", conservative substitutions are linked with a "+" and non-conservative substitutions with ".". In the consensus sequence (Q Consensus), "~" denotes non-consensus residues. Gaps in the alignment are represented by "-".

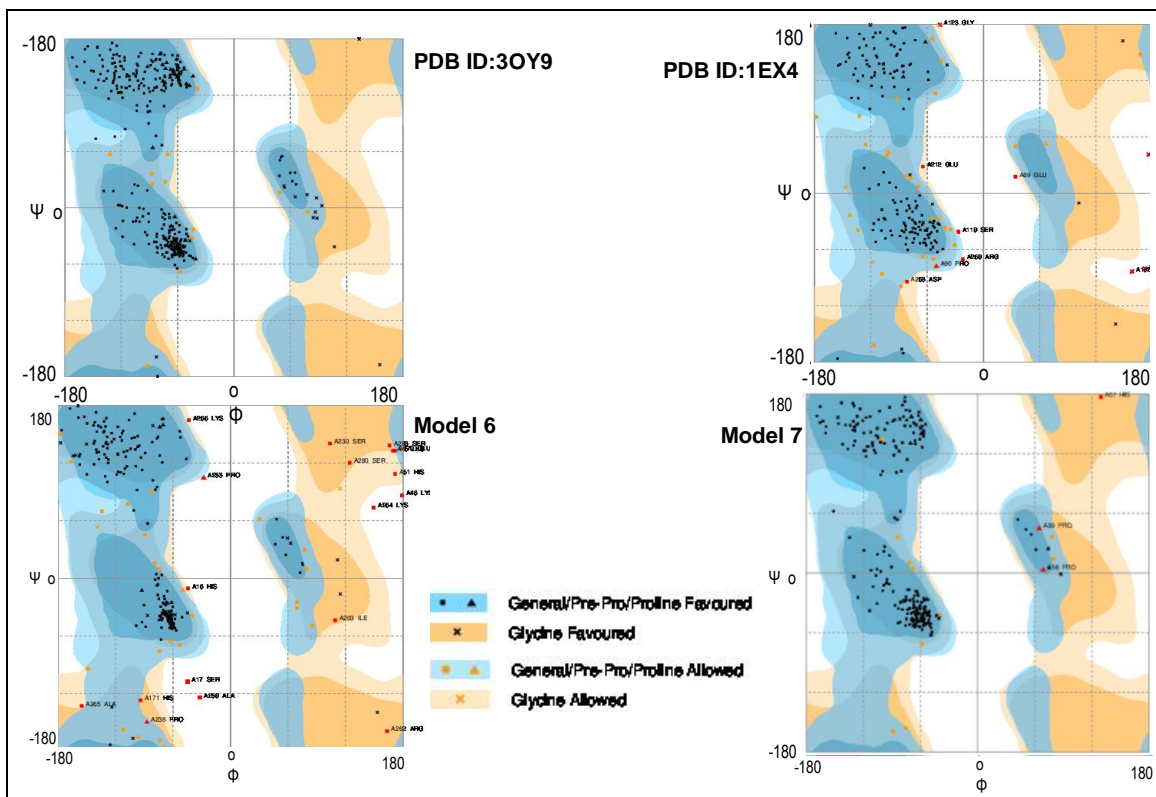
Uppercase letters are strong trends and lowercase letters represent lower confidence trends.



S5. Modeling of the CRF02\_A/G integrase model 4 ( Figure A) and (Figure B) the alignment of the model with the 'best' two possible templates. RMSD values are indicated for the structurally aligned portions only.



S6. Structural alignment of model 5 (yellow) with 3OY9 (cyan) and 1EX4 (dark green)



S7. Ramachandran plot analysis of models 6 and 7 compared to the two lead templates

**S8. Summary comparison of the top 100 binding energies of compounds and their relative displacements as calculated using AutoDock Vina**

Ligand	Binding Affinity	rmsd/ub	rmsd/lb	Ligand	Binding Affinity	rmsd/ub	rmsd/lb
AGwtINdimer_2_ZINC00337691	-8.4	0	0	AGwtINdimer_2_ZINC04689544	-7.4	15.93	15.4
AGwtINdimer_2_ZINC00337691.	-8.3	0	0	AGwtINdimer_2_ZINC05331807	-7.3	4.649	2.972
AGwtINdimer_2_ZINC05004388	-8.2	0	0	AGwtINdimer_2_ZINC05331807	-7.3	7.312	4.22
AGwtINdimer_2_ZINC00337691.	-7.9	6.627	2.713	AGwtINdimer_2_ZINC05331807	-7.3	2.256	1.573
AGwtINdimer_2_ZINC00337691.	-7.9	7.149	4.708	AGwtINdimer_2_ZINC01680992	-6.4	12.271	11.035
AGwtINdimer_2_ZINC00337691.	-7.9	6.552	3.915	AGwtINdimer_2_ZINC01680992	-6.4	0	0
AGwtINdimer_2_ZINC01703953	-7.9	3.33	2.262	AGwtINdimer_2_ZINC01680992	-6.3	7.637	6.626
AGwtINdimer_2_ZINC00337691.	-7.9	5.237	3.26	AGwtINdimer_2_ZINC01680992	-6.3	8.487	7.295
AGwtINdimer_2_ZINC05004388	-7.9	11.109	9.632	AGwtINdimer_2_ZINC01680992	-6.3	8.548	7.38
AGwtINdimer_2_ZINC01703953	-7.9	5.783	3.589	AGwtINdimer_2_ZINC01680992	-6.3	8.282	7.092
AGwtINdimer_2_ZINC00337691.	-7.9	7.14	4.14	AGwtINdimer_2_ZINC01680992	-6.3	9.054	7.779
AGwtINdimer_2_ZINC04689544	-7.9	0	0	AGwtINdimer_2_ZINC01680992	-6.3	7.528	6.343
AGwtINdimer_2_ZINC01703953	-7.9	0	0	AGwtINdimer_2_ZINC01680992	-6.2	8.269	7.085
AGwtINdimer_2_ZINC00337691.	-7.8	7.383	4.632	AGwtINdimer_2_ZINC00334492.	-6	0	0
AGwtINdimer_2_ZINC00337691.	-7.8	4.165	3	AGwtINdimer_2_ZINC00334492	-6	0	0
AGwtINdimer_2_ZINC00337691.	-7.8	7.235	4.474	AGwtINdimer_2_ZINC00334492	-5.9	18.186	16.532
AGwtINdimer_2_ZINC01703953	-7.8	18.71	17.47	AGwtINdimer_2_ZINC00334492	-5.9	17.511	15.879
AGwtINdimer_2_ZINC00337691	-7.8	5.178	3.25	AGwtINdimer_2_ZINC00334492.	-5.8	3.504	2.631
AGwtINdimer_2_ZINC05004388	-7.8	18.142	16.428	AGwtINdimer_2_ZINC00334492	-5.6	22.069	18.823
AGwtINdimer_2_ZINC00337691	-7.8	7.12	4.658	AGwtINdimer_2_ZINC00334492	-5.6	20.464	17.864
AGwtINdimer_2_ZINC04689544	-7.8	2.889	1.802	AGwtINdimer_2_ZINC00334492.	-5.5	4.024	2.605
AGwtINdimer_2_ZINC00337691	-7.8	6.389	3.811	AGwtINdimer_2_ZINC00334492.	-5.5	20.555	17.974
AGwtINdimer_2_ZINC05004388	-7.7	18.486	15.679	AGwtINdimer_2_ZINC00334492	-5.4	16.714	14.709
AGwtINdimer_2_ZINC05004388	-7.7	17.859	16.239	AGwtINdimer_2_ZINC00334492	-5.4	16.908	14.871
AGwtINdimer_2_ZINC00337691	-7.7	8.732	5.32	AGwtINdimer_2_ZINC00334492.	-5.4	4.462	3.161
AGwtINdimer_2_ZINC05004388	-7.7	21.411	18.008	AGwtINdimer_2_ZINC00334492	-5.3	10.409	8.763
AGwtINdimer_2_ZINC00337691	-7.7	4.204	2.969	AGwtINdimer_2_ZINC00334492	-5.3	15.72	14.396
AGwtINdimer_2_ZINC05004388	-7.7	4.832	1.87	AGwtINdimer_2_ZINC00334492.	-5.3	10.316	8.609
AGwtINdimer_2_ZINC01703953	-7.7	8.066	6.588	AGwtINdimer_2_ZINC00334492.	-5.1	11.459	10.074
AGwtINdimer_2_ZINC00337691	-7.7	6.628	2.642	AGwtINdimer_2_ZINC00334492.	-5.1	2.597	1.992
AGwtINdimer_2_ZINC05004388	-7.7	17.901	16.488	AGwtINdimer_2_ZINC00334492.	-5.1	2.846	2.012
AGwtINdimer_2_ZINC04689544	-7.7	11.156	9.968	AGwtINdimer_2_ZINC02554713.	-5	0	0
AGwtINdimer_2_ZINC04689544	-7.7	8.958	5.878	AGwtINdimer_2_ZINC02554713	-5	0	0
AGwtINdimer_2_ZINC05331807	-7.7	0	0	AGwtINdimer_2_ZINC02554713	-4.9	11.108	10.605
AGwtINdimer_2_ZINC05004388	-7.6	17.403	15.161	AGwtINdimer_2_ZINC02554713.	-4.8	23.532	22.052
AGwtINdimer_2_ZINC01703953	-7.6	5.444	3.816	AGwtINdimer_2_ZINC02554713	-4.7	10.723	10.123
AGwtINdimer_2_ZINC00337691	-7.6	7.059	2.805	AGwtINdimer_2_ZINC02554713	-4.6	18.798	18.365
AGwtINdimer_2_ZINC01703953	-7.6	8.628	6.613	AGwtINdimer_2_ZINC02554713	-4.6	14.503	13.617
AGwtINdimer_2_ZINC00337691	-7.6	6.921	4.698	AGwtINdimer_2_ZINC02554713	-4.6	19.184	18.311
AGwtINdimer_2_ZINC01703953	-7.6	3.174	1.917	AGwtINdimer_2_ZINC02554713.	-4.6	19.097	18.229
AGwtINdimer_2_ZINC01703953	-7.6	4.596	3.154	AGwtINdimer_2_ZINC02554713	-4.6	12.874	12.146
AGwtINdimer_2_ZINC04689544	-7.6	8.899	5.939	AGwtINdimer_2_ZINC02554713.	-4.6	22.456	21.635
AGwtINdimer_2_ZINC05331807	-7.6	6.987	1.252	AGwtINdimer_2_ZINC02554713	-4.6	24.896	23.392
AGwtINdimer_2_ZINC05331807	-7.6	9.426	5.977	AGwtINdimer_2_ZINC02554713.	-4.6	19.136	18.538
AGwtINdimer_2_ZINC05331807	-7.6	7.311	1.397	AGwtINdimer_2_ZINC02554713.	-4.5	19.156	18.531
AGwtINdimer_2_ZINC04689544	-7.5	8.336	7.432	AGwtINdimer_2_ZINC02554713	-4.5	9.515	9.033
AGwtINdimer_2_ZINC05331807	-7.5	7.487	2.041	AGwtINdimer_2_ZINC02554713.	-4.5	19.48	18.64
AGwtINdimer_2_ZINC04689544	-7.5	4.714	3.305	AGwtINdimer_2_ZINC02554713.	-4.5	19.662	18.982
AGwtINdimer_2_ZINC05331807	-7.5	3.579	2.576	AGwtINdimer_2_ZINC02554713.	-4.5	13.795	13.031

## Chapter 3

### Characterization of the R263K mutational pathway in HIV-1 integrase that confers resistance to the second-generation integrase strand transfer inhibitor Dolutegravir

The majority of work presented in this chapter was previously published in the Journal of Virology article below:

- Quashie PK, Mesplède T, Han Y, Oliveira M, Singhroy DN, Fujiwara T, Underwood MR, Wainberg MA. **Characterization of the R263K mutation in HIV-1 integrase that confers low-level resistance to the second-generation integrase strand transfer inhibitor Dolutegravir.** *J Virol.* 2012 Mar;86(5):2696-705. Epub 2011 Dec 28 Copyright © 2012, American Society for Microbiology.

PKQ and TM wrote the bulk of the manuscript. PKQ performed most biochemical and *in silico* work, TM performed all virology, DNS and YH performed additional experiments, MO performed the selection study, TF, MRW and MAW wrote and edited parts of the manuscript and MAW supervised the work.



A small amount of work presented here was previously included in the Retrovirology journal article shown below:

- Mesplède T, Quashie PK, Osman N, Han Y, Singhroy DN, Lie Y, Petropoulos CJ, Huang W, Wainberg MA. **Viral fitness cost prevents HIV-1 from evading dolutegravir drug pressure.** Retrovirology. 2013 Feb 22;10:22. doi: 10.1186/1742-4690-10-22 © 2013 Mesplède et al.; licensee BioMed Central Ltd.

T.M. designed and performed experiments, analysed data and wrote the manuscript; P.K.Q. performed the molecular modeling analyses and performed experiments; N.O. performed experiments and analysed data; Y.H. developed analytical tools; D.N.S. performed experiments; Y.L., C.J.P and W.H. performed the PhenoSense® assays; and M.A.W. supervised the project and revised the manuscript.

### 3.1 ABSTRACT

Integrase (IN) strand transfer inhibitors (INSTIs) have been developed to inhibit the ability of HIV-1 integrase to irreversibly link the reverse-transcribed viral DNA to the host genome. INSTIs have proven their high efficiency in inhibiting viral replication *in vitro* and in patients. However, first-generation INSTIs have only a modest genetic barrier to resistance, allowing the virus to escape these powerful drugs through several resistance pathways. Second-generation INSTIs, such as Dolutegravir (DTG, S/GSK1349572), have been reported to have a higher resistance barrier, and no novel drug resistance mutation has yet been described for this drug. Therefore, we performed *in vitro* selection experiments with DTG using viruses of subtypes B, C and A/G, and showed that the most common mutation to emerge was R263K with H51Y as a common secondary substitution. Further analysis by site-directed mutagenesis showed that R263K does confer low-level resistance to DTG and decreased integration in cell culture without altering reverse transcription. Biochemical cell-free assays performed with purified integrase (IN) enzyme containing R263K confirmed the absence of major resistance against DTG and showed a slight decrease in 3'-processing and strand transfer activities compared to wild-type. Additional studies on the impact of the secondary mutation H51Y shows that H51Y in combination with R263K increases resistance to dolutegravir but is accompanied by dramatic decreases

in both enzymatic activity and viral replication. Since H51Y and R263K may define a unique resistance pathway to dolutegravir, our results are consistent with the absence of resistance mutations in antiretroviral drug-naive patients treated with this drug. Structural modeling and *in vitro* IN-DNA binding assays show that the R263K and H51Y mutations affect IN-DNA interactions.

### 3.2 INTRODUCTION

The high mutation rate of HIV-1 reverse transcriptase allows the virus to escape pressure through adaptive mutations that include drug resistance mutations that limit the effectiveness of antiretroviral drugs [466-470]. The use of multiple drugs in combination can hamper this process by restraining viral replication, limiting the emergence of resistant strains. The addition of integrase inhibitors to the arsenal of drugs against HIV-1 is important since these inhibitors are active against viruses resistant to other drug classes [471-473].

The HIV-1 integrase enzyme catalyzes two reactions. The first is 3'-processing, which consists of cleavage of a dinucleotide at both 3' ends of the retrotranscribed linear viral DNA and results in the exposure of reactive hydroxyl groups. The second step termed strand transfer is carried out through a nucleophilic attack by exposed 3' hydroxyl groups on host genomic DNA [283, 474]. Even though 3'-processing may be a suitable therapeutic target, the integrase inhibitors developed so far are integrase strand transfer inhibitors (INSTIs) such as RAL [211] and EVG [331] that preferentially inhibit strand transfer while only modestly affecting 3'-processing [283, 287, 289];

Although first-generation INSTIs strongly inhibit HIV-1 replication, they possess only a modest genetic barrier to resistance. Three main resistance pathways have been identified for RAL, involving initial mutations of the N155, Q148 and

Y143 residues within IN [475]. Both N155 and Q148 confer cross-resistance to EVG [474, 476-478], while Y143 has been reported to be specific for RAL [479]. Numerous secondary mutations confer low levels of resistance against both drugs (reviewed in [474]). Second-generation INSTIs have been developed that possess a more robust resistance profile than RAL and EVG [290, 409, 478, 480, 481]. These include MK-2048 [478, 481-483] and dolutegravir (DTG) [409, 478, 481, 482, 484-486].

Selection studies have shown that MK-2048 can select a G118R resistance mutation [481] and similar studies with DTG have led to the selection of mutations at positions L101, T124 and S153 [409, 487, 488]. However, fold changes (FC) in susceptibility were moderate (FC<10) for most of these substitutions. Although no major resistance mutation against DTG has been identified to date, the accumulation of multiple mutations can result in a FC>10, confirming that second-generation INSTIs possess a higher genetic barrier for resistance than their first-generation counterparts [409, 482].

To further investigate this subject, we performed *in vitro* selections with DTG using viruses of subtypes B, C and recombinant A/G. The most common mutation selected was R263K and introduction of R263K into HIV-1 pNL4-3 by site-directed mutagenesis revealed low-level resistance to DTG. In addition, R263K diminished both viral fitness and integration without affecting reverse

transcription. Cell-free assays indicated that R263K had minimal effect on DTG susceptibility but decreased integrase 3'-processing and strand transfer activities. Molecular modeling suggests that R263K can trigger structural and catalytic changes within IN that explain its selection by DTG. The use of an IN-DNA binding assay confirmed that R263K partially impairs IN-DNA binding. This is the first characterization of a drug resistance mutation consistently selected in both B and non-B subtype viruses passaged with DTG. This is also the first report of selection with DTG in primary human cells.

### **3.3 MATERIALS AND METHODS**

#### **3.3.1 Cells and antiviral compounds.**

TZM-bl and PM1 cells were obtained through the NIH AIDS Research and Reference Reagent Program (see Acknowledgments for details). The 293T cell line was obtained from the American Type Culture Collection (CRL-11268). Cells were subcultured every 3–4 days in Dulbecco's minimal essential medium (DMEM for TZM-bl and 293T cells) or RPMI medium for PM1 cells supplemented with 10% fetal bovine serum (FBS), 2 mM L-glutamine, 50 U/ml penicillin and 50 · g/ml streptomycin and maintained at 37°C and 5% CO<sub>2</sub>. Umbilical cord blood mononuclear cells (CBMCs) were isolated by Ficoll-Hypaque (GE Healthcare) gradient centrifugation from blood obtained through the Department of Obstetrics, Jewish General Hospital, Montreal, Canada. CBMCs were cultured as previously described [489].

Merck & Co., Inc., Gilead Sciences and GSK kindly provided both RAL and MK-2048, EVG, and DTG, respectively. Compounds were solubilised in dimethyl sulfoxide.

#### **3.3.2 Serial passage experiments.**

Selections were performed as previously described [481, 490]. Briefly, CBMCs infected with the specified viruses were serially passaged in the presence of increasing concentrations of DTG. Mutations were identified by sequencing the

IN region of the *pol* gene according to the procedure described in [491]. Viral strains 5331, 5326, 12197, 6399 and 4742 are primary isolates.

### 3.3.3 Generation of replication-competent genetically homogeneous HIV-1.

pNL4-3<sub>INR263K</sub> was created by site-directed mutagenesis of the wild-type pNL4-3 obtained through the NIH AIDS Research and Reference Reagent Program with the following primers: sense 5'-GTAGTGCCAAGAAAAAAGCAAAGATCATCAGGG-3' and antisense 5'-CCCTGATGATCTTTGCTTTTTTTCTTGGCACTAC-3'. The presence of the mutation was confirmed by sequencing. To study the H51Y mutation and the H51Y/R263K combination, pNL4.3<sub>IN(H51Y)</sub> and pNL4.3<sub>IN(H51Y/R263K)</sub> were generated by site-directed mutagenesis using H51Y primers (sense: 5'-CTAAAAGGGGAAGCCATGTATGGACAAGTAGACTGTA-3' and antisense: 5'-TACAGTCTACTTGTCCATACATGGCTTCCCCTTTTAG-3'), and the QuickChange II XL Site-Directed mutagenesis kit (Stratagene). To produce genetically homogeneous HIV-1, 16 µg of plasmid coding for pNL4-3 or pNL4-3<sub>INR263K</sub> were transfected into 293T cells using Lipofectamine 2000 as recommended by the manufacturer (Invitrogen). Fresh medium was added 6 hrs after transfection. After 48 hrs, culture supernatants were harvested, centrifuged and passed through a 0.45 µm filter to remove cellular debris, treated with benzonase (EMD) to degrade the transfected plasmids and stored at -80°C for



future use. Levels of p24 in culture fluids were measured by ELISA (Perkin Elmer). Virion-associated reverse transcriptase (RT) activity was measured as previously described [489].

#### **3.3.4 Replication capacity in TZM-bl cells.**

Relative replication of the recombinant wild-type and mutant viruses was evaluated using a non-competitive short-term infectivity assay with TZM-bl cells as previously described [489, 492]. Briefly, 20,000 cells per well were seeded into 96-well culture plates (Corning). After 24 hrs, cells were infected with the indicated amount of virus normalized by p24. Luciferase activity was measured at 48 hrs post-infection using the Luciferase Assay System (Promega) and a MicroBeta2 luminometer (Perkin Elmer).

#### **3.3.5 Q-PCR for reverse transcripts and integrated viral DNA.**

Quantification of reverse transcripts and integrated DNA in PM1 T-cell lines was performed as previously described [481], with minor modifications. Briefly, cellular DNA was extracted with a DNeasy blood and tissue kit (Qiagen). PCR was performed with Platinum qPCR SuperMix-UDG (Invitrogen) on a Corbett Rotor-Gene 6000 thermocycler (Corbett). The samples were normalized for their  $\beta$ -globin DNA contents. The cycling conditions were 50°C for 2 min, 95°C for 2 min and 50 repeats of 95°C for 10 s, 60°C for 10 s and 72°C for 30 s. For the quantification of reverse transcripts, reactions were performed in the presence of

65 ng of DNA template. Integrated DNA was quantified as previously described [481] in a two-step PCR. Late reverse transcripts, Alu-LTR and  $\beta$ -globin primers and probes have been described previously [481].

### 3.3.6 Protein Expression and Purification.

*E. coli* strain XL10-Gold ultracompetent cells Tet<sup>r</sup>,  $\Delta(mcrA)183$ ,  $\Delta(mcrCB$ -*hsdSMR-mrr)*173, *endA1*, *supE44*, *thi-1*, *recA1*, *gyrA96*, *relA1*, *lac* Hte, [F', *proAB*, *lac*<sup>q</sup> Tn10(tet<sup>r</sup>) Amy Cam<sup>r</sup>]<sup>a</sup> (Stratagene), were used for plasmid production while BL21(DE3) Gold cells F<sup>-</sup>, *ompT*, *hsdS<sub>B</sub>*(r<sub>B</sub><sup>-</sup>, m<sub>B</sub><sup>-</sup>), *dcm*, *gal*,  $\lambda$ (DE3) were used for protein expression. Luria-Bertani (LB) broth (Multicell), prepared in MilliQ water and supplemented with 100  $\mu$ g/mL ampicillin was used for all bacterial growth. Expression and purification of integrase recombinant proteins were performed as previously described for his-tagged integrase [493] with some modifications. Fractions containing purified integrase as judged by SDS-PAGE were dialyzed into storage buffer (20 mM Hepes, 1 M NaCl, 1mM EDTA, 5 mM DTT, 10 % glycerol, pH7.5), aliquoted and stored at -80°C. Protein aliquots could be kept for several months at -80°C without loss of activity.

### 3.3.7 Protein concentration and identity.

Protein concentrations were measured using an extinction coefficient of 50420 M<sup>-1</sup>cm<sup>-1</sup> calculated using ProtParam [494] and verified using the Bio-Rad protein assay with bovine serum albumin (BSA, Sigma) as a standard. BSA

concentration was determined by OD280 readings using its published extinction coefficient [495].

### 3.3.8 DNA substrates for *in vitro* assays.

The following DNA substrates were used for strand transfer assays: donor LTR

DNA sense (A): \*5AmMC12-ACCCTTTTAGTCAGTGTGGAAAATCTCTAGCAGT-3' (where \*5AmMC12 refers

to a reactive amino group attached to the 5' end of the oligonucleotide using a 12 carbon linker) and antisense (B): 5'-

ACTGCTAGAGATTTTCCCACTGACTAAAAG-3'; target DNA: sense (C): 5'-TGACCAAGGGCTAATTCCT-3Bio and antisense (D): 5'-

AGTGAATTAGCCCTTGGTCA-3Bio. For 3' processing assay, primer B was used together with the LTR-3'-sense oligonucleotide (E): \*5AmMC12-

ACCCTTTTAGTCAGTGTGGAAAATCTCTAGCAGT-BioTEG. The following pairs of oligonucleotides, LTR-D1: 5'-CTTTTAGTCAGTGTGGAAAATCTCTAGCAGT-

3' and LTR-D2: 5'-RhoR-XN/ACTGCTAGAGATTTTCCCACTGACTAAAAG-3' were used for DNA binding assays. To make functional duplexes, equimolar

amounts of sense and antisense primers were mixed in a microcentrifuge tube and annealed by heating for ten minutes at 95°C and slow cooling to room

temperature over a period of 4 hours.

### 3.3.9 Strand transfer activity.

Strand transfer reactions with the wild-type and R263K integrase proteins were carried out using a microtiter plate assay as published [493, 496], with the major difference being the choice of Time Resolved Fluorescence (TRF) over fluorescence for signal detection. Donor DNA LTR oligonucleotide duplex A/B diluted to 100 nM in PBS pH7.4 (Bioshop) was covalently linked to Costar DNA-Bind 96-well plates (Corning) by incubation at room temperature for 4 hrs; negative control wells lacked any DNA duplex. The plates were blocked with 0.5% BSA in blocking buffer for 18 hrs. Before use, the plates were washed twice with each of PBS pH 7.4 and assay buffer (50 mM MOPS pH 6.8, 50 µg/mL BSA, 50 mM NaCl, 0.15% CHAPS, 30 mM MnCl<sub>2</sub>/MgCl<sub>2</sub>). Purified integrase proteins, diluted in assay buffer supplemented with 5 mM DTT, were added followed by a 1.5 hr incubation at 37°C for the 3' processing reaction. Then INSTIs were added or not, followed by an additional 1 hr incubation at 37°C in the presence of the biotinylated target DNA duplex C/D for the strand transfer reaction to occur. Following the strand transfer reaction, the plates were washed three times with wash buffer (50 mM Tris pH 7.5, 150 mM NaCl, 0.05% Tween20, 2 mg/mL BSA). The plates were then incubated with Eu-labelled Streptavidin (Perkin Elmer) diluted to 0.025 µg/mL in wash buffer in the presence of 50 µM DTPA (Sigma). After additional washes with the same buffer, Wallac enhancement solution was added (Perkin Elmer). The low pH of the enhancement solution caused the

charging of conjugated Eu to yield  $\text{Eu}^{3+}$  ions. The TRF of  $\text{Eu}^{3+}$  in the Wallac enhancement solution was measured on FLUOStar OPTIMA multi-label plate reader (BMG Labtech) in TRF mode with excitation and emission slits of 355 nm and 612 nm respectively.

#### **3.3.10 3' processing activity.**

The determination of 3' processing activity of purified recombinant integrase proteins by microtiter plate assay was also performed. Briefly, 3'-biotinylated DNA duplex E/B was covalently linked to Costar DNA-bind plates under similar conditions as for strand transfer. Purified IN was added and after 2 hrs of incubation, 3'-biotinylated ends cleaved by the enzyme were washed away and the remaining signal measured as described for the strand transfer assay.

#### **3.3.11 Microplate-based assay for IN-DNA binding.**

An IN-DNA binding assay was established by modifying a previously described procedure [497]. Briefly, various concentrations of IN in PBS (pH 7.4) were loaded into NUNC FluoroNunc™ microplate wells (200  $\mu\text{L}$  per well) and the plate was incubated at room temperature for 2 h; excess unbound proteins were removed by three washes with PBS (200  $\mu\text{L}$ , pH 7.4). The plate was then blocked with 200  $\mu\text{L}$  PBS/well containing 2% BSA (w/v) for 2h and washed three times in PBS. A 5'-rhodamine-labelled LTR duplex (20 nM) was then added in 100  $\mu\text{L}$  of binding buffer (20 mM MOPS, pH 7.2, 20 mM NaCl, 5 mM DTT, 7.5 mM  $\text{MgCl}_2$ ),

and the plate was incubated at room temperature for 1 h. The plate was then washed three times in PBS. After removal of the final wash by inversion, 100  $\mu$ L PBS was added to each well, and fluorescence was measured in a FLUOStar Optima plate reader (BMG Labtech) at excitation and emission wavelengths of 544 and 590 nm. All measurements were performed in duplicate, and experiments were repeated at least twice.

### **3.3.12 Monogram Biosciences PhenoSense replication capacity and phenotyping assays**

HIV replication capacity and susceptibility to dolutegravir, raltegravir, and elvitegravir were measured as previously described [24]. Briefly, murine leukemia virus envelope-pseudotyped viruses bearing the integrase H51Y and R263K mutations and a luciferase reporter gene were used to inoculate human embryonic kidney HEK-293 cells. The resultant luciferase activity was used to calculate changes in both HIV replication capacity relative to a wild-type reference strain. Drug susceptibility was expressed as a fold-change in IC<sub>50</sub>.

### **3.3.13 Data processing.**

All cell-free experiments, except when otherwise indicated, were the result of at least 3 sets of experiments, performed in triplicate to yield 9 independent values. To determine the kinetic parameters for target-dependent strand transfer activity, the results of at least 4 sets of triplicate results ( $n \geq 12$ ) were fit to a Michaelis-

Menten algorithm using GraphPad Prism 4.0. software.  $IC_{50}$  values were calculated on the basis of 9 independent experiments performed with wild-type B and IN<sub>R263K</sub> enzymes by using the sigmoid dose-response function of the same software. Values of strand transfer activity in the absence of drug for each experiment were determined arbitrarily as 100%. The extent of resistance for individual inhibitors was measured by using an unpaired Student's t-test with Welch's correction. Mean  $IC_{50}$  values were expressed together with the standard error of the mean (SEM).

### **3.3.14 Homology modeling.**

Homology models of full-length HIV-1 IN intasome and strand transfer complex (STC) were created based on the available partial crystal structures of HIV-1 integrase [412, 435, 498, 499] and the published intasome [283] and STC [286] of PFV using the I-TASSER 3D protein prediction server [432]. Model quality was assessed based on root mean square deviation (RMSD) of the global homology structure from the PFV lead templates and available HIV-1 IN using the RCSB PDB Protein Comparison Tool [443]. Pymol (<http://pymol.org/>, The PyMOL Molecular Graphics System, Version 1.3, Schrödinger, LLC) was used for structural visualization and image processing.

## 3.4 RESULTS

### 3.4.1 Isolation of R263K mutant viruses with DTG

Previous serial passage experiments with DTG have led to the emergence of T124A, S153F/Y and L101I from HIV-1 subtype B virus [409, 487, 488]. To extend these observations, we performed serial passage experiments with DTG using healthy donor primary human cord blood mononuclear cells (CBMCs) infected with various subtype B, C and A/G viruses (Table 3.1).

After 20 weeks, the R263K mutation was observed in all five subtype B (5/5) and one of two subtype A/G selections. Of note, only a fraction of the 5326 viral population carried this substitution. During the selections, neither L101I nor T124A appeared. However, the S153Y substitution was observed in combination with R263K for one subtype B virus and S153T was partially detected in one subtype C virus. Importantly, the only subtype B or A/G virus that did not bear the R263K mutation carried the G118R mutation; the same mutation (G118R) was observed in one subtype C virus. The R263K mutation was detected alone or in combination with other substitutions that varied among virus strains (Table 3.1). R263K emerged early in culture in both subtype B and A/G viruses and was the most frequent mutation at weeks 34/37, observable in 4/6 subtype B and A/G viruses. At this same time, G118R was present in one subtype C and one subtype A/G virus. Various secondary mutations accumulated with R263K and



G118R, in particular H51Y, a secondary mutation previously associated with EVG resistance [500, 501]. For one subtype B virus, 5326, the initial R263K mutation was lost and a single substitution S153Y was detected at week 37. Together, these results identified R263K as a common mutation that emerges in the presence of DTG and prompted us to further investigate this substitution.

#### **3.4.2 R263K confers resistance against DTG *in vitro*.**

To study the R263K substitution in the context of a homogeneous genetic background, this mutation was introduced by site-directed mutagenesis into pNL4-3 proviral DNA. The resulting pNL4-3<sub>IN(R263K)</sub> virus and its wild-type counterpart, pNL4-3, were produced by transfecting proviral DNA into 293T cells. The activity of DTG was tested in TZM-bl cells against pNL4-3 and pNL4-3<sub>IN(R263K)</sub> (Table 3.2). Dose-response studies to determine half maximal inhibitory concentrations (IC<sub>50</sub>) showed that DTG inhibited wild-type pNL4-3 with an IC<sub>50</sub> of 3.273 nM (with a 90%-confidence interval of 1.178 to 9.095 nM). The calculated IC<sub>50</sub> was 36.69 nM (17.49 to 76.98 nM) for pNL4-3<sub>IN(R263K)</sub>. These values were statistically different according to the extra sum-of-squares F test ( $p < 0.02$ ). This corresponds to a 11.2 fold decrease in DTG susceptibility in the presence of the R263K mutation.

**Table 3.1 Serial passage experiments with CBMCs infected with subtype B, A/G and C HIV-1 viruses in the presence of increasing concentrations of DTG. Baseline polymorphisms and acquired substitutions are indicated.**

Subtype	Virus	Baseline polymorphisms	Week 20		Week 37	
			DTG Concentration ( $\cdot$ M)	Acquired mutations	DTG Concentration ( $\cdot$ M)	Acquired mutations
<b>B</b>	5331	I72V	0.05	R263K		
	BK-132	M154I, V201I	0.05	W243G/W, R263K	0.05	E138E/K, R263K
	5326	V72I, I203M	0.05	S153Y, R166K/R, R263K/R	0.05	S153Y
	PNL4.3	I72V, I113V, L234V	0.05	M50I/M, V151I, R263K	0.05	M50I, V151I, R263K
	12197 Ral TI WT for INI	I203M	0.01	R263K, D288E	0.025	R263K, D288E (week 34)
<b>AG</b>	6399	V72I, T125A, V201I	0.025	E69E/K, G118R	0.05	G118R
	96USSN20	V72I, T125A, V201I	0.1	R263K	0.1	H51H/Y; R263K
<b>C</b>	4742	V72I, Q95P, T125A, V201I, I203M	0.05	G118R	0.05	H51Y, G118R
	96USNG31	V72I, T125A, V201I	0.01	S153S/T	0.025	H51Y, G139E/G

**Table 3.2 R263K susceptibility to DTG.**

Backbone	Genotype	DTG		FC
		IC <sub>50</sub> (nM)	90% confidence intervals (nM)	
pNL4-3	wt <sup>a</sup>	3.273	1.178 to 9.095	11.2
	IN <sub>R263K</sub>	36.69	17.49 to 76.98	

<sup>a</sup> wt, wild type.

### 3.4.3 Characterization of R263K in cell-based assays.

To analyze how R263K impacts viral infectivity, we performed TZM-bl infection assays with increasing amounts of wild-type pNL4-3 and pNL4-3<sub>IN(R263K)</sub> viruses (Figure 3.1A). For both viruses, the measured luciferase activity from TZM-bl cells was directly proportional to the amount of virus, measured in ng of p24. These experiments indicated that R263K slightly decreases viral infectivity, as shown by the reduction in luciferase activity induced by pNL4-3<sub>IN(R263K)</sub> compared to wild-type pNL4-3. Best-fit linear regressions were created for each virus to determine the slope as an estimate of infectivity (Figure 3.1B). This analysis shows that R263K decreases viral infectiousness by approximately 20%.

R263K mutation had no effect on reverse transcription. DNA reverse transcripts from pNL4-3 and pNL4-3<sub>IN(R263K)</sub> were quantified in PM1 cells by Q-PCR at 7h and 24h after infection (Figure 3.1C). Both viruses produced similar amounts of reverse transcripts, suggesting that R263K did not affect RT activity. To test the role of integration in decreased infectivity observed with the R263K mutation, we

quantified viral integration (Alu-LTR) by Q-PCR (Figure 3.1D), as described previously [481].

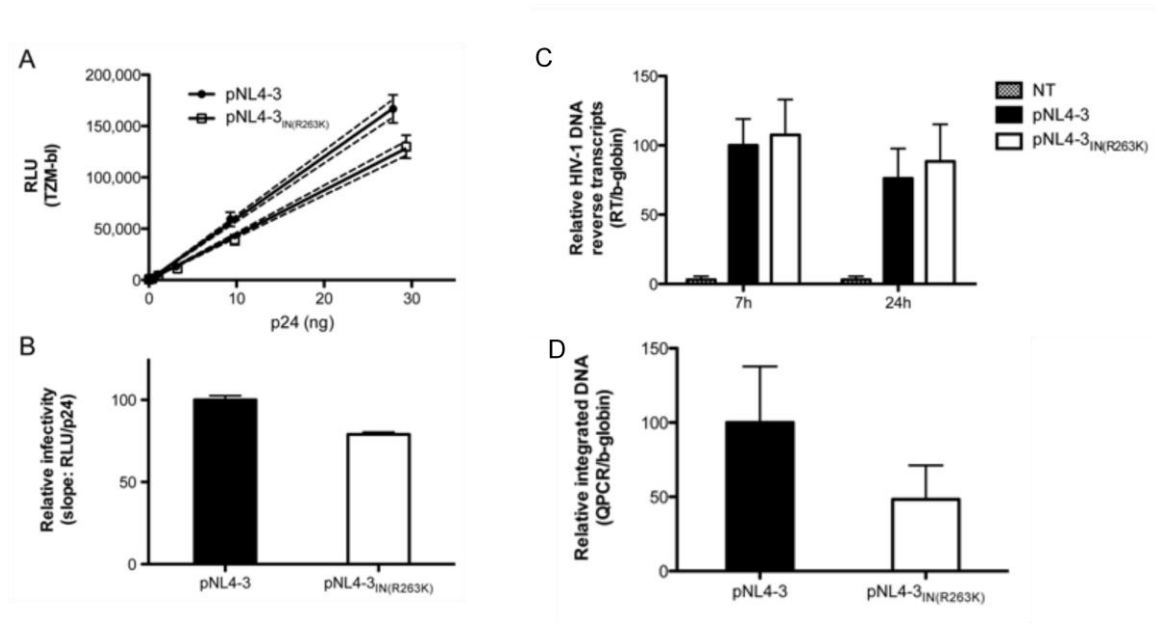


**Figure 3.1: The R263K mutation specifically decreases HIV-1 integration.**

(A-B) The R263K mutation in the IN region decreases HIV-1 pNL4-3 infectivity.

(A) Relative luciferase units (RLU) produced by TZM-bl cells 48h after infection with WT and IN<sub>R263K</sub> pNL4-3 viruses. The calculated linear regressions are shown as solid lines and the 95% confidence intervals as dotted lines. The results presented are representative of three independent experiments. (B) Infectivity of wild-type and R263K mutant virus represented by the mean  $\pm$ SD of the calculated slopes for three independent TZMbl infectivity assays ( $p < 0.01$ , t-test), normalized against the wild-type slope, arbitrarily set at 100%. (C) The R263K

mutation does not affect HIV-1 pNL4-3 reverse transcripts production. Reverse transcription products were measured by Q-PCR at 7h and 24h after infection of PM1 cells with wild-type and R263K mutant viruses. Infections were performed in duplicate with two different viral stocks for each virus for a total of 4 independent infections for each time-point and each virus. Q-PCR reactions were performed in duplicate for each sample. Results were normalized for globin gene expression and expressed relative to the normalized signal measured for the wild-type virus 7h post-infection, arbitrarily fixed at 100% for each set of infections. Results from non-infected cells (NI) are indicated. Means  $\pm$ SD are shown. (D) HIV-1 pNL4-3 integration is diminished in the presence of the R263K mutation. Integrated DNA was quantified by Q-PCR in PM1 cells infected with wild-type and R263K pNL4-3 viruses for 72h. Infections were performed twice in duplicate with two separate viral stocks, for a total of 8 independent infections for each virus. Q-PCR reactions were performed in duplicate for each sample. Results were normalized for  $\alpha$ -globin gene expression and expressed relative to the signal detected for wild-type virus, arbitrarily set at 100% for each set of infections. Means  $\pm$ SD are shown.

#### **3.4.4 Expression and purification of IN<sub>R263K</sub>.**

We next carried out a biochemical characterization of IN carrying the R263K mutation. Although arginine (R) and lysine (K) are hydrophilic, basic, and

positively charged at neutral pH, with only small differences in their biochemical properties, substitution from R to K leads to a change from a guanidine to an amine side chain. To investigate the effect of this change on the biochemical properties of HIV-1 integrase, the R263K mutation was introduced by site-directed mutagenesis into the coding sequence of the subtype B integrase carrying the solubility mutations F185H and C280S. These latter substitutions have been previously shown to increase solubility of recombinant integrase without changing its activity in vitro [483, 493]. Both the wild-type and R263K enzymes were expressed fused to a hexa-histidine tag and purified simultaneously, as previously described [483, 493]. The purity of the recombinant enzymes was shown to be better than 90% as measured by gel analysis and their identity was confirmed by western blot (not shown).

#### **3.4.5 Strand transfer and 3'-processing activities of IN<sub>R263K</sub>.**

Since cell-based experiments suggest a defect in the activity of integrase carrying the R263K substitution, we analyzed the biochemical properties of the wild-type and variant (IN<sub>R263K</sub>) enzymes in cell-free assays. We measured both 3'-processing and strand transfer activities of the IN<sub>R263K</sub> protein and compared the results to those obtained with wild-type IN protein (Figure 3.2). Both assays were performed in microtiter plates in the absence of drug inhibitors. First, the optimal protein concentration for the strand transfer assay was determined by

using increasing amounts of wild-type and IN<sub>R263K</sub> recombinant proteins (Figure 3.2A). Wild-type IN showed a maximal strand transfer activity at 300 nM whereas IN<sub>R263K</sub> reached a maximum at 150 nM. IN<sub>R263K</sub> strand transfer activity was lower than wild-type at all protein concentrations.

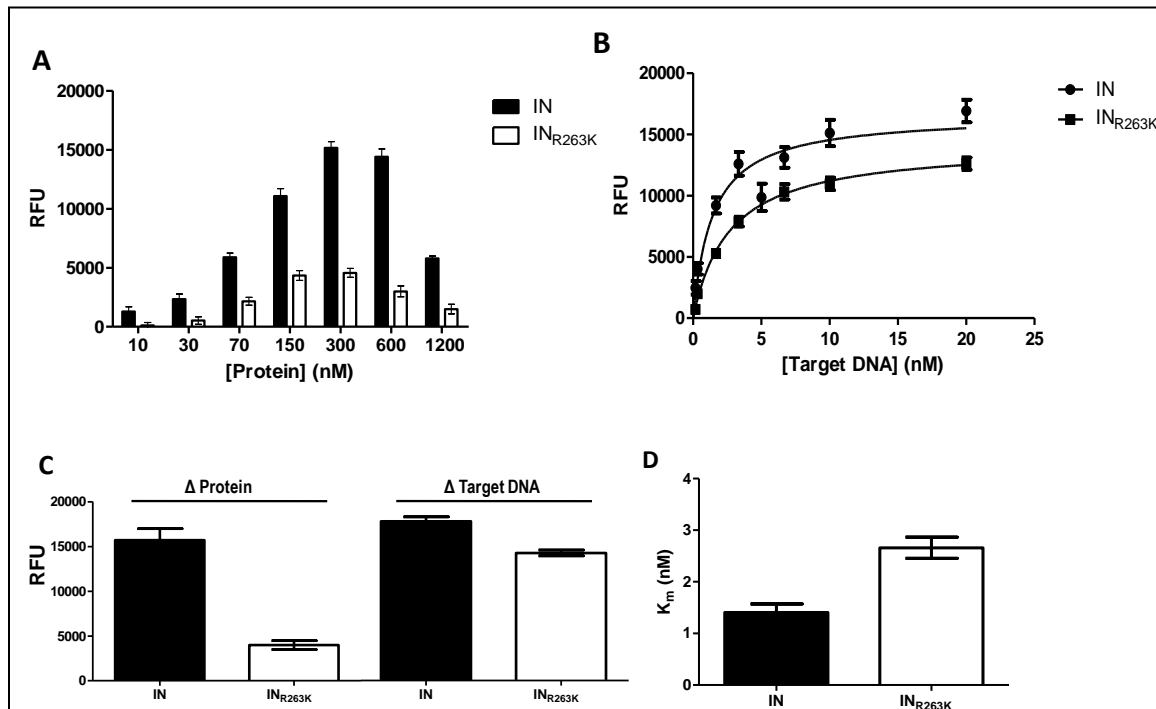


**Figure 3.2: Strand transfer activity of purified recombinant wild-type (IN) and R263K (IN<sub>R263K</sub>) integrase proteins.**

(A) Strand transfer activity expressed in relative fluorescent units (RFU) in the presence of 3 nM target DNA and variable concentrations of purified recombinant protein. (B) Strand transfer activity (RFU) in the presence of 300 nM purified recombinant protein and variable concentrations of target DNA. (C) Calculated maximum strand transfer activities for wild-type IN and IN<sub>R263K</sub> with variable protein or target DNA concentration. The maximum activities in the presence of

increasing concentrations of proteins ( $\Delta$ Protein) were calculated by excluding the higher concentration (1200 nM). (D) Calculated Michaelis-Menten constant ( $K_m$ ) for purified IN and INR263K.

Similar experiments were also performed in the presence of increasing concentrations of target DNA (Figure 3.2B) and saturation curves were generated for each enzyme to determine maximal activity. The results indicate that IN<sub>R263K</sub> has a lower maximal strand transfer activity than does wild-type IN (17,679 $\pm$ 503 relative fluorescence units (RFU)/hr for wild-type compared to 14,166 $\pm$ 321 RFU/hr for IN<sub>R263K</sub>), corresponding to a 20% decrease in activity. Calculated apparent maximum activities ( $V_{max}$ ) and Michaelis-Menten constants ( $K_m$ ) are summarized in Figure 3.2C and 3.2D, respectively. The  $K_m$  was 1.40 nM for wild-type and 2.66 nM for IN<sub>R263K</sub>, confirming the inhibitory effect of the R263K mutation on the integration process.

The strand transfer assay measures both integration steps, i.e. 3'-processing and strand transfer of the processed donor DNA to target DNA. To discriminate between the two reactions, we measured 3'-processing activity using the purified recombinant wild-type and IN<sub>R263K</sub> proteins in separate assays. First, 3'-processing activity was measured over time (Figure 3.3A). 3'-processing activity increased with time, reaching linear progression between 90 and 160 minutes.



Next, we performed similar experiments in the presence of increasing concentrations of integrase proteins (Figure 3.3B). Calculated maximum activities ( $V_{max}$ ) after 2 hrs were  $17,414 \pm 277$  and  $14,489 \pm 1,158$  RFU for wild-type and  $IN_{R263K}$  enzyme, respectively. The same assay was also performed with increasing concentrations of donor LTR DNA (Figure 3.3C). The values for wild-type and  $IN_{R263K}$   $V_{max}$  were  $9,535 \pm 946$  and  $7,404 \pm 863$  RFU, respectively. Calculated  $V_{max}$  values are summarized in Figure 3.3D. Together, these results show that integrase 3'-processing and strand transfer activities were decreased by approximately 20% when the R263K mutation was present.

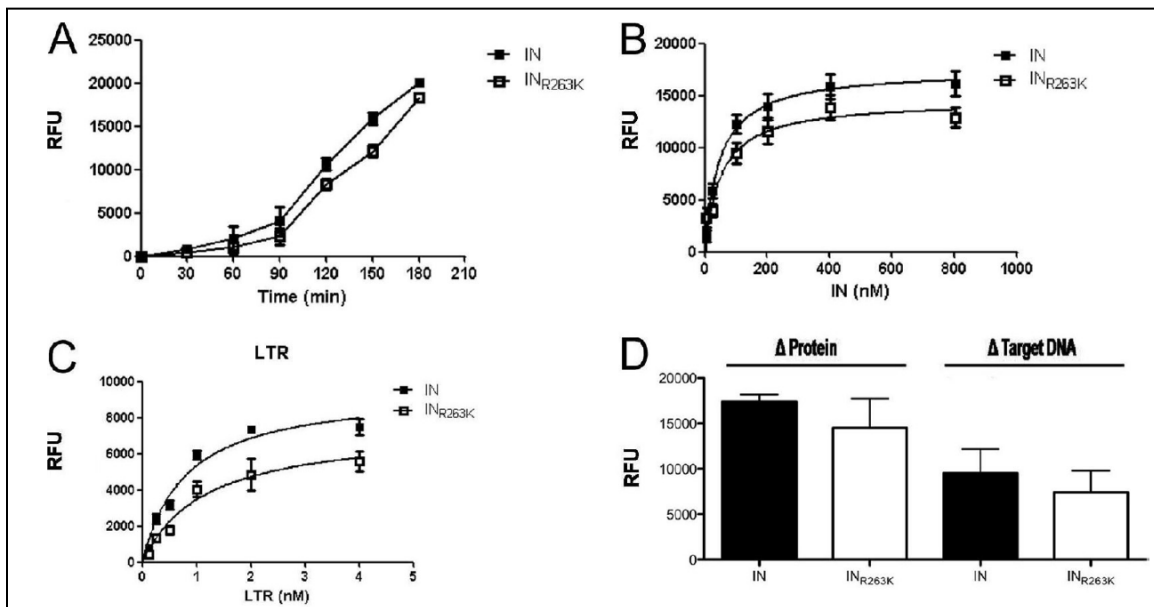


**Figure 3.3: 3'-processing activity of purified recombinant wild-type (IN) and R263K ( $IN_{R263K}$ ) integrase proteins.**

(A) Time-dependent 3'-processing activity expressed in relative units of time-resolved fluorescence (RFU) in the presence of 100 nM protein and 10 nM target

DNA. (B) 3'-processing activity (RFU) after 2 h incubation with 10 nM target DNA and increasing concentrations of protein. (C) 3'-processing activity (RFU) after 2 h incubation with 400 nM protein and increasing concentrations of target DNA (LTR). (D) Calculated maximum 3'-processing activities for WT IN and INR263K with variable protein or target DNA concentration.

#### **3.4.6 Effects of the R263K mutation on susceptibility to INSTIs *in vitro*.**

Next, we measured the effects of DTG, EVG, RAL, and MK-2048 on wild-type and IN<sub>R263K</sub> enzymes *in vitro* (Table 3.3). Strand transfer assays were performed with the wild-type and mutant IN, in the presence of increasing concentrations of each of these drugs and the resulting strand transfer activity was measured.

Dose-response curves were calculated to determine IC<sub>50</sub> values. DTG inhibited wild-type and R263K IN with an IC<sub>50</sub> of 3.49 nM and 3.74 nM, respectively. The 95% confidence interval for IN<sub>R263K</sub> was wider than that for wild-type enzyme, with a higher limit that was twice that of wild-type integrase. Our results indicate that R263K confers marginal resistance to EVG (1.8 fold change) with the same trend observed in the 95% confidence interval for the variant enzyme as observed for DTG. In addition, our results show that R263K slightly increases integrase susceptibility to RAL and MK-2048. None of the drugs tested showed any significant inhibition of 3' processing (not shown), as previously reported [287].



**Table 3.3 Effects of R263K mutation on half-inhibitory concentrations ( $IC_{50}$ , nM) and 95% confidence intervals (nM) for various INSTIs.**

	<b>DTG</b>		<b>RAL</b>		<b>EVG</b>		<b>MK-2048</b>	
	$IC_{50}$	95% Confidence intervals	$IC_{50}$	95% Confidence intervals	$IC_{50}$	95% Confidence intervals	$IC_{50}$	95% Confidence intervals
<b>IN</b>	3.485	2.672 to 4.546	10.38	7.407 to 14.54	1.239	0.4682 to 3.278	2.578	1.923 to 3.455
<b>IN<sub>R263K</sub></b>	3.738	1.589 to 8.796	6.587	2.863 to 15.15	2.170	0.5246 to 8.977	1.472	0.5283 to 4.104

### 3.4.7 Addition of H51Y to R263K

In experiments with purified integrase enzyme, the H51Y substitution was found to have no effect on wild-type activity but in when combined with R263K, the double mutant showed increased loss of wild-type strand transfer activity compared to the R263K in isolation (Figure 3.4B).

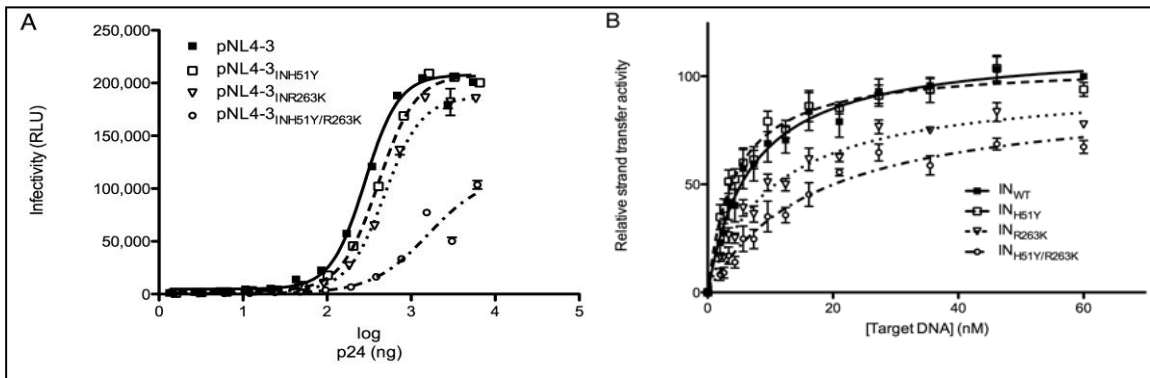


**Figure 3.4: H51Y reduces viral infectivity of integrase R263K virus by reducing integration.**

(A) pNL4.3IN(WT), pNL4.3IN(H51Y), pNL4.3IN(R263K), and pNL4.3IN(H51Y/R263K) infectivity was measured as the luciferase activity expressed in relative luminescent units (RLU) in the presence of increasing concentrations of virus (in ng of p24 antigen). (B) Strand transfer activity (in RFU/h) in the presence of 450 nM purified recombinant protein and the indicated concentration of target DNA.

This effect was also observed in cell culture with a drastic impact of the H51Y mutation on the infectivity of an R263K containing virus (Figure 3.4A) as measured by the Monogram Phenosense Integrase assay (Table 3.4). Conversely, the H51Y/R263K

combination resulted in higher levels of DTG resistance than R263K in isolation, with significant observed cross-resistance to EVG (Table 3.4).

**Table 3.4: H51Y increases resistance of R263K containing virus to DTG and EVG but drastically reduces viral replication.**

		<b>DTG</b>	<b>RAL</b>	<b>EVG</b>	<b>Replication capacity</b>
Backbone	Genotype	Fold change	Fold change	Fold change	
pNL4-3	WT	0.92	0.91	1.03	100%
	H51Y	1.25	1.11	2.06	89%
	R263K	1.95	1.21	3.28	70%
	H51Y/R263K	6.95	2.94	41.5	11%

### 3.4.8 *In silico* studies of R263K and H51Y/R263K mutant integrase.

The crystal structures of integrase from the prototype foamy virus (PFV) bound to DNA [283, 286] and DTG [290] have recently been elucidated. Other studies demonstrated that the structure of the HIV-1 IN is analogous to that of PFV [282, 284, 290]. Accordingly, we used protein data bank (PDB) IDs 3L2R [283], 3S3M [290] and 3OS0 [286] as starting points for structural refinement of wild-type and R263K intasome, drug-bound intasome, and the strand transfer complex (STC) respectively. Modeled HIV-1 integrase structures showed good global agreement with their template structures and with each other (Figure 3.5A). When integrase intasome and STC models were overlaid with the DNA ligands of their respective templates, R263 in wild-type integrase was

within 4Å of the viral long terminal repeat (LTR) fragment in both the intasome (not shown) and STC (Figure 3.5A).

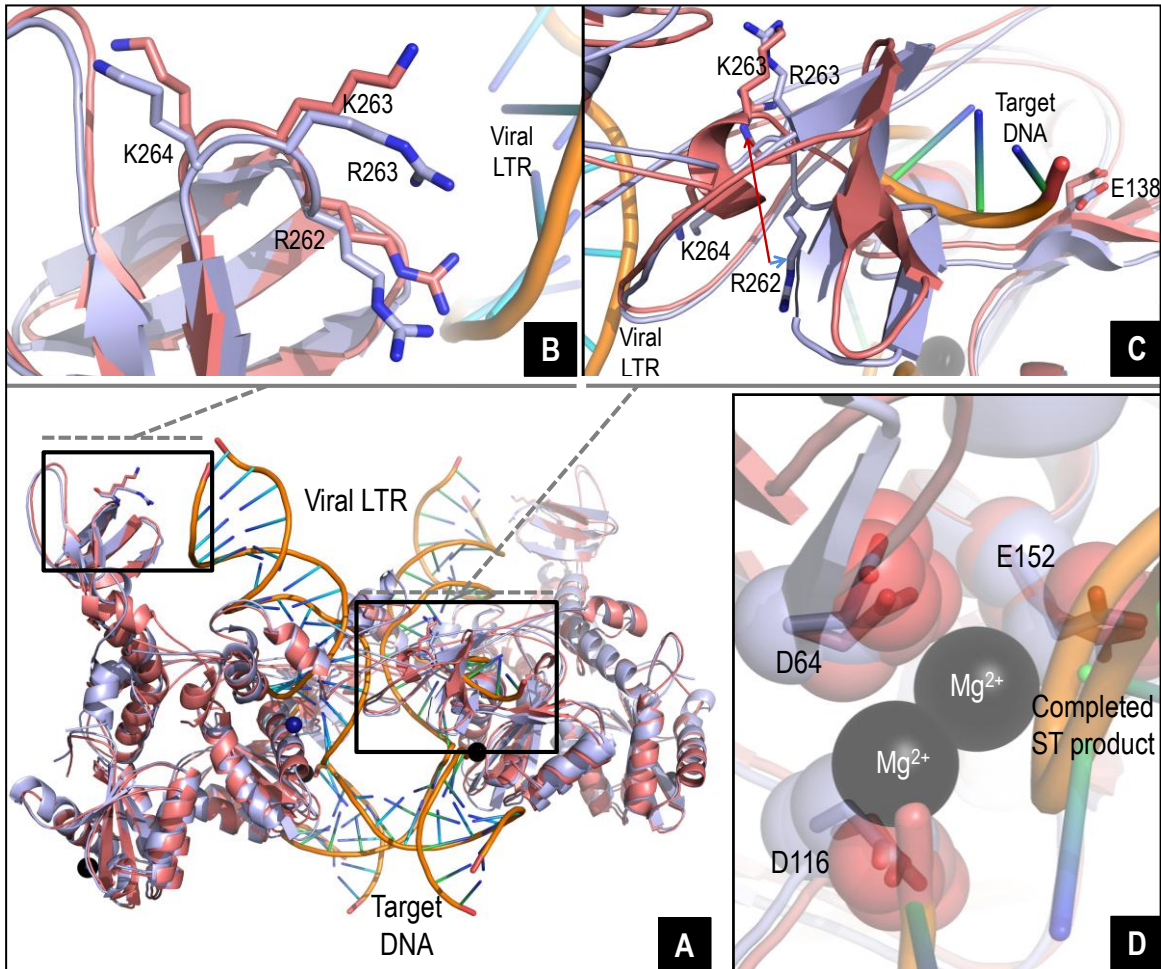


**Figure 3.5:** *In silico* studies of the wild-type and R263K integrase proteins.

(A-D) Overlay of the WT IN and INR263K integrase proteins, intasome, and strand transfer complex models with the viral LTR DNA and target DNA. The tetrameric IN structure is composed of the inner and outer subunits. (B) Detailed view (8Å) of the overlay showing proximity between residue 263 (R or K) in one of the outer subunits and the viral LTR. (C) Detailed view (12Å) showing the pronounced shift in localization and orientation of residue R262 in the presence of the R263K mutation at the vicinity of the

target DNA in one of the inner subunits. (D) Close-up overlay showing the relative positions of the D64D116E152 core catalytic residues in the WT and INR263K enzymes in the inner subunits.

The R263K mutation brings the R262 and K263 residues closer to the viral LTR mimic (Figure 3.5B), possibly affecting LTR binding. The short length of the LTR template prevented proper analysis of these differences in integrase-DNA interactions, but it is possible that this basic rich region, which has already been shown to be important for DNA binding and 3' processing [502, 503], has more DNA interactions than are obvious from modeling. A more dramatic spatial and orientation shift of R262 relative to its wild-type position was observed in the inner integrase subunits (Figure 3.5C), causing steric clashes that translate to the target DNA binding site and the active site periphery. A close-up of one active site shows insignificant differences in the relative positions of the D<sub>64</sub>D<sub>116</sub>E<sub>152</sub> catalytic residues between wild-type and R263K (Figure 3.5D), leading to the conclusion that the reduction in both integrase activities caused by this mutation is the effect of altered DNA substrate interactions. Additionally, in looking at the impact of the H51Y mutation, a comparison of wild-type IN (Figure 3.6A) to H51Y IN (Figure 3.6B) revealed no significant differences in secondary structure; however, a comparison of wild-type to R263K (Figure 3.6C) and H51Y/R263K (Figure 3.6D) demonstrated incremental disruptions in orientation of R262 and K264 that may contribute to viral DNA interactions [502, 504], resulting in a larger scale disruption of electrostatic interactions



in the C-terminus of integrase, which are transferred to key residues in INSTI drug resistance, P145, Q148 and Y143 [504]. Additionally, in the case of both R263K and H51Y/R263K, the orientation of the residue at position 51 is inverted (Figure 3.6C and 3.6D), which may have an impact on HIV-1 DNA binding ability, explaining the loss in fitness of the R263K and H51Y/R263K viruses.

#### **3.4.9 R263K impairs IN-DNA binding *in vitro*.**

To confirm our *in silico* studies, we performed *in vitro* IN-DNA binding assays using increasing concentrations of both wild-type IN and R263K IN (Figure 3.7). DNA binding was detected within a range of 62.5 to 2000 nM of purified IN. The results show that IN-DNA binding was significantly reduced in experiments performed with R263K as opposed to wild-type IN. These experiments confirm that the R263K mutation decreases IN-DNA binding under cell-free conditions

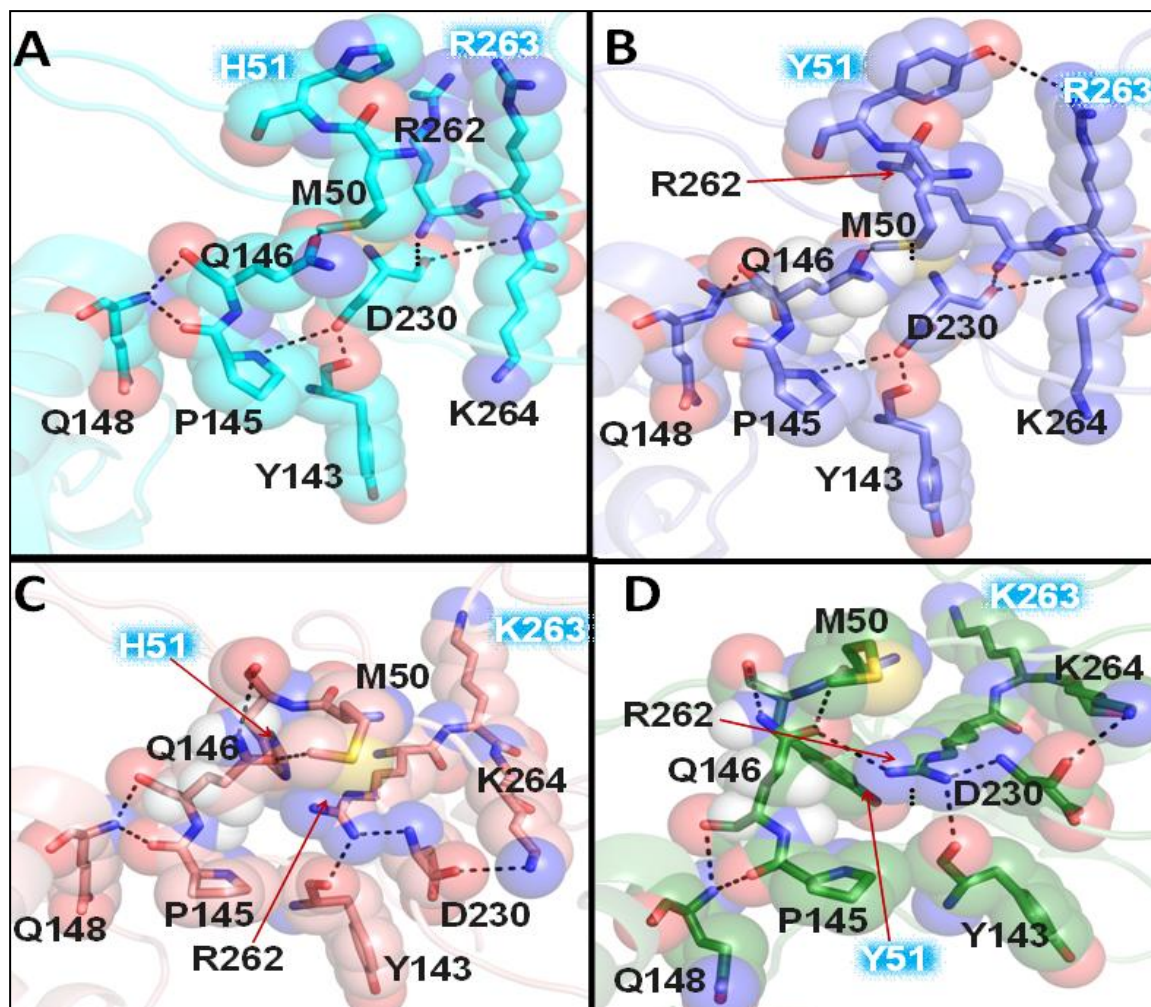


Figure 3.6: Effect of residues at position 51 and 263 on local side-chain electrostatic interactions and side-chain mobility in IN CTD.

(A) INwt (turquoise backbone) ; (B) INH51Y (purple backbone); (C) INR263K (salmon backbone) and (D) INH51Y/R263K (Dark green backbone). Highlighted residues are shown as sticks within partly transparent space-filling structures coloured according to standard atomic colouration. Suspected hydrogen-bonding ( $<3.5\text{\AA}$ ) and electrostatic interactions ( $<4.5\text{\AA}$ ) are represented by dotted black lines.

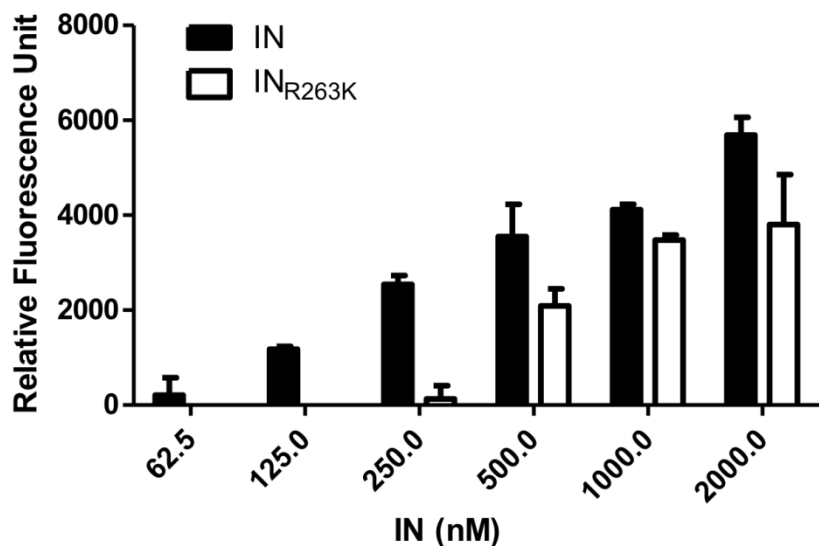


Figure 3.7: DNA-binding activity of purified recombinant wild-type (IN) and R263K (IN<sub>R263K</sub>) integrase proteins.

DNA-binding expressed in relative fluorescence units (RFU) in the presence of 10 nM target DNA and increasing concentrations of protein.

### 3.5 DISCUSSION

To extend previous studies [409, 487, 488], we performed *in vitro* selection experiments with DTG using viruses of several subtypes, B, C and A/G. The inclusion of non-B viruses in this study was necessary since such variants represent more than 90% of the HIV-1 pandemic [470]. It is important to determine the role that subtype-specific polymorphisms might play in the emergence of DTG-resistance [469].

Our serial passage study did not lead to the isolation of highly resistant viruses, in agreement with previous selection studies [409, 487, 488]. Our results show that subtype A/G and C viruses are not more likely to develop resistance to DTG than

subtype B viruses. Furthermore, we report the selection of several mutations with DTG *in vitro*, with R263K being the most common after 20 weeks of culture, i.e. 6/9 viruses. R263K was present in the selections with all five subtype B (5/5) and 1 of 2 A/G viruses (Table 3.1). At weeks 34-37, this mutation was detected in 3 of 4 B and 1 of 2 A/G subtypes. R263K was absent in the subtype C selections, although not enough viruses may have been tested. The partial R263K substitution identified at week 20 with the subtype C 5236 virus was replaced by S153Y after 37 weeks (Table 3.1). S153Y was previously documented during serial passage experiments with DTG [409]. Whether resistance or fitness accounts for the change from R263K to S153Y is currently under investigation.

Initially, R263K was identified as a secondary resistance mutation for EVG, arising in the presence of the major resistance mutation T66I [500] and has also been reported in patients treated with RAL [491]. Other selection studies with EVG did not show the emergence of R263K [501]. Most resistance mutations emerge from within the catalytic core domain (a.a. 50 to 212). Of more than 33 amino acids involved in resistance to INSTIs, only 2 (6%) are located in the C-terminal region of integrase. Hence, R263K, which is also located in this region, is an unusual mutation. We have shown that IN carrying R263K is less active than wild-type IN, resulting in a decrease in infectiousness (Figure 3.1A-B), that correlates with a specific decrease in viral DNA integration (Figures 3.1C-D). These results agree with biochemical studies that confirmed that IN<sub>R263K</sub> is impaired in regard to integration (Figure 3.2). In fact, each of infectivity in TZM-bl cells as

well as both 3' processing and strand transfer activities with variable DNA substrates were all reduced by approximately 20% if the R263K mutation was present (Figures 3.1, 3.2 and 3.3). Although R263K was shown in a previous study to be devoid of significant impact on DNA binding on its own, the presence of three mutations, i.e. R262D/R263V/K264E, severely impaired the ability of integrase to bind and cleave DNA [502]. In contrast, our results show that DNA binding is inhibited in the presence of the single R263K mutation. This discrepancy may be due to the fact that previous workers used only a minimal DNA-binding region to test for DNA binding (IN<sub>210-270</sub>) [502]. In addition, our data show that both 3'-processing and strand transfer activities were impeded by the R263K mutation (Figures 3.2 and 3.3), highlighting the importance of the R263 residue for integrase activity. *In silico* studies (Figure 3.5) supports this observation, since R263K can mediate structural changes in the HIV-1 IN intasome and strand transfer complex, ultimately impacting on integrase catalytic activities. Indeed, structural modeling of the HIV-1 intasome and strand transfer complex suggests that R263K causes a deviation in the spatial positioning and orientation of R262 in both the inner and outer subunits of IN. In the inner subunit, this deviation possibly affects IN-target interactions and hence strand transfer. The coordination of Mg<sup>2+</sup> by D<sub>64</sub>D<sub>112</sub>E<sub>152</sub> does not appear to be significantly affected by the R263K mutation.

Structural modeling might also shed light on experimental differences between cell-based and biochemical cell-free assays. Despite its selection in cell culture with DTG (Table 3.1) and a modest-level of resistance to DTG in cell-based assays (Table 3.2),

R263K did not confer significant levels of resistance to DTG in cell-free biochemical assays (Table 3.3). The difference between cell culture and biochemical assays could be due to the regulation of biological events that are not measured *in vitro* with purified recombinant proteins. For example, the presence of cellular co-factors that are important but non-essential for integrase activity *in vitro* and that are not included in the strand transfer assay could play an important role. Furthermore, the polypeptide 262-RRKAK-266 has recently been identified as important for integrase nuclear import [505]. Whether interaction with cellular co-factors and nuclear localization contribute to susceptibility to INSTIs is unknown. We previously identified another substitution, G118R, that also translates into a decrease in integrase activity and confers resistance to MK-2048 [481]. In this regard, integrase activities with other DTG-associated mutations [409] remain to be investigated. Importantly, neither these mutations nor R263K confers major resistance to DTG in cell culture or *in vitro*, confirming the potency of this drug. Interestingly, it is possible that second-generation INSTIs may favour the selection of R263K in subtype B viruses whereas G118R may be favoured in subtype C.

A number of secondary mutations, M50I, H51Y, E138K, V151I and D288E, were co-selected with R263K in the various cultures (Table 3.1). The absence of homogeneity in these secondary mutations suggests that they do not result in a major resistance pathway, although combination of these substitutions with R263K by site-directed mutagenesis will be necessary to confirm this point. M50I and D288E are natural polymorphisms detected in clinical isolates (<http://hivdb.stanford.edu/>, Stanford

University HIV drug resistance database). V151I is a polymorphic substitution that has been selected by several INSTIs, without having significant effects on RAL and EVG susceptibility [506-509]. H51Y is a E92Q-linked secondary mutation selected in the presence of EVG *in vitro* and in patients [501, 508]. Our current data suggests that the H51Y mutation does not compensate for the primary resistance mutation R263K but rather has an additional detrimental effect on IN-associated viral fitness and infectivity when R263K is present (Figure 3.5; Table 3.4). We believe that the fitness cost of the unique H51Y/R263K combination explains the absence of resistance mutations in previously drug-naïve patients treated to date with DTG.

In addition to R263K, our study shows that G118R was also occasionally selected with DTG (Table 3.1). We have previously shown that G118R is selected *in vitro* by MK-2048 and confers resistance to this INSTI [481]. Here, we also show that G118R emerged with subtype C and A/G viruses selected with DTG. No subtype B virus displayed this mutation over the course of the selection. Despite this, G118R was the second most common substitution observed during *in vitro* selection with DTG. From these studies and others [290], it appears that G118R bears further investigation in the context of DTG and MK-2048 and DTG.

## Chapter 4

### Biochemical analysis of the role of G118R-linked dolutegravir drug resistance substitutions in HIV-1 integrase

The majority of work presented in this chapter was previously published in the journal *Antimicrobial Agents and Chemotherapy* article below:

- Quashie PK, Mesplède T, Han YS, Veres T, Osman N, Hassounah S, Sloan R, Xu HT, Wainberg MA. **Biochemical analysis of the role of G118R-linked dolutegravir drug resistance substitutions in HIV-1 integrase.** *Antimicrob Agents Chemother.* 2013 Dec;57(12):6223-35. doi: 10.1128/AAC.01835-13. Epub 2013 Sep 30.

PKQ designed the project, performed most of the biochemistry, all the *in silico* simulations, and wrote the manuscript. TM performed molecular biology and edited the manuscript, YH, TV, NO and SH performed additional experiments, RS and HX helped in experimental design, MAW supervised the work and edited the manuscript.



## 4.1 Abstract

Drug resistance mutations (DRMs) have been reported for all currently approved anti-HIV drugs, including the latest integrase strand transfer inhibitors (INSTIs). We previously used the new INSTI dolutegravir (DTG) to select a G118R integrase resistance substitution in tissue culture and also showed that secondary substitutions emerged at positions H51Y and E138K. Now, we have characterized the impact of the G118R substitution, alone or in combination with either H51Y or E138K, on 3' processing and integrase strand-transfer activity. The results show that G118R primarily impacted the strand transfer step of integration by diminishing the ability of integrase-LTR complexes to bind target-DNA. The addition of H51Y and E138K to G118R partially restored strand transfer activity by modulating the formation of integrase-LTR complexes through increasing LTR-DNA affinity and total DNA binding, respectively. This unique compensatory mechanism in which one function of HIV integrase partially compensates for the defect in another function, has not been previously reported. G118R resulted in low-level resistance against DTG, raltegravir (RAL) and elvitegravir (EVG). The addition of either of H51Y or E138K, to G118R did not enhance resistance against DTG, RAL, or EVG. Homology modeling provided insight into the mechanism of resistance conferred by G118R as well as the effects of H51Y or E138K on enzyme activity. The G118R substitution therefore represents a potential avenue for resistance against DTG, similar to that previously described for the R263K substitution. For both pathways, secondary

substitutions can lead to either diminished integrase activity or increased INSTI susceptibility.

## 4.2 Introduction

The HIV integrase enzyme catalyzes the insertion of viral DNA into host DNA, a process known as integration [510]. In a reaction termed 3' processing, integrase recognizes and cleaves off a dinucleotide GT downstream of a conserved dinucleotide CA signal located within the last 15 bps of the long terminal repeats (LTR) that flank the viral DNA and this effectively creates new 3'- hydroxyl ends [511]. The second step in integration, termed strand transfer, is the integrase-mediated insertion of the processed viral DNA into host DNA by a 5- base-pair staggered cleavage of target-DNA. The exposed 3'- hydroxyl groups on the viral insert interact with exposed 5'- phosphates on the host DNA. Integration, which occurs primarily in highly expressed genes [512], causes the host machinery to transcribe viral genes and leads to successful propagation of viral particles. Integration is essential for productive infection and the establishment of viral persistence; therefore, integration was an early choice for the development of inhibitory compounds [513].

The development of *in vitro* microtiter plate-based biochemical assays for the measurement of the various biochemical activities of integrase facilitated compound screening and identification of viable integrase inhibitors [276]. The first specific integrase inhibitors, identified in 2000 [276], possessed diketoacid motifs and targeted the strand transfer activity of integrase; these compounds were thus termed integrase strand transfer inhibitors (INSTIs). The first INSTIs to be approved for therapy were raltegravir (RAL) in 2007 [211] and elvitegravir (EVG) in 2012 [514]. These compounds

have been shown to be highly potent, bioavailable inhibitors of integrase strand transfer [414], but have demonstrated low-moderate genetic barriers to the development of drug resistance substitutions (DRMs) [515]. There are three major pathways that are involved in resistance for RAL, commencing with substitutions at any of positions 155, 143 or 148 [317, 515, 516]]; EVG exhibits extensive cross-resistance with RAL due to substitutions at positions 155 and 148 [311, 336, 349, 515] and demonstrates other resistance pathways as well. This cross-resistance between RAL and EVG has necessitated the development of other INSTIs that possess higher barriers to resistance development as well as non-overlapping resistance profiles.

A newer INSTI, dolutegravir (DTG), has been shown in both preclinical and clinical studies to have higher potency and a higher barrier to resistance than either RAL or EVG [361]. DTG [154, 366, 373, 386, 414, 517-520] also binds to integrase protein with a longer residence time than either RAL and EVG [368] and has yet to select for resistance substitutions in HIV-positive previously antiretroviral (ARV)-naive patients receiving ARVs for the first time, despite having been used over a period of 96 weeks [154, 366, 521]. It is important to better understand the resistance profile of DTG as well as to determine whether differences in HIV subtype might ultimately affect the clinical performance of this drug.

We previously identified a G118R substitution in the integrase of subtype C HIV through cell-culture selections; G118R resulted in moderate levels of resistance to an experimental INSTI MK-2048 [352] and was also observed in a patient harboring HIV-1

CRF02\_A/G virus in whom it conferred high level resistance to RAL [408]. Prior to these reports, G118ACR mutants had only been selected in cell culture with the early INSTI S-1360, resulting in resistance to this compound [411]. More recent cell culture selections with DTG selected for the G118R substitution in subtype C and CRF02\_A/G clonal viruses but not in subtype B viruses [418]. In our MK-2048 selections, E138K was a secondary substitution that appeared after G118R and seemed to partially rescue its replication activity as well as to enhance resistance levels to MK-2048 [352]; E138K was also observed as a secondary substitution in one instance alongside R263K, the most common substitution associated with resistance to DTG in selection studies [418], although the role of E138K in the R263K resistance pathway has not been characterized. The primary RAL substitutions Q148H/K/R are often found together with E138K as a second or third substitution and, in this context, E138K has been shown to restore fitness and enhance resistance [317, 414].

The H51Y substitution was first reported as a secondary substitution to E92Q in the context of EVG treatment. It has also recently been observed as a secondary substitution to both R263K and G118R in DTG passage experiments [177, 418]. In our recently published work, we observed that the double mutant H51Y/R263K had lower LTR binding affinity and resulted in a virus that was less fit and less infectious than that containing only R263K [177].

Here we present a biochemical characterization of subtype B integrase proteins that harbor the G118R substitution, in isolation or in combination with either of the secondary

substitutions H51Y and E138K. We investigated the impact of these substitutions on the strand transfer activity of integrase and its ability to bind to substrates, i.e. the LTR and target-DNA. We also present homology modeling of the active site of integrase, based on the published foamy virus (PFV) strand transfer complex [380], and explain the cross-resistance profiles of integrase proteins for the three clinically relevant INSTIs, i.e. DTG, RAL and EVG. This work provides a detailed analysis of mechanistic, structural and sequence specific factors that may affect the *in vivo* development and maintenance of resistance substitutions and may be instrumental in predicting resistance pathways for INSTIs.

## 4.3 Materials and Methods

### 4.3.1 Antiviral compounds

The integrase inhibitor drugs RAL was provided by Merck & Co. Inc.; EVG and DTG were kindly provided by Gilead Sciences and GlaxoSmithKline, respectively. Prior to use, compounds were solubilised in dimethyl sulfoxide and stored at -20°C. All other reagents used were enzyme grade and of the highest available purity.

### 4.3.2 Site-directed mutagenesis

The generation of a  $\rho$ ET-15b expression plasmid containing soluble wild-type (WT) HIV subtype B integrase has already been described [305, 359]. PCR-mediated site-directed mutagenesis was performed on this plasmid to yield plasmid DNA encoding the G118R substitution, either in isolation or together with one of two additional substitutions, H51Y or E138K. The following primers were used for mutagenesis: G118R (CCAGTAAAAACAGTACATACAGACAATCGCAGCAATTTCCACC); G118R\_antisense (GGTGAAATTGCTGCGATTGTCTGTATGTACTGTTTTTACTGG); H51Y (CTAAAAGGGGAAGCCATGTATGGACAAGTAGACTGTA); H51Y\_antisense (TACAGTC TACTTGTCCATACATGGCTTCCCCTTTTAG); E138K\_sense (GGCGGGGATCAAGCAGA AATTTGGCATTCCCTA); and E138K\_antisense (TAGGGAATGCCAAATTTCTGCTTGAT CCCC GCC). Plasmid DNA was amplified and maintained in *E. coli* XL10-Gold ultracompetent cells Tet<sup>r</sup>,  $\Delta(mcrA)183$ ,  $\Delta(mcrCB-hsdSMR-mrr)173$ , *endA1*, *supE44*, *thi-1*, *recA1*, *gyrA96*, *relA1*, *lac Hte*, [ F', *proAB*,

*ladqZΔM15*, Tn10(Tet<sup>r</sup>) Amy Cam<sup>r</sup>] (Stratagene). Successful mutagenesis was confirmed by sequencing (Genome Quebec).

#### 4.3.3 Protein expression, purification and quantification

Plasmids bearing either WT or a G118R mutated IN gene were transformed into BL21(DE3) Gold cells F<sup>-</sup>, *ompT*, *hsdS*(<sub>r<sub>B</sub></sub><sup>-</sup>, <sub>m<sub>B</sub></sub><sup>-</sup>), *dcm*<sup>+</sup>, Tet<sup>r</sup>, *gal*, λ(DE3), *endA* Hte (Stratagene) for protein expression. Luria-Bertani (LB) broth (Multicell), prepared in MilliQ water and supplemented with 100 μg/mL ampicillin, was used for all bacterial growth. Expression and purification of integrase recombinant proteins were performed as previously described for His-tagged integrase [418]. Fractions containing purified integrase as judged by SDS-PAGE were dialyzed into storage buffer (20 mM Hepes, 1 M NaCl, 1mM EDTA, 5 mM DTT, 10 % glycerol, pH 7.5) with a molecular cut-off of 30 kDa. Protein concentrations were measured using a calculated extinction coefficient of 50420 M<sup>-1</sup>cm<sup>-1</sup>[418]. Protein aliquots could be kept for several months at -80°C without significant loss of activity or integrity.

#### 4.3.4 DNA substrates for *in vitro* assays

All oligonucleotide substrates were purchased from Integrated DNA Technologies (IDT, Coralville, IA, USA). The following oligonucleotides were used for strand transfer assays:

pre-processed	donor	LTR-DNA	sense	(A):	5'AmMC12-
ACCCTTTTAGTCAGTGTGGAAAATCTCTAGCA-3'			and	antisense	(B): 5'-
ACTGCTAGAGATTTTCCCACTGACTAAAAG-3';	target-DNA:	sense	(C):	5'-	
TGACCAAGGGCTAATTCAC-3'		and	antisense	(D):	5'-



AGTGAATTAGCCCTTGGTCA-3Bio-3'. The following oligonucleotides were used for LTR-DNA binding assays: (E) 5'-CTTTTAGTCAGTGTGGAAAATCTCTAGCAGT-3' and (F) 5'-/Rhodamine-XN/ACTGCTAGAGATTTTCCCACTGACTAAAAG-3'. For 3' processing assays, primer B was used together with the LTR-3'-sense oligonucleotide (G): \*5'AmMC12-ACCCTTTTAGTCAGTGTGGAAAATCTCTAGCAGT-BioTEG-3'. All these oligonucleotides have been previously described [177, 418, 450, 451]. Functional DNA duplexes were made by combining equimolar amounts of sense and antisense primers to appropriate concentrations in low-chelate TE buffer (10 mM Tris, 0.1mM EDTA pH 7.8), heated for ten minutes at 95°C, and annealed by slow cooling to room temperature over a period of 4 hours. Duplexes were stored at -20°C for several months without loss of integrity.

#### **4.3.5 Preparation of pre-processed LTR-coated plates for strand transfer activity**

Eighty µL of pre-processed viral LTR-mimic (donor DNA) duplex A/B, diluted to 150 nM (except as dictated by experiment design) in PBS pH 7.4 (Bioshop), was covalently linked to Costar DNA-Bind 96-well plates (Corning#2499) by overnight incubation at 4°C; negative control wells lacked any DNA duplex. The plates were blocked with 0.5% BSA in blocking buffer (20 mM Tris pH 7.8, 150 mM NaCl) and were stored in blocking buffer for several weeks without detectable loss in integrity. Before use, the plates were washed twice with each of PBS pH 7.4 and assay buffer (50 mM MOPS pH 6.8, 50 µg/mL BSA, 50 mM NaCl, 0.15% CHAPS, 30 mM MnCl<sub>2</sub>/MgCl<sub>2</sub>) except as dictated by experimental design.

#### 4.3.6 Protein calibration for strand transfer activity

The optimum concentration of protein to use in subsequent strand transfer experiments was determined by titrating protein concentration (effective [protein]= 0-1.8 $\mu$ M) in the presence of varying target-DNA concentrations (0-128nM). Pre-processed LTR-coated plates were prepared as described above. Purified integrase proteins, diluted appropriately in assay buffer supplemented with 5 mM DTT, were added followed by a 30 min incubation at room temperature to allow for assembly of integrase onto the pre-processed LTR duplexes. Biotinylated target-DNA duplex C/D was added and the plates were incubated for 1 h at 37°C (except when specified otherwise) for the strand transfer reaction to occur. The plates were then rinsed three times with wash buffer (50 mM Tris pH 7.5, 150 mM NaCl, 0.05% Tween20, 0.2 mg/mL BSA) and incubated with Eu-labeled Streptavidin (Perkin Elmer) diluted to 0.025  $\mu$ g/mL in wash buffer in the presence of 50  $\mu$ M DTPA (Sigma). After additional rinses with wash buffer, 100  $\mu$ L of Wallac enhancement solution (Perkin Elmer) was added. Ionization of conjugated-Eu to free aqueous Eu<sup>3+</sup> is caused by the low pH of the enhancement solution (pH <4). Excitation of Eu<sup>3+</sup> ions by incident wavelength at 355 nm resulted in time-resolved emission of fluorescence (TRF) that was measured at 612 nm on a FLUOStar OPTIMA multi-label plate reader (BMG Labtech) in TRF mode.

Protein concentrations that yielded the highest activity (300 nM) as measured by RFU were chosen for subsequent experiments. A common target concentration was also chosen in this experiment for subsequent experiments.

#### **4.3.7 Time-phase strand transfer activity assay**

Pre-processed LTR plates were prepared and washed as above. Fifty  $\mu\text{L}$  of reaction buffer (assay buffer supplemented with 5 mM DTT) were then added to each well. At time intervals of 10 min, 50  $\mu\text{L}$  of 3X WT integrase enzyme (900 nM) was added to one column of wells followed immediately by addition of 50  $\mu\text{L}$  of target-DNA (0-128 nM). Incubation at 37°C follows immediately to initiate transfer reaction in that column. All transfers between the incubator and pipetting station were done with the aid of heating blocks pre-calibrated to 38°C; this reduced temperature variations that might have impacted ongoing strand transfer reactions. After two hours, integrase and target were added to the final column and the plates were immediately inverted to stop the reactions. The plate was quickly washed three times with wash buffer to remove all traces of unreacted protein and target. All subsequent steps of the assay were as described above for the strand transfer assay. Following detection of TRF, the raw data was processed in GraphPad Prism V5.0 (GraphPad Software, San Diego California USA, [www.graphpad.com](http://www.graphpad.com)) using Michaelis-Menten settings, and kinetic parameters obtained for the particular enzyme employed. Departure from linearity for data-points in the range of 0- 70 min were tested using linear regression analysis in GraphPad Prism. The mean of at least three independent experiments is reported.

#### **4.3.8 Fixed [LTR]- variable [target] strand transfer activity assay**

In order to obtain kinetic activity parameters for WT and variant integrase proteins, strand transfer reactions were carried out as described based on the same design as

that for the protein calibration assay described above. The major difference is that effective LTR and integrase concentrations 80 nM and 300 nM, respectively, were used for these assays. All other experimental procedures were as described above. The mean of at least three independent experiments, each performed in triplicate for each integrase protein was calculated. The data were analyzed using Michaelis-Menten kinetics in GraphPad Prism.

#### **4.3.9 Variable [LTR]- variable [target] strand transfer activity assay**

In order to test the binding dynamics of LTR mimic and target-DNA, twelve concentrations of pre-processed LTR-DNA mimic (effective assay concentrations: 0-160 nM) were used to coat Costar DNA-Bind 96-well plates as described above. The plates were incubated overnight at 4°C, followed by an overnight incubation with blocking buffer (4°C). An equimolar amount of integrase (effective concentration = 450 nM) was added to each well followed by 50 µL of 0-128 nM target-DNA. The plates were then incubated at 37°C. After 1 h, the reaction was stopped by inversion of the plates followed by appropriate washing, and the Eu-Streps hybridization and detection steps. Data for three independent experiments for each integrase protein were fit by GraphPad Prism to the user-defined bisubstrate equilibrium-ordered kinetic equation [522, 523] shown below:

$$K_{App} = K_b (A + K_{ia}) / A$$

$$V = V_{max} B / (K_{App} + B)$$

In the above equations,  $A = [\text{LTR}]$  in nM,  $B = [\text{Target}]$  in nM,  $K_{ia}$  refers to the stability of the enzyme-LTR complex,  $V$  refers to enzyme activity in RFU/h,  $V_{\max}$  refers to the maximum activity in RFU/h,  $K_{App}$  refers to the apparent  $K_m$  for target observed for a given concentration of LTR. To reflect the likely order of substrate addition *in vivo*, LTR was assumed to bind first, followed by target-DNA.

#### 4.3.10 LTR-DNA binding assay

The LTR binding ability of our purified integrase proteins was measured as previously described [451]. Briefly, Corning® 96 well black flat bottom polystyrene high bind microplate wells (Corning #3925) were coated overnight at 4°C with HIV integrase proteins (500 nM) diluted in PBS pH 7.4; negative control wells were only incubated with PBS. Unbound proteins were removed by rapid inversion and subsequent wash with 200  $\mu\text{L}$ /well of PBS (pH 7.4). The plates were then blocked with 200  $\mu\text{L}$  of PBS (pH 7.4) containing 5% BSA at room temperature for 2 h. After blocking, the coated plates were washed twice with PBS and once with binding buffer (20 mM MOPS pH 7.2, 20 mM NaCl, 7.5 mM  $\text{MgCl}_2$ , 5 mM DTT). Fluorescently labeled RhoR-LTR (duplex E/F: 0- 200 nM) was then added into each well, and the plates were incubated at room temperature in the dark for 1 h. After the incubation, the reaction mixtures were removed by rapid inversion and plates washed 3 times with 200  $\mu\text{L}$  of PBS. After removal of the final wash, 100  $\mu\text{L}$  of PBS were added to each well and the fluorescent signals were measured at an excitation wavelength of 544 nm and an emission wavelength of 590 nm using a FLOUstar Optima plate reader.

Control reactions without IN (protein-free) or LTR were performed under the same reaction conditions to monitor the background signal ( $B_{\text{background}}$ ). Reactions with immobilized HIV-1 IN under different conditions were performed to measure the total binding activity ( $B_{\text{total}}$ ). The HIV-1 IN DNA binding activity for each sample was calculated using the following equation:

$$BA_{\text{sample}} = (B_{\text{total}} - B_{\text{background}})$$

To determine the apparent  $K_d$  value, IN (500 nM) was incubated with increasing concentrations of RhoR-LTR (from 0 to 200 nM), and the  $K_d$  value was calculated by directly fitting the titration curve using GraphPad Prism with nonlinear one-site binding regression.

#### **4.3.11 3' processing assay**

The determination of 3' processing activity of the purified recombinant integrase proteins was performed as previously described [450]. Briefly, 3' biotinylated LTR duplex G/B was covalently linked at varying concentrations (0-36 nM) to Costar DNA-bind plates under similar conditions as for strand transfer. To initiate 3' processing, purified integrase protein (300 nM) in reaction buffer (50 mM MOPS pH6.8, 50 mg/mL BSA, 50 mM NaCl, 20 mM  $\text{MnCl}_2$ , 0.015% CHAPS, 5 mM DTT) and the plates were incubated at 37°C. Negative protein control wells had only reaction buffer added. After 2h of incubation, the plate was quickly washed three times with wash buffer to remove all traces of protein and cleaved 3'GT-BIOTEG. All subsequent steps of the assay were as described above for the strand transfer assay with the exception of data analysis. For

each plate and concentration of LTR, four negative protein controls contained unprocessed LTR and the average signal from these represented the maximum possible TRF signal ( $3'OH_{max}$ ). For each protein, the TRF signal observed ( $3'OH_{obs}$ ) represented unprocessed LTR. Thus the TRF signal representing actual 3' processing activity ( $3'OH_{actual}$ ) was determined by the calculation:

$$(3'OH_{actual}) = (3'OH_{max}) - (3'OH_{obs})$$

The calculated 3' processing readings ( $n \geq 8$ ) were then processed in GraphPad Prism to yield 3' processing kinetic parameters for the particular integrase protein employed.

#### **4.3.12 Competitive inhibition of strand transfer inhibition by DTG, RAL and EVG**

The susceptibilities of our purified integrase proteins to INSTIs were tested in competitive inhibition assays using the compounds DTG, RAL and EVG. Drug stock solutions were prepared as 6× working solutions at a concentration of 6 μM and subsequently serially diluted 4-fold in compound dilution buffer (assay buffer containing 10% DMSO) to concentrations between 1.2- 6000 nM; inhibition assays were performed in the presence of varying target-DNA concentrations (0-128 nM). Briefly, pre-processed LTR-coated plates (effective LTR concentration= 160 nM) were prepared as described above. Purified integrase proteins (effective concentration= 300 nM) in assay buffer supplemented with 5 mM DTT were added to each well followed by a 30 min incubation at room temperature to allow for assembly of integrase onto the pre-processed LTR duplexes. Twenty-five μL of appropriately diluted compound were added to each well followed immediately by 25 μL of appropriately diluted biotinylated target-DNA duplex.

The plates were then incubated for 1 h at 37°C, followed by the usual post strand transfer steps described above. Data from three independent competition assays for each protein were fit to the competitive inhibition algorithm using GraphPad Prism. Inhibitory constants ( $K_i$ ) calculated by this algorithm were transformed to fold-change (FC) values by division with the  $K_i$  value for WT B integrase enzyme.

#### **Data processing.**

All cell-free experiments presented herein, except when otherwise indicated, were the result of at least 3 independent sets of experiments. When relevant, statistical significances of differences between datasets for two or more integrase proteins were determined using a one sample two-tailed t test. Probability values equal to or below 0.05 ( $p \leq 0.05$ ) were used to indicate statistically significant differences between different proteins.

#### **4.3.13 Homology modeling.**

Homology models of the HIV-1 integrase strand transfer complex (STC) were created based on the STC [380] of PFV. Amino-acid sequences that were of WT origin or that had been point mutated at desired positions were submitted to the I-TASSER 3D protein prediction server [453]; the prototype foamy virus (PFV) crystal structure PDB ID: 3OY9 [380] was selected as a lead template for the modeling. Rotamer orientations for key residues in the active site, especially the mutated residues, were interrogated; whenever possible, the best backbone-dependent rotamers were selected [524, 525]. Model quality was assessed based on root mean square deviation (RMSD) of the global



homology structure from the PFV lead template using the RCSB PDB Protein Comparison Tool. Superimposition of the HIV-1 homology models with the published co-crystal structures of PFV with DTG (PDB ID: 3S3M) [370], RAL (PDB ID:30YA) [380] and EVG (PDB ID: 3L2U) [380] provided insights into the mechanism of resistance caused by G118R substitution in regard to these three INSTIs. DNA interaction hints were obtained by overlaying the HIV-1 homology models with the PFV crystal structure PDB ID: 4E7K, representing the target capture complex (TCC) [416]. The molecular visualization program PyMOL (<http://pymol.org/>, The PyMOL Molecular Graphics System, Version 1.3, Schrödinger, LLC) was used for structural visualization and image processing.

## 4.4 Results

### 4.4.1 Generation of recombinant integrase proteins and calibration of enzyme activity

HIV integrase encoding plasmids that carried the G118R substitution alone or in combination with either of the H51Y or E138K substitutions were created. Generation of the G118R substitution was by a single G→C nucleotide change at position 118 in integrase from GGC to CGC; the other two substitutions, H51Y and E138K, occurred by more common G→A single base-pair changes (Figure 4.1A). Mutated or WT proteins were expressed in and purified from *E. coli* BL-21 DE3 cells to greater than 90% homogeneity (Figure 4.2B).

The HIV integrase protein has been shown to lose activity at high concentrations due to non-specific aggregation [376-378, 510] and it is thus necessary to determine the dynamic range of its activity before its use in enzyme assays. In order to determine appropriate protein and target-DNA concentrations, the strand transfer activity of both WT and mutated integrase preparations were monitored as previously described [418] in the presence of varying protein (37 nM- 1800 nM) and target-DNA concentrations (0- 256 nM) (Figure 4.1C). From these experiments, an optimum integrase protein concentration of 300 nM and a maximum target-DNA concentration of 128 nM were employed; significant differences were not observed between variants and/or purifications. Since most of our experiments were performed for a fixed period of 1h, we confirmed that the results using WT enzyme were within the linear phase of the strand transfer reaction over this time through use of time-resolved activity assays (not shown).

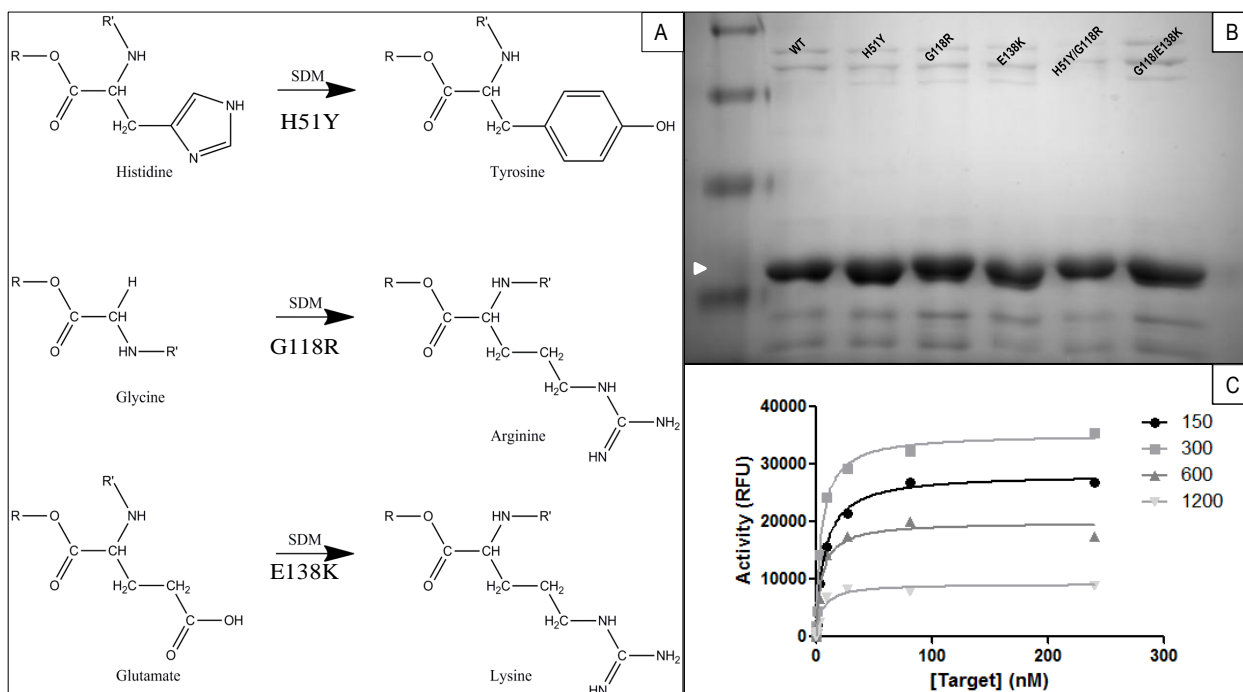


**Figure 4.15: Generation and quantitation of drug resistant HIV-1 integrase proteins.**

Site-directed mutagenesis was used to change the nucleotide sequences at codons 51, 118 and 138 resulting in plasmids encoding G118R, H51Y/G118R and G118R/E138K integrase proteins (A). Successful purification of integrase (white arrow) proteins was confirmed by SDS page analysis (B). Optimum protein and target DNA concentrations were determined by performing strand transfer reactions in the presence of varying concentrations of integrase protein. Although these experiments were performed for all the proteins tested at concentrations ranging from 37 to 1800 nM, only wild-type is shown at concentrations between 150 and 1200 nM.(C).

#### 4.4.2 G118R causes a deficit in integrase strand transfer activity

The G118R substitution had previously been shown by our group to reduce viral replication and infectivity; the addition of E138K partially rescued this defect [352]. We

also showed that the addition of H51Y to R263K further reduced each of strand transfer activity, viral replication, and infectiousness [177] In both cases neither H51Y nor E138K alone had any significant effect on integration and/or viral replication or infectivity [177].

**Table 4.1: Strand transfer activity parameters for purified integrase proteins**

Subtype B Integrase Protein	Fixed [LTR] Strand transfer Activity			Variable LTR/Variable Target Assay		
	$V_{max} \pm SEM$ (RFU/hr)	Target $K_m \pm SEM$ (nM)	$V_{max}/K_m \pm SEM$ (RFU/hr/nM)	$V_{max} \pm SEM$ (RFU/hr)	Target $K_m \pm SEM$ (nM)	$V_{max}/K_m \pm SEM$ (RFU/hr/nM)
Wild-type	21300 ± 1371	2.13 ± 0.42	10208 ± 1842	18896 ± 4460	2.54 ± 0.562	21273 ± 11493
G118R	10815 ± 2185	22.0 ± 7.21	458 ± 21	20490 ± 2870	24.5 ± 8.80	1962 ± 473
G118R/H51Y	16615 ± 1987	24.3 ± 6.72	880 ± 141	19715 ± 3242	5.43 ± 0.886	4886 ± 1303
G118R/E138K	12730 ± 4001	13.2 ± 7.84	995 ± 45	19793 ± 2644	8.00 ± 1.65	9278 ± 4989

♠ $K_m=K_b$  from variable LTR/variable target assays. All data presented is the result of at least 3 independent experiments

We wished to confirm that the partial rescue of G118R by E138K occurred at the level of strand transfer. To study this, we used pre-processed LTR in our assays, and decoupled the strand transfer activity of integrase from its 3' processing activity to uniquely examine strand transfer. Target-saturation strand transfer experiments were performed using fixed concentrations of integrase protein (300 nM) and viral LTR mimic (80 nM) at variable target-DNA concentrations (0-128 nM) (Figure 4.2). In agreement with previous work [352], the presence of G118R resulted in > 50% loss in maximal strand transfer activity ( $V_{max}$ ); this loss was partially rescued by the addition of H51Y and E138K (Figure 4.2A). The  $K_m$  for the strand transfer reaction for the G118R enzyme was increased by

~10-fold over WT, indicating lower target-DNA affinity, and - the addition of E138K reduced this deficit to ~6-fold, although this effect was not statistically significant (Table 4.1).

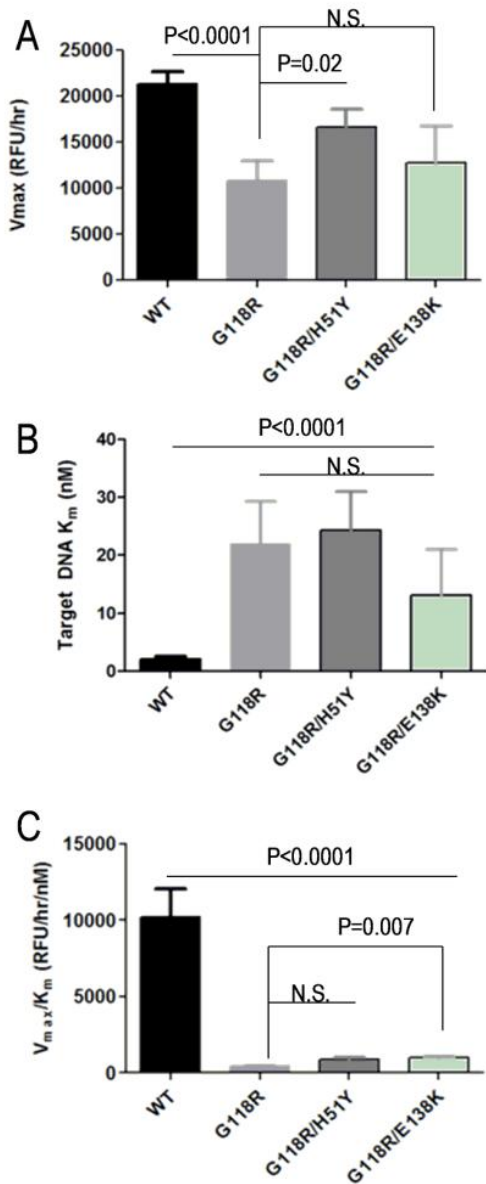


**Figure 4.2: Strand transfer activities of purified recombinant integrase proteins at target saturation.**

Strand transfer activities were measured using an immobilized pre-processed LTR plate-based assay. Graph Pad Prism was used to transform TRF data using the Michaelis-Menten functionality to obtain Vmax (A) and Km values (B). Enzyme performance was determined by division of Vmax with Km (C). Data presented is the mean of at least 3 independent experiments each performed in triplicate (n≥9). Error bars represent the standard error of the mean (SEM). Statistical significance was calculated for individual data pairs using a one sample two-tailed test with a statistical cut-off of p≤0.05. N.S.= not significant.

Since *in vivo* enzyme activity does not differentiate between  $V_{\max}$  and  $K_m$  effects, enzyme performance calculations ( $V_{\max}/K_m$ ) can be used to assess the effect of substitutions in enzymes *in vivo*, when substrates may be in limiting concentration [526]. Additionally, this analysis provides a more accurate representation of the activity of single-turnover enzymes such as integrase [527]. We observed that G118R caused a ~96 % reduction in enzyme performance and that the secondary substitutions H51Y and E138K minimally rescued activity by 2% and 4%, respectively (Figure 4.2C). Only the E138K rescue reached statistical significance ( $P=0.007$ ).

#### **4.4.3 Addition of H51Y and E138K to G118R regulates the formation of integrase-LTR complexes**

The ability of integrase to bind viral LTR impacts on the efficiency of the strand transfer reaction [378]. We thus investigated if the loss in enzyme activity and performance, attributed to the G118R substitution, was related to deficits in LTR affinity or solely to deficits in target-DNA binding and catalytic activity. A LTR-DNA binding assay, performed as previously described [451] showed that G118R did not affect either the dissociation constant ( $K_d$ ) or the ability of integrase to bind to the LTR mimic in our assay (Figure 4.3). The  $K_d$  values for WT integrase in these experiments were in agreement with previous reports [451, 527, 528] (Table 4.2).

Binding of LTR by G118R/H51Y integrase was tighter than that by WT enzyme, indicating an increase in substrate selectivity but was associated with a reduction in total LTR bound (Figure 4.3A-C).

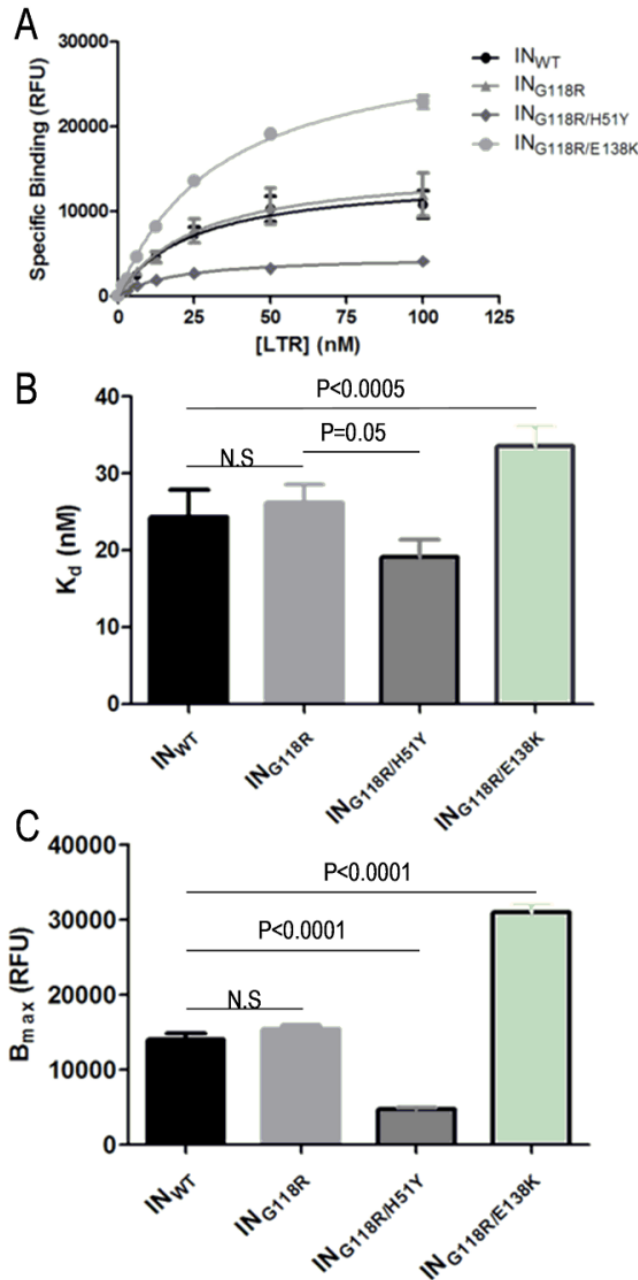


**Figure 4.3: LTR binding experiments using purified integrase proteins.**

IN-DNA binding reactions were performed with varying concentrations of RhoR-LTR and were fitted to nonlinear one-site binding regression (A) to obtain values of  $K_d$  (B) and  $B_{max}$  (C). Data presented is the mean of at least 3 independent experiments each performed in duplicate ( $n \geq 6$ ). Error bars represent the standard error of the mean (SEM). Statistical significance was calculated for individual data pairs using a one sample two-tailed test with a statistical cut-off of  $p \leq 0.05$ . N.S.= not significant.

The G118R/E138K integrase variant showed less tight binding to the LTR (Figure 4.3A, B) but possessed twice the maximal LTR binding ability of WT enzyme (Figure 4.3A, C). Taken together, these results suggest that a deficit in target-DNA binding but not LTR-DNA usage may account, at least in part, for the diminished enzymatic performance of the G118R integrase. The partial compensatory mechanism described here for both the H51Y and E138K secondary substitutions has not been reported previously.

#### 4.4.4 G118R reduces 3' processing activity yet G118R/H51Y and G118R/E138K are fully active

We showed above that the G118R substitution caused no difference in the ability of mutant enzyme to bind viral LTR-DNA and that G118R/H51Y and G118R/E138K increased binding specificity or total DNA binding relative to WT, respectively (Figure 4.3B). We thus wanted to see the effect of these differences in LTR binding on the 3' processing reaction.

**Table 4.2: 3' processing parameters for purified integrase proteins**

Subtype B Integrase Protein	LTR Binding Assay			3' processing Assay	
	$K_d \pm \text{SEM}$ (nM)	$B_{\text{max}} \pm \text{SEM}$ (RFU)	$V_{\text{max}} \pm \text{SEM}$ (RFU)	LTR $K_m \pm \text{SEM}$ (nM)	$V_{\text{max}}/K_m \pm \text{SEM}$ (RFU/nM)
Wild-type	24.2 ± 3.58	14079 ± 796.5	13101 ± 217	10.6 ± 0.46	1235 ± 18.8
G118R	26.2 ± 2.42	15419 ± 559.1	11887 ± 1292	17.9 ± 3.99	675 ± 46.3
G118R/H51Y	19.1 ± 2.24	4715 ± 198.2	35497 ± 3098	17.0 ± 2.42	2099 ± 68.2
G118R/E138K	33.5 ± 2.55	31022 ± 1002	19958 ± 1903	11.7 ± 2.04	1727 ± 81.6

All data presented is the result of at least 4 independent experiments, each performed in duplicate.



Using a previously reported and validated assay [450], we observed no significant differences between the 3' processing activity of WT and G118R integrase proteins, while both G118R/H51Y and G118R/E138K had significantly higher 3' processing activity than WT (Figure 4.4A-B). This led to significantly higher enzyme performance levels for the two double mutants relative to both the WT and G118R enzymes (Figure 4.4C). The G118R substitution, despite having a similar  $V_{max}$  to WT enzyme, showed a 40% increase in its  $K_m$  (Table 4.2); this, however, does not represent a major reduction in enzyme activity and would not account for the drastic reduction in viral integration and replication ability previously reported [352].

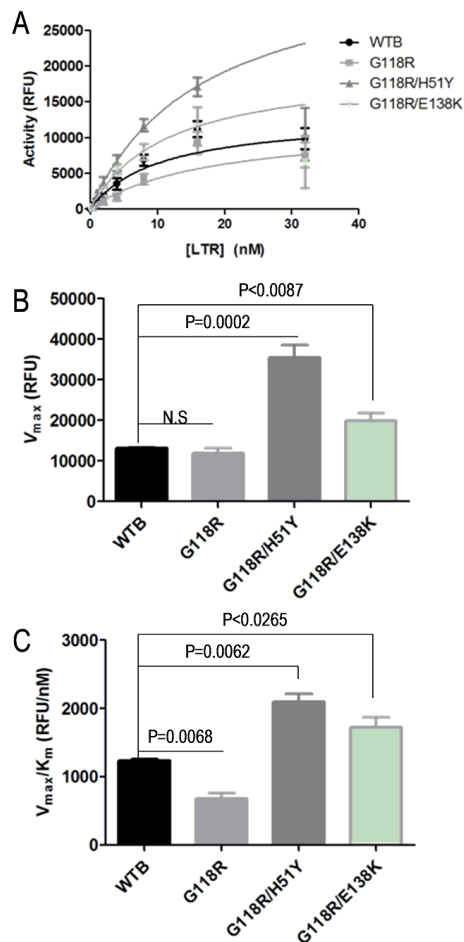


**Figure 4.4: Measurements of the 3' processing activities of integrase.**

3' processing activities of the various integrase proteins were determined using a fixed enzyme concentration and varying concentrations of immobilized LTR-DNA. The raw TRF data for 3' processing were calculated as described in the Methods section and data were fitted in GraphPad Prism to Michaelis-Menten kinetics (A) to obtain

values of  $V_{max}$  (B) and  $K_m$ . Enzyme performance (C) was determined by division of  $V_{max}$  by  $K_m$ . Data presented is the mean of at least 4 independent experiments each performed in duplicate ( $n \geq 8$ ). Error bars represent the standard error of the mean (SEM). Statistical significance was calculated for individual data pairs using a one sample two-tailed test with a statistical cut-off of  $p \leq 0.05$ . N.S.= not significant.

#### **4.4.5 H51Y and E138K partially rescue G118R activity by enhancing LTR-DNA binding**

The LTR-DNA binding assay indicated that a loss in enzyme performance may be partially attributable to deficits in target binding to the integrase-LTR-DNA complexes. Integration requires two substrates, i.e. viral LTR and target-DNA. In addition, LTR binding and 3' processing take place in the cytoplasm while strand transfer occurs in the nucleus, thus the addition of DNA substrates to integrase is essentially a sequential ordered bi-substrate reaction [522] with the LTR binding first. In order to obtain a more accurate measure of the strand transfer reaction in an ordered sequential addition bi-substrate reaction model, we varied both the concentrations of LTR-DNA (0- 160nM) and target-DNA (0- 128 nM) in the presence of a fixed enzyme concentration (Figure 4.5).

Integrase strand transfer  $V_{max}$  values calculated by this approach did not differ significantly between proteins (Table 4.1) and both the G118R/H51Y and G118R/E138K enzymes possessed target affinity ( $K_b$ ) similar to WT integrase (Figure 4.5E), with enzyme performance levels for G118R/H51Y and G118R/E138K being 22% and 44% of

WT, respectively. However, the G118R variant showed similar target-DNA affinity as was seen in our initial assays (Figure 4.2), with enzyme performance levels being 91% below that of WT enzyme (Figure 4.5F, Table 4.1). Thus, the G118R substitution appears to reduce integration by affecting target-DNA binding, and the addition of either H51Y or E138K increases strand transfer efficiency by enhancing LTR binding to integrase.

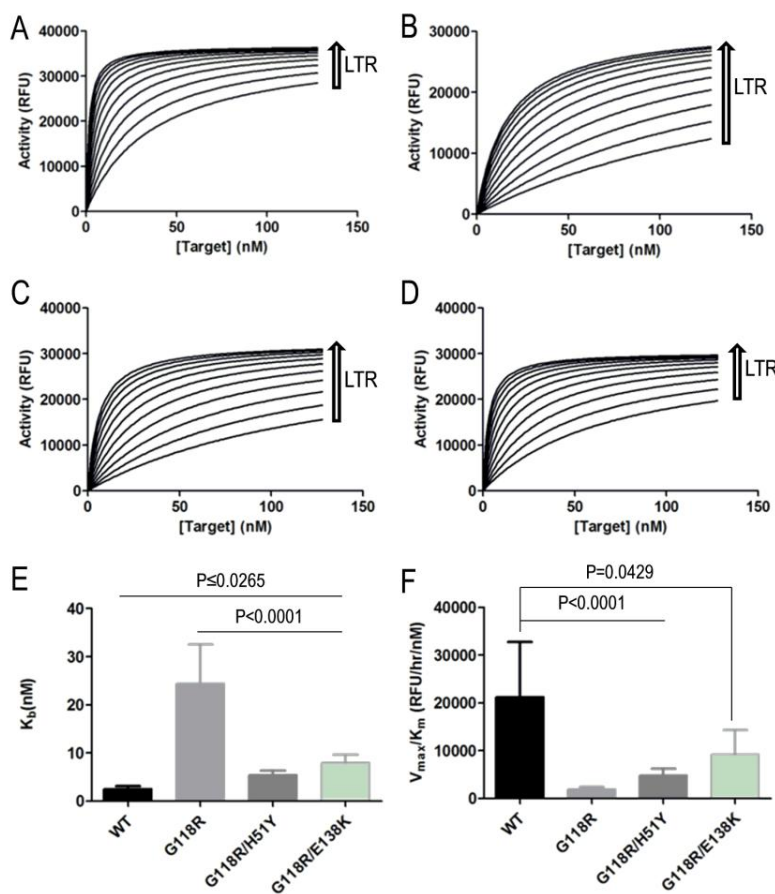


**Figure 4.5: Measurements of the strand transfer activities of integrase with bisubstrate variation.**

Strand transfer activities of the various integrase proteins were determined by using a fixed enzyme concentration and varying concentrations of LTR-DNA and target-DNA. The raw TRF data were fitted in GraphPad Prism to an

ordered sequential-addition kinetic mechanism for WT (A), G118R (B), G118R/H51Y (C) and G118R/E138K (D) integrase proteins. The affinity of target-DNA for enzyme was assessed by the calculated  $K_b$  values (E). Enzyme performance (F) was determined by

division of  $V_{\max}$  by the  $K_m$ . Data presented is the mean of 3 independent experiments (n=3). Error bars represent the standard error of the mean (SEM). Statistical significance was calculated for individual data pairs using a one sample two-tailed test with a statistical cut-off of  $p \leq 0.05$ . N.S.= not significant.

#### **4.4.6 The H51Y and E138K double mutants do not show increased resistance to DTG, RAL and EVG**

Primary drug resistance substitutions tend to cause deficits in enzyme activity and the presence of secondary substitutions usually restore fitness and increase the level of resistance to a particular inhibitor [336]. We have shown above that the performance loss caused by the G118R substitution in integrase can be partially rescued by either the H51Y or E138K secondary substitutions and therefore also wished to learn whether the addition of either of these substitutions to G118R would also affect levels of resistance to DTG, RAL and EVG. Numerous reports have confirmed that INSTIs act by direct competition with target-DNA and can also coordinate to divalent cations that are bound at the active site of integrase [276, 280, 359, 529]. Now, we performed target saturation assays in the presence of varying concentrations of RAL, EVG or DTG (0-5 $\mu$ M) (Figure 4.6A).

**Table 4.3: Susceptibilities of purified integrase proteins to DTG, RAL and EVG**

Subtype B Integrase Protein	$K_i \pm \text{SEM}$ (nM)			~FC		
	RAL	EVG	DTG	RAL	EVG	DTG
WT	1.83 $\pm$ 0.44	2.22 $\pm$ 0.92	1.25 $\pm$ 0.13	1	1	1
G118R	6.29 $\pm$ 2.66	10.2 $\pm$ 2.46	3.94 $\pm$ 0.60	3.4	4.6	3.1
G118R/H51Y	5.16 $\pm$ 1.30	7.08 $\pm$ 0.69	4.26 $\pm$ 0.50	2.8	3.2	3.4
G118R/E138K	4.12 $\pm$ 0.34	1.95 $\pm$ 0.19	0.78 $\pm$ 0.26	2.3	0.88	0.64

All data presented in the result of at least 3 independent experiments

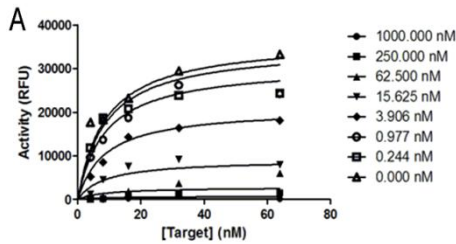
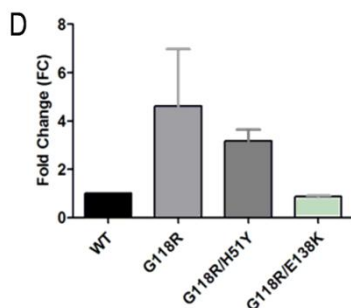
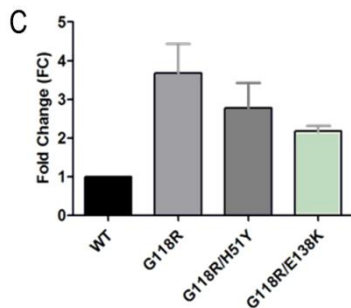
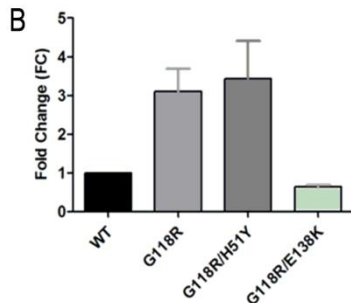


**Figure 4.6: Competitive inhibition of strand transfer by DTG, RAL and EVG. Strand transfer reactions were carried out in the presence of 300 nM integrase.**



Transfer of target-DNA was competitively inhibited with each of DTG, RAL and EVG. Raw data from three independent experiments were fit to the competitive inhibition equation using GraphPad Prism. A representative plot for the competitive inhibition of WT integrase DTG is shown (A). The fold-change in susceptibility of each variant to DTG (B), RAL (C) and EVG (D) was calculated by division of the  $K_i$  for each variant by that for WT integrase. Data presented is the mean of at least 3

independent experiments ( $n \geq 3$ ). Error bars represent the standard error of the mean (SEM).

The data were fitted by non-linear regression analysis to a competitive inhibition algorithm using GraphPad Prism to yield an inhibitory constant ( $K_i$ ) for each drug-enzyme combination (Table 4.3). Unlike  $IC_{50}$  measurements, which can vary if substrate concentrations are not sufficiently saturating, the  $K_i$  is an intrinsic property of each enzyme-inhibitor complex and is independent of substrate concentration [522].  $K_i$  fold-change (FC) results were obtained by dividing the  $K_i$ s of the individual variants by that of WT enzyme (Figure 4.6B-D). The presence of G118R caused a 3.1 fold-change in resistance to DTG. The addition of H51Y to G118R did not have significant effect on resistance to DTG (Figure 4.6B). As previously reported [352], G118R conferred low-level resistance to both RAL (Figure 4.6C) and EVG (Figure 4.6D). In both cases, the addition of either H51Y or E138K to G118R caused reductions in level of resistance to RAL and EVG (Figure 4.6C and 4.6D).

#### **4.4.7 Structural analysis of the impact of G118R, E138K, and H51Y on the integrase active site**

Homology models of the integrase active site for WT, G118R, G118R/H51Y and G118R/E138K (Figures 4.7 and 4.8) were created using the I-TASSER server [453, 531] with the recently published structures of PFV integrase as lead modeling templates [380]. Rotamer analysis of WT active site residues showed a similar propensity for the

D64, D116 and E152 to co-orient in a manner similar to that described for the amino acid pairs in the PFV structure (Figure 4.7A); in these orientations, the DDE motif of the wt HIV-1 integrase had good coordination interactions with the two  $Mn^{2+}$  ions derived from the PFV structure (Figure 4.7A; 4.7C). When the WT model was overlaid with the latest PFV TCC [416], residue G118 was within 4Å of the target-DNA, and it is a logical assumption that any bulky substitution at this position would interfere with target-DNA binding. This complements our data shown above in regard to a deficit in target-DNA binding caused by the G118R substitution.

In an effort to gain insight into the mechanism of resistance caused by G118R we superimposed the WT and G118R homology models with co-crystal PFV structures containing DTG, RAL or EVG (Figure 4.8) and examined interactions of G118 and 118R with the various inhibitors as well as with other residues implicated in INSTI resistance [317, 346, 532]. The G118R substitution may cause 118R to form a salt bridge with E92, effectively breaking an electrostatic interaction of E92 with N120. E92 is implicated in EVG resistance. Additionally all residues implicated in high level RAL and EVG resistance [317, 336, 346, 532] were within 8Å of position 118; in particular T66 and L74 are within 4Å of the guanidino group of 118R. L74M was an accessory substitution to G118R in the only clinically reported instance of this substitution [408] (Figure 4.8).

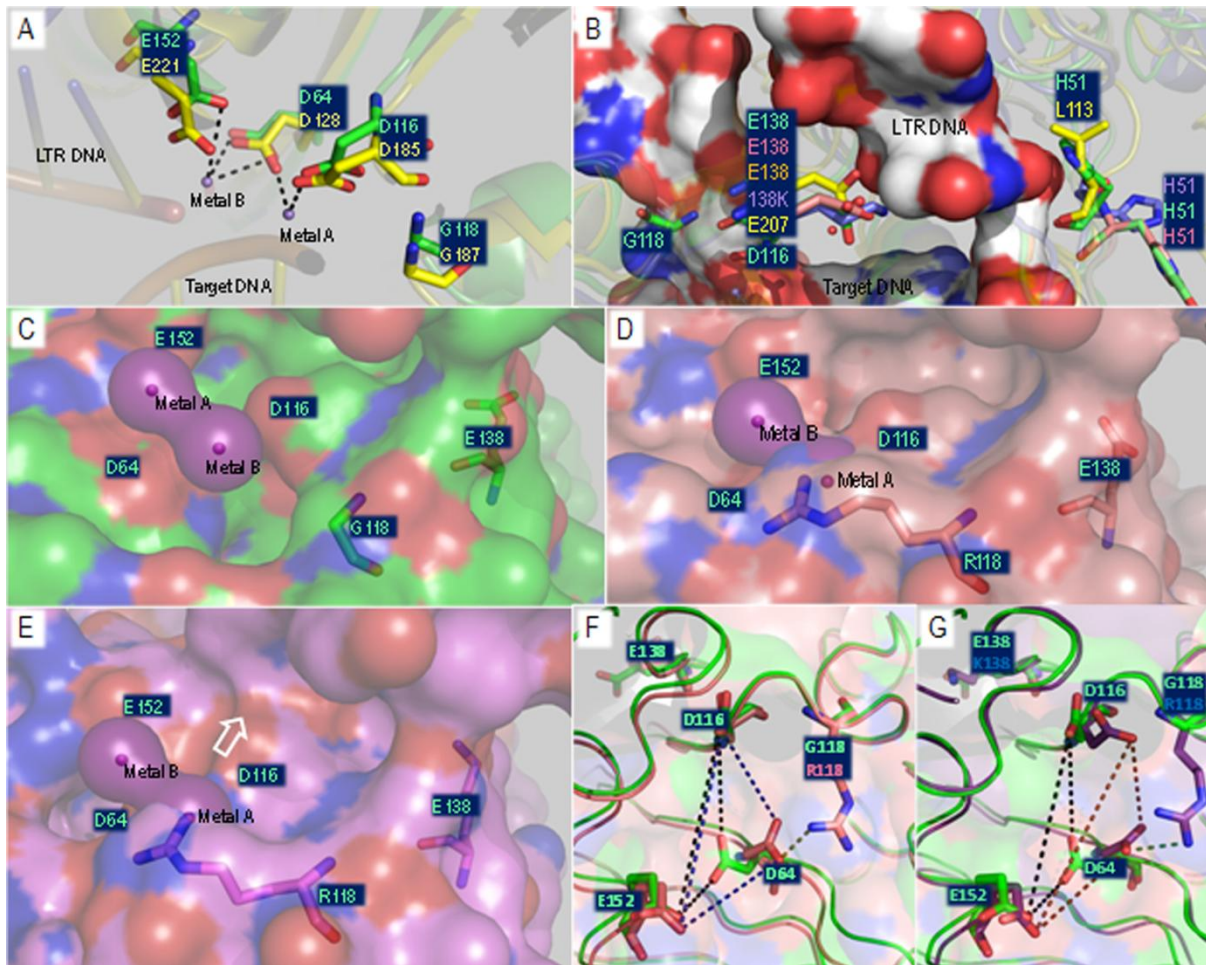


**Figure 4.7: Modeling of the HIV integrase active site.**

Energetically minimized homology models with sequences corresponding to either WT, G118R, G118R/H51Y or G118R/E138K HIV-1 integrase were created based on the PFV strand transfer structure PDB ID:3OY9. Rotamer interrogation in WT model showed that catalytic residues had similar propensity as PFV integrase to coordinate two divalent-cations  $Mn^{2+}$  (A). The positions of the mutated residues, G118R, H51Y and E138K, relative to the corresponding residues in PFV integrase and to target and LTR-DNA, was obtained by direct superimposition of all the homology models with the PFV TCC (B). Coordination of  $Mn^{2+}$  by the integrase active sites was simulated by insertion



of the Mn<sup>2+</sup> coordinates from the PDB structure 3OY9 into the active sites of modeled WT (C), G118R (D) and G118R/E138K (E) HIV-1 integrase enzymes. Differences in orientations of catalytic residues in the presence or absence of G118R were investigated by superimposition of the WT and G118R homology models (F) and of G118R/E138K (G). All images were processed in PyMOL. Secondary structures are represented by partially transparent cartoon structures with key residues shown in stick-form. Cartoon and carbon atom coloration differentiated WT (light green), G118R (salmon) and G118R/E138K (magenta). Mn<sup>2+</sup> cations are shown as small purple spheres with acidic (red) and basic (blue) moieties identified by standard atomic coloration.

## 4.5 DISCUSSION

The HIV integrase G118R substitution was selected by two drugs, RAL [408] and DTG [418], in CRF02\_AG virus and by MK-2048 [408] and DTG [418] in subtype C viruses. Prior to these selections, G118A, G118C and G118R had been selected by a preclinical inhibitor S-1360 in a non-B context [411]. G118R in subtype B was shown to display resistance to MK-2048 [352] and DTG [370]. The current work focuses on the enzymatic cost of the G118R substitution in a subtype B background as well as the effects of the secondary H51Y and E138K substitutions on enzyme activity and level of drug resistance.

We have shown in this study that the G118R substitution results in a loss in both 3' processing (Figure 4.4 and Table 4.2) and strand transfer activity (Figure 4.3 and Table 4.1). Our findings further indicate that the major block to integration ability caused by this substitution occurs at the level of strand transfer. There was no serious deficit in 3' processing ability caused by the G118R substitution (Figure 4.4A-C), and the ability of the secondary substitutions H51Y and E138K to compensate G118R to higher than WT 3' processing levels did not correlate with their inability to restore total integration activity [352] (unpublished data). The G118R substitution resulted in a > 90% reduction in strand transfer efficiency (Figure 4.3C, 4.5F and Table 4.1). The secondary substitutions H51Y and E138K partially repaired this deficit (Figure 4.5E) but by different mechanisms: H51Y increased the specificity of LTR binding (Figure 4.3B) while E138K increased total overall DNA binding ability. Both of these secondary substitutions

increased the number of integrase-LTR complexes; this resulted in increased overall enzyme performance, thereby implying that the deficit was partially due to the ability of the LTR-integrase complex to bind to target-DNA (Figure 4.5F). Although the G118R/H51Y and G118R/E138K enzymes had increased enzyme strand transfer performance relative to the G118R variant, this was still <50% of WT enzyme (Figure 4.5F). Additionally, an increase in the number of integrase-LTR complexes did not completely rescue the deficit in enzyme performance by the G118R variant. Thus, factors other than target-DNA might be involved in the G118R mediated reduction in enzyme performance. There was no major defect in the ability of the various integrase proteins to multimerize and to form the strand transfer complexes with the LTR and target DNA molecules (data not shown), as this would have changed the protein concentration at which integration was optimal (300 nM).

Homology modeling based on the PFV crystal structure provided some insight into the effects of the various substitutions described here on the active site residues of HIV subtype B integrase (Figures 4.7 and 4.8). The formation of a salt-bridge between 118R and D64 represents the most energetically favorable backbone dependent rotamer for 118R (Figure 4.7A). The formation of this salt-bridge causes a distortion in the orientation of D64 relative to the other two catalytic residues and this could conceivably affect the ability of the G118R variant to coordinate the cofactor  $Mg^{2+}/Mn^{2+}$  ions. This could also be related to the ability of the variant to bind to target-DNA. It has been suggested that only one cation initially binds the enzyme and that the binding of the

second cation is facilitated by DNA binding [279, 413, 451, 529, 533]. This can also be inferred from the difficulty of obtaining integrase crystal structures with two bound  $Mg^{2+}$  ions [370, 380, 381, 413, 533]. In the initial PFV crystal structures, the only structures that co-crystallized with  $Mn^{2+}$  had two ions bound at the active site whereas those formed with  $Mg^{2+}$  had only one ion bound despite evidence of effective 3' processing activity [380]. It has previously been reported that LTR binding to integrase is independent of cation binding [413, 416, 451], which may explain why there were no appreciable defects on the ability of the variant proteins to bind LTR-DNA with the exception of the G118R/H51Y double variant (Figure 4.3). Additionally, it had been postulated that the roles of the two ions differ during the two integration steps [534], and this has recently been experimentally demonstrated [416]. A single cation of  $Mn^{2+}$  (metal B) primes a water molecule for nucleophilic attack on the cytidine-guanine phosphodiester bond, facilitating 3' processing. It subsequently keeps the reactive 3'OH end stabilized and primed for strand transfer. The other  $Mn^{2+}$  cation (metal A) (Figure 4.8) polarizes and destabilizes the scissile phosphodiester bond in the target-DNA, permitting a nucleophilic attack on the target-DNA by the reactive 3'OH of the viral DNA. The G118R enzyme and doubly mutated variants may have been impaired in their ability to bind metal A. Alternatively, the coordination sphere may have been altered towards D116 and E152 (Figure 4.7E- indicated by arrow). The addition of E138K to G118R resulted in an altered orientation for D116, bringing it closer to D64 relative to WT enzyme (Figure 4.7G) and G118R (Figure 4.7F), and this may account for the partial

rescue in activity and target-DNA affinity that we observed in our experiments. Additionally, the G118R/E138K active site appeared to be slightly more acidic than that of WT enzyme (Figure 4.8) and this may have increased the ability of the G118R/E138K integrase enzyme to coordinate  $Mg^{2+}/Mn^{2+}$  ions and target-DNA.

The E138K substitution was observed at the integrase- LTR interface; the change of an E to a K may have increased the non-specific DNA binding abilities of integrase, leading to a concomitant increase in affinity for the target-DNA relative to the G118R single variant (Figure 4.5E). However, the addition of E138K to G118R did not abrogate the salt-bridge between 118R and D64 and this may thus account for the fact that the G118R/E138K enzyme was seriously compromised in enzyme performance (Figure 4.3C, Figure 4.5F). In contrast, the G118R and H51Y substitutions did not appear to interact in the doubly mutated enzyme. This is in contradiction to interactions between H51Y and R263K [177] in the H51Y/R263K double mutant. The effect of H51Y on G118R may be due to the likelihood that each of G118R and H51Y have separate effects on the enzyme. We previously reported that H51Y enzyme was less able to bind to the viral LTR [177], a finding consistent with the reduction in total LTR binding seen with the G118R/H51Y double mutant and the inability of H51Y to rescue enzyme performance.

The G118R substitution caused low-level resistance to DTG (3.1-fold) and the addition of H51Y to G118R did not significantly increase the level of resistance (3.4-fold) (Table 4.3). Superimposition of the HIV integrase models with PFV integrase bound to DTG

(Figure 4.8A), RAL (Figure 4.8B) and EVG into the homology models (Figure 4.8C), showed that the activity of these INSTIs would be compromised by the G118R substitution. It had been previously reported that the G118R substitution may result in steric hindrance to DTG binding [370].

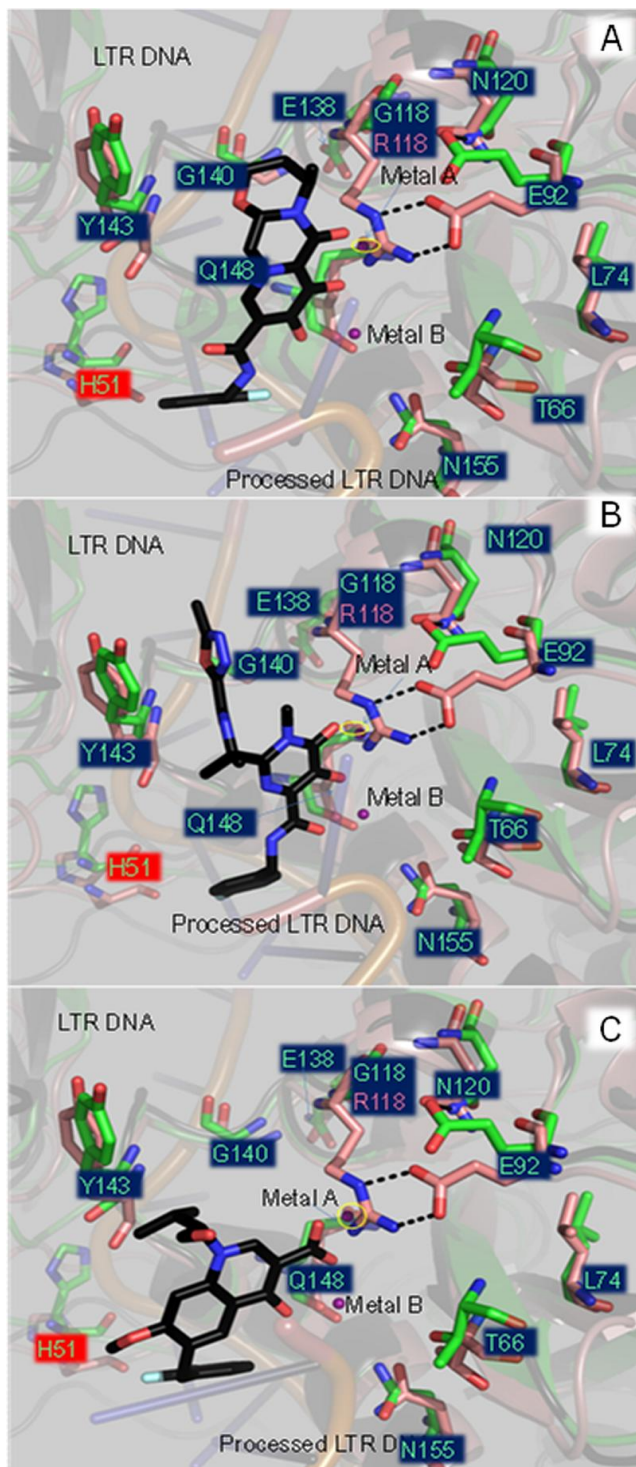


**Figure 4.8. The G118R mutation in the context of INSTI drug resistance.**

Coordinates of DTG (A), RAL (B) and EVG (C) structures were inserted into the active site of the WT HIV-1 integrase homology model by overlap with the PFV integrase co-crystal structures, i.e. PDB ID: 3S3M, PDB ID: 30YA, and PDB ID: 3L2U, respectively. WT and G118R homology models were superimposed, with the side-chains of most major integrase drug resistance mutations within 12Å of the side-chain of 118R being shown as stick representations. PyMOL was used for all image processing. All residues shown with

the exception of H51Y (red highlight) are within a 10Å sphere of the active site. INSTI molecules are shown as sticks with carbon molecules colored black and all other residues colored by standard atomic coloration. Coloration of WT and G118R models is as shown for Figure 4.7. Yellow oval marks presence of Metal A.

Our homology model of G118R provides additional possibilities for the mechanism(s) of resistance to DTG and other INSTIs. The side-chain of 118R, in addition to forming a salt-bridge with D64, forms a strong salt-bridge with E92 and is within 4Å of T66 and N155 (Figure 4.8); each of these three residues has previously been implicated in resistance to both EVG and RAL [311, 317, 349, 414, 532]. The salt-bridge between 118R and E92 may break the interaction between E92 and N120 (Figure 4.8A). Additionally, the E92-118R salt-bridge may abrogate the interaction between E92 and the coordination scaffold of EVG (Figure 4.8C); potentially explaining the slightly higher resistance levels conferred by G118R to EVG (Figure 4.6C), compared to the other INSTIs.

The addition of E138K in a background of G118R caused striking reductions in resistance to all drugs tested, and the G118R/E138K enzyme displayed slightly higher susceptibility to DTG than WT enzyme (Table 4.3; Figure 4.6B), while the G118R substitution alone apparently conferred low-level resistance to both RAL (Figure 4.6C) and EVG (Figure 4.6 D). The G118R/H51Y and G118R/E138K doubly mutated enzymes displayed less resistance to both EVG and RAL than G118R integrase while

G118R/E138K enzyme was hypersensitive to EVG. Both H51Y and E138K have been selected in the clinic and have been shown to play a role in clinical resistance against EVG and RAL [177, 311, 317, 336, 346, 532].

In summary this study presents an analysis of biochemical and structural data that define the G118R substitution in the context of subtype B and its interactions with integrase substitutions at positions H51Y and E138K. We show that multiple factors may preclude G118R from occurring spontaneously, extend to the ability of G118R mutated enzyme to efficiently catalyze integration. Structural insights provided through PFV crystal structures and modeling alignments imply that combinations of G118R together with multiple other substitutions might result in an enzyme that most likely would be catalytically defective. Should G118R develop in patients receiving DTG therapy we believe that the resultant virus would be extremely unfit and the development of further substitutions such as E138K might render the virus hyper-susceptible to EVG and other INSTIs. Ongoing work will quantify the effects of these same substitutions in non-B subtypes.



## Chapter 5

### Differential effects of the G118R, H51Y and E138K resistance substitutions in HIV integrase of different subtypes

The work presented in this chapter has been published previously, in the manuscript below:

- Quashie PK, Oliviera M, Veres T, Osman N, Han YS, Hassounah S, Lie Y, Huang W, Mesplède T, Wainberg MA. **Differential effects of the G118R, H51Y and E138K resistance substitutions in HIV integrase of different subtypes**. J Virol. 2015 Mar 15;89(6):3163-75. doi: 10.1128/JVI.03353-14. Epub 2014 Dec 31.

PKQ designed the study, performed most experiments and simulations, and wrote the manuscript. MO performed viral phenotyping studies. TV and SH performed some biochemical assays. NO and YH designed analysis tools and performed some simulations. YL and WH performed Monogram assays. TM performed molecular biology and helped write the manuscript. MAW oversaw all aspects of the work and edited the manuscript. All authors read and approved the final published manuscript.

## 5.1 ABSTRACT

Dolutegravir (DTG) is the latest antiviral (ARV) approved for treatment of human immunodeficiency virus (HIV) infection. The G118R substitution, previously identified with MK-2048 and raltegravir may represent the initial substitution in a dolutegravir resistance pathway. We have found that subtype C integrase proteins have a lower enzymatic cost associated with the G118R substitution, mostly at the strand transfer step of integration, when compared to either subtype B or recombinant CRF02\_AG proteins. Subtype B and circulating recombinant form AG (CRF02\_AG) clonal viruses encoding G118R-bearing integrase were severely restricted in viral replication capacity, and G118R/E138K-bearing viruses had varying levels of resistance to dolutegravir, raltegravir and elvitegravir. In cell-free, the impacts of the H51Y and E138K substitutions on resistance and enzyme efficiency, when present with G118R, were highly dependent on viral subtype. Sequence alignment and homology modeling showed that the subtype-specific effects of these mutations were likely due to differential amino acid residue networks in the different integrase proteins, caused by polymorphic residues, which do significantly affect native protein activity, structure or function and are important for drug-mediated inhibition of enzyme activity. By characterizing G118R, this chapter also preemptively defines parameters for a potentially important pathway in some HIV non-B subtype viruses treated with dolutegravir, and will aid in the inhibition of such virus, if detected. The general inability of strand transfer -related substitutions to diminish 3'

processing indicates the importance of the 3' processing step and highlights a therapeutic angle that needs to be better exploited.

## 5.2 INTRODUCTION

During the past thirty years, the human immunodeficiency virus (HIV) has infected over 68 million people, killing ~34 million [190]. The advent of combination antiretroviral (ARV) regimens in 1995 has played a key role in reducing HIV/AIDS-related deaths and prolonging the life-span of people living with HIV [175].

The integration of viral DNA into the human genome prevents the facile eradication of HIV from the cells of infected individuals, even during suppressive ARV therapy [173]. Additionally, HIV quickly develops drug resistance in the face of suboptimum drug pressure (as happens in poorly adherent patients or due to low drug bioavailability) [535], and this is facilitated by the high mutation and recombination rates of HIV reverse transcriptase [536]. The inability to eradicate HIV combined with high rates of drug resistance has necessitated the ongoing development of new potent ARVs with novel targets, unique resistance patterns, and/or better bioavailability in a context of simplified dosing [414, 537].

Raltegravir (RAL) was the first approved drug to target the HIV integrase (IN) enzyme. RAL acts as an integrase strand transfer inhibitor (INSTI) and was approved in 2007 [211] followed by a second INSTI termed elvitegravir (EVG) in 2012 [330]. These two compounds, as well as dolutegravir, the most recently approved INSTI (2013) [355], target the strand transfer step of integration, by three binding mechanisms: i) chelation

of active site divalent cations ( $Mg^{2+}$  or  $Mn^{2+}$ ), ii) pi-stacking interactions between INSTI halobenzyl groups and the viral long terminal repeat (LTR) base immediately upstream of CA-OH and iii) interactions between INSTIs and specific IN residues [382]. Both RAL and EVG are associated with a low barrier to resistance in both treatment-naïve and -experienced patients and share many of the same resistance mutations, hence establishing a problem of cross-resistance among these drugs [311, 317, 346, 538].

In contrast, no resistance mutations have yet been associated with DTG in drug-naïve patients, after more than five years of experience in clinical trials [414, 538]. Tissue culture selection studies identified two DTG mutational pathways for resistance initiated by either R263K in subtypes B and CRF02\_AG or G118R in subtypes C and CRF02\_AG [418]. We showed that R263K and a subsequent substitution at positions H51Y conferred DTG resistance but that the addition of secondary H51Y mutation caused an additional drop in viral fitness below that conferred by R263K alone [177]. This is in contrast to the usual situation whereby secondary resistance mutations commonly play a compensatory role in regard to viral fitness while also increasing levels of drug resistance. The R263K mutation has also been identified in at least two ARV-experienced patients who were treated with a DTG-containing regimen [539]. Our results also showed that the G118R substitution can confer resistance against DTG in subtype B integrase [419]. The G118R substitution alone and in conjunction with E138K had previously been identified in subtype C but not in subtype B in selections utilizing an investigational INSTI, MK-2048 [352]. Similar to DTG, integrase complex- drug binding

studies had shown that MK-2048 stayed bound to the pre-integration complex for far longer than either RAL or EVG, explaining its superior barrier to resistance development [369]. The clinical development of MK-2048 has not continued beyond Phase IIb clinical trials, yet the selection of G118R by both DTG and MK-2048 as well as the increased susceptibility of R263K containing integrase protein to MK-2048 [418] points to intersections and similarities between the resistance profiles of DTG and MK-2048.

The purpose of this study was to gain mechanistic understanding, through cell culture, biochemical and structural analysis, for the differential selection of G118R and its associated substitutions, H51Y and E138K, in HIV subtypes B and C as well as in CRF02\_AG, and to evaluate the impact of these substitutions on integrase activity.

## 5.3 MATERIALS AND METHODS

### 5.3.1 Cells and antiviral compounds.

*E. coli* strain XL10-Gold ultracompetent cells Tet<sup>r</sup>Δ(*mcrA*)183, *mcrCB-hsdSMR-mrr*173, *endA1*, *supE44*, *thi-1*, *recA1*, *gyrA96*, *relA1*, *lac Hte*, [F', *proAB*, *lac*<sup>q</sup> Tn10(*tet*<sup>r</sup>) Amy Cam<sup>r</sup>]<sup>a</sup> (Stratagene) were used for plasmid production. The integrase inhibitor drugs, RAL and MK-2048 were kindly provided by Merck Inc., while EVG and DTG were kindly provided by Gilead Sciences and GlaxoSmithKline, respectively. Prior to use, compounds were solubilized in dimethyl sulfoxide (DMSO) and stored at -20°C. All reagents used were enzyme grade and of high purity.

### 5.3.2 Plasmids and site-directed mutagenesis

The generation of a  $\rho$ ET15b expression plasmid containing soluble HIV subtype B and C integrase has been demonstrated [359, 418]. In order to construct a  $\rho$ ET-15b expression plasmid containing soluble HIV circulating recombinant form (CRF02\_AG), the CRF02\_AG integrase coding sequence was amplified from p97AG proviral plasmid DNA (GenBank accession number: AB052867.1) by PCR using the following primers: p97-INT-FWD: 5'-GCCAGGATCCTTTTTAGATGGCATAGATAAAGCCCAAGAAG-3' and p97-INT-RVS: 5'-GTTATCTAGATTAATCCTCATCCTGTCTATCTGCCACACAATC-3'. Amplification products were purified using the QIAquick PCR purification kit (QIAGEN, Toronto, ON), digested using the BamHI and XbaI restriction enzymes (NEB, Whitby, ON) and ligated inside the  $\rho$ ET15b plasmid using T4 DNA ligase (NEB). The resulting  $\rho$ ET15b-INAG plasmid was verified by sequencing.

PCR-mediated site-directed mutagenesis performed on this plasmid yielded plasmid DNA coding for the G118R mutation, in isolation or together with either of two additional mutations, H51Y or E138K. The following primers were used for mutagenesis:

G118R<sub>AG\_sense</sub> (CCAGTGAAAGTGATACACACAGACAATCGCAGAAATTTCCACC);

G118R<sub>AG\_antisense</sub> (GGTGAAATTTCTGCGATTGTCTGTGTGTATCACTTTCACTGG);

H51Y<sub>AG\_sense</sub> (GCTAAAAGGGGAAGCCATATATGGACAAGTAGACTGT);

H51Y<sub>AG\_antisense</sub> (ACAGTCTACTTGTCCATATATGGCTTCCCCTTTTAGC);

E138K<sub>AG\_sense</sub> (TTGGTGGACAAATGTTACACAAAATTTGGAATTCCCTACAATCC),

E138K<sub>AG\_antisense</sub>

(GGATTGTAGGGAATTCCAAATTTTTGTGTAACATTTGTCCACCAA), G118R<sub>C\_sense</sub>

(GGCCAGTCAAAGTAATACATACAGACAATCGTAGTAATTTACCAG);

G118R<sub>C</sub>\_antisense

(CTGGTGAAATTACTACGATTGTCTGTATGTATTACTTTGACTGGCC); H51Y<sub>C</sub>\_sense

(CAAAGGGGAAGCCATGTATGGACAAGTAGACTGT); H51Y<sub>C</sub>\_antisense

(ACAGTCTACTTGTCCATACATGGCTTCCCCTTTTG); E138K<sub>C</sub>\_sense

(GGGCAGGTATCCAACAGAAATTTGGGATTCCCTAC); and E138K<sub>C</sub>\_antisense

(GTAGGGAATCCCAAATTTCTGTTGGATACCTGCCC). Successful mutagenesis was confirmed by sequencing (Genome Quebec).

### 5.3.3 Protein expression, purification and quantification

Plasmids bearing either a wild-type or an appropriately mutated IN coding sequence were transformed into BL21(DE3) Gold cells F<sup>-</sup>, *ompT*, *hsdS<sub>B</sub>*(r<sub>B</sub><sup>-</sup>, m<sub>B</sub><sup>-</sup>), *dcm* + Tet<sup>r</sup>, *gal*, for protein expression. Luria-Bertani (LB) broth (Multicell), prepared in MilliQ water and supplemented with 100 µg/mL ampicillin was used for all bacterial growth. Expression and purification of integrase recombinant proteins were performed as previously described for hexa-His-tagged integrase [418]. Fractions containing purified integrase as judged by SDS-PAGE were dialyzed into storage buffer (20 mM Hepes, 1 M NaCl, 1mM EDTA, 5 mM DTT, 10 % glycerol, pH7.5). Protein concentrations were measured using a calculated molar extinction coefficient of 50420 M<sup>-1</sup>cm<sup>-1</sup>; of note, the molar extinction coefficients of all integrase proteins were the same and in congruence with that calculated for subtype B integrase [418]. Protein aliquots were kept for several months at -80°C without significant loss of enzymatic activity.

### 5.3.4 DNA substrates for *in vitro* assays

All oligonucleotide substrates were purchased from Integrated DNA Technologies (IDT, Coralville, IA, USA). The following oligonucleotides were used for strand transfer assays:

pre-processed donor LTR DNA sense (A): 5AmMC12-ACCCTTTTAGTCAGTGTGGAAAATCT CTAGCA-3' and antisense (B): 5'-ACTGCTAGAGATTTTCCACACTGACTAAAAG-3'; target DNA: sense (C): 5'-TGACCAAGGGCTAATTCACCT-3Bio and antisense (D): 5'-AGTGAATTAGCCCTTGGTCA-3Bio. For 3' processing assays, primer (B) was used together with the LTR -3'-sense oligonucleotide (E): \*5'AmMC12-ACCCTTTTAGTCAGTGTGGAAAATCTCTAGCAGT-BioTEG-3'.

The key features of these oligonucleotides have been previously described [418, 450]. Functional DNA duplexes were made by combining equimolar quantities of sense and antisense primers to appropriate concentrations in low-chelate TE buffer (10mM Tris, 0.1mM EDTA pH7.8). The combined primers were heated for ten minutes at 95°C and annealed by slow cooling to room temperature over a period of 4 hours. Duplexes were stored at -20°C for several months without a loss in integrity.

### 5.3.5 Preparation of pre-processed LTR-coated plates for strand transfer activity

Eighty microliters of pre-processed viral LTR-mimic (donor DNA) duplex A/B diluted to 300 nM (except as dictated by experiment design) in PBS pH7.4 (Bioshop) were covalently linked to Costar DNA-Bind 96-well plates (Corning#2499) by overnight incubation at 4°C. The plates were blocked with 0.5% BSA in blocking buffer (20 mM



Tris pH7.8, 150 mM NaCl) and were stored in blocking buffer for several weeks without detectable loss in integrity. Before use, the plates were washed twice with each of PBS pH7.4 and assay buffer (50 mM MOPS pH6.8, 50 µg/mL BSA, 50 mM NaCl, 0.15% CHAPS, 30 mM MnCl<sub>2</sub>/MgCl<sub>2</sub>) except as dictated by experiment design.

### **5.3.6 Protein calibration for strand transfer activity**

In order to better elucidate the impact of resistance substitutions, the strand transfer and 3' processing steps of the HIV integration reactions have been decoupled, as previously described [418, 419]. The optimum concentration of protein for use in strand transfer experiments was determined by titration as previously described [418, 419]. Briefly, purified integrase proteins, appropriately diluted in reaction buffer (50 mM MOPS pH6.8, 50 mg/mL BSA, 50 mM NaCl, 30 mM MnCl<sub>2</sub>, 0.015% CHAPS, 5 mM DTT), were added to pre-processed LTR bound plates as described above. This was followed by 30 min incubation at room temperature to allow for assembly of integrase onto the pre-processed LTR duplexes. Varying concentrations of biotinylated target DNA duplex C/D (0-240 nM) were added, followed by a 1 hr incubation at 37°C for the strand transfer reaction to occur. The plates were then rinsed three times with wash buffer (50 mM Tris pH7.5, 150 mM NaCl, 0.05% Tween20, 0.2 mg/mL BSA) and incubated with 150 µL of Eu-labeled Streptavidin (Perkin Elmer) diluted to 0.025 µg/mL in wash buffer in the presence of 50 µM DTPA (Sigma). After additional rinses with wash buffer, 100 µL of Wallac enhancement solution (Perkin Elmer) was added. The amount of target DNA covalently linked to the LTR was then measured by quantifying the amount of bound Eu-

labeled streptavidin. The low pH of the Wallac solution caused the ionization of Eu to  $\text{Eu}^{3+}$ . Excitation of  $\text{Eu}^{3+}$  ions by incident wavelength at 355 nm resulted in time-resolved emission of fluorescence (TRF) which was measured at 612 nm on a FLUOStar OPTIMA multi-label plate reader (BMG Labtech).

Protein concentrations that yielded the highest activity as measured by relative fluorescence units (RFU) were chosen for subsequent experiments.

### **5.3.7 Strand transfer activity assay**

Michaelis-Menten enzyme analysis has previously been used to determine enzyme parameters of HIV integrase [341]. Whilst 3' processing has been conclusively shown to follow non-Michaelis-Menten kinetics [527, 540], there has been no similar study of HIV integrase strand transfer. In order to obtain relative activity parameters for wild-type and variant integrase proteins, strand transfer reactions were carried out as described based on the same design as the protein calibration assay described above. The major deviation was that an effective [LTR] of 160 nM and effective [integrase] of 300 nM were used for these assays while [target DNA] was varied from 0-128 nM. All other experimental procedures are as described above. The mean of at least three independent experiments, each performed in triplicate for wild-type and each variant integrase proteins, were calculated. The values of enzyme activity in RFU ( $A$ ) and [target DNA] ( $S$ ) were fit by non-linear regression using GraphPad Prism V5 (GraphPad Software, San Diego California USA, [www.graphpad.com](http://www.graphpad.com)) to the Michaelis-Menten derivative equations below:

$$A = A_{\max}' * [S] / ([S] + K_m')$$

$$K_m' = A_{\max}' * [S] / A - [S]$$

In this case, the pseudo-Michaelis constant ( $K_m'$ ) reflects the apparent affinity of the enzyme for the target DNA substrate ( $[S]$ ), and the maximum activity ( $A_{\max}'$ ) reflects the maximum activity obtainable with same concentration of the protein in a similar assay, regardless of substrate concentration. To determine overall enzyme efficiency, we calculated the ratio of  $A_{\max}'$  to  $K_m'$ , as previously described [419], presented as a percentage of wild-type values.

### 5.3.8 3' processing activity assay

The 3' processing activity of the purified recombinant integrase proteins was determined as previously described [450]. Briefly, 3' biotinylated LTR duplex G/B was covalently linked at varying concentrations (effective concentration: 0-160 nM) to Costar DNA-bind plates under similar conditions as for strand transfer. To initiate 3' processing, purified integrase protein (300 nM) diluted in reaction buffer was added and the plates incubated at 37°C. Negative protein control wells had only reaction buffer added. After 2h of incubation the reaction was within the linear phase [450], and the plates were quickly washed three times with wash buffer to remove all traces of protein and cleaved 3'GT dinucleotide. All subsequent steps of the assay were as described above for the strand transfer assay with the exception of data analysis. For each plate and concentration of LTR, four negative protein controls contained unprocessed LTR and the average signal

from these represented the maximum possible signal ( $3'OH_{max}$ ). Thus the RFU representing actual 3' processing activity ( $3'OH_{actual}$ ) was determined by the calculation:

$$(3'OH_{actual}) = (3'OH_{max}) - (3'OH_{obs}).$$

The calculated 3' processing readings ( $n \geq 3$ ) were then processed using GraphPad Prism to yield 3' processing enzyme parameters as previously described [450]. The data within the linear phase of the 3' processing reaction were used to calculate kinetic parameters by fitting to Michaelis Menten equation [341]. As such relative enzyme efficiency calculations of 3' processing activity was calculated in the same manner described above for strand transfer.

### **5.3.9 Confirmation of the impact of G118R and E138K on subtype C integrase inhibition by MK-2048**

Since the selection of G118R in cell culture was initially driven by MK-2048 drug pressure [352] in a subtype C HIV-1 backbone, we performed preliminary confirmation that G118R and the associated E138K substitution caused resistance to MK-2048. The concentration-dependent susceptibility of subtype C WT, G118R, E138K and G118R/E138K proteins to MK-2048 was tested. Briefly, strand transfer assays were performed as described above with slight modifications. Following incubation of subtype C WT, G118R, E138K and G118R/E138K proteins with LTR DNA, of dose-ranging amounts of MK-2048 (20 pM- 20  $\mu$ M) dissolved in compound dilution buffer in a total of 25  $\mu$ L was added in each well. After an incubation period of 10 minutes at room temperature, 25  $\mu$ L of target DNA (6 nM) was added in each well and the strand transfer

reaction allowed to proceed as above. All subsequent steps were as described above for the strand transfer assay. Data obtained were normalized and fit to the log (inhibitor) vs. normalized response equation shown below in GraphPad Prism to yield estimates of the half inhibitory concentration (IC<sub>50</sub>) of the drug for the different proteins:

$$A = 100 / (1 + 10^{([I] - \log IC_{50})})$$

In the above equation, *A* represents residual strand transfer activity at a given drug concentration [*I*]. Each experiment was done in triplicate. Fold change (FC) susceptibility of each variant to MK-2048 was calculated by dividing the IC<sub>50</sub> for that variant by that of the WT subtype C integrase protein tested at the same time. Mean FC susceptibility data from at least three independent experiments were graphed using GraphPad Prism.

#### **5.3.10 Competitive inhibition of strand transfer by DTG, RAL and EVG**

The susceptibilities of our purified integrase proteins to INSTIs were tested in competitive inhibition assays using DTG, RAL and EVG. Drug stock solutions were prepared as a 6X working solution (6000 nM) and subsequently serially diluted 4-fold into compound dilution buffer (assay buffer without cations and containing 10% DMSO). The assay concentrations varied from 0.2- 1000 nM; inhibition assays were performed in the presence of varying target DNA concentrations (0-128 nM). Briefly, pre-processed LTR-coated plates (effective [LTR] = 160 nM) were prepared as described above. Purified integrase proteins (effective concentration = 300 nM), in assay buffer supplemented with 5 mM DTT, were added to each well followed by a 30 min incubation at room temperature to allow for assembly of integrase onto the pre-processed LTR

duplexes. Twenty-five microliters of appropriately diluted compound were added to each well, followed immediately by 25  $\mu$ L of appropriately diluted biotinylated target DNA duplex. The plates were then incubated for 1 hr at 37°C, followed by the post strand transfer steps described above. The data from at least three independent competitions assays for each protein were fit to the competitive inhibition algorithm using GraphPad Prism as shown below:

$$K_{mObs} = K_m' * (1 + [I] / K_i)$$

$$A = A_{max}' * [S] / (K_{mObs} + [S])$$

In the above equation,  $K_{mObs}$  represents the Michaelis constant obtained in the presence of inhibitor,  $[I]$  represents the inhibitor concentration, and  $K_i$  is the inhibition constant of the inhibitor for that particular protein. All other abbreviations are as defined above. During analysis, the  $K_m'$  for each protein was constrained to that previously determined in the strand transfer activity assays above while  $V_{max}'$  was left unconstrained.

Inhibitory constants  $K_i$  calculated by this algorithm were transformed to fold-change (FC) values by division of the  $K_i$  values for variant proteins with the  $K_i$  value for the appropriate wild-type integrase enzyme. FC calculations from multiple inhibition assays were compiled and analyzed using GraphPad Prism.

### **5.3.11 Monogram biosciences PhenoSense replication capacity and phenotyping assays**

HIV replication capacity and susceptibilities to DTG, RAL, and EVG were measured as previously described [31]. Briefly, murine leukemia virus envelope-pseudotyped HIV

viruses bearing WT, H51Y, G118R, E138K or G118R/E138K integrase substitutions and a luciferase reporter gene were used to inoculate human embryonic kidney HEK-293 cells. The resultant luciferase activity was used to calculate changes in HIV replication capacity relative to a wild-type reference strain. Drug susceptibility was expressed as a fold-change in IC50 relative to wild-type.

#### **5.3.12 Data processing.**

All cell-free experiments presented herein, except when otherwise indicated, were the result of at least 3 independent sets of experiments. When relevant, statistical significance of differences between datasets for two or more integrase proteins was determined using a one sample two-tailed t-test using GraphPad Prism. Probability values equal to or below 0.05 ( $p \leq 0.05$ ) were indicative of statistically significant differences between the different proteins tested.

#### **5.3.13 Homology modeling and active site analysis.**

Homology models of integrase proteins were generated using the ProtMod server (<http://ffas.burnham.org>) based on lead subtype B model templates which were initially generated using the I-TASSER protein modeling server [453]. The PFV structure PDB ID: 4E7K [416] was utilized as a lead template to generate a subtype B WT monomeric model for the formation of the target capture complex (TCC). The prototype foamy virus (PFV) integrase structure PDB ID:3S3M was used as a lead template to create the I-TASSER model for DTG-bound HIV-integrase. The ProtMod server was used to minimize stochastic error between the models and remove any sampling errors

introduced by the multi-template modeling method [421] of I-TASSER. Briefly, single template (subtype B WT)-single query (each integrase sequence including subtype B WT) alignments were performed using the alignment program SCWRL [442]. The program Modeller [434] was then used to create monomeric homology models of each integrase based on the SCWRL sequence alignment and the subtype B WT I-TASSER structure. Model quality was assessed based on root mean square deviation (RMSD) of the global homology structure from the PFV lead template using the RCSB PDB Protein Comparison Tool [443]. All structures were also verified by Ramachandran plot analysis [541, 542] as having greater than 89% of residues in allowed and favorable orientations. Superimposition of the HIV-1 homology models with the published co-crystal structure of PFV with DTG (PDB ID: 3S3M) provided insights into the mechanism of resistance caused by the G118R substitution in regard to this and other INSTIs. DNA interaction hints were obtained by overlaying the HIV-1 homology models with the PFV crystal structure PDB ID: 4E7K, representing the target capture complex (TCC) [416]. The molecular visualization program PyMOL (<http://PyMOL.org/>, The PyMOL Molecular Graphics System, Version 1.3, Schrödinger, LLC) was used for structural visualization and image processing.

## **5.4 RESULTS**

### **5.4.1 Generation of recombinant HIV subtype C and CRF02\_AG integrase enzymes**

Two resistance selection studies performed in our laboratory with the investigative drugs MK-2048 and S/GSK139572 (DTG) yielded the G118R mutation in subtypes C [352] and



CRF02\_AG [418], respectively. Key amino acid changes observed in these selection studies are presented in Table 5.1. Recombinant enzymes of either wild-type sequence or site-mutated to contain H51Y, G118R, or E138K, H51Y/G118R and G118R/E138K were expressed and purified as previously described [177, 418, 419]. As in previous studies, protein calibration confirmed that maximum protein activity occurred with 300 nM of protein for all subtypes [(not shown)]. Therefore subsequent experiments utilized 300 nM of integrase protein. When relevant, we compared our results with those obtained using subtype B protein.

**Table 5.1: Selection of substitutions in cell-culture by MK-2048 and DTG.**

<i>MK-2048 Selections</i>						
<b>Subtype</b>	<b>Baseline Polymorphisms</b>	<b>Week</b>	<b>Acquired mutations</b>	<b>Week</b>	<b>Acquired mutations</b>	<b>References</b>
<b>B</b>	M154I, V201I	34	None			(5)
<b>C</b>	V72I, Q95P, T125A	25	<b>G118R</b>	29	<b>G118R, E138K</b>	
<i>DTG Selections</i>						
<b>B</b>	M154I, V201I	20	R263K	37	<b>E138E/K, R263K</b>	(3)
<b>AG</b>	V72I, T125A, V201I	20	R263K	37	<b>H51H/Y, R263K</b>	
<b>AG</b>	V72I, T125A, V201I	20	E69E/K, <b>G118R</b>	37	<b>G118R</b>	
<b>C</b>	V72I, Q95P, T125A	20	<b>G118R</b>	37	<b>H51Y, G118R</b>	
<b>C</b>	V72I, T125A, V201I	20	S153S/T	37	<b>H51Y, G193G/E</b>	
Substitutions tested in this manuscript are shown in highlighted in bold.						

#### 5.4.2 Effect of the G118R on integrase strand transfer efficiency when alone or in combination with H51Y or E138K

Given that G118R and mutations associated with it arose during serial passage with several INSTIs, we expected these mutations to impact on the strand transfer reaction.

In CRF02\_AG integrase, the presence of any of the H51Y, G118R and E138K substitutions significantly reduced the enzyme parameters of the strand transfer reaction (Figure 5.1A) and led to reductions in enzyme efficiency > 50% (Figure 5.1C). H51Y caused a significant loss in enzyme efficiency in CRF02\_AG and subtype B but not in subtype C integrase (Figure 5.1B, C). The E138K single mutation was also not associated with a drop in enzyme efficiency in subtypes B and C integrase proteins but caused > 55% loss of activity when present in CRF02\_AG integrase. Of note, G118R caused significant diminutions in activity in all subtypes treated, i.e. subtype C 43% of WT activity, CRF02\_AG, (27%), subtype B (12%) (Figure 5.1C). The addition of H51Y and E138K to G118R partially restored the strand transfer efficiency of subtype B integrase, but less so with the subtype C or CRF02\_AG integrase enzymes (Figure 5.1C).

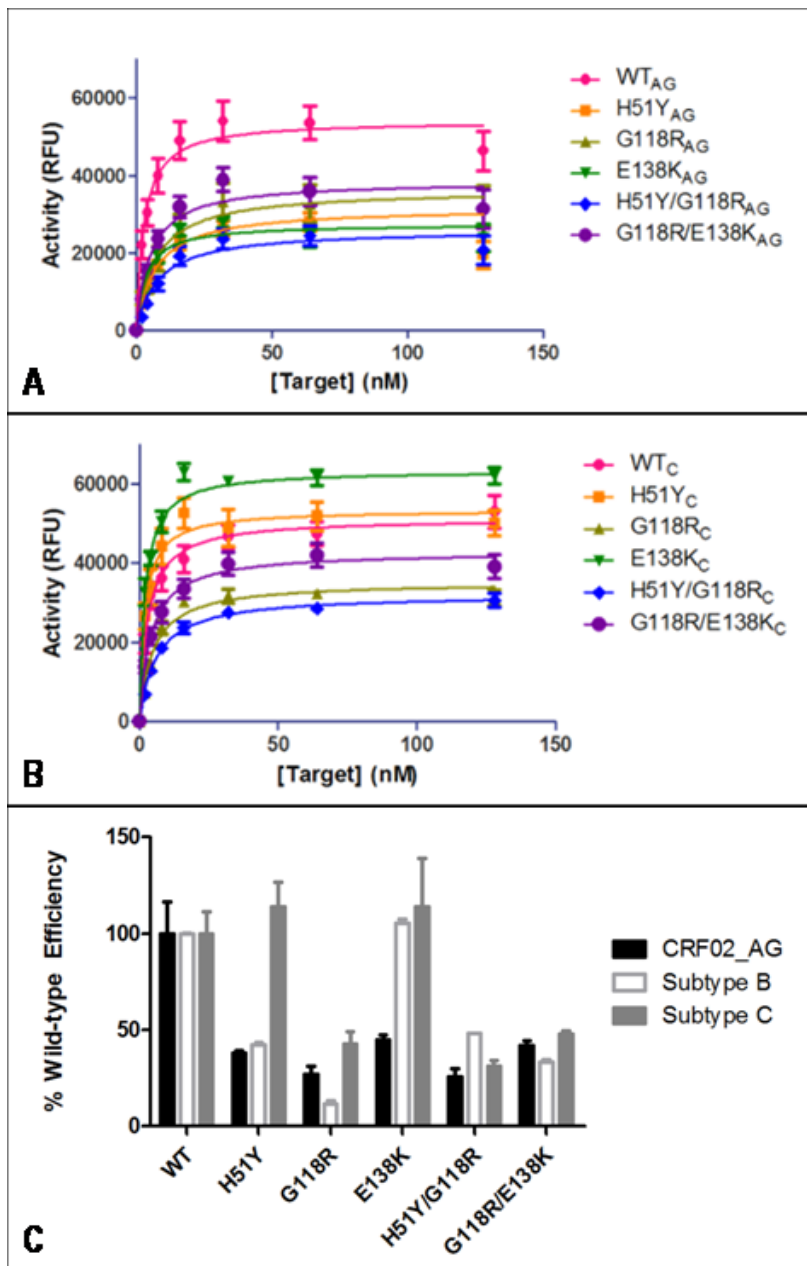


Figure 5.1: Comparative strand transfer activities of purified HIV-1 WT and variant integrase proteins of CRF02\_AG, subtype C and subtype B (A-C) origin.

(A) Target DNA saturation (0-128 nM) plots showing activity of CRF02\_AG proteins in the presence of fixed protein and LTR concentrations (300 nM and 160 nM respectively).

(B) Target DNA saturation plots showing activity of subtype C proteins in the presence of

fixed protein and LTR concentrations (300 nM and 160 nM, respectively). (C) Comparison of strand transfer reaction efficiencies for CRF02\_AG, subtype B and subtype C integrase proteins. All data presented reflect at least three independent experiments, each performed in duplicate or triplicate.

#### **5.4.3 Impact of the G118R, H51Y, and E138K substitutions on 3' processing ability**

To fully assess the impact of G118R, H51Y and E138K substitutions on integration, it is essential that the 3' processing ability of the various integrase proteins be evaluated. Accordingly, cell-free 3' processing experiments were performed using dose ranging levels of viral LTR mimic as previously described (Figure 5.2) [419]. The LTR DNA binding ability of the recombinant proteins, as indirectly inferred from  $K_m$  values, was not significantly different from WT except for H51Y for both non-B subtypes and E138K for subtype C (Figure 5.2 A, B). H51Y resulted in markedly tighter binding to the LTR for both the CRF02\_AG and subtype C integrase proteins while the opposite result was obtained for subtype C integrase containing the E138K substitution (Figure 5.2 A, B). G118R alone or in combination with either H51Y or E138K did not cause a significant change in LTR binding for either subtype. However, the doubly substituted H51Y/G118R CRF02\_AG protein showed lowered LTR DNA binding relative to WT.

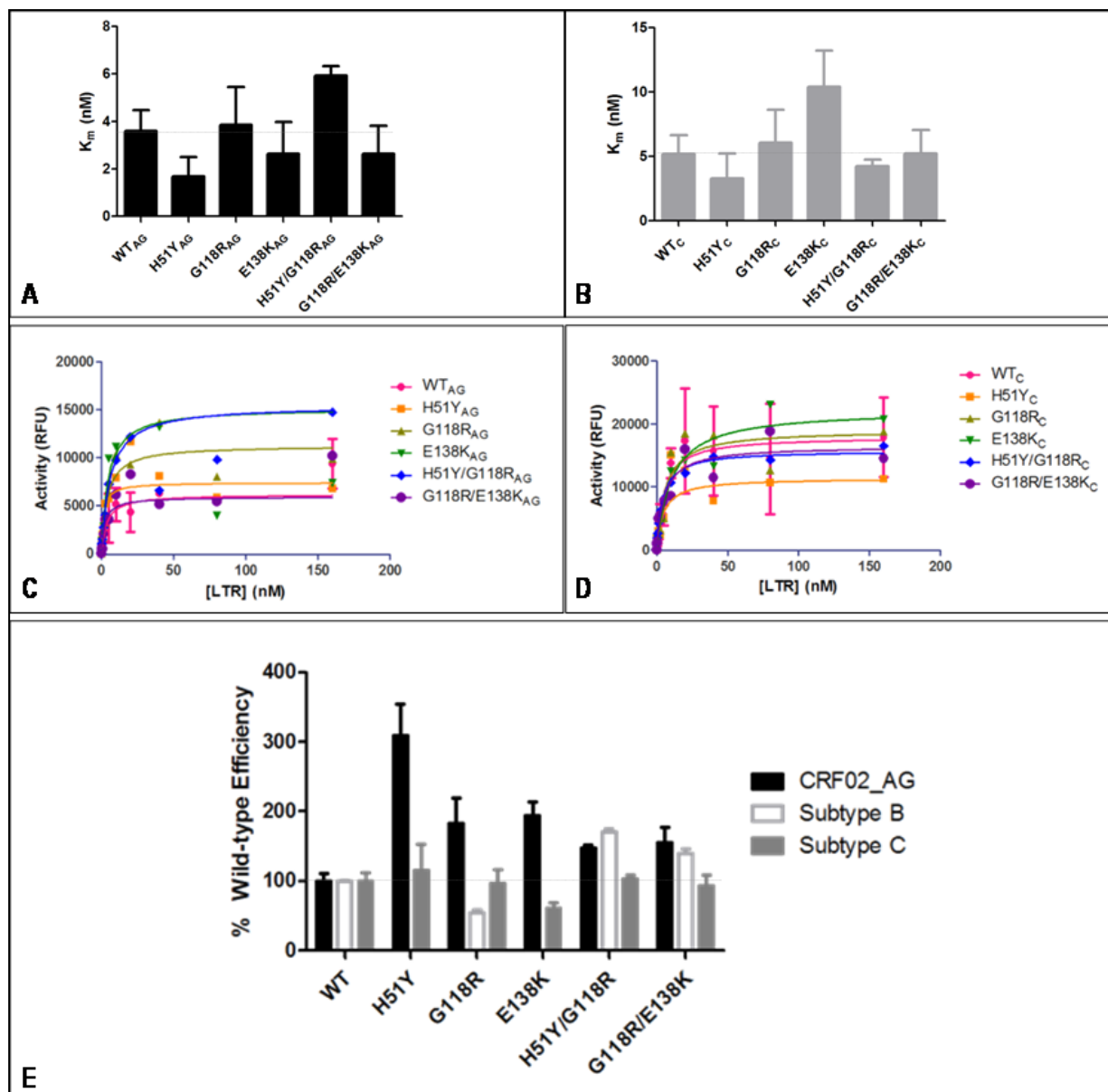


Figure 5.2: Comparative 3' processing activities of purified HIV-1 WT and variant integrase proteins of CRF02\_AG, subtype C and subtype B (A-E) origin.

Effect of amino acid substitution on functional binding ( $K_m$ ) of viral LTR mimic by CRF02\_AG integrase (A) or subtype C integrase (B). LTR DNA saturation plots showing activity of CRF02\_AG (C) or subtype C (D) proteins in the presence of fixed protein concentration (300 nM). Comparison of 3' processing reaction efficiencies for subtype B,

C and CRF02\_AG integrase proteins (E). All data presented reflect at least three independent experiments, each performed in duplicate or triplicate. This figure appears in color in the online version of the manuscript only.

The impact of these mutations on overall 3' processing activity was markedly different among the subtypes tested (Figure 5.2C-E). All CRF02\_AG variant proteins exhibited significantly higher 3' processing activity than WT (Figure 5.2C) and thus higher enzyme efficiency (Figure 5.2E). In subtype C, the presence of the E138K substitution resulted in a 38% reduction in efficiency of 3' processing, while H51Y and E138K were without effect. Diminished 3' processing ability was served for the G118R integrase protein of subtype B but not subtypes C or CRF02\_AG.

#### **5.4.4 The effect of G118R, and E138K on subtype C integrase protein resistance to MK-2048**

The G118R substitution was selected in cell culture by MK-2048 in a subtype C virus [352]. Despite being selected by the subtype C isolate 4742, the addition of E138K (within 4 weeks) was necessary to engender significant resistance in the virus to MK-2048 with a fold-change (FC) in  $EC_{50}$  of ~139 (Figure 5.3A) and lower levels of cross-resistance to RAL (~4.4 FC) and EVG (~ 4.1 FC). We also studied the susceptibility of subtype C WT integrase or integrase containing the G118R, E138K or G118R/E138K substitutions on susceptibility to MK-2048 (Figure 5.3; Table 5.2). As previously

reported for subtype B in cell culture [352], G118R resulted in minimal resistance to MK-2048 (~ 1.5 FC) (Figure 5.3A,B) and this level of resistance was significantly increased by the presence of the E138K mutation (~11 FC). Of note, the FC in resistance to MK-2048 reported for clonal G118R/E138K subtype C virus is ~100-fold higher than previously reported for subtype B [352]. This result may partially account for the emergence of G118R and the additional selection of E138K in subtype C [352].

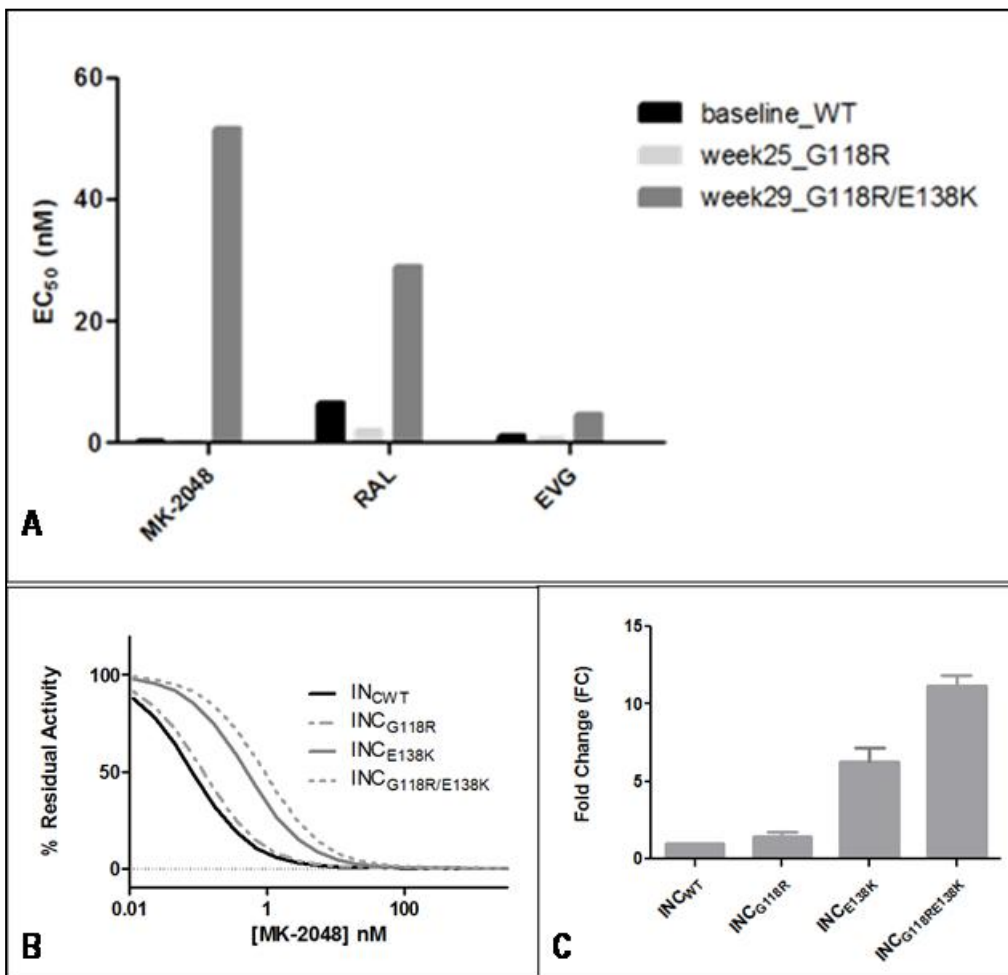


Figure 5.3: Confirmation of the role of G118R and E138K substitutions in conferring resistance to MK-2048 in subtype C integrase.

(A) Susceptibility of MK-2048 selected subtype C variant viruses to MK-2048, RAL and EVG. (B) Concentration-dependent inhibition of the strand transfer reaction of subtype C WT, G118R-, E138K- and G118R/E138K-containing integrase proteins by the INSTI MK-2048 (0.173 nM - 5000 nM). (C) Calculation of IC<sub>50</sub> fold-changes (FC) relative to WT shows that the G118R/E138K double variant protein has high in vitro resistance to MK-2048. Data presented here are the result of at least three independent experiments performed in triplicate.

#### **5.4.5 Effect of G118R on susceptibility to DTG, RAL and EVG**

We next tested the susceptibility of subtype C and CRF02\_AG integrase proteins containing G118R, alone or in combination with H51Y or E138K, as well as H51Y and E138K alone, on susceptibility to DTG, RAL and EVG (Figure 5.4; Table 5.2). The G118R substitution in all three subtypes resulted in statistically similar levels of resistance to DTG (Figure 5.4A; Table 5.2) and significant cross resistance with RAL (Figure 5.4B) and EVG (Figure 5.4C). However, G118R in subtypes B and C resulted in only low-level resistance to RAL, whereas an 8-fold change in susceptibility to RAL was noted for subtype CFF02\_AG consistent with clinical results [408]; no statistical differences between subtypes was observed in regard to resistance to EVG. The impact of the two secondary mutations H51Y and E138K on G118R-bearing protein differed between subtypes. The H51Y/G118R combination in subtype C resulted in slightly elevated levels of resistance to DTG compared to G118R alone but not in CRF02\_AG or



subtype B (Figure 5.4A; Table 5.2). Consistent with this, G118R/H51Y were selected by DTG in subtype C (Table 5.1). Although the H51Y/G118R variant integrase enzyme showed low levels of cross-resistance to both RAL and EVG in subtype B (~3 FC), susceptibility levels were comparable to WT for the subtype C protein (<2 FC). H51Y/G118R displayed greater susceptibility than WT for CRF02\_AG protein to both RAL and EVG (~0.6 FC) (Figure 5.4B, C; Table 5.2). Variant enzymes bearing E138K showed the greatest subtype-dependent variability; the G118R/E138K variant protein, when compared to WT, showed decreased susceptibility, increased susceptibility and similar susceptibility to DTG in subtypes B, C and CRF02\_AG integrase proteins respectively (Figure 5.4A; Table 5.2). However, all 3 subtypes exhibited similar levels of cross-resistance to RAL (~2 FC) (Figure 5.4B; Table 5.2) and WT-levels of susceptibility to EVG (Figure 5.4C; Table 5.2). The E138K variant in the three subtypes exhibited low level resistance to DTG (~1.5-2 FC) (Figure 5.4A; Table 5.2), low-level cross-resistance to RAL in subtype B (Figure 5.4B; Table 5.2) and high-level cross-resistance to EVG in CRF02\_AG (Figure 5.4C; Table 5.2).

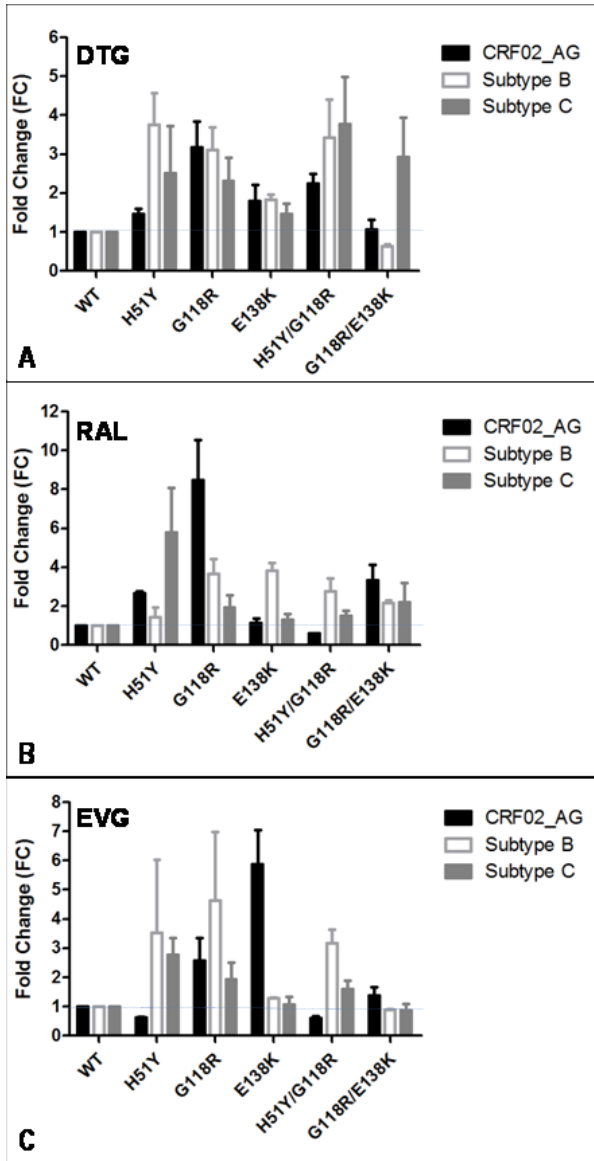


Figure 5.4: Subtype-specific susceptibility of WT and variant integrase proteins to clinically relevant INSTIs.

(A) DTG, (B) RAL, and (C) EVG. Drug inhibitory constants ( $K_i$ s) were derived by performing variable drug (0.2 nM-1000 nM)/variable target DNA (0 nM-128 nM) strand transfer assays in the presence of fixed concentrations of LTR (160 nM) and integrase protein (300 nM). Data were fit by non-linear regression analysis using GraphPad Prism and a competitive inhibition equation as detailed in Experimental Procedures. Fold-change (FC) values were

calculated in each experiment by dividing the observed  $K_i$  value of each variant for a particular INSTI by that observed for WT with the same INSTI. For each subtype, FC calculations from at least three individual experiments, analyzed using column statistics are presented.

Table 5.2: Enzymatic and virological parameters of variant HIV-1 integrase protein and viruses in CRF02\_AG and subtypes B and C

HIV-1 subtype	Integrase phenotype	Enzyme efficiency (EE) (% WT)		Viral Replication Capacity (% WT RC)	INSTI susceptibility (Fold change relative to WT)					
		3' processing (3P)	Strand transfer (ST)		DTG		RAL		EVG	
					Cell-free	Cell Culture	Cell-free	Cell Culture	Cell-free	Cell Culture
CRF02_AG	WT	100 ± 10.9	100 ± 16.4	100	1.00	1.0	1.00	1.0	1.00	1.0
	H51Y	309 ± 45.1	38.0 ± 1.4	69	1.47 ± 0.13	1.4	2.68 ± 0.08	1.0	0.631 ± 0.009	2.1
	G118R	182 ± 37.4	27.0 ± 4.4	8	3.17 ± 0.67	15.5	8.48 ± 2.05	17.2	2.58 ± 0.77	7.7
	E138K	193 ± 20.4	44.8 ± 2.5	91	2.61 ± 0.18	0.8	1.14 ± 0.23	0.8	5.87 ± 1.18	1.0
	H51Y/G118R	147 ± 4.1	25.9 ± 4.4	ND	2.24 ± 0.26	ND	0.595 ± 0.018	ND	0.617 ± 0.048	ND
	G118R/E138K	155 ± 21.4	41.9 ± 2.4	32	1.33 ± 0.35	12.7	3.33 ± 0.78	20.2	1.39 ± 0.28	5.2
Subtype B	WT	100 ± 1.5	100 ± 0.4	100	1.00	1.0	1.00	1.0	1.00	1.0
	H51Y	ND	42.5 ± 1.2	89	3.75 ± 0.82	1.4	1.43 ± 0.53	1.2	3.53 ± 2.49	2.0
	G118R	54.7 ± 3.8	11.8 ± 1.7	30	3.11 ± 0.58	8.2	3.68 ± 0.75	10.6	4.62 ± 2.35	5.5
	E138K	ND	105 ± 2.2	77	1.83 ± 0.13	0.8	3.84 ± 0.37	1.0	1.30 ± 0.03	0.8
	H51Y/G118R	170 ± 5.5	48.4 ± 0.04	ND	3.43 ± 0.97	ND	2.78 ± 0.65	ND	3.18 ± 0.45	ND
	G118R/E138K	140 ± 6.6	33.4 ± 1.46	43	0.644 ± .047	8.0	2.18 ± 0.13	14.1	0.884 ± 0.029	4.8
Subtype C	WT	100 ± 12.5	100 ± 11.2	ND	1.00	ND	1.00	1.0*	1.00	1.0*
	H51Y	116 ± 36.8	114 ± 12.6	ND	2.51 ± 1.22	ND	5.80 ± 2.28	ND	2.77 ± 0.57	ND
	G118R	96.4 ± 19.9	42.6 ± 6.6	ND	2.31 ± 0.60	ND	1.93 ± 0.64	0.3*	1.93 ± 0.58	0.78*
	E138K	61.4 ± 7.3	114 ± 12.6	ND	1.47 ± 0.26	ND	1.30 ± 0.31	ND	1.07 ± 0.26	ND
	H51Y/G118R	103 ± 5.5	31.3 ± 3.0	ND	3.78 ± 1.21	ND	1.51 ± 0.26	ND	1.61 ± 0.29	ND
	G118R/E138K	93.1 ± 15.3	47.9 ± 1.6	ND	2.93 ± 1.00	ND	2.20 ± 1.01	4.4*	0.876 ± 0.221	4.1*

\* Phenotyping studies performed on infectious viruses selected during MK-2048 selections in CBMCs

Table 5.3: Comparative analysis of biochemical and virology data

HIV-1 subtype	Integrase phenotype	Extent of INSTI susceptibility (FC relative to WT) <sup>a</sup>						% Integration activity <sup>b</sup>	
		DTG		RAL		EVG		EE	RC
		Cell-free	Cell culture	Cell-free	Cell culture	Cell-free	Cell culture		
CRF02_AG	WT	-						100	100
	H51Y	-	-	++	-	-	+	117	69
	G118R	++	+++	+++	+++	++	++	49.1	8
	E138K	++	-	-	-	+++	-	86.5	91
	H51Y/G118R	+	ND	-	ND	-	ND	38.1	ND
	G118R/E138K	-	+++	++	+++	++	++	64.9	32
Subtype B	WT	-	-	-	-	-	-	100	100
	H51Y	++	-	-	-	++	+	ND	89
	G118R	++	++	++	+++	+++	+++	54.7	30
	E138K	+	-	++	-	-	-	ND	77
	H51Y/G118R	++	ND	++	ND	++	ND	82.3	ND
	G118R/E138K		++	+	+++	-	+	46.8	43
Subtype C	WT		ND	-	ND	-	ND	100	ND
	H51Y	++	ND	+++	ND	++	ND	132	ND
	G118R	+	ND	+	ND	+	ND	96.4	ND

	E138K	-	ND	-	ND	-	ND	70.0	ND
	H51Y/G118R	++	ND	+	ND	+	ND	32.2	ND
	G118R/E138K	++	ND	+	ND	-	ND	93.1	ND

<sup>a</sup> Cell culture experiments tends to yield higher FC values than cell-free assays [418]. In the above table, susceptibility ranking for FC values in cell-free versus cell culture assays reported in the following format cell-free/cell culture is as follows: 0<-<1.5/0<-<2.0; 1.5≤+<2.5/2.0≤+<5.0; 2.5<++<4.0/5.0<++<10.0; 4.0<+++ /10.0 <+++.

<sup>b</sup> In the cell, 3'processing is the rate limiting step for integration [540], therefore we calculated overall integration efficiency is either calculated by multiplication of the EE values for 3' processing and strand transfer (if EE for 3' processing is lower that higher than ST or the EE for 3'processing is retained (if 3' processing is much lower than ST). Scenarios not tested are marked as ND

Clonal viruses that were WT, H51Y, G118R, E138K or G118R/E138K were phenotyped by Monogram Biosciences in subtype B and CRF02\_AG backgrounds (Tables 5.2 and 5.3). Difficulties generating subtype C clonal variants precluded its similar analysis. The phenotyping data implies that G118R alone conferred significant yet low-level resistance to DTG in both subtype B and CRF02\_AG but with significant loss of viral replication capacity (Table 5.2). G118R also caused significant cross resistance to EVG and RAL particularly, in CRF02\_A/G, for RAL [408]. Where possible, when resistance levels and viral replication calculated in cell culture were compared to resistance and integration activity calculated in biochemical assays (Table 5.3), there was good agreement between the two methods for most variants.

#### **5.4.6 Amino acid sequences differ at key positions between the three subtypes**

We performed multiple sequence alignments using ClustalW v1.8 software[543] to try to explain subtype specific differences in these experimental data. Integrase subtype amino acid sequences from subtype B (pNL4\_3), subtype C (pINDieC) and CRF02\_AG (p97) were aligned (Figure 5.5). The three integrase amino acid sequences share > 93% sequence identity and differed at only at a few positions, mostly through conservative polymorphisms. Interestingly, several polymorphic positions appear to be close to 2<sup>nd</sup> generation INSTI-resistance associated positions. As an example, the amino acid at position 50 in treatment-naïve patients is mostly M in treatment naïve subtype B [544] with polymorphisms in other subtypes . The M50I substitution appeared as a secondary

mutation to R263K during passage of subtype B HIV in the presence of DTG [418] and increased levels of resistance to DTG, together with R263K, without affecting the viral fitness cost imposed by R263K [544]. Position 50 is also only one residue downstream of the DTG-resistance associated substitution H51Y, that appears to be a secondary substitution for both G118R and R263K that increased levels of resistance to both DTG and EVG while also increasing the fitness cost imposed by R263K in subtype B HIV [177].

Another key polymorphic position at residue 91 is naturally A in both subtypes B and C and E in CRF02\_AG. CRF02\_AG integrase possesses an R at position 119 while subtype B and C have an S at this position, and all three subtypes have different residues at positions 133-136. Of note, positions 140, 143, 148 and 155 (Figure 5.5; boxed in blue)- that are associated with primary drug resistance to RAL and EVG, all occur within highly invariant motifs. Although the C-terminus of integrase is known to be highly polymorphic across retroviral genera, it is highly conserved among the three subtypes studied here.

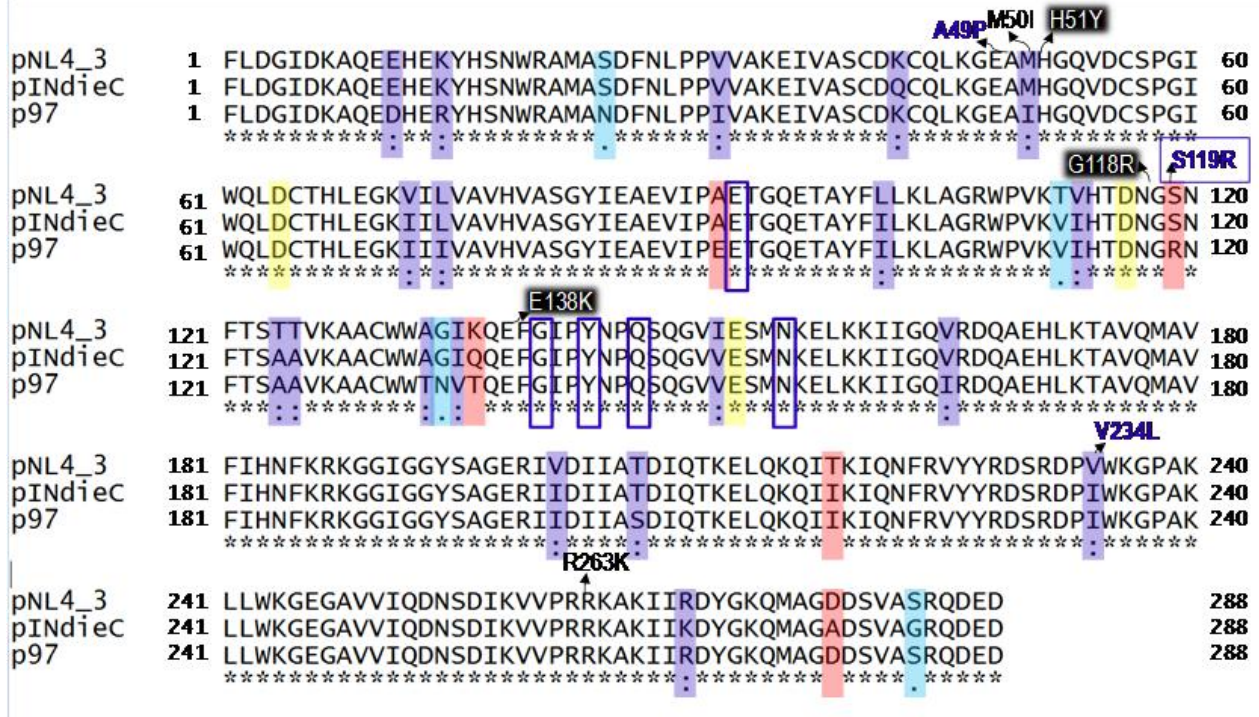


Figure 5.5: Multiple sequence alignment of subtype B, subtype C and CRF02\_AG integrase sequences from the plasmids pNL4\_3, pINdieC and p97, respectively, performed using ClustalW (1.8).

The catalytic site residues, D64, D116 and E152, are highlighted in yellow. Perfectly conserved residues are marked with (\*), conservative substitutions are marked with (:) and highlighted blue, while semi-conservative substitutions are marked with (.) and light blue highlights. Non-conservative substitutions are highlighted in red. Positions E92, G140, Y143, Q148, and N155, implicated in primary resistance to RAL and EVG, are boxed in blue. Labeled residues have been adequately characterized as affecting DTG susceptibility in, this study (White text with black highlight), or previous studies [177, 418, 544, 545] (bolded blue).



## 5.5 DISCUSSION

The integrase inhibitor associated substitution, G118R has never been selected in subtype B by any drug, in either the clinic or in a laboratory setting. In contrast, it has been selected in culture in subtype C and CRF02\_AG clonal viruses (Table 5.1) [352, 418] and in the clinic in a CRF02\_AG virus [408]. We subsequently showed that the presence of this mutation, when introduced into subtype B integrase caused resistance to DTG, EVG and RAL [419] at both an integrative [419] and fitness cost to the virus [352]. In this manuscript, we investigated the biochemical basis for the differential selection of G118R and its associated H51Y and E138K amino acid substitutions in HIV subtypes B and C as well as CRF02\_AG. We evaluated the impact of G118R alone or in concert with either H51Y or E138K on the ability of recombinant integrase proteins from subtypes B, C and CRF02\_AG to perform strand transfer and 3' processing activities and the individual impacts of H51Y and E138K were determined. We also evaluated the phenotypes of HIV-1 clonal viruses bearing wild-type or variant integrase sequences. After verifying that the sequential selection of G118R and E138K caused resistance to MK-2048, we also tested the susceptibility of the various recombinant enzymes to the clinically relevant INSTIs, DTG, RAL and EVG. Molecular modeling was used to provide an understanding of inter-residue and integrase-DNA interactions that drive the differential impact of G118R, H51Y and E138K in different HIV-1 subtypes. Of all the recombinant proteins tested, subtype B G118R integrase had the greatest loss in enzyme efficiency relative to WT (~90% for strand transfer and ~50% in 3'

processing), perhaps explaining why G118R is not selected in subtype B (15). In both the CRF02\_AG and subtype C proteins, the G118R mutation alone resulted in ~70% and ~60% loss in WT strand transfer efficiency. In all subtypes tested, the G118R mutation involves a G→C transversion that is less common than the G→A transition that is seen in the case of many drug resistance mutations such as R263K [546]. In subtype B, the addition of H51Y or E138K, neither of which has a major impact on strand transfer and 3' processing, partially rescued G118R-containing enzymes, while not significantly increasing the activities of G118R-containing subtype C or CRF02\_AG enzymes (Figure 5.1B, C; Figure 5.2B, C). Thus, the impact of H51Y and E138K may be related to resistance particularly since H51Y selected together with G118R in subtype C DTG selections.

The highly subtype-dependent protein activities revealed here in enzyme activity assays shows that minor polymorphic differences among subtypes may play important roles in fitness and in pathways for resistance. A key experiment (Figure 5.3) showed that G118R in subtype C, caused minimal if any resistance to MK-2048 (cell-free/cell culture; ~2.0/0.87 FC), but the addition of E138K significantly augmented levels of such resistance (~11/139 FC). This was important since MK-2048 was the first compound to select sequentially for G118R and E138K in a subtype C viral backbone [352]. More relevant clinically, the G118R mutation caused ~1.8-3.5 FC resistance to DTG in all three subtypes (Figure 5.4A) and resulted in varying levels of cross-resistance to RAL (Figure 5.4B) and EVG (Figure 5.4C). In CRF02\_AG integrase, G118R caused high-

level resistance to RAL (~8/17 FC), consistent with a clinical report of G118R in a patient harboring CRF02\_AG virus who failed a RAL containing regimen [408].

The impact of H51Y and E138K on resistance, whether alone or together with G118R, varied depending on subtype (Figure 5.4). Based on integrase homology modeling and structural overlays, the G118R substitution inhibits strand transfer activity by sterically hindering the access of target DNA to the strand transfer hotspot (Figure 5.6, yellow dotted circle) and by impeding hydrogen bond formation with D116. This effect is not seen with G118R in CRF02\_AG (Figure 5.6B) or subtype C (Figure 5.6C), nor is there interference with cation coordination or interaction with D64, the most important catalytic residue [105]. By contrast, 118R in subtype B forms strong electrostatic interactions with D64, C65 as well as D116 (Figure 5.6A). The subtype B 118R also extends in a manner that might force the repositioning of active site  $Mg^{2+}$  ions. In a subtype B DTG-bound model, the G118R side chain was shown to be physically overlapped with the DTG binding site [370]. The presence of either H51Y or E138K caused the partial (H51Y) or complete (E138K) repositioning of the G118R side chain (Figure 5.7J). In the DTG bound models, G118R formed salt-bridge interactions with D64 and hydrogen-bonding with D116 in both CRF02\_AG (Figure 5.7H) and subtype C (Figure 5.7I). In these cases, the active site would be seriously affected and the repositioning of at least one active site  $Mg^{2+}$  ion would be necessary (Figure 5.7 H, I; potential  $Mg^{2+}$  movement indicated by dotted red outlined arrow). In both scenarios, the long side-chain of 118R is completely within the DTG binding pocket (Figure 5.7K, L). The addition of either H51Y or E138K in

a G118R background, partially (E138K) or completely (H51Y) repositioned the 118R side chain out of the DTG binding pocket in CRF02\_AG (Figure 5.7K). In subtype C, the addition of either H51Y or E138K was insufficient to significantly reposition the 118R side chain. This result, coupled with the slightly better activity profile caused by either substitution, may explain the slight increase in resistance associated with these secondary mutations.

The variable impact of H51Y and E138K on integrase activity and drug resistance can be due to proximity with various polymorphic positions (Figure 5.5). Position 51 is clearly important for DTG resistance; H51Y was a secondary resistance mutation to R263K and augmented resistance to DTG [177] and was also selected together with G118R or alone by DTG [418]. The adjacent M50 position is polymorphic among subtypes, and M50I, which is a secondary substitution to R263K in subtype B [418], was shown to augment R263K-associated resistance to DTG and EVG [544]. Because DTG binds primarily to DNA and does not have as many protein contacts as RAL, and because it is more flexible than EVG [290], DNA binding may be impacted by a number of the DTG-selected substitutions: H51Y (LTR DNA), G118R (target DNA), M50I (LTR DNA), R263K and E138K (both LTR and target DNA) [177, 418-420, 544]. In the case of G118R and associated substitutions, slight active site perturbations caused by the 118R may be linked. Most DTG-associated mutations appear to interact with the L46-T66 loop which spans the DNA binding trough and interacts with both C-terminal and active site residues.

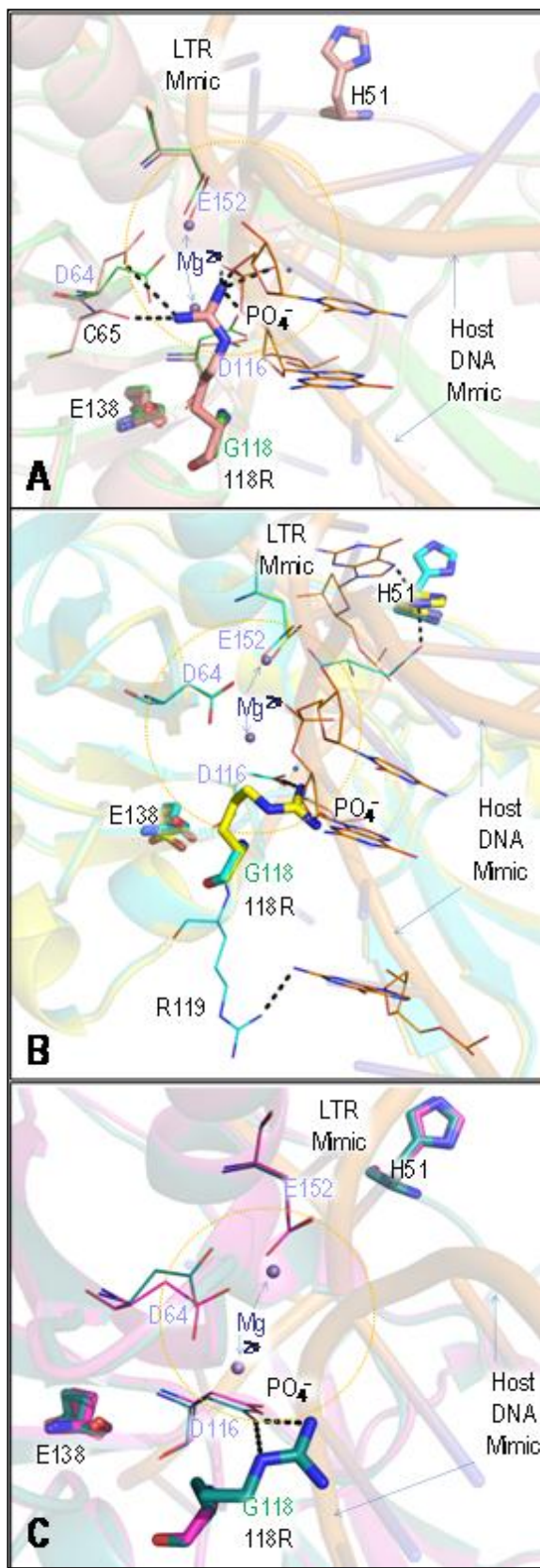


**Figure 5.6: Modeled HIV-1 WT and G118R target capture complexes show differential impact of G118R in the active sites of the three integrase subtypes.**

HIV-1 WT or G118R monomeric homology models for each of the three subtypes were created based on the structure of the freeze-trapped PFV target capture complex (PDB ID: 4E7K). These models were then used to build dimers as described in Experimental Procedures. Integrase-DNA interaction clues as well as cation binding in the TCC were mimicked by direct overlay of the LTR DNA, target DNA and the Mn<sup>2+</sup> and Zn<sup>2+</sup> ligands from the PFV structure. The impact of the G118R substitution in the strand transfer reaction with the active site of (A) subtype B, (B) CRF02\_AG and (C) subtype C was analyzed by visual assessment of the differing side-chain and backbone

interactions as well as residue-DNA clashes that occur with the G118R substitution,

particularly within the putative strand transfer zone (yellow circle). Structural visualization and manipulation were performed using PyMOL. Protein and DNA structure are shown as cartoons, with the residues under investigation shown as sticks. The catalytic triad residues are labeled in blue and shown as line traces. Structures of active site residues interacting with residues 118, 51 and 138 are shown as line traces. Possible hydrophilic interactions between atoms separated by  $< 3.5\text{\AA}$  are shown by black dashed lines. Coloration of lines and sticks are based on main chain color as well as standard atomic coloration. For clarity and where necessary, the colors of residue labels are the same as in the cartoons for that particular model.

The concomitant appearance of A49P, V234L and S119R substitutions, in a previously DTG-susceptible N155H-containing subtype B virus, was associated with clinical resistance to DTG [545]. These substitutions propelled a significant shift in the highly conserved loop region spanning L46-T66, drastically altering the active site and resulting in a severely compromised virus that was also highly resistant to DTG [545]. M50I is the sole polymorphic residue in this stretch and its impact on residue 49 as well as 51 may vary between subtypes. The presence of multiple subtype specific polymorphisms in association with E138K (Figure 5.5) may not affect overall protein structure (Figure 5.6), but altered side-chain interactions (Figure 5.7) may be sufficient to cause a differential impact on DNA binding as well as the G118R-associated DTG resistance reported here. Modeling studies suggest that E138K in a DTG-bound state communicates with

G118G/R primarily through the interaction of Q137 with the backbone amide of the 118 residue. E138 also interacts indirectly with the Q148 INSTI resistance position, Q148, by sequential hydrogen bonding with H114 [547]. The charged nature of H114 implies that the presence of 138K may affect H114 orientation and, ultimately, the orientation of Q148, with variable consequences for INSTI cross-resistance. The fact that E138K, in addition to having electrostatic interactions with H114, also forms such interactions with E136 in subtype B (residue 136 is T in CRF02\_AG and Q in subtype C) (Figures 5.5 and 5.7) implies that the impact of E138K on the orientation of Q148 may differ between subtypes and that the impact on drug susceptibility might also differ among subtypes.

The classical G140, Y143 and Q148 substitutions, associated with resistance to RAL and EVG, are in the active site loop and N155, also associated with resistance to RAL and EVG, is located deep in the active site. Any changes to these residues directly impact the ability of the active site to interact with the drug versus the substrate and can directly influence resistance and enzyme activity without the need for significant inter-residue interactions. In these cases, the subtype may be irrelevant to the level of drug resistance that results. The EVG E92Q mutation like G118R, is on the periphery of the INSTI binding pocket and variable interactions involving HIV subtypes can affect the level of resistance that is associated with this substitution [305].

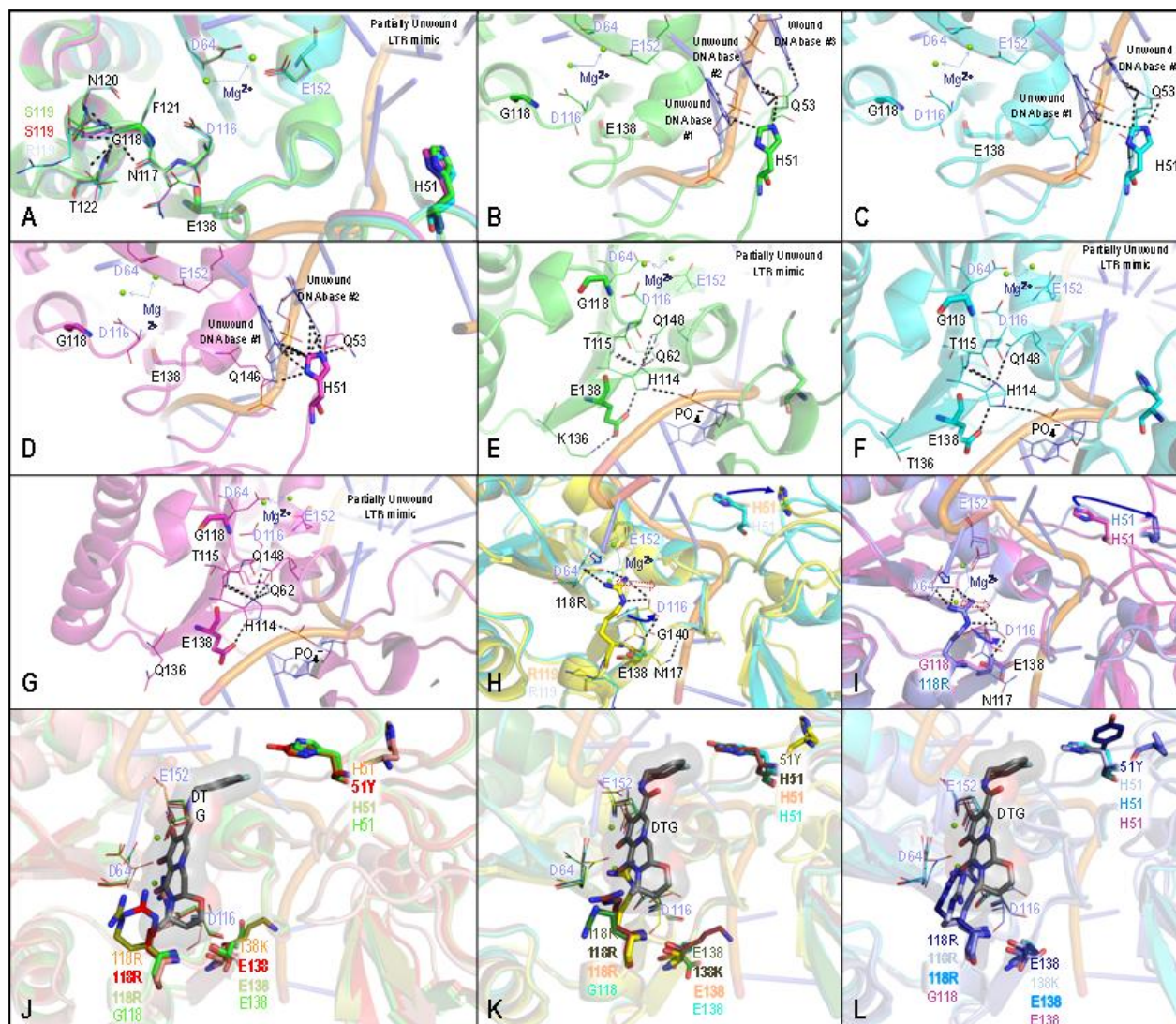


**Figure 5.7: Active site modeling of DTG-bound integrase.**

For each subtype, HIV-1 monomeric models which were WT, G118R, H51Y/G118R or G118R/E138K were created based on the structure of the DTG-bound PFV structure (PDB ID: 3S3M). These models were then used to build dimers as described in Experimental Procedures. Integrase-DNA interaction clues, cation binding and DTG - integrase interactions were mimicked by direct overlay of the LTR DNA, the Mn<sup>2+</sup> and Zn<sup>2+</sup> ligands, and DTG from the PFV structure 3S3M. (A) Overlay of WT models from



subtype B (green), subtype C (pink) and CRF02\_AG (turquoise) showing key backbone interactions of G118. (B) Close-up of subtype B WT showing inter-residue and DNA-integrase interactions of H51. (C) Close-up of CRF02\_AG WT showing inter-residue and DNA-integrase interactions of H51. (D) Close-up of subtype C WT showing inter-residue and DNA-integrase interactions of H51. (E) Close-up of subtype B WT showing inter-residue and DNA-integrase interactions of E138. (F) Close-up of CRF02\_AG WT showing inter-residue and DNA-integrase interactions of E138. (G) Close-up of subtype C WT showing inter-residue and DNA-integrase interactions of E138. (H) Overlay of WT (turquoise) and G118R (yellow) active sites showing impact of G118R substitution in the CRF02\_AG active site: changes in the D64 side-chain orientation caused by 118R is indicated (Open blue arrow) and other key side chain orientation changes are indicated by a solid blue arrow; possible repositioning of at least one Mg<sup>2+</sup> cation is indicated by the dotted red arrow. (I) Overlay of WT (pink) and G118R (purple) active sites showing the impact of the G118R substitution in the subtype C active site: changes in D64 side-chain orientation caused by 118R are indicated (open blue arrow) and other key side chain orientation changes are indicated by a solid blue arrow; possible repositioning of at least one Mg<sup>2+</sup> cation is indicated by the dotted red arrow. (J) Overlay of subtype B models; WT (green), G118R (tan), H51Y/G118R (red) and G118R/E138K (orange) showing the relative positioning of the three residues H51Y, G118R and E138K to DTG. (K) Overlay of CRF02\_AG models: WT (turquoise), G118R (yellow), H51Y/G118R (olive green) and G118R/E138K (tan) showing the relative positioning of the three residues

H51Y, G118R and E138K to DTG. (L) Overlay of subtype C models: WT (pink), G118R (purple), H51Y/G118R (navy) and G118R/E138K (light blue) showing the relative positioning of the three residues H51Y, G118R and E138K to DTG. Structural visualization and manipulation were performed using PyMOL. Protein and DNA structure are shown as cartoons, with the residues under investigation shown as sticks. The catalytic triad residues are labeled in blue and shown as line traces. Structures of active site residues interacting with residues 118, 51 and 138 are shown as line traces. Possible hydrophilic interactions between atoms separated by  $< 3.5\text{\AA}$  are shown as black dashed lines. Coloration of lines and sticks are based on main chain color as well as standard atomic coloration. For clarity and where necessary, the colors of residue labels are the same color as in the cartoon for that particular model.

DTG is able to evade these primary EVG and RAL substitutions because it forms hydrophobic stacking interactions with the terminal processed viral LTR CA dinucleotide [370] and coordinates optimally to active site  $\text{Mg}^{2+}$  ions without the need to interact significantly with the integrase protein [381]. Thus, it is more difficult to develop resistance to DTG. Evidence that G118R and R263K are two mutations that can engender resistance to DTG is growing [177, 418-420, 539, 544, 548] and both substitutions have also been shown to engender INSTI resistance in simian

immunodeficiency virus [549]. In this context, minor polymorphisms that vary among subtypes may be able to play a major role in the development of drug resistance.

In all three subtypes tested here, G118R results in highly deficient integration activity, and the secondary substitutions, E138K and H51Y are likely primarily rescue substitutions though their effectiveness varies between different integrase sequences.

This work highlights the need to better characterize polymorphic integrase positions, particularly in treatment experienced patients undergoing DTG therapy and especially in patients failing therapy without previously reported resistance substitutions.

## Chapter 6

### General Discussion

The introduction of integrase inhibitors into the fold of anti-retroviral therapy has been successful in terms of drug potency, *in vivo* pharmacokinetics and general patient outcomes [538]. As a novel class of anti- HIV drugs, integrase inhibitors offer a unique resistance profile that have made them useful for therapy in both drug-experienced and drug naïve patients [532, 538]. Elucidation of prototype foamy virus (PFV) integrase crystal structure [245, 370, 380, 381] and subsequent modeling of HIV-1 integrase structures [382] has led to a very good understanding of the molecular basis for the efficacy and potency of INSTIs as well as each of the mechanisms of resistance to INSTIs imparted by the "classical" E92, Y143, Q148 and N155 resistance pathways [336, 381] and limited cross-resistance with second-generation INSTIs such as MK-2048 and DTG [290]. In this thesis, we have examined resistance pathways that are relevant to second generation INSTIs, ie the R263K and G118R integrase substitution pathways, and have attempted to understand the influence of HIV subtype on development of resistance pathways and cross-resistance.

#### **6.1 Important considerations in homology modeling of HIV-1 integrase structures**

The lack of a viable HIV integrase structure or model was probably the single biggest impediment to integrase drug development for the first 25 years of HIV

research [550]. Just prior to and during this study, numerous partial structures of PFV integrase were crystallized by Peter Cherepanov and colleagues at Imperial College, London [245, 370, 379-381, 416]. Most of these were co-crystallized with viral and target DNA mimics, divalent cations and other relevant ligands such as INSTIs. These crystal structures and subsequent models have yielded an integrase drug discovery revolution and there are currently numerous candidate INSTI molecules at different stages of development [400, 414, 551]. Despite numerous HIV-1 integrase partial structures and despite a low sequence identity between HIV-1 and PFV integrase, the latter remains the only truly viable template for accurate creation of HIV integrase homology models.

By utilizing the I-TASSER server for protein structure and prediction of function [453], we were able to obtain full-length HIV-integrase structures that showed good spatial agreement with most HIV-1 partial structures as well as with the PFV crystal structures (Chapter 2). Considering that we are not close to resolution of a full-length HIV-1 integrase structure, let alone one with bound DNA molecules, and given the computing challenges of advanced methods such as molecular dynamics, we have developed methods in this thesis (Chapter 2) that provide easy and credible HIV integrase models that can be utilized for drug screening and/or predictions of comparative drug binding affinity. This

modelling also provides valuable insights into the G118R and R263K resistance pathways, which are discussed further below.

## **6.2 Comparing G118R and R263K and their associated secondary substitutions**

The classical G140, Y143 and Q148 substitutions, associated with resistance to RAL and EVG, are in the active site loop. N155, also associated with resistance to RAL and EVG, is located deep in the active site. Any residue substitutions at these positions thus directly impact the ability of the active site to interact with drugs and DNA substrate(s), thereby leading to major impacts on resistance and enzyme activity without the need for significant inter-residue interactions. In these cases, the viral subtype may be irrelevant to the level of drug resistance.

It is clear from the evidence presented in this thesis that G118R and R263K are two mutations that can engender resistance to DTG. Susceptibility to MK-2048 is also imparted by G118R in subtype C, providing evidence of subtype variability. Of the two substitutions, G118R and R263K, the latter has been seen clinically in relation to DTG treatment in two treatment-experienced INSTI-naïve patients, one with subtype B virus and the other with subtype C virus [539]. In tissue culture selections under DTG pressure, R263K has been selected by subtype B virus and G118R has been selected by subtype C virus; both mutations were selected by a CRF02\_AG recombinant virus [418]. Both of these substitutions

have been shown to engender broad INSTI resistance in simian immunodeficiency virus [549].

What separates DTG and MK-2048 from first generation integrase inhibitors is the extent of inhibitor-viral DNA interactions that are observed with these compounds [370, 547]. In separate studies, DTG and MK-2048 have been reported to have significantly longer binding half-lives to HIV pre-integration complexes than either RAL or EVG [341, 368, 369, 547]. DTG is able to evade primary EVG and RAL substitutions because it forms extensive hydrophobic stacking interactions with the terminal processed viral LTR CA dinucleotide [370, 547] and coordinates optimally to active site  $Mg^{2+}$  ions without the need to interact as much with the integrase protein as do RAL and EVG [380, 382]. Thus, it is more difficult to develop resistance to DTG and MK-2048. In this context, minor polymorphisms that vary among subtypes may be able to play a major role in the development of drug resistance, consistent with the results of the VIKING studies, in which patients received DTG after having first failed either RAL or EVG [547]. This is consistent with the work presented in the preceding chapters.

In all three subtypes tested here, G118R resulted in the lowest levels of integration activity; secondary substitutions such as E138K and H51Y may be able to partially rescue integrase activity, although their effectiveness varied between different integrase sequences. The G118R residue is perfectly

conserved among retroviral genera and it is likely indispensable for normal integrative functions of integrase. This is buoyed by the fact that substitutions at residue G118 have been detected in cell culture selections with the two experimental drugs S-1360 and MK-2048 as well as with the approved inhibitor DTG but not with RAL or EVG. In the clinic, only one patient has developed G118R while being treated with RAL. Our experimental results support the idea that a high fitness cost is associated with G118R, that only gives rise to low levels of drug resistance. This may explain why G118R seems to always be co-selected with another substitution, both in the clinic [408] and in culture [352, 418].

The R263K substitution imparts a major fitness cost to HIV and was identified in subtype B selections, either alone or together with complementary substitutions. [418]. Subtype C viruses, in our selections, failed to yield R263K. However, when this substitution was introduced into a subtype C viral backbone, R263K conferred similar INSTI resistance levels as seen in subtype B and CRF02AG viruses, although at a higher fitness cost similar to that of G118R in subtype B virus (Unpublished). Our modeling work has shown that there are significant differences in inter-residue interactions involving R263K in subtype C versus subtype B, which may explain why the only clinical report of R263K in subtype C occurred in the context of a V260I substitution [539].



Subtype differences aside, both G118R and R263K affect DNA binding [418-420, 544]. The G118 residue had previously been postulated to be involved in target DNA binding whilst the R263K substitution has been shown to reduce binding to integrase of both viral and target DNA (Chapter 3) [418].

The G118R and R263K mutations involve residues that have been postulated to be involved in DNA binding and/or active site architecture. The G118R substitution has been selected in the clinic together with L74M (by RAL) [408] and in culture together with substitutions at positions 51 (with DTG)[418], 66 (MK-2048, DTG)), 74 (MK-2048), and 138 (MK-2048) [352]. R263K leads to low levels of resistance at only a small cost in activity and viral fitness. Additional substitutions at positions 50, 51, 138, 151 have been associated with R263K and DTG treatment[177, 418, 420, 544] What is key and unique is that R263K, in the presence of tested secondary substitutions, did not lead to a gain in fitness and that viral replicative capacity was commonly even further impacted. The possibility that the R263K substitution might represent a dead-end resistance pathway is now being explored in our lab.

Structural modeling has shown that most, if not all, of these residues that are implicated in DTG and MK-2048 resistance interact with each other and with DNA within the quaternary integrase structure [177, 418-420, 462, 544, 545, 549]. The higher fitness cost of the G118R substitution in subtype B has been

attributed to the formation of a salt bridge between the substituted 118R and the key D64 catalytic residue in the viral intasome (Figure 4.7), an interaction that has not been observed in the intasomes of subtypes C and A/G. Unlike the situation in subtype B, residue 263K in subtype C is in close proximity to the active site, with contacts to both viral and target DNA mimics (Mesplede, Quashie et al, submitted). This is supported by biochemical evidence, which shows that R263K results in a 30-fold decrease in the ability of subtype C integrase to bind to DNA (Mesplède, Quashie et al, submitted), compared to mere 2-3 fold decreases in subtype B [418] and CRF02\_A/G [552]. The significant structural, biochemical and virological differences imparted by identical substitutions in these three different HIV subtypes are surprising, given their close genetic identity (Figure 5.5). In subtype B, the fitness cost for selection of G118R appears too great to overcome the resistance benefit that is conferred by this mutation [419]. The same may be true for the R263K substitution in subtype C (Mesplede, Quashie et al, submitted).

The current work highlights the need to better characterize polymorphic integrase positions, particularly in treatment experienced patients undergoing DTG therapy and in patients failing therapy without common resistance substitutions in integrase.

### 6.3 How has our work advanced the field?

Our work has preempted the appearance of R263K and G118R in the clinic as dolutegravir associated substitutions- more clinical usage of dolutegravir usage are needed to show whether these substitutions are truly clinically relevant. A combination of R263K with N155H had previously been observed in a study of RAL treated patients in the United States [553]. Current ongoing work in our lab suggests that this N155H/R263K combination engenders DTG resistance but at a mild fitness cost [554]. Combinations of R263K together with any of E92Q, Q148K, Y143R or G140S/Q148K resulted in viruses that were highly resistant to DTG but severely deficient in replication [554, 555]. In the clinic, a patient previously treated with RAL and harboring a virus bearing the N155H substitution was completely suppressed under DTG treatment but later developed DTG resistance ( $FC \approx 55$ ); however, virus recovered from this patient had reduced replication capacity ( $RC \approx 41\%$ ). This latter virus was also highly resistant to RAL ( $FC > 150$ ) and EVG ( $FC > 150$ ) [545] and contained the following substitutions: A49P, L68FL, T97A, E38K and L234V. This implies that the N155H pathway may be important in regard to DTG resistance. The additional impact of these accessory substitutions on DTG resistance are consistent with our findings. Using our modeling methodology from Chapter 2, we generated various integrase structural models based on the genotype of these viruses and showed

that the interaction of A49P and L234V as well as the N155H substitution may drive reorganization of the active site, affecting activity and preventing the binding of DTG [545]. The results of the VIKING clinical trials also showed that the presence of Q148K/R plus at least two additional substitutions can yield DTG resistance [163]; this has been corroborated by *in vitro* studies [556]. Despite this, twice-daily dosing of 50mg DTG was sufficient to suppress RAL-resistant viruses in the majority of patients.

#### **6.4 Conclusions**

Our work shows that development of resistance to second generation INSTIs such as DTG is likely to be rare in drug naïve HIV-infected patients. Furthermore, any resistant viruses might be highly deficient in replication capacity. Integrase sequences will need to be evaluated during therapy to fully quantify and understand the nature of any resistance that develops during therapy. The importance of understanding resistance mechanisms towards INSTIs are even more important now because in the 2015 recommended guidelines for treating antiretroviral-naïve patients, issued by the NIH, four out of five recommended options for firstline therapy were INSTI-based regimen, with DTG being in two of the four options (DTG+TDF+FTC or DTG+ABC+3TC in certain patients) [557]. The high potency of DTG and the low fitness of DTG-resistant variants may therefore significantly define the future of HIV therapy.

## References

1. Time 80 days that changed the world. 1st ed. New York, NY: Time Inc. Home Entertainment; 2003. p. p.
2. Wintrebert F, Certain A. [Evolution of the definition of AIDS. The main classifications of HIV infection]. *Presse Med.* 1990;19(41):1892-8. Epub 1990/12/01. PubMed PMID: 1980014.
3. Gallo RC. A reflection on HIV/AIDS research after 25 years. *Retrovirology.* 2006;3:72. Epub 2006/10/24. doi: 10.1186/1742-4690-3-72. PubMed PMID: 17054781; PubMed Central PMCID: PMC1629027.
4. Gallo RC, Montagnier L. The discovery of HIV as the cause of AIDS. *N Engl J Med.* 2003;349(24):2283-5. Epub 2003/12/12. doi: 10.1056/NEJMp038194. PubMed PMID: 14668451.
5. Quagliarello V. The Acquired Immunodeficiency Syndrome: current status. *The Yale journal of biology and medicine.* 1982;55(5-6):443-52. Epub 1982/09/01. PubMed PMID: 6134399; PubMed Central PMCID: PMC2596573.
6. Nahmias AJ, Weiss J, Yao X, Lee F, Kodosi R, Schanfield M, et al. Evidence for human infection with an HTLV III/LAV-like virus in Central Africa, 1959. *Lancet.* 1986;1(8492):1279-80. Epub 1986/05/31. PubMed PMID: 2872424.
7. Corbitt G, Bailey AS, Williams G. HIV infection in Manchester, 1959. *Lancet.* 1990;336(8706):51. Epub 1990/07/07. PubMed PMID: 1973229.
8. Pepin J. *The origins of AIDS.* Cambridge, UK ; New York: Cambridge University Press; 2011. xiv, 293 p. p.
9. Wayengera M. Searching for new clues about the molecular cause of endomyocardial fibrosis by way of in silico proteomics and analytical chemistry. *Plos One.* 2009;4(10):e7420. Epub 2009/10/14. doi: 10.1371/journal.pone.0007420. PubMed PMID: 19823676; PubMed Central PMCID: PMC2757908.
10. Larpin R, Chave JP, Schaller MD, Perret C. [Survival of HIV-positive patients hospitalized in intensive care for respiratory insufficiency and

pneumocystis carinii pneumonia]. Schweizerische medizinische Wochenschrift. 1990;120(50):1928-33. Epub 1990/12/15. PubMed PMID: 2270446.

11. Lee CA. Natural history of HIV and AIDS. AIDS care. 1990;2(4):353-7. Epub 1990/01/01. doi: 10.1080/09540129008257752. PubMed PMID: 1982504.

12. Fiore JR, Calabro ML, Angarano G, De Rossi A, Fico C, Pastore G, et al. HIV-1 variability and progression to AIDS: a longitudinal study. J Med Virol. 1990;32(4):252-6. Epub 1990/12/01. PubMed PMID: 1982010.

13. Plettenberg A, Reisinger E, Lenzner U, Listemann H, Ernst M, Kern P, et al. Oral candidosis in HIV-infected patients. Prognostic value and correlation with immunological parameters. Mycoses. 1990;33(9-10):421-5. Epub 1990/09/01. PubMed PMID: 1982718.

14. Green D, Deutsche J, Tang M, Goldsmith J. Effect of HIV-1 infection on CD4 cells in a hemophilia cohort. Haematologica. 1990;75 Suppl 5:132-41. Epub 1990/09/01. PubMed PMID: 1982277.

15. Harrer T, Messing K, Bienzle U, Meyer E, Giedl J, Kalden JR. [Manifestation of AIDS in HIV infected homosexual males with lymphadenopathy syndrome]. Klinische Wochenschrift. 1989;67(18):936-9. Epub 1989/09/15. PubMed PMID: 2571742.

16. Tindall B, Tillett G. HIV-related discrimination. AIDS. 1990;4 Suppl 1:S251-6. Epub 1990/01/01. PubMed PMID: 2152577.

17. West J. Public opinion, public policy, and HIV infection. Mental retardation. 1989;27(4):245-8. Epub 1989/08/01. PubMed PMID: 2586315.

18. Neumann PW, Benning BJ, Robinson DG, Gilmore N, O'Shaughnessy MV. HTLV-III infection in Canada in 1985. CMAJ : Canadian Medical Association journal = journal de l'Association medicale canadienne. 1986;135(5):477-80. Epub 1986/09/01. PubMed PMID: 3461870; PubMed Central PMCID: PMC1491537.

19. Lever AM, Berkhout B. 2008 Nobel prize in medicine for discoverers of HIV. Retrovirology. 2008;5:91. Epub 2008/10/16. doi: 10.1186/1742-4690-5-91. PubMed PMID: 18854052; PubMed Central PMCID: PMC2579300.

20. Cohen J, Enserink M. Nobel Prize in Physiology or Medicine. HIV, HPV researchers honored, but one scientist is left out. *Science*. 2008;322(5899):174-5. Epub 2008/10/11. doi: 10.1126/science.322.5899.174. PubMed PMID: 18845715.
21. Barre-Sinoussi F, Chermann JC, Rey F, Nugeyre MT, Chamaret S, Gruest J, et al. Isolation of a T-lymphotropic retrovirus from a patient at risk for acquired immune deficiency syndrome (AIDS). *Science*. 1983;220(4599):868-71. Epub 1983/05/20. PubMed PMID: 6189183.
22. Sarin PS, Gallo RC. Human T-cell leukemia-lymphoma virus (HTLV). *Progress in hematology*. 1983;13:149-61. Epub 1983/01/01. PubMed PMID: 6322228.
23. von Knebel Doeberitz M, Rittmuller C, zur Hausen H, Durst M. Inhibition of tumorigenicity of cervical cancer cells in nude mice by HPV E6-E7 anti-sense RNA. *International journal of cancer Journal international du cancer*. 1992;51(5):831-4. Epub 1992/07/09. PubMed PMID: 1319412.
24. Durst M, Glitz D, Schneider A, zur Hausen H. Human papillomavirus type 16 (HPV 16) gene expression and DNA replication in cervical neoplasia: analysis by in situ hybridization. *Virology*. 1992;189(1):132-40. Epub 1992/07/01. PubMed PMID: 1318602.
25. Sarngadharan MG, DeVico AL, Bruch L, Schupbach J, Gallo RC. HTLV-III: the etiologic agent of AIDS. *Princess Takamatsu symposia*. 1984;15:301-8. Epub 1984/01/01. PubMed PMID: 6100648.
26. Coffin J, Haase A, Levy JA, Montagnier L, Oroszlan S, Teich N, et al. Human immunodeficiency viruses. *Science*. 1986;232(4751):697. Epub 1986/05/09. PubMed PMID: 3008335.
27. Coffin J, Haase A, Levy JA, Montagnier L, Oroszlan S, Teich N, et al. What to call the AIDS virus? *Nature*. 1986;321(6065):10. Epub 1986/05/01. PubMed PMID: 3010128.
28. Cohen J. HHS: Gallo guilty of misconduct. *Science*. 1993;259(5092):168-70. Epub 1993/01/08. PubMed PMID: 8380653.

29. Gallo RC. Mechanism of disease induction by HIV. *J Acquir Immune Defic Syndr*. 1990;3(4):380-9. Epub 1990/01/01. PubMed PMID: 2156044.
30. Gallo RC, Robert-Guroff M, Wong-Staal F, Reitz MS, Jr., Arya SK, Streicher HZ. HTLV-III/LAV and the origin and pathogenesis of AIDS. *International archives of allergy and applied immunology*. 1987;82(3-4):471-5. Epub 1987/01/01. PubMed PMID: 3032803.
31. Popovic M, Sarngadharan MG, Read E, Gallo RC. Detection, isolation, and continuous production of cytopathic retroviruses (HTLV-III) from patients with AIDS and pre-AIDS. *Science*. 1984;224(4648):497-500. Epub 1984/05/04. PubMed PMID: 6200935.
32. Natrass N. *The AIDS conspiracy : science fights back*. New York: Columbia University Press; 2012. p. p.
33. Kalichman SC. *Denying AIDS : conspiracy theories, pseudoscience, and human tragedy*. New York: Copernicus Books; 2009. xxiii, 205 p. p.
34. Rödlach A. *Witches, Westerners, and HIV : AIDS & cultures of blame in Africa*. Walnut Creek, CA: Left Coast Press; 2006. ix, 247 p. p.
35. Hooper E. *The river : a journey to the source of HIV and AIDS*. 1st ed. Boston, MA: Little, Brown and Co.; 1999. xxxiii, 1070 p. p.
36. Marx PA, Drucker EM, Schneider WH. The serial passage theory of HIV emergence. *Clin Infect Dis*. 2011;52(3):421; author reply -2. Epub 2011/01/11. doi: 10.1093/cid/ciq166. PubMed PMID: 21217190; PubMed Central PMCID: PMC3106251.
37. Apetrei C, Becker J, Metzger M, Gautam R, Engle J, Wales AK, et al. Potential for HIV transmission through unsafe injections. *AIDS*. 2006;20(7):1074-6. Epub 2006/04/11. doi: 10.1097/01.aids.0000222085.21540.8a. PubMed PMID: 16603865.
38. Sharp PM, Hahn BH. Origins of HIV and the AIDS pandemic. *Cold Spring Harbor perspectives in medicine*. 2011;1(1):a006841. Epub 2012/01/10. doi: 10.1101/cshperspect.a006841. PubMed PMID: 22229120; PubMed Central PMCID: PMC3234451.



39. Korber B, Muldoon M, Theiler J, Gao F, Gupta R, Lapedes A, et al. Timing the ancestor of the HIV-1 pandemic strains. *Science*. 2000;288(5472):1789-96. Epub 2000/06/10. PubMed PMID: 10846155.
40. Gao F, Bailes E, Robertson DL, Chen Y, Rodenburg CM, Michael SF, et al. Origin of HIV-1 in the chimpanzee *Pan troglodytes troglodytes*. *Nature*. 1999;397(6718):436-41. Epub 1999/02/16. doi: 10.1038/17130. PubMed PMID: 9989410.
41. Sharp PM, Bailes E, Chaudhuri RR, Rodenburg CM, Santiago MO, Hahn BH. The origins of acquired immune deficiency syndrome viruses: where and when? *Philosophical transactions of the Royal Society of London Series B, Biological sciences*. 2001;356(1410):867-76. Epub 2001/06/19. doi: 10.1098/rstb.2001.0863. PubMed PMID: 11405934; PubMed Central PMCID: PMC1088480.
42. Kawamura M, Ishikawa K, Mingle JA, Osei-Kwasi M, Afoakwa SN, Nettey VB, et al. Immunological reactivities of Ghanaian sera with HIV-1, HIV-2, and simian immunodeficiency virus SIVagm. *AIDS*. 1989;3(9):609-11. Epub 1989/09/01. PubMed PMID: 2551342.
43. Hirsch VM, Olmsted RA, Murphey-Corb M, Purcell RH, Johnson PR. An African primate lentivirus (SIVsm) closely related to HIV-2. *Nature*. 1989;339(6223):389-92. Epub 1989/06/01. doi: 10.1038/339389a0. PubMed PMID: 2786147.
44. Chen Z, Luckay A, Sodora DL, Telfer P, Reed P, Gettie A, et al. Human immunodeficiency virus type 2 (HIV-2) seroprevalence and characterization of a distinct HIV-2 genetic subtype from the natural range of simian immunodeficiency virus-infected sooty mangabeys. *J Virol*. 1997;71(5):3953-60. Epub 1997/05/01. PubMed PMID: 9094672; PubMed Central PMCID: PMC191547.
45. Chen Z, Telfer P, Gettie A, Reed P, Zhang L, Ho DD, et al. Genetic characterization of new West African simian immunodeficiency virus SIVsm: geographic clustering of household-derived SIV strains with human immunodeficiency virus type 2 subtypes and genetically diverse viruses from a

- single feral sooty mangabey troop. *J Virol.* 1996;70(6):3617-27. Epub 1996/06/01. PubMed PMID: 8648696; PubMed Central PMCID: PMC190237.
46. Marx PA, Li Y, Lerche NW, Sutjipto S, Gettie A, Yee JA, et al. Isolation of a simian immunodeficiency virus related to human immunodeficiency virus type 2 from a west African pet sooty mangabey. *J Virol.* 1991;65(8):4480-5. Epub 1991/08/01. PubMed PMID: 1840620; PubMed Central PMCID: PMC248889.
47. Reitz MS, Jr., Guo HG, Oleske J, Hoxie J, Popovic M, Read-Connole E, et al. On the historical origins of HIV-1 (MN) and (RF). *AIDS research and human retroviruses.* 1992;8(11):1950. Epub 1992/11/11. PubMed PMID: 1489582.
48. Taya K, Nakayama EE, Shioda T. Moderate Restriction of Macrophage-Tropic Human Immunodeficiency Virus Type 1 by SAMHD1 in Monocyte-Derived Macrophages. *PLoS One.* 2014;9(3):e90969. Epub 2014/03/07. doi: 10.1371/journal.pone.0090969. PubMed PMID: 24599229; PubMed Central PMCID: PMC3944824.
49. Chen Z, Telfer P, Reed P, Zhang L, Getti A, Ho DD, et al. Isolation and characterization of the first simian immunodeficiency virus from a feral sooty mangabey (*Cercocebus atys*) in West Africa. *Journal of medical primatology.* 1995;24(3):108-15. Epub 1995/05/01. PubMed PMID: 8751049.
50. Lisse IM, Poulsen AG, Aaby P, Normark M, Kvinesdal B, Dias F, et al. Immunodeficiency in HIV-2 infection: a community study from Guinea-Bissau. *AIDS.* 1990;4(12):1263-6. Epub 1990/12/01. PubMed PMID: 1982411.
51. Lau KA, Wong JJ. Current Trends of HIV Recombination Worldwide. *Infectious disease reports.* 2013;5(Suppl 1):e4. Epub 2014/01/29. doi: 10.4081/idr.2013.s1.e4. PubMed PMID: 24470968; PubMed Central PMCID: PMC3892622.
52. Aldrich C, Hemelaar J. Global HIV-1 diversity surveillance. *Trends in molecular medicine.* 2012;18(12):691-4. Epub 2012/07/17. doi: 10.1016/j.molmed.2012.06.004. PubMed PMID: 22796205.
53. Hemelaar J, Gouws E, Ghys PD, Osmanov S. Global trends in molecular epidemiology of HIV-1 during 2000-2007. *AIDS.* 2011;25(5):679-89. Epub

2011/02/08. doi: 10.1097/QAD.0b013e328342ff93. PubMed PMID: 21297424; PubMed Central PMCID: PMC3755761.

54. Marx PA, Alcabes PG, Drucker E. Serial human passage of simian immunodeficiency virus by unsterile injections and the emergence of epidemic human immunodeficiency virus in Africa. *Philosophical transactions of the Royal Society of London Series B, Biological sciences*. 2001;356(1410):911-20. Epub 2001/06/19. doi: 10.1098/rstb.2001.0867. PubMed PMID: 11405938; PubMed Central PMCID: PMC1088484.

55. Locatelli S, Peeters M. Non-Human Primates, Retroviruses, and Zoonotic Infection Risks in the Human Population. *Nature Education Knowledge*. 2012;3(10):62-83. Epub 2012.

56. Kourouma K, Foucault-Fretz C, Diallo MP, Sabbatani S, Rezza G, Titti F, et al. HIV-1 and HIV-2 seropositivity among AIDS cases in Guinea. *AIDS*. 1990;4(12):1299-300. Epub 1990/12/01. PubMed PMID: 2088411.

57. Tebit DM, Arts EJ. Tracking a century of global expansion and evolution of HIV to drive understanding and to combat disease. *Lancet Infect Dis*. 2011;11(1):45-56. Epub 2010/12/04. doi: 10.1016/S1473-3099(10)70186-9. PubMed PMID: 21126914.

58. Drucker E, Alcabes PG, Marx PA. The injection century: massive unsterile injections and the emergence of human pathogens. *Lancet*. 2001;358(9297):1989-92. Epub 2001/12/19. doi: 10.1016/S0140-6736(01)06967-7. PubMed PMID: 11747942.

59. Gostin L. The needle-borne HIV epidemic: causes and public health responses. *Behavioral sciences & the law*. 1991;9(3):287-304. Epub 1991/07/01. PubMed PMID: 10148824.

60. Tahir M, Sharma SK, Smith-Rohrberg D. Unsafe medical injections and HIV transmission in India. *Lancet Infect Dis*. 2007;7(3):178-9. Epub 2007/02/24. doi: 10.1016/S1473-3099(07)70034-8. PubMed PMID: 17317597.

61. Hayes RJ, White RG. How important are unsafe medical injections in the spread of HIV in Africa? *Sexually transmitted diseases*. 2006;33(3):135-6. Epub

2006/03/02. doi: 10.1097/01.olq.0000204772.27981.d4. PubMed PMID: 16508524.

62. French K, Riley S, Garnett G. Simulations of the HIV epidemic in sub-Saharan Africa: sexual transmission versus transmission through unsafe medical injections. *Sexually transmitted diseases*. 2006;33(3):127-34. Epub 2006/03/02. doi: 10.1097/01.olq.0000204505.78077.e5. PubMed PMID: 16508523.

63. Gisselquist D, Rothenberg R, Potterat J, Drucker E. HIV infections in sub-Saharan Africa not explained by sexual or vertical transmission. *International journal of STD & AIDS*. 2002;13(10):657-66. Epub 2002/10/25. doi: 10.1258/095646202760326390. PubMed PMID: 12396534.

64. Gisselquist DP. Estimating HIV-1 transmission efficiency through unsafe medical injections. *International journal of STD & AIDS*. 2002;13(3):152-9. Epub 2002/02/28. PubMed PMID: 11860690.

65. Pepin J, Abou Chakra CN, Pepin E, Nault V. Evolution of the global use of unsafe medical injections, 2000-2010. *PLoS One*. 2013;8(12):e80948. Epub 2013/12/11. doi: 10.1371/journal.pone.0080948. PubMed PMID: 24324650; PubMed Central PMCID: PMC3851995.

66. Hoelscher M, Riedner G, Hemed Y, Wagner HU, Korte R, von Sonnenburg F. Estimating the number of HIV transmissions through reused syringes and needles in the Mbeya Region, Tanzania. *AIDS*. 1994;8(11):1609-15. Epub 1994/11/01. PubMed PMID: 7848599.

67. James B. Clean needles save lives. *HIV and injecting drug use. AIDS action*. 1993;(21):4-5. Epub 1993/06/01. PubMed PMID: 12345208.

68. Drug abuse. Study says clean drug needles cut HIV infections in half. *AIDS policy & law*. 1994;9(23):1, 7. Epub 1994/12/16. PubMed PMID: 12166378.

69. Tabor E, Gerety RJ, Cairns J, Bayley AC. Did HIV and HTLV originate in Africa? *JAMA : the journal of the American Medical Association*. 1990;264(6):691-2. Epub 1990/08/08. PubMed PMID: 2374268.

70. Nagelkerke NJ, Plummer FA, Holton D, Anzala AO, Manji F, Ngugi EN, et al. Transition dynamics of HIV disease in a cohort of African prostitutes: a

Markov model approach. *AIDS*. 1990;4(8):743-7. Epub 1990/08/01. PubMed PMID: 2175619.

71. Cayabyab M, Karlsson GB, Etemad-Moghadam BA, Hofmann W, Steenbeke T, Halloran M, et al. Changes in human immunodeficiency virus type 1 envelope glycoproteins responsible for the pathogenicity of a multiply passaged simian-human immunodeficiency virus (SHIV-HXBc2). *J Virol*. 1999;73(2):976-84. Epub 1999/01/09. PubMed PMID: 9882298; PubMed Central PMCID: PMC103917.

72. Reimann KA, Li JT, Veazey R, Halloran M, Park IW, Karlsson GB, et al. A chimeric simian/human immunodeficiency virus expressing a primary patient human immunodeficiency virus type 1 isolate env causes an AIDS-like disease after in vivo passage in rhesus monkeys. *J Virol*. 1996;70(10):6922-8. Epub 1996/10/01. PubMed PMID: 8794335; PubMed Central PMCID: PMC190741.

73. Lin X, van den Driessche P. A threshold result for an epidemiological model. *Journal of mathematical biology*. 1992;30(6):647-54. Epub 1992/01/01. PubMed PMID: 1640184.

74. Ulm K. A statistical method for assessing a threshold in epidemiological studies. *Statistics in medicine*. 1991;10(3):341-9. Epub 1991/03/01. PubMed PMID: 2028118.

75. Hayes R, Weiss H. Epidemiology. Understanding HIV epidemic trends in Africa. *Science*. 2006;311(5761):620-1. Epub 2006/02/04. doi: 10.1126/science.1124072. PubMed PMID: 16456070.

76. Tee KK, Pybus OG, Li XJ, Han X, Shang H, Kamarulzaman A, et al. Temporal and spatial dynamics of human immunodeficiency virus type 1 circulating recombinant forms 08\_BC and 07\_BC in Asia. *J Virol*. 2008;82(18):9206-15. Epub 2008/07/04. doi: 10.1128/JVI.00399-08. PubMed PMID: 18596096; PubMed Central PMCID: PMC2546895.

77. UNAIDS report focuses on Asia and cites growing epidemic in the East, particularly China, Indonesia, Vietnam. HIV has spread to all 31 China provinces. *AIDS Alert*. 2005;20(8):suppl 1-3. Epub 2005/08/30. PubMed PMID: 16124116.

78. Fields Virology. 5 ed. Philadelphia: Lippincott Williams & Wilkins; 2007.
79. Hemelaar J. Implications of HIV diversity for the HIV-1 pandemic. *The Journal of infection*. 2013;66(5):391-400. Epub 2012/10/30. doi: 10.1016/j.jinf.2012.10.026. PubMed PMID: 23103289.
80. Keele BF, Van Heuverswyn F, Li Y, Bailes E, Takehisa J, Santiago ML, et al. Chimpanzee reservoirs of pandemic and nonpandemic HIV-1. *Science*. 2006;313(5786):523-6. Epub 2006/05/27. doi: 10.1126/science.1126531. PubMed PMID: 16728595; PubMed Central PMCID: PMC2442710.
81. Coffin JM, Hughes SH, Varmus H. *Retroviruses*. Plainview, N.Y.: Cold Spring Harbor Laboratory Press; 1997. xv, 843 p. p.
82. Goto T, Nakai M, Ikuta K. The life-cycle of human immunodeficiency virus type 1. *Micron*. 1998;29(2-3):123-38. Epub 1998/07/31. PubMed PMID: 9684349.
83. Sierra S, Kupfer B, Kaiser R. Basics of the virology of HIV-1 and its replication. *Journal of clinical virology : the official publication of the Pan American Society for Clinical Virology*. 2005;34(4):233-44. Epub 2005/10/04. doi: 10.1016/j.jcv.2005.09.004. PubMed PMID: 16198625.
84. Frankel AD, Young JA. HIV-1: fifteen proteins and an RNA. *Annual review of biochemistry*. 1998;67:1-25. Epub 1998/10/06. doi: 10.1146/annurev.biochem.67.1.1. PubMed PMID: 9759480.
85. Woodward CL, Cheng SN, Jensen GJ. Electron cryotomography studies of maturing HIV-1 particles reveal the assembly pathway of the viral core. *J Virol*. 2015;89(2):1267-77. Epub 2014/11/14. doi: 10.1128/JVI.02997-14. PubMed PMID: 25392219; PubMed Central PMCID: PMC4300640.
86. Shibata R, Miura T, Hayami M, Ogawa K, Sakai H, Kiyomasu T, et al. Mutational analysis of the human immunodeficiency virus type 2 (HIV-2) genome in relation to HIV-1 and simian immunodeficiency virus SIV (AGM). *J Virol*. 1990;64(2):742-7. Epub 1990/02/01. PubMed PMID: 2296082; PubMed Central PMCID: PMC249168.

87. Hu W, Vander Heyden N, Ratner L. Analysis of the function of viral protein X (VPX) of HIV-2. *Virology*. 1989;173(2):624-30. Epub 1989/12/01. PubMed PMID: 2596032.
88. Liu J, Bartesaghi A, Borgnia M, Sapiro G, Subramaniam S. Molecular architecture of native HIV-1 gp120 trimers. *Nature*. 2008;455(7209):109-U76. doi: DOI 10.1038/nature07159. PubMed PMID: ISI:000258890200047.
89. Klatzmann DR, McDougal JS, Maddon PJ. The CD4 molecule and HIV infection. *Immunodeficiency reviews*. 1990;2(1):43-66. Epub 1990/01/01. PubMed PMID: 1973616.
90. Tzakis AG, Cooper MH, Dummer JS, Ragni M, Ward JW, Starzl TE. Transplantation in HIV+ patients. *Transplantation*. 1990;49(2):354-8. Epub 1990/02/01. PubMed PMID: 2305465; PubMed Central PMCID: PMC3234112.
91. Li H, Liu TJ, Hong ZH. Gene polymorphisms in CCR5, CCR2, SDF1 and RANTES among Chinese Han Population with HIV-1 infection. *Infection, genetics and evolution : journal of molecular epidemiology and evolutionary genetics in infectious diseases*. 2014. Epub 2014/03/22. doi: 10.1016/j.meegid.2014.03.009. PubMed PMID: 24650919.
92. Puissant B, Roubinet F, Massip P, Sandres-Saune K, Apoil PA, Abbal M, et al. Analysis of CCR5, CCR2, CX3CR1, and SDF1 polymorphisms in HIV-positive treated patients: impact on response to HAART and on peripheral T lymphocyte counts. *AIDS research and human retroviruses*. 2006;22(2):153-62. Epub 2006/02/16. doi: 10.1089/aid.2006.22.153. PubMed PMID: 16478397.
93. Ross TM, Cullen BR. The ability of HIV type 1 to use CCR-3 as a coreceptor is controlled by envelope V1/V2 sequences acting in conjunction with a CCR-5 tropic V3 loop. *Proc Natl Acad Sci U S A*. 1998;95(13):7682-6. Epub 1998/06/24. PubMed PMID: 9636210; PubMed Central PMCID: PMC22722.
94. O'Brien TR, Padian NS, Hodge T, Goedert JJ, O'Brien SJ, Carrington M. CCR-5 genotype and sexual transmission of HIV-1. *AIDS*. 1998;12(4):444-5. Epub 1998/03/31. PubMed PMID: 9520179.

95. Rooke R, Tremblay M, Wainberg MA. AZT (zidovudine) may act postintegrally to inhibit generation of HIV-1 progeny virus in chronically infected cells. *Virology*. 1990;176(1):205-15. Epub 1990/05/01. PubMed PMID: 1691885.
96. Prasad VR, Goff SP. Structure-function studies of HIV reverse transcriptase. *Annals of the New York Academy of Sciences*. 1990;616:11-21. Epub 1990/01/01. PubMed PMID: 1706569.
97. Piguet V, Trono D. Living in oblivion: HIV immune evasion. *Seminars in immunology*. 2001;13(1):51-7. Epub 2001/04/06. doi: 10.1006/smim.2000.0295. PubMed PMID: 11289799.
98. Wainberg MA, Tremblay M, Rooke R, Blain N, Soudeyns H, Parniak MA, et al. Characterization of reverse transcriptase activity and susceptibility to other nucleosides of AZT-resistant variants of HIV-1. Results from the Canadian AZT Multicentre Study. *Annals of the New York Academy of Sciences*. 1990;616:346-55. Epub 1990/01/01. PubMed PMID: 1706573.
99. Larder BA, Kemp SD. Multiple mutations in HIV-1 reverse transcriptase confer high-level resistance to zidovudine (AZT). *Science*. 1989;246(4934):1155-8. Epub 1989/12/01. PubMed PMID: 2479983.
100. Clinical trials of zidovudine in HIV infection. *Lancet*. 1989;2(8661):483-4. Epub 1989/08/26. PubMed PMID: 2570190.
101. Rooke R, Tremblay M, Soudeyns H, DeStephano L, Yao XJ, Fanning M, et al. Isolation of drug-resistant variants of HIV-1 from patients on long-term zidovudine therapy. Canadian Zidovudine Multi-Centre Study Group. *AIDS*. 1989;3(7):411-5. Epub 1989/07/01. PubMed PMID: 2504243.
102. Hehl EA, Joshi P, Kalpana GV, Prasad VR. Interaction between human immunodeficiency virus type 1 reverse transcriptase and integrase proteins. *J Virol*. 2004;78(10):5056-67. Epub 2004/04/29. PubMed PMID: 15113887; PubMed Central PMCID: PMC400328.



103. Tasara T, Maga G, Hottiger MO, Hubscher U. HIV-1 reverse transcriptase and integrase enzymes physically interact and inhibit each other. *FEBS letters*. 2001;507(1):39-44. Epub 2001/10/30. PubMed PMID: 11682056.
104. Sloan RD, Wainberg MA. The role of unintegrated DNA in HIV infection. *Retrovirology*. 2011;8:52. doi: 1742-4690-8-52 [pii] 10.1186/1742-4690-8-52. PubMed PMID: 21722380; PubMed Central PMCID: PMC3148978.
105. Engelman A, Liu Y, Chen H, Farzan M, Dyda F. Structure-based mutagenesis of the catalytic domain of human immunodeficiency virus type 1 integrase. *J Virol*. 1997;71(5):3507-14. PubMed PMID: 9094622; PubMed Central PMCID: PMC191497.
106. Marciniak RA, Calnan BJ, Frankel AD, Sharp PA. HIV-1 Tat protein trans-activates transcription in vitro. *Cell*. 1990;63(4):791-802. Epub 1990/11/16. PubMed PMID: 2225077.
107. Viscidi RP, Mayur K, Lederman HM, Frankel AD. Inhibition of antigen-induced lymphocyte proliferation by Tat protein from HIV-1. *Science*. 1989;246(4937):1606-8. Epub 1989/12/22. PubMed PMID: 2556795.
108. Sloan RD, Kuhl BD, Donahue DA, Roland A, Bar-Magen T, Wainberg MA. Transcription of preintegrated HIV-1 cDNA modulates cell surface expression of major histocompatibility complex class I via Nef. *J Virol*. 2011;85(6):2828-36. Epub 2011/01/07. doi: 10.1128/JVI.01854-10. PubMed PMID: 21209113; PubMed Central PMCID: PMC3067938.
109. Sloan RD, Donahue DA, Kuhl BD, Bar-Magen T, Wainberg MA. Expression of Nef from unintegrated HIV-1 DNA downregulates cell surface CXCR4 and CCR5 on T-lymphocytes. *Retrovirology*. 2010;7:44. Epub 2010/05/15. doi: 10.1186/1742-4690-7-44. PubMed PMID: 20465832; PubMed Central PMCID: PMC2881062.
110. Kuhl BD, Cheng V, Wainberg MA, Liang C. Tetherin and its viral antagonists. *Journal of neuroimmune pharmacology : the official journal of the Society on NeuroImmune Pharmacology*. 2011;6(2):188-201. Epub 2011/01/12.

doi: 10.1007/s11481-010-9256-1. PubMed PMID: 21222046; PubMed Central PMCID: PMC3087111.

111. Franke EK, Yuan HE, Luban J. Specific incorporation of cyclophilin A into HIV-1 virions. *Nature*. 1994;372(6504):359-62. Epub 1994/11/24. doi: 10.1038/372359a0. PubMed PMID: 7969494.

112. Giroud C, Chazal N, Briant L. Cellular kinases incorporated into HIV-1 particles: passive or active passengers? *Retrovirology*. 2011;8:71. Epub 2011/09/06. doi: 10.1186/1742-4690-8-71. PubMed PMID: 21888651; PubMed Central PMCID: PMC3182982.

113. Joshi A, Garg H, Ablan SD, Freed EO. Evidence of a role for soluble N-ethylmaleimide-sensitive factor attachment protein receptor (SNARE) machinery in HIV-1 assembly and release. *J Biol Chem*. 2011;286(34):29861-71. Epub 2011/06/18. doi: 10.1074/jbc.M111.241521. PubMed PMID: 21680744; PubMed Central PMCID: PMC3191027.

114. Matreyek KA, Engelman A. The requirement for nucleoporin NUP153 during human immunodeficiency virus type 1 infection is determined by the viral capsid. *J Virol*. 2011;85(15):7818-27. doi: JVI.00325-11 [pii] 10.1128/JVI.00325-11. PubMed PMID: 21593146; PubMed Central PMCID: PMC3147902.

115. Fujii K, Hurley JH, Freed EO. Beyond Tsg101: the role of Alix in 'ESCRTing' HIV-1. *Nature reviews Microbiology*. 2007;5(12):912-6. Epub 2007/11/06. doi: 10.1038/nrmicro1790. PubMed PMID: 17982468.

116. Wapling J, Srivastava S, Shehu-Xhilaga M, Tachedjian G. Targeting human immunodeficiency virus type 1 assembly, maturation and budding. *Drug target insights*. 2007;2:159-82. Epub 2007/01/01. PubMed PMID: 21901072; PubMed Central PMCID: PMC3155237.

117. Promadej-Lanier N, Thielen C, Hu DJ, Chaowanachan T, Gvetadze R, Choopanya K, et al. Cross-reactive T cell responses in HIV CRF01\_AE and B'-infected intravenous drug users: implications for superinfection and vaccines.

- AIDS research and human retroviruses. 2009;25(1):73-81. Epub 2009/02/03. doi: 10.1089/aid.2008.0169. PubMed PMID: 19182923.
118. Casado C, Pernas M, Alvaro T, Sandonis V, Garcia S, Rodriguez C, et al. Coinfection and superinfection in patients with long-term, nonprogressive HIV-1 disease. *J Infect Dis.* 2007;196(6):895-9. Epub 2007/08/19. doi: 10.1086/520885. PubMed PMID: 17703421.
119. Piantadosi A, Chohan B, Chohan V, McClelland RS, Overbaugh J. Chronic HIV-1 infection frequently fails to protect against superinfection. *PLoS Pathog.* 2007;3(11):e177. Epub 2007/11/21. doi: 10.1371/journal.ppat.0030177. PubMed PMID: 18020705; PubMed Central PMCID: PMC2077901.
120. Plantier JC, Lemee V, Dorval I, Gueudin M, Braun J, Hutin P, et al. HIV-1 group M superinfection in an HIV-1 group O-infected patient. *AIDS.* 2004;18(18):2444-6. Epub 2004/12/29. PubMed PMID: 15622327.
121. Griffin GE. Superinfection in HIV disease. *The Quarterly journal of medicine.* 1993;86(1):69-70. Epub 1993/01/01. PubMed PMID: 8438053.
122. Ragupathy V, Zhao J, Wood O, Tang S, Lee S, Nyambi P, et al. Identification of new, emerging HIV-1 unique recombinant forms and drug resistant viruses circulating in Cameroon. *Virology journal.* 2011;8:185. Epub 2011/04/26. doi: 10.1186/1743-422X-8-185. PubMed PMID: 21513545; PubMed Central PMCID: PMC3118203.
123. Liang B, Luo M, Ball TB, Plummer FA. QUASI analysis of the HIV-1 envelope sequences in the Los Alamos National Laboratory HIV sequence database: pattern and distribution of positive selection sites and their frequencies over years. *Biochemistry and cell biology = Biochimie et biologie cellulaire.* 2007;85(2):259-64. Epub 2007/05/31. doi: 10.1139/o06-143. PubMed PMID: 17534408.
124. Arts EJ, Hazuda DJ. HIV-1 antiretroviral drug therapy. *Cold Spring Harbor perspectives in medicine.* 2012;2(4):a007161. Epub 2012/04/05. doi: 10.1101/cshperspect.a007161. PubMed PMID: 22474613; PubMed Central PMCID: PMC3312400.

125. Guidelines for HIV and AIDS student support services. *The Journal of school health*. 1990;60(6):249-55. Epub 1990/08/01. PubMed PMID: 2232727.
126. Stimson GV. The fourth Okey memorial lecture. AIDS and HIV: the challenge for British drug services. *British journal of addiction*. 1990;85(3):329-39; discussion 41-51. Epub 1990/03/01. PubMed PMID: 2334820.
127. Graham MM, Bonini LA, Verdi MM. A multi-center study: clinical practices of HIV infected patients on CAPD/CCPD. *Advances in peritoneal dialysis Conference on Peritoneal Dialysis*. 1990;6:88-91. Epub 1990/01/01. PubMed PMID: 1982848.
128. Volberding PA, McCutchan JA. The HIV epidemic: medical and social challenges. *Biochimica et biophysica acta*. 1989;989(3):227-36. Epub 1989/12/27. PubMed PMID: 2695167.
129. Sonigo P, Montagnier L, Tiollais P, Girard M. AIDS vaccines: concepts and first trials. *Immunodeficiency reviews*. 1989;1(4):349-66. Epub 1989/01/01. PubMed PMID: 2698645.
130. Montagnier L, Chermann JC, Barre-Sinoussi F, Klatzmann D, Wain-Hobson S, Alizon M, et al. Lymphadenopathy associated virus and its etiological role in AIDS. *Princess Takamatsu symposia*. 1984;15:319-31. Epub 1984/01/01. PubMed PMID: 6100650.
131. Horwitz JP, Chua J, Noel M, Darooge MA. Nucleosides. Iv. 1-(2-Deoxy-Beta-D-Lyxofuranosyl)-5-Iodouracil. *J Med Chem*. 1964;7:385-6. Epub 1964/01/01. PubMed PMID: 14204995.
132. Wright K. AIDS therapy. First tentative signs of therapeutic promise. *Nature*. 1986;323(6086):283. Epub 1986/09/01. doi: 10.1038/323283a0. PubMed PMID: 3463865.
133. Wright K. AIDS protein made. *Nature*. 1986;319(6054):525. Epub 1986/02/13. doi: 10.1038/319525b0. PubMed PMID: 3003583.
134. Santangelo J, Large KM. Future hope? Antiretroviral therapy to treat HIV. *Today's OR nurse*. 1989;11(10):27-32. Epub 1989/10/01. PubMed PMID: 2683256.

135. Marcus U. [HIV positive: when to begin azidothymidine (AZT)?]. *Fortschritte der Medizin*. 1989;107(21):9. Epub 1989/07/20. PubMed PMID: 2670715.
136. Rooke R, Parniak MA, Tremblay M, Soudeyns H, Li XG, Gao Q, et al. Biological comparison of wild-type and zidovudine-resistant isolates of human immunodeficiency virus type 1 from the same subjects: susceptibility and resistance to other drugs. *Antimicrob Agents Chemother*. 1991;35(5):988-91. Epub 1991/05/01. PubMed PMID: 1649576; PubMed Central PMCID: PMC245142.
137. Soudeyns H, Yao XI, Gao Q, Belleau B, Kraus JL, Nguyen-Ba N, et al. Anti-human immunodeficiency virus type 1 activity and in vitro toxicity of 2'-deoxy-3'-thiacytidine (BCH-189), a novel heterocyclic nucleoside analog. *Antimicrob Agents Chemother*. 1991;35(7):1386-90. Epub 1991/07/01. PubMed PMID: 1929298; PubMed Central PMCID: PMC245177.
138. Yarchoan R, Mitsuya H, Thomas RV, Pluda JM, Hartman NR, Perno CF, et al. In vivo activity against HIV and favorable toxicity profile of 2',3'-dideoxyinosine. *Science*. 1989;245(4916):412-5. Epub 1989/07/28. PubMed PMID: 2502840.
139. Horwitz JR, Chua J, Da Rooze MA, Noel M, Klundt IL. Nucleosides. IX. The formation of 2',2'-unsaturated pyrimidine nucleosides via a novel beta-elimination reaction. *The Journal of organic chemistry*. 1966;31(1):205-11. Epub 1966/01/01. PubMed PMID: 5900814.
140. Bartlett JA. Current and future treatment of HIV infection. *Oncology (Williston Park)*. 1990;4(11):19-26, 9. Epub 1990/11/01. PubMed PMID: 2150323.
141. Watanabe KA, Harada K, Zeidler J, Matulic-Adamic J, Takahashi K, Ren WY, et al. Synthesis and anti-HIV-1 activity of 2'-"up"-fluoro analogues of active anti-AIDS nucleosides 3'-azido-3'-deoxythymidine (AZT) and 2',3'-dideoxycytidine (DDC). *J Med Chem*. 1990;33(8):2145-50. Epub 1990/08/01. PubMed PMID: 1695683.

142. Szebeni J, Wahl SM, Betageri GV, Wahl LM, Gartner S, Popovic M, et al. Inhibition of HIV-1 in monocyte/macrophage cultures by 2',3'-dideoxycytidine-5'-triphosphate, free and in liposomes. *AIDS research and human retroviruses*. 1990;6(5):691-702. Epub 1990/05/01. PubMed PMID: 2163269.
143. Russell JW, Whiterock VJ, Marrero D, Klunk LJ. Disposition in animals of a new anti-HIV agent: 2',3'-didehydro-3'-deoxythymidine. *Drug metabolism and disposition: the biological fate of chemicals*. 1990;18(2):153-7. Epub 1990/03/01. PubMed PMID: 1971565.
144. Nakashima H, Pauwels R, Baba M, Schols D, Desmyter J, De Clercq E. Tetrazolium-based plaque assay for HIV-1 and HIV-2, and its use in the evaluation of antiviral compounds. *Journal of virological methods*. 1989;26(3):319-29. Epub 1989/12/01. PubMed PMID: 2482843.
145. Kaul S, Dandekar KA, Pittman KA. Analytical method for the quantification of 2',3'-didehydro-3'-deoxythymidine, a new anti-human immunodeficiency virus (HIV) agent, by high-performance liquid chromatography (HPLC) and ultraviolet (UV) detection in rat and monkey plasma. *Pharmaceutical research*. 1989;6(10):895-9. Epub 1989/10/01. PubMed PMID: 2558374.
146. Yusa K, Oh-hara T, Yamazaki A, Tsukahara S, Satoh W, Tsuruo T. Cross-resistance to anti-HIV nucleoside analogs in multidrug-resistant human cells. *Biochemical and biophysical research communications*. 1990;169(3):986-90. Epub 1990/06/29. PubMed PMID: 2163639.
147. Ganser A, Greher J, Volkens B, Staszewski S, Hoelzer D. Inhibitory effect of azidothymidine, 2'-3'-dideoxyadenosine, and 2'-3'-dideoxycytidine on in vitro growth of hematopoietic progenitor cells from normal persons and from patients with AIDS. *Experimental hematology*. 1989;17(4):321-5. Epub 1989/05/01. PubMed PMID: 2540017.
148. Sterzycki RZ, Ghazzouli I, Brankovan V, Martin JC, Mansuri MM. Synthesis and anti-HIV activity of several 2'-fluoro-containing pyrimidine nucleosides. *J Med Chem*. 1990;33(8):2150-7. Epub 1990/08/01. PubMed PMID: 2165162.

149. Nakashima H, Balzarini J, Pauwels R, Schols D, Desmyter J, De Clercq E. Anti-HIV-1 activity of antiviral compounds, as quantitated by a focal immunoassay in CD4+ HeLa cells and a plaque assay in MT-4 cells. *Journal of virological methods*. 1990;29(2):197-208. Epub 1990/08/01. PubMed PMID: 1980126.
150. Reiss P, Casula M, de Ronde A, Weverling GJ, Goudsmit J, Lange JM. Greater and more rapid depletion of mitochondrial DNA in blood of patients treated with dual (zidovudine+didanosine or zidovudine+zalcitabine) vs. single (zidovudine) nucleoside reverse transcriptase inhibitors. *HIV medicine*. 2004;5(1):11-4. Epub 2004/01/21. PubMed PMID: 14731163.
151. Dalakas MC, Semino-Mora C, Leon-Monzon M. Mitochondrial alterations with mitochondrial DNA depletion in the nerves of AIDS patients with peripheral neuropathy induced by 2'3'-dideoxycytidine (ddC). *Laboratory investigation; a journal of technical methods and pathology*. 2001;81(11):1537-44. Epub 2001/11/14. PubMed PMID: 11706061.
152. Lewis LD, Hamzeh FM, Lietman PS. Ultrastructural changes associated with reduced mitochondrial DNA and impaired mitochondrial function in the presence of 2'3'-dideoxycytidine. *Antimicrob Agents Chemother*. 1992;36(9):2061-5. Epub 1992/09/01. PubMed PMID: 1329643; PubMed Central PMCID: PMC192440.
153. Grodeck B. AZT plus 3TC produces best results to date. *Positively aware : the monthly journal of the Test Positive Aware Network*. 1995;6. Epub 1995/01/01. PubMed PMID: 11362209.
154. Raffi F, Rachlis A, Stellbrink HJ, Hardy WD, Torti C, Orkin C, et al. Once-daily dolutegravir versus raltegravir in antiretroviral-naive adults with HIV-1 infection: 48 week results from the randomised, double-blind, non-inferiority SPRING-2 study. *Lancet*. 2013;381(9868):735-43. Epub 2013/01/12. doi: 10.1016/S0140-6736(12)61853-4. PubMed PMID: 23306000.
155. Grob PM, Wu JC, Cohen KA, Ingraham RH, Shih CK, Hargrave KD, et al. Nonnucleoside inhibitors of HIV-1 reverse transcriptase: nevirapine as a

prototype drug. *AIDS research and human retroviruses*. 1992;8(2):145-52. Epub 1992/02/01. PubMed PMID: 1371691.

156. Skoog MT, Hargrave KD, Miglietta JJ, Kopp EB, Merluzzi VJ. Inhibition of HIV-1 reverse transcriptase and virus replication by a non-nucleoside dipyridodiazepinone BI-RG-587 (Nevirapine). *Medicinal research reviews*. 1992;12(1):27-40. Epub 1992/01/01. PubMed PMID: 1371177.

157. Merluzzi VJ, Hargrave KD, Labadia M, Grozinger K, Skoog M, Wu JC, et al. Inhibition of HIV-1 replication by a nonnucleoside reverse transcriptase inhibitor. *Science*. 1990;250(4986):1411-3. Epub 1990/12/07. PubMed PMID: 1701568.

158. Collier AC, Coombs RW, Schoenfeld DA, Bassett R, Baruch A, Corey L. Combination therapy with zidovudine, didanosine and saquinavir. *Antiviral Res*. 1996;29(1):99. Epub 1996/01/01. PubMed PMID: 8721557.

159. Baker R. FDA approves 3TC and saquinavir. *Food and Drug Administration. BETA bulletin of experimental treatments for AIDS : a publication of the San Francisco AIDS foundation*. 1995;5, 9. Epub 1995/12/01. PubMed PMID: 11363011.

160. Kitchen VS, Skinner C, Ariyoshi K, Lane EA, Duncan IB, Burckhardt J, et al. Safety and activity of saquinavir in HIV infection. *Lancet*. 1995;345(8955):952-5. Epub 1995/04/15. PubMed PMID: 7715294.

161. Ritonavir, saquinavir combination--& warning. *AIDS treatment news*. 1995;(no 231):6. Epub 1995/09/29. PubMed PMID: 11362871.

162. Grodeck B. Triple combination superior to double combination. *Positively aware : the monthly journal of the Test Positive Aware Network*. 1995;6. Epub 1995/01/01. PubMed PMID: 11362210.

163. Castagna A, Maggiolo F, Penco G, Wright D, Mills A, Grossberg R, et al. Dolutegravir in Antiretroviral-Experienced Patients With Raltegravir- and/or Elvitegravir-Resistant HIV-1: 24-Week Results of the Phase III VIKING-3 Study. *J Infect Dis*. 2014. Epub 2014/01/22. doi: 10.1093/infdis/jiu051. PubMed PMID: 24446523.



164. The rules for successful HAART (highly active antiretroviral therapy). *Newsline People AIDS Coalit N Y.* 1998;30. Epub 2001/05/22. PubMed PMID: 11367500.
165. Goguel J, Katlama C, Sarfati C, Maslo C, Leport C, Molina JM. Remission of AIDS-associated intestinal microsporidiosis with highly active antiretroviral therapy. *AIDS.* 1997;11(13):1658-9. Epub 1997/11/20. PubMed PMID: 9365777.
166. Klaus BD, Grodesky MJ. HIV and HAART in 1997. Highly active antiretroviral therapy. *The Nurse practitioner.* 1997;22(8):139-42. Epub 1997/08/01. PubMed PMID: 9279851.
167. Zuger A. Adherence to highly active antiretroviral therapy. *AIDS clinical care.* 1997;9(11):86-7. Epub 2001/05/22. PubMed PMID: 11364775.
168. Teto G, Kanmogne GD, Torimiro JN, Alemnji G, Nguemaim FN, Takou D, et al. Lipid peroxidation and total cholesterol in HAART-naive patients infected with circulating recombinant forms of human immunodeficiency virus type-1 in Cameroon. *Plos One.* 2013;8(6):e65126. Epub 2013/06/14. doi: 10.1371/journal.pone.0065126. PubMed PMID: 23762297; PubMed Central PMCID: PMC3676401.
169. Martinez LJ. Why the fat lady hasn't sung: the limits of HAART. *Research initiative, treatment action : RITA.* 1999;5(5):8-10. Epub 2001/05/22. PubMed PMID: 11366892.
170. Gilden D. When HAART is not enough. *GMHC treatment issues : the Gay Men's Health Crisis newsletter of experimental AIDS therapies.* 1996;10(10):1-6. Epub 1996/10/01. PubMed PMID: 11364005.
171. Harrington M. Ten years of HAART. *Research initiative, treatment action : RITA.* 2005;11(1):28-38. Epub 2005/10/08. PubMed PMID: 16208817.
172. Laurence J. HAART, side effects, and viral transmission. *The AIDS reader.* 2004;14(5):210-1. Epub 2004/06/17. PubMed PMID: 15198078.
173. HAART does not stop all HIV replication. *Research initiative, treatment action : RITA.* 1999;5(5):23-4. Epub 2001/05/22. PubMed PMID: 11366891.

174. HAART won't completely eradicate HIV in semen. *AIDS Alert*. 1999;14(5):56-7. Epub 2001/05/22. PubMed PMID: 11366401.
175. HAART slashed AIDS death rates by 80 percent. *IAPAC monthly*. 2003;9(11):279. Epub 2004/03/03. PubMed PMID: 14989186.
176. Mayer K, Beyrer C. WHO's new HIV guidelines: opportunities and challenges. *Lancet*. 2013;382(9889):287-8. Epub 2013/07/31. doi: 10.1016/S0140-6736(13)61578-0. PubMed PMID: 23890033.
177. Mesplede T, Quashie PK, Osman N, Han Y, Singhroy DN, Lie Y, et al. Viral fitness cost prevents HIV-1 from evading dolutegravir drug pressure. *Retrovirology*. 2013;10:22. Epub 2013/02/26. doi: 10.1186/1742-4690-10-22. PubMed PMID: 23432922; PubMed Central PMCID: PMC3598531.
178. Gebo KA, Chaisson RE, Folkemer JG, Bartlett JG, Moore RD. Costs of HIV medical care in the era of highly active antiretroviral therapy. *AIDS*. 1999;13(8):963-9. Epub 1999/06/17. PubMed PMID: 10371178.
179. Hassig SE, Perriens J, Baende E, Kahotwa M, Bishagara K, Kinkela N, et al. An analysis of the economic impact of HIV infection among patients at Mama Yemo Hospital, Kinshasa, Zaire. *AIDS*. 1990;4(9):883-7. Epub 1990/09/01. PubMed PMID: 2252561.
180. The costs of HIV infections. *JAMA : the journal of the American Medical Association*. 1990;263(8):1067-8. Epub 1990/02/23. PubMed PMID: 2299777.
181. Pisani E. *The wisdom of whores : bureaucrats, brothels, and the business of AIDS*. 1st American ed. New York: W.W. Norton & Co.; 2008. xvii, 372 p. p.
182. Chaisson RE. The world AIDS conference in Durban, South Africa--science, politics, and health. *The Hopkins HIV report : a bimonthly newsletter for healthcare providers / Johns Hopkins University AIDS Service*. 2000;12(4):1, 6-7. Epub 2002/08/20. PubMed PMID: 12184236.
183. The XIII International AIDS Conference, held this summer in Durban, South Africa. *Canadian HIV/AIDS policy & law review / Canadian HIV/AIDS Legal Network*. 2000;5(4):3-4. Epub 2002/02/09. PubMed PMID: 11833165.

184. Marshall E. Gene patents. Patent on HIV receptor provokes an outcry. *Science*. 2000;287(5457):1375, 7. Epub 2000/03/18. PubMed PMID: 10722375.
185. Patel M, Mandava NK, Vadlapatla RK, Mitra AK. Recent patents and emerging therapeutics for HIV infections: a focus on protease inhibitors. *Pharmaceutical patent analyst*. 2013;2(4):513-38. Epub 2013/11/19. doi: 10.4155/ppa.13.33. PubMed PMID: 24237127.
186. Boelaert M, Lynen L, Van Damme W, Colebunders R. Do patents prevent access to drugs for HIV in developing countries? *JAMA : the journal of the American Medical Association*. 2002;287(7):840-1; author reply 2-3. Epub 2002/02/20. PubMed PMID: 11851568.
187. Nderitu T. Balancing pills and patents: intellectual property and the HIV/AIDS crisis. *E law : Murdoch University electronic journal of law*. 2001;8(3):E5. Epub 2006/08/15. PubMed PMID: 16903022.
188. Aspen manufactures Africa's first generic ARVs. *South African medical journal = Suid-Afrikaanse tydskrif vir geneeskunde*. 2003;93(10):744. Epub 2003/12/05. PubMed PMID: 14652958.
189. Aspen to manufacture AIDS drugs for Clinton Foundation. *South African medical journal = Suid-Afrikaanse tydskrif vir geneeskunde*. 2003;93(12):896-7. Epub 2004/01/31. PubMed PMID: 14750487.
190. Kommer C. [New UNAIDS figures]. *Kinderkrankenschwester : Organ der Sektion Kinderkrankenpflege / Deutsche Gesellschaft für Sozialpädiatrie und Deutsche Gesellschaft für Kinderheilkunde*. 2013;32(2):78. Epub 2013/03/13. PubMed PMID: 23477062.
191. Hargreaves S. Increase funding to ensure universal access, warns UNAIDS. *Lancet Infect Dis*. 2007;7(11):705. Epub 2007/11/08. PubMed PMID: 17987676.
192. UNAIDS guidelines update includes expanded agenda. Changes occur with sixth guideline. *AIDS Alert*. 2002;17(11):141-2. Epub 2002/11/05. PubMed PMID: 12412566.

193. Carmichael J. UNAIDS priorities in the battle against AIDS. *AIDS Patient Care STDS*. 1999;13(4):235-8. Epub 1999/06/03. PubMed PMID: 10351892.
194. Funding. Gates Foundation gives record \$150 million to AIDS efforts. *AIDS policy & law*. 2004;19(15):5. Epub 2004/09/16. PubMed PMID: 15366114.
195. Walgate R. Gates Foundation picks 14 grand challenges for global disease research. *Bulletin of the World Health Organization*. 2003;81(12):915-6. Epub 2004/03/05. PubMed PMID: 14997247; PubMed Central PMCID: PMC2572382.
196. Bill & Melinda Gates Foundation announces dollar 200 million grant to accelerate research on biggest problems in global health. *Journal of investigative medicine : the official publication of the American Federation for Clinical Research*. 2003;51(2):62. Epub 2003/03/20. PubMed PMID: 12643508.
197. Drug access. WTO, Clinton Foundation cut red tape over drug dispute. *AIDS policy & law*. 2007;22(16):2. Epub 2008/01/22. PubMed PMID: 18203380.
198. Kerr C. Clinton Foundation to help Ethiopian HIV/AIDS plan. *Lancet Infect Dis*. 2006;6(3):132. Epub 2006/03/16. PubMed PMID: 16535798.
199. Clinton Foundation gets big price reduction--to 40 cents a day for three-drug combination. *AIDS treatment news*. 2003;(395):3. Epub 2003/12/12. PubMed PMID: 14666911.
200. Hanefeld J. The Global Fund to Fight AIDS, Tuberculosis and Malaria: 10 years on. *Clin Med*. 2014;14(1):54-7. Epub 2014/02/18. doi: 10.7861/clinmedicine.14-1-54. PubMed PMID: 24532746.
201. Hoen E, Berger J, Calmy A, Moon S. Driving a decade of change: HIV/AIDS, patents and access to medicines for all. *J Int Aids Soc*. 2011;14:15. Epub 2011/03/29. doi: 10.1186/1758-2652-14-15. PubMed PMID: 21439089; PubMed Central PMCID: PMC3078828.
202. Poore P. The Global Fund to fight AIDS, Tuberculosis and Malaria (GFATM). *Health policy and planning*. 2004;19(1):52-3; discussion 4-6. Epub 2003/12/18. PubMed PMID: 14679285.

203. Bush signs bills to fund domestic, global AIDS programs. *AIDS policy & law*. 2002;17(2):5. Epub 2002/02/20. PubMed PMID: 11851131.
204. Weschler J, Malinowski T. U.S. loses U.N. seat, pledges \$200 million to global AIDS fund. *AIDS policy & law*. 2001;16(10):3. Epub 2001/09/26. PubMed PMID: 11569979.
205. Amin T, Kesselheim AS. Secondary patenting of branded pharmaceuticals: a case study of how patents on two HIV drugs could be extended for decades. *Health Aff (Millwood)*. 2012;31(10):2286-94. Epub 2012/10/11. doi: 10.1377/hlthaff.2012.0107. PubMed PMID: 23048110.
206. Morris K. HIV drug patents in the spotlight. *Lancet Infect Dis*. 2009;9(11):660-1. Epub 2009/10/29. PubMed PMID: 19860026.
207. Kintisch E. Dan Ravicher profile. A 'Robin Hood' declares war on lucrative U.S. patents. *Science*. 2005;309(5739):1319-20. Epub 2005/08/27. doi: 10.1126/science.309.5739.1319. PubMed PMID: 16123280.
208. Enfuvirtide (Fuzeon) for HIV Infection. *The Medical letter on drugs and therapeutics*. 2003;45(1159):49-50. Epub 2003/06/21. PubMed PMID: 12817195.
209. Carr A. Enfuvirtide, an HIV-1 fusion inhibitor. *N Engl J Med*. 2003;349(18):1770-1; author reply -1. Epub 2003/10/31. doi: 10.1056/NEJM200310303491815. PubMed PMID: 14585947.
210. Ball RA, Kinchelow T. Injection site reactions with the HIV-1 fusion inhibitor enfuvirtide. *Journal of the American Academy of Dermatology*. 2003;49(5):826-31. Epub 2003/10/25. doi: 10.1067/S0190. PubMed PMID: 14576660.
211. FDA. FDA approval of Isentress (raltegravir) <http://www.fda.gov/ForConsumers/ByAudience/ForPatientAdvocates/HIVandAIDSActivities/ucm124040.htm>2007 [cited 2011 07/08/2011].
212. Demberg T, Robert-Guroff M. Controlling the HIV/AIDS epidemic: current status and global challenges. *Frontiers in immunology*. 2012;3:250. Epub 2012/08/23. doi: 10.3389/fimmu.2012.00250. PubMed PMID: 22912636; PubMed Central PMCID: PMC3418522.

213. Stablein DM. Challenges of HIV vaccine development. *Statistics in medicine*. 1990;9(12):1425-31; discussion 33-7. Epub 1990/12/01. PubMed PMID: 2281230.
214. Robinson WE, Jr., Kawamura T, Lake D, Masuho Y, Mitchell WM, Hersh EM. Antibodies to the primary immunodominant domain of human immunodeficiency virus type 1 (HIV-1) glycoprotein gp41 enhance HIV-1 infection in vitro. *J Virol*. 1990;64(11):5301-5. Epub 1990/11/11. PubMed PMID: 1698995; PubMed Central PMCID: PMC248578.
215. Vzorov AN, Tentsov I, Grigor'ev VB, Shulenin SA, Garaev MM, Bogdan OP, et al. [Formation of virus-like particles by HIV-1 Gag proteins, expressed by a recombinant vaccinia virus]. *Molekuliarnaia biologii*. 1990;24(6):1666-74. Epub 1990/11/01. PubMed PMID: 2094814.
216. Gee CF. Cocktail vaccine may protect against HIV. *Nursing*. 1990;4(14):8. Epub 1990/07/12. PubMed PMID: 2381586.
217. Berman PW, Gregory TJ, Riddle L, Nakamura GR, Champe MA, Porter JP, et al. Protection of chimpanzees from infection by HIV-1 after vaccination with recombinant glycoprotein gp120 but not gp160. *Nature*. 1990;345(6276):622-5. Epub 1990/06/14. doi: 10.1038/345622a0. PubMed PMID: 2190095.
218. Bolognesi D. Vaccine development for HIV infection. *Journal of the American Academy of Dermatology*. 1990;22(6 Pt 2):1295-9. Epub 1990/06/01. PubMed PMID: 2362019.
219. Study of HIV vaccine begins. *American family physician*. 1990;41(6):1859, 61. Epub 1990/06/01. PubMed PMID: 2190459.
220. Robinson WE, Jr., Kawamura T, Gorny MK, Lake D, Xu JY, Matsumoto Y, et al. Human monoclonal antibodies to the human immunodeficiency virus type 1 (HIV-1) transmembrane glycoprotein gp41 enhance HIV-1 infection in vitro. *Proc Natl Acad Sci U S A*. 1990;87(8):3185-9. Epub 1990/04/01. PubMed PMID: 2326277; PubMed Central PMCID: PMC53860.

221. Ruby J, Brinkman C, Jones S, Ramshaw I. Response of monkeys to vaccination with recombinant vaccinia virus which coexpress HIV gp160 and human interleukin-2. *Immunology and cell biology*. 1990;68 ( Pt 2):113-7. Epub 1990/04/01. doi: 10.1038/icb.1990.16. PubMed PMID: 2200748.
222. Tacket CO, Baqar S, Munoz C, Murphy JR. Lymphoproliferative responses to mitogens and HIV-1 envelope glycoprotein among volunteers vaccinated with recombinant gp160. *AIDS research and human retroviruses*. 1990;6(4):535-42. Epub 1990/04/01. PubMed PMID: 2187503.
223. Rosenberg ZF, Fauci AS. Immunology of AIDS: approaches to understanding the immunopathogenesis of HIV infection. *La Ricerca in clinica e in laboratorio*. 1989;19(3):189-209. Epub 1989/07/01. PubMed PMID: 2688039.
224. Report of a WHO informal consultation on animal models for evaluation of drugs and vaccines for HIV infection and AIDS. W.H.O., Geneva, 14-15 September 1989. *Biologicals : journal of the International Association of Biological Standardization*. 1990;18(3):225-33. Epub 1990/07/01. PubMed PMID: 2175206.
225. Casazza JP, Bowman KA, Adzaku S, Smith EC, Enama ME, Bailer RT, et al. Therapeutic vaccination expands and improves the function of the HIV-specific memory T-cell repertoire. *J Infect Dis*. 2013;207(12):1829-40. Epub 2013/03/14. doi: 10.1093/infdis/jit098. PubMed PMID: 23482645; PubMed Central PMCID: PMC3654747.
226. Ramirez LA, Arango T, Boyer J. Therapeutic and prophylactic DNA vaccines for HIV-1. *Expert opinion on biological therapy*. 2013;13(4):563-73. Epub 2013/03/13. doi: 10.1517/14712598.2013.758709. PubMed PMID: 23477730.
227. Cohen J. HIV/AIDS. Gates Foundation doubles support for AIDS vaccine research. *Science*. 2006;313(5785):283. Epub 2006/07/22. doi: 10.1126/science.313.5785.283a. PubMed PMID: 16857908.
228. Gates Foundation donates \$25 million for AIDS vaccine. *AIDS treatment news*. 1999;(No 318):4-5. Epub 2001/05/22. PubMed PMID: 11366457.

229. Alcorn K. Raltegravir shows promise for use as a PrEP drug <http://www.aidsmap.com/Raltegravir-shows-potential-for-use-as-PrEP-drug/page/1434320/2009> [cited 2011 27/08/2011]. Available from: <http://www.aidsmap.com/Raltegravir-shows-potential-for-use-as-PrEP-drug/page/1434320/>.
230. Holmes D. FDA treads carefully with PrEP. *Lancet Infect Dis.* 2012;12(7):515-6. Epub 2012/08/30. PubMed PMID: 22930826.
231. Marcus JL, Glidden DV, Mayer KH, Liu AY, Buchbinder SP, Amico KR, et al. No evidence of sexual risk compensation in the iPrEx trial of daily oral HIV preexposure prophylaxis. *PLoS One.* 2013;8(12):e81997. Epub 2013/12/25. doi: 10.1371/journal.pone.0081997. PubMed PMID: 24367497; PubMed Central PMCID: PMC3867330.
232. Auerbach JD. The iPrEx results: lifting hopes, raising questions. *BETA bulletin of experimental treatments for AIDS : a publication of the San Francisco AIDS foundation.* 2010;22(4):47-9. Epub 2011/05/20. PubMed PMID: 21591604.
233. Baeten JM, Donnell D, Ndase P, Mugo NR, Campbell JD, Wangisi J, et al. Antiretroviral prophylaxis for HIV prevention in heterosexual men and women. *N Engl J Med.* 2012;367(5):399-410. Epub 2012/07/13. doi: 10.1056/NEJMoa1108524. PubMed PMID: 22784037; PubMed Central PMCID: PMC3770474.
234. Choopanya K, Martin M, Suntharasamai P, Sangkum U, Mock PA, Leethochawalit M, et al. Antiretroviral prophylaxis for HIV infection in injecting drug users in Bangkok, Thailand (the Bangkok Tenofovir Study): a randomised, double-blind, placebo-controlled phase 3 trial. *Lancet.* 2013;381(9883):2083-90. Epub 2013/06/19. doi: 10.1016/S0140-6736(13)61127-7. PubMed PMID: 23769234.
235. Richman DD, Margolis DM, Delaney M, Greene WC, Hazuda D, Pomerantz RJ. The challenge of finding a cure for HIV infection. *Science.* 2009;323(5919):1304-7. Epub 2009/03/07. doi: 10.1126/science.1165706. PubMed PMID: 19265012.



236. Vanham G, Buve A, Florence E, Seguin-Devaux C, Saez-Cirion A. What is the significance of posttreatment control of HIV infection vis-a-vis functional cure? *AIDS*. 2014;28(4):603-5. Epub 2014/01/10. doi: 10.1097/QAD.0000000000000147. PubMed PMID: 24401643.
237. Katlama C, Deeks SG, Autran B, Martinez-Picado J, van Lunzen J, Rouzioux C, et al. Barriers to a cure for HIV: new ways to target and eradicate HIV-1 reservoirs. *Lancet*. 2013;381(9883):2109-17. Epub 2013/04/02. doi: 10.1016/S0140-6736(13)60104-X. PubMed PMID: 23541541; PubMed Central PMCID: PMC3815451.
238. Kent SJ, Reece JC, Petravic J, Martyushev A, Kramski M, De Rose R, et al. The search for an HIV cure: tackling latent infection. *Lancet Infect Dis*. 2013;13(7):614-21. Epub 2013/03/14. doi: 10.1016/S1473-3099(13)70043-4. PubMed PMID: 23481675.
239. Yukl SA, Boritz E, Busch M, Bentsen C, Chun TW, Douek D, et al. Challenges in detecting HIV persistence during potentially curative interventions: a study of the Berlin patient. *PLoS Pathog*. 2013;9(5):e1003347. Epub 2013/05/15. doi: 10.1371/journal.ppat.1003347. PubMed PMID: 23671416; PubMed Central PMCID: PMC3649997.
240. Mbonye U, Karn J. Transcriptional control of HIV latency: Cellular signaling pathways, epigenetics, happenstance and the hope for a cure. *Virology*. 2014;454-455C:328-39. Epub 2014/02/26. doi: 10.1016/j.virol.2014.02.008. PubMed PMID: 24565118.
241. Hutter G. [History of the "Berlin patient" and the promise of a zinc-finger based HIV gene therapy]. *MMW Fortschritte der Medizin*. 2013;155 Suppl 1:17, 9. Epub 2013/08/22. PubMed PMID: 23961646.
242. Allers K, Hutter G, Hofmann J, Loddenkemper C, Rieger K, Thiel E, et al. Evidence for the cure of HIV infection by CCR5Delta32/Delta32 stem cell transplantation. *Blood*. 2011;117(10):2791-9. Epub 2010/12/15. doi: 10.1182/blood-2010-09-309591. PubMed PMID: 21148083.

243. Bukrinsky M. A hard way to the nucleus. *Mol Med.* 2004;10(1-6):1-5. PubMed PMID: 15502876; PubMed Central PMCID: PMC1431348.
244. Al-Mawsawi LQ, Neamati N. Blocking interactions between HIV-1 integrase and cellular cofactors: an emerging anti-retroviral strategy. *Trends Pharmacol Sci.* 2007;28(10):526-35. doi: S0165-6147(07)00209-X [pii] 10.1016/j.tips.2007.09.005. PubMed PMID: 17888520.
245. Maertens GN, Hare S, Cherepanov P. The mechanism of retroviral integration from X-ray structures of its key intermediates. *Nature.* 2010;468(7321):326-9. doi: nature09517 [pii] 10.1038/nature09517. PubMed PMID: 21068843; PubMed Central PMCID: PMC2999894.
246. Van Maele B, Busschots K, Vandekerckhove L, Christ F, Debyser Z. Cellular co-factors of HIV-1 integration. *Trends Biochem Sci.* 2006;31(2):98-105. doi: S0968-0004(05)00346-4 [pii] 10.1016/j.tibs.2005.12.002. PubMed PMID: 16403635.
247. Kalpana GV, Marmon S, Wang W, Crabtree GR, Goff SP. Binding and stimulation of HIV-1 integrase by a human homolog of yeast transcription factor SNF5. *Science.* 1994;266(5193):2002-6. PubMed PMID: 7801128.
248. Lesbats P, Botbol Y, Chevereau G, Vaillant C, Calmels C, Arneodo A, et al. Functional coupling between HIV-1 integrase and the SWI/SNF chromatin remodeling complex for efficient in vitro integration into stable nucleosomes. *PLoS Pathog.* 2011;7(2):e1001280. doi: 10.1371/journal.ppat.1001280. PubMed PMID: 21347347; PubMed Central PMCID: PMC3037357.
249. Lin CW, Engelman A. The barrier-to-autointegration factor is a component of functional human immunodeficiency virus type 1 preintegration complexes. *J Virol.* 2003;77(8):5030-6. PubMed PMID: 12663813; PubMed Central PMCID: PMC152146.
250. Suzuki Y, Yang H, Craigie R. LAP2alpha and BAF collaborate to organize the Moloney murine leukemia virus preintegration complex. *EMBO J.* 2004;23(23):4670-8. doi: 7600452 [pii]

10.1038/sj.emboj.7600452. PubMed PMID: 15510219; PubMed Central PMCID: PMC533042.

251. Cherepanov P, Maertens G, Proost P, Devreese B, Van Beeumen J, Engelborghs Y, et al. HIV-1 integrase forms stable tetramers and associates with LEDGF/p75 protein in human cells. *J Biol Chem.* 2003;278(1):372-81. doi: M209278200 [pii]

10.1074/jbc.M209278200. PubMed PMID: 12407101.

252. Cherepanov P, Ambrosio AL, Rahman S, Ellenberger T, Engelman A. Structural basis for the recognition between HIV-1 integrase and transcriptional coactivator p75. *Proc Natl Acad Sci U S A.* 2005;102(48):17308-13. doi: 0506924102 [pii]

10.1073/pnas.0506924102. PubMed PMID: 16260736; PubMed Central PMCID: PMC1297672.

253. Busschots K, Vercammen J, Emiliani S, Benarous R, Engelborghs Y, Christ F, et al. The interaction of LEDGF/p75 with integrase is lentivirus-specific and promotes DNA binding. *J Biol Chem.* 2005;280(18):17841-7. doi: M411681200 [pii]

10.1074/jbc.M411681200. PubMed PMID: 15749713.

254. Emiliani S, Mousnier A, Busschots K, Maroun M, Van Maele B, Tempé D, et al. Integrase mutants defective for interaction with LEDGF/p75 are impaired in chromosome tethering and HIV-1 replication. *J Biol Chem.* 2005;280(27):25517-23. doi: M501378200 [pii]

10.1074/jbc.M501378200. PubMed PMID: 15855167.

255. Maertens G, Vercammen J, Debyser Z, Engelborghs Y. Measuring protein-protein interactions inside living cells using single color fluorescence correlation spectroscopy. Application to human immunodeficiency virus type 1 integrase and LEDGF/p75. *FASEB J.* 2005;19(8):1039-41. doi: 04-3373fje [pii]

10.1096/fj.04-3373fje. PubMed PMID: 15788449.

256. Christ F, Voet A, Marchand A, Nicolet S, Desimmie BA, Marchand D, et al. Rational design of small-molecule inhibitors of the LEDGF/p75-integrase

- interaction and HIV replication. *Nat Chem Biol.* 2010;6(6):442-8. doi: nchembio.370 [pii]  
10.1038/nchembio.370. PubMed PMID: 20473303.
257. McNeely M, Hendrix J, Busschots K, Boons E, Deleersnijder A, Gerard M, et al. In vitro DNA tethering of HIV-1 integrase by the transcriptional coactivator LEDGF/p75. *J Mol Biol.* 2011;410(5):811-30. doi: S0022-2836(11)00376-7 [pii]  
10.1016/j.jmb.2011.03.073. PubMed PMID: 21763490.
258. De Luca L, Ferro S, Gitto R, Barreca ML, Agnello S, Christ F, et al. Small molecules targeting the interaction between HIV-1 integrase and LEDGF/p75 cofactor. *Bioorg Med Chem.* 2010;18(21):7515-21. doi: S0968-0896(10)00807-2 [pii]  
10.1016/j.bmc.2010.08.051. PubMed PMID: 20850978.
259. Madlala P, Gijssbers R, Christ F, Hombrouck A, Werner L, Mlisana K, et al. Association of polymorphisms in the LEDGF/p75 gene (PSIP1) with susceptibility to HIV-1 infection and disease progression. *AIDS.* 2011;25(14):1711-9. doi: 10.1097/QAD.0b013e328349c693. PubMed PMID: 21681054.
260. Cereseto A, Manganaro L, Gutierrez MI, Terreni M, Fittipaldi A, Lusic M, et al. Acetylation of HIV-1 integrase by p300 regulates viral integration. *EMBO J.* 2005;24(17):3070-81. doi: 7600770 [pii]  
10.1038/sj.emboj.7600770. PubMed PMID: 16096645; PubMed Central PMCID: PMC1201351.
261. Allouch A, Cereseto A. Identification of cellular factors binding to acetylated HIV-1 integrase. *Amino Acids.* 2011;41(5):1137-45. doi: 10.1007/s00726-009-0444-3. PubMed PMID: 20016921.
262. Allouch A, Di Primio C, Alpi E, Lusic M, Arosio D, Giacca M, et al. The TRIM family protein KAP1 inhibits HIV-1 integration. *Cell Host Microbe.* 2011;9(6):484-95. doi: S1931-3128(11)00168-5 [pii]  
10.1016/j.chom.2011.05.004. PubMed PMID: 21669397.
263. Ocwieja KE, Brady TL, Ronen K, Huegel A, Roth SL, Schaller T, et al. HIV integration targeting: a pathway involving Transportin-3 and the nuclear pore

protein RanBP2. PLoS Pathog. 2011;7(3):e1001313. doi: 10.1371/journal.ppat.1001313. PubMed PMID: 21423673; PubMed Central PMCID: PMC3053352.

264. Krishnan L, Matreyek KA, Oztop I, Lee K, Tipper CH, Li X, et al. The requirement for cellular transportin 3 (TNPO3 or TRN-SR2) during infection maps to human immunodeficiency virus type 1 capsid and not integrase. J Virol. 2010;84(1):397-406. doi: JVI.01899-09 [pii]

10.1128/JVI.01899-09. PubMed PMID: 19846519; PubMed Central PMCID: PMC2798409.

265. Lee K, Ambrose Z, Martin TD, Oztop I, Mulky A, Julias JG, et al. Flexible use of nuclear import pathways by HIV-1. Cell Host Microbe. 2010;7(3):221-33. doi: S1931-3128(10)00070-3 [pii]

10.1016/j.chom.2010.02.007. PubMed PMID: 20227665; PubMed Central PMCID: PMC2841689.

266. Levin A, Hayouka Z, Friedler A, Loyter A. Transportin 3 and importin  $\alpha$  are required for effective nuclear import of HIV-1 integrase in virus-infected cells. Nucleus. 2010;1(5):422-31. doi: 10.4161/nucl.1.5.12903. PubMed PMID: 21326825; PubMed Central PMCID: PMC3037538.

267. Ao Z, Danappa Jayappa K, Wang B, Zheng Y, Kung S, Rassart E, et al. Importin alpha3 interacts with HIV-1 integrase and contributes to HIV-1 nuclear import and replication. J Virol. 2010;84(17):8650-63. doi: JVI.00508-10 [pii]

10.1128/JVI.00508-10. PubMed PMID: 20554775; PubMed Central PMCID: PMC2919037.

268. Jayappa KD, Ao Z, Yang M, Wang J, Yao X. Identification of critical motifs within HIV-1 integrase required for importin  $\alpha$ 3 interaction and viral cDNA nuclear import. J Mol Biol. 2011;410(5):847-62. doi: S0022-2836(11)00426-8 [pii]

10.1016/j.jmb.2011.04.011. PubMed PMID: 21763491.

269. Zheng Y, Ao Z, Wang B, Jayappa KD, Yao X. Host protein Ku70 binds and protects HIV-1 integrase from proteasomal degradation and is required for HIV replication. J Biol Chem. 2011;286(20):17722-35. doi: M110.184739 [pii]

10.1074/jbc.M110.184739. PubMed PMID: 21454661; PubMed Central PMCID: PMC3093848.

270. Gupta SP, Nagappa AN. Design and development of integrase inhibitors as anti-HIV agents. *Curr Med Chem*. 2003;10(18):1779-94. PubMed PMID: 12871104.

271. Sluis-Cremer N, Tachedjian G. Modulation of the oligomeric structures of HIV-1 retroviral enzymes by synthetic peptides and small molecules. *Eur J Biochem*. 2002;269(21):5103-11. doi: 3216 [pii]. PubMed PMID: 12392542.

272. Maurin C, Bailly F, Cotelle P. Structure-activity relationships of HIV-1 integrase inhibitors--enzyme-ligand interactions. *Curr Med Chem*. 2003;10(18):1795-810. PubMed PMID: 12871105.

273. Singh SB, Jayasuriya H, Salituro GM, Zink DL, Shafiee A, Heimbuch B, et al. The complestatins as HIV-1 integrase inhibitors. Efficient isolation, structure elucidation, and inhibitory activities of isocomplestatin, chloropectin I, new complestatins, A and B, and acid-hydrolysis products of chloropectin I. *J Nat Prod*. 2001;64(7):874-82. doi: np000632z [pii]. PubMed PMID: 11473415.

274. Jing N, Xu X. Rational drug design of DNA oligonucleotides as HIV inhibitors. *Curr Drug Targets Infect Disord*. 2001;1(2):79-90. PubMed PMID: 12455406.

275. Brigo A, Mustata GI, Briggs JM, Moro S. Discovery of HIV-1 integrase inhibitors through a novel combination of ligand and structure-based drug design. *Med Chem*. 2005;1(3):263-75. PubMed PMID: 16787322.

276. Hazuda DJ, Felock P, Witmer M, Wolfe A, Stillmock K, Grobler JA, et al. Inhibitors of strand transfer that prevent integration and inhibit HIV-1 replication in cells. *Science*. 2000;287(5453):646-50. doi: 8227 [pii]. PubMed PMID: 10649997.

277. Reinke R, Lee DJ, Robinson WE. Inhibition of human immunodeficiency virus type 1 isolates by the integrase inhibitor L-731,988, a diketo Acid. *Antimicrob Agents Chemother*. 2002;46(10):3301-3. PubMed PMID: 12234866; PubMed Central PMCID: PMC3093848.

278. Hazuda D, Iwamoto M, Wenning L. Emerging pharmacology: inhibitors of human immunodeficiency virus integration. *Annu Rev Pharmacol Toxicol.* 2009;49:377-94. doi: 10.1146/annurev.pharmtox.011008.145553. PubMed PMID: 18928385.
279. Marchand C, Zhang X, Pais GC, Cowansage K, Neamati N, Burke TR, et al. Structural determinants for HIV-1 integrase inhibition by beta-diketo acids. *J Biol Chem.* 2002;277(15):12596-603. doi: M110758200 [pii] 10.1074/jbc.M110758200. PubMed PMID: 11805103.
280. Goldgur Y, Craigie R, Cohen GH, Fujiwara T, Yoshinaga T, Fujishita T, et al. Structure of the HIV-1 integrase catalytic domain complexed with an inhibitor: a platform for antiviral drug design. *Proc Natl Acad Sci U S A.* 1999;96(23):13040-3. PubMed PMID: 10557269; PubMed Central PMCID: PMC23896.
281. Rosemond MJ, St John-Williams L, Yamaguchi T, Fujishita T, Walsh JS. Enzymology of a carbonyl reduction clearance pathway for the HIV integrase inhibitor, S-1360: role of human liver cytosolic aldo-keto reductases. *Chem Biol Interact.* 2004;147(2):129-39. doi: S0009279703001534 [pii] 10.1016/j.cbi.2003.12.001. PubMed PMID: 15013815.
282. Krishnan L, Li X, Naraharisetty HL, Hare S, Cherepanov P, Engelman A. Structure-based modeling of the functional HIV-1 intasome and its inhibition. *Proc Natl Acad Sci U S A.* 2010;107(36):15910-5. PubMed PMID: 20733078.
283. Hare S, Gupta SS, Valkov E, Engelman A, Cherepanov P. Retroviral intasome assembly and inhibition of DNA strand transfer. *Nature.* 2010;464(7286):232-6. PubMed PMID: 20118915.
284. Cherepanov P, Maertens GN, Hare S. Structural insights into the retroviral DNA integration apparatus. *Curr Opin Struct Biol.* 2011;21(2):249-56. PubMed PMID: 21277766.
285. Engelman A, Cherepanov P. The structural biology of HIV-1: mechanistic and therapeutic insights. *Nature reviews Microbiology.* 2012;10(4):279-90. Epub 2012/03/17. doi: 10.1038/nrmicro2747. PubMed PMID: 22421880.

286. Maertens GN, Hare S, Cherepanov P. The mechanism of retroviral integration from X-ray structures of its key intermediates. *Nature*. 2010;468(7321):326-9. PubMed PMID: 21068843.
287. Espeseth AS, Felock P, Wolfe A, Witmer M, Grobler J, Anthony N, et al. HIV-1 integrase inhibitors that compete with the target DNA substrate define a unique strand transfer conformation for integrase. *Proc Natl Acad Sci U S A*. 2000;97(21):11244-9. PubMed PMID: 11016953.
288. Hare S, Vos AM, Clayton RF, Thuring JW, Cummings MD, Cherepanov P. Molecular mechanisms of retroviral integrase inhibition and the evolution of viral resistance. *Proc Natl Acad Sci U S A*. 2010;107(46):20057-62. Epub 2010/10/30. doi: 10.1073/pnas.1010246107. PubMed PMID: 21030679; PubMed Central PMCID: PMC2993412.
289. Grobler JA, Stillmock K, Hu B, Witmer M, Felock P, Espeseth AS, et al. Diketo acid inhibitor mechanism and HIV-1 integrase: implications for metal binding in the active site of phosphotransferase enzymes. *Proc Natl Acad Sci U S A*. 2002;99(10):6661-6. PubMed PMID: 11997448.
290. Hare S, Smith SJ, Metifiot M, Jaxa-Chamiec A, Pommier Y, Hughes SH, et al. Structural and Functional Analyses of the Second-generation Integrase Strand Transfer Inhibitor Dolutegravir (S/GSK1349572). *Mol Pharmacol*. 2011. PubMed PMID: 21719464.
291. Li X, Krishnan L, Cherepanov P, Engelman A. Structural biology of retroviral DNA integration. *Virology*. 2011;411(2):194-205. Epub 2011/01/11. doi: 10.1016/j.virol.2010.12.008. PubMed PMID: 21216426.
292. Bacchi A, Carcelli M, Compari C, Fiscaro E, Pala N, Rispoli G, et al. Investigating the role of metal chelation in HIV-1 integrase strand transfer inhibitors. *J Med Chem*. 2011;54(24):8407-20. Epub 2011/11/10. doi: 10.1021/jm200851g. PubMed PMID: 22066494.
293. Bacchi A, Carcelli M, Compari C, Fiscaro E, Pala N, Rispoli G, et al. HIV-1 IN strand transfer chelating inhibitors: a focus on metal binding. *Molecular*



pharmaceutics. 2011;8(2):507-19. Epub 2011/02/18. doi: 10.1021/mp100343x. PubMed PMID: 21323359.

294. Hazuda DJ, Felock P, Witmer M, Wolfe A, Stillmock K, Grobler JA, et al. Inhibitors of strand transfer that prevent integration and inhibit HIV-1 replication in cells. *Science*. 2000;287(5453):646-50. Epub 2000/01/29. PubMed PMID: 10649997.

295. FDA notifications. FDA approves raltegravir for HIV-1 treatment-naive patients. *AIDS Alert*. 2009;24(9):106-7. PubMed PMID: 19938313.

296. Steigbigel RT, Cooper DA, Tepler H, Eron JJ, Gatell JM, Kumar PN, et al. Long-term efficacy and safety of Raltegravir combined with optimized background therapy in treatment-experienced patients with drug-resistant HIV infection: week 96 results of the BENCHMRK 1 and 2 Phase III trials. *Clin Infect Dis*. 2010;50(4):605-12. doi: 10.1086/650002. PubMed PMID: 20085491.

297. Donahue DA, Sloan RD, Kuhl BD, Bar-Magen T, Schader SM, Wainberg MA. Stage-dependent inhibition of HIV-1 replication by antiretroviral drugs in cell culture. *Antimicrob Agents Chemother*. 2010;54(3):1047-54. doi: AAC.01537-09 [pii] 10.1128/AAC.01537-09. PubMed PMID: 20038621; PubMed Central PMCID: PMC2826010.

298. Grinsztejn B, Nguyen BY, Katlama C, Gatell JM, Lazzarin A, Vittecoq D, et al. Safety and efficacy of the HIV-1 integrase inhibitor raltegravir (MK-0518) in treatment-experienced patients with multidrug-resistant virus: a phase II randomised controlled trial. *Lancet*. 2007;369(9569):1261-9. doi: S0140-6736(07)60597-2 [pii] 10.1016/S0140-6736(07)60597-2. PubMed PMID: 17434401.

299. Iwamoto M. Rifampin (RIF) modestly reduces plasma levels of MK-0518. In: Wenning LA LS, Kost JT, Mangin E, et al, editor. 8th Int Congr Drug Therapy in HIV Infection (HIV-8). Glasgow, Scotland2006.

300. Eron JJ, Rockstroh JK, Reynes J, Andrade-Villanueva J, Ramalho-Madruga JV, Bekker LG, et al. Raltegravir once daily or twice daily in previously

- untreated patients with HIV-1: a randomised, active-controlled, phase 3 non-inferiority trial. *Lancet Infect Dis*. 2011. doi: S1473-3099(11)70196-7 [pii] 10.1016/S1473-3099(11)70196-7. PubMed PMID: 21933752.
301. Vispo E, Barreiro P, Maida I, Mena A, Blanco F, Rodríguez-Novoa S, et al. Simplification from protease inhibitors to once- or twice-daily raltegravir: the ODIS trial. *HIV Clin Trials*. 2010;11(4):197-204. doi: 02N7N1575R25410N [pii] 10.1310/hct1104-197. PubMed PMID: 20974575.
302. Lanzafame M, Hill A, Lattuada E, Calcagno A, Bonora S. Raltegravir: is a 400 mg once-daily dose enough? *J Antimicrob Chemother*. 2010;65(3):595-7. doi: dkp488 [pii] 10.1093/jac/dkp488. PubMed PMID: 20071368.
303. Malet I, Delelis O, Valantin MA, Montes B, Soulie C, Wirden M, et al. Mutations associated with failure of raltegravir treatment affect integrase sensitivity to the inhibitor in vitro. *Antimicrob Agents Chemother*. 2008;52(4):1351-8. doi: AAC.01228-07 [pii] 10.1128/AAC.01228-07. PubMed PMID: 18227187; PubMed Central PMCID: PMC2292515.
304. Garrido C, de Mendoza C, Soriano V. [Resistance to integrase inhibitors]. *Enferm Infecc Microbiol Clin*. 2008;26 Suppl 12:40-6. PubMed PMID: 19572425.
305. Bar-Magen T, Donahue DA, McDonough EI, Kuhl BD, Faltenbacher VH, Xu H, et al. HIV-1 subtype B and C integrase enzymes exhibit differential patterns of resistance to integrase inhibitors in biochemical assays. *AIDS*. 2010;24(14):2171-9. doi: 10.1097/QAD.0b013e32833cf265. PubMed PMID: 20647908.
306. Delelis O, Malet I, Na L, Tchertanov L, Calvez V, Marcelin AG, et al. The G140S mutation in HIV integrases from raltegravir-resistant patients rescues catalytic defect due to the resistance Q148H mutation. *Nucleic Acids Res*. 2009;37(4):1193-201. doi: gkn1050 [pii] 10.1093/nar/gkn1050. PubMed PMID: 19129221; PubMed Central PMCID: PMC2651800.

307. Johnson VA, Brun-Vézinet F, Clotet B, Günthard HF, Kuritzkes DR, Pillay D, et al. Update of the drug resistance mutations in HIV-1: December 2010. *Top HIV Med.* 2010;18(5):156-63. PubMed PMID: 21245516.
308. Hu Z, Kuritzkes DR. Effect of raltegravir resistance mutations in HIV-1 integrase on viral fitness. *J Acquir Immune Defic Syndr.* 2010;55(2):148-55. doi: 10.1097/QAI.0b013e3181e9a87a. PubMed PMID: 20634701; PubMed Central PMCID: PMC2943977.
309. Canducci F, Barda B, Ceresola E, Spagnuolo V, Sampaolo M, Boeri E, et al. Evolution patterns of raltegravir-resistant mutations after integrase inhibitor interruption. *Clin Microbiol Infect.* 2011;17(6):928-34. doi: 10.1111/j.1469-0691.2010.03375.x. PubMed PMID: 20854427.
310. Cooper DA, Steigbigel RT, Gatell JM, Rockstroh JK, Katlama C, Yeni P, et al. Subgroup and resistance analyses of raltegravir for resistant HIV-1 infection. *N Engl J Med.* 2008;359(4):355-65. doi: 359/4/355 [pii] 10.1056/NEJMoa0708978. PubMed PMID: 18650513.
311. Blanco JL, Varghese V, Rhee SY, Gatell JM, Shafer RW. HIV-1 integrase inhibitor resistance and its clinical implications. *J Infect Dis.* 2011;203(9):1204-14. doi: jir025 [pii] 10.1093/infdis/jir025. PubMed PMID: 21459813; PubMed Central PMCID: PMC3069732.
312. Eron JJ, Young B, Cooper DA, Youle M, Dejesus E, Andrade-Villanueva J, et al. Switch to a raltegravir-based regimen versus continuation of a lopinavir-ritonavir-based regimen in stable HIV-infected patients with suppressed viraemia (SWITCHMRK 1 and 2): two multicentre, double-blind, randomised controlled trials. *Lancet.* 2010;375(9712):396-407. doi: S0140-6736(09)62041-9 [pii] 10.1016/S0140-6736(09)62041-9. PubMed PMID: 20074791.
313. Fransen S, Gupta S, Frantzell A, Petropoulos CJ, Huang W. Substitutions at amino acid positions 143, 148, and 155 of HIV-1 integrase define distinct genetic barriers to raltegravir resistance in vivo. *J Virol.* 2012;86(13):7249-55.

Epub 2012/05/04. doi: 10.1128/JVI.06618-11. PubMed PMID: 22553340; PubMed Central PMCID: PMC3416338.

314. Fransen S, Gupta S, Danovich R, Hazuda D, Miller M, Witmer M, et al. Loss of raltegravir susceptibility by human immunodeficiency virus type 1 is conferred via multiple nonoverlapping genetic pathways. *J Virol.* 2009;83(22):11440-6. Epub 2009/09/18. doi: 10.1128/JVI.01168-09. PubMed PMID: 19759152; PubMed Central PMCID: PMC2772690.

315. Fransen S, Karmochkine M, Huang W, Weiss L, Petropoulos CJ, Charpentier C. Longitudinal analysis of raltegravir susceptibility and integrase replication capacity of human immunodeficiency virus type 1 during virologic failure. *Antimicrob Agents Chemother.* 2009;53(10):4522-4. Epub 2009/08/12. doi: 10.1128/AAC.00651-09. PubMed PMID: 19667293; PubMed Central PMCID: PMC2764161.

316. Codoner FM, Pou C, Thielen A, Garcia F, Delgado R, Dalmau D, et al. Dynamic escape of pre-existing raltegravir-resistant HIV-1 from raltegravir selection pressure. *Antiviral Res.* 2010;88(3):281-6. Epub 2010/10/05. doi: 10.1016/j.antiviral.2010.09.016. PubMed PMID: 20883724.

317. Mesplede T, Quashie PK, Wainberg MA. Resistance to HIV integrase inhibitors. *Current opinion in HIV and AIDS.* 2012;7(5):401-8. Epub 2012/07/14. doi: 10.1097/COH.0b013e328356db89. PubMed PMID: 22789986.

318. Young TP, Napolitano LA, Paquet AC, Parkin NT, Fransen S, Trinh R, et al. Minimal sequence variability of the region of HIV-1 integrase targeted by the Abbott RealTime HIV-1 viral load assay in clinical specimens with reduced susceptibility to raltegravir. *Journal of virological methods.* 2013;193(2):693-6. Epub 2013/07/31. doi: 10.1016/j.jviromet.2013.07.028. PubMed PMID: 23892128.

319. Hurt CB. Transmitted resistance to HIV integrase strand-transfer inhibitors: right on schedule. *Antivir Ther.* 2011;16(2):137-40. Epub 2011/03/31. doi: 10.3851/IMP1750. PubMed PMID: 21447861; PubMed Central PMCID: PMC3139474.

320. Hightow-Weidman LB, Hurt CB, Phillips G, 2nd, Jones K, Magnus M, Giordano TP, et al. Transmitted HIV-1 drug resistance among young men of color who have sex with men: a multicenter cohort analysis. *The Journal of adolescent health : official publication of the Society for Adolescent Medicine*. 2011;48(1):94-9. Epub 2010/12/28. doi: 10.1016/j.jadohealth.2010.05.011. PubMed PMID: 21185530.
321. Seki T KM, Wakasa-Morimoto C, Yoshinaga T, Sato A, Fujiwara T, Underwood M, Garvey EP, Johns BA. No Impact of HIV Integrase Polymorphisms at Position 101 and 124 on in vitro Resistance Isolation with Dolutegravir (DTG, S/GSK1349572), A Potent Next Generation HIV Integrase Inhibitor. 17th International Conference on Retroviruses and Opportunistic Infections; San Francisco, California2010.
322. Armenia D, Vandenbroucke I, Fabeni L, Van Marck H, Cento V, D'Arrigo R, et al. Study of genotypic and phenotypic HIV-1 dynamics of integrase mutations during raltegravir treatment: a refined analysis by ultra-deep 454 pyrosequencing. *J Infect Dis*. 2012;205(4):557-67. Epub 2012/01/13. doi: 10.1093/infdis/jir821. PubMed PMID: 22238474; PubMed Central PMCID: PMC3266134.
323. Winters MA, Lloyd RM, Jr., Shafer RW, Kozal MJ, Miller MD, Holodniy M. Development of elvitegravir resistance and linkage of integrase inhibitor mutations with protease and reverse transcriptase resistance mutations. *PLoS One*. 2012;7(7):e40514. Epub 2012/07/21. doi: 10.1371/journal.pone.0040514. PubMed PMID: 22815755; PubMed Central PMCID: PMC3399858.
324. Klibanov OM. Elvitegravir, an oral HIV integrase inhibitor, for the potential treatment of HIV infection. *Curr Opin Investig Drugs*. 2009;10(2):190-200. PubMed PMID: 19197797.
325. Sato M, Motomura T, Aramaki H, Matsuda T, Yamashita M, Ito Y, et al. Novel HIV-1 integrase inhibitors derived from quinolone antibiotics. *J Med Chem*. 2006;49(5):1506-8. doi: 10.1021/jm0600139. PubMed PMID: 16509568.

326. Matsuzaki Y, editor JTK-303/GS 9137, a Novel Small-molecule Inhibitor of HIV-1 Integrase: Anti-HIV Activity Profile and Pharmacokinetics in Animals. 13th Conference on Retroviruses and Opportunistic Infections; 2006; Denver, Colorado, USA.
327. Anonymous. Single-tablet Quad regimen achieves high rate of virologic suppression. *AIDS Patient Care STDS*. 2010;24(3):197. doi: 10.1089/apc.2010.9909. PubMed PMID: 20214488.
328. Ramanathan S, Mathias AA, German P, Kearney BP. Clinical pharmacokinetic and pharmacodynamic profile of the HIV integrase inhibitor elvitegravir. *Clin Pharmacokinet*. 2011;50(4):229-44. doi: 2 [pii] 10.2165/11584570-000000000-00000. PubMed PMID: 21348537.
329. Breeze S. Novel HIV-1 treatment Stribild gains regulatory approval. *Expert review of clinical pharmacology*. 2012;5(6):613. Epub 2012/12/14. doi: 10.1586/ecp.12.67. PubMed PMID: 23234321.
330. A 4-drug combination (Stribild) for HIV. *The Medical letter on drugs and therapeutics*. 2012;54(1404):95-6. Epub 2012/11/28. PubMed PMID: 23183388.
331. HIV/AIDS Update - Approval of Vitekta: *Health News Med*; [01/07/2015]. Available from: <http://healthnewsmed.blogspot.ca/2014/09/hivaids-update-approval-of-vitekta.html>.
332. Mathias AA, West S, Hui J, Kearney BP. Dose-response of ritonavir on hepatic CYP3A activity and elvitegravir oral exposure. *Clin Pharmacol Ther*. 2009;85(1):64-70. doi: clpt2008168 [pii] 10.1038/clpt.2008.168. PubMed PMID: 18815591.
333. Isao K, Ishikawa T, Ishibashi M, Irie S, Kakee A, Japan Tobacco Inc. T, Japan, et al., editors. Safety and Pharmacokinetics of Single Oral Dose of JTK-303/GS-9137, a Novel HIV Integrase Inhibitor, in Healthy Volunteers. 13th Conference on Retroviruses and Opportunistic Infections; 2006; Denver, Colorado, USA.
334. Elion R, Gathe J, Rashburn B, et al, editors. The single-tablet regimen elvitegravir/cobicistat/emtricitabine/tenofovir disoproxil fumarate

(EVG/COBI/FTC/TDF; "QUAD") maintains a high rate of virologic suppression, and cobicistat (COBI) is an effective pharmacoenhancer through 48 weeks. 50th International Conference on Antimicrobial Agents and Chemotherapy; 2010; Boston, Ma, USA.

335. Zolopa AR, Berger DS, Lampiris H, Zhong L, Chuck SL, Enejosa JV, et al. Activity of elvitegravir, a once-daily integrase inhibitor, against resistant HIV Type 1: results of a phase 2, randomized, controlled, dose-ranging clinical trial. *J Infect Dis.* 2010;201(6):814-22. doi: 10.1086/650698. PubMed PMID: 20146631.

336. Quashie PK, Mesplede T, Wainberg MA. Evolution of HIV integrase resistance mutations. *Current opinion in infectious diseases.* 2013;26(1):43-9. Epub 2012/12/18. doi: 10.1097/QCO.0b013e32835ba81c. PubMed PMID: 23242340.

337. Goethals O, Clayton R, Van Ginderen M, Vereycken I, Wagemans E, Geluykens P, et al. Resistance mutations in human immunodeficiency virus type 1 integrase selected with elvitegravir confer reduced susceptibility to a wide range of integrase inhibitors. *J Virol.* 2008;82(21):10366-74. doi: JVI.00470-08 [pii] 10.1128/JVI.00470-08. PubMed PMID: 18715920; PubMed Central PMCID: PMC2573211.

338. Taiwo B, Zheng L, Gallien S, Matining RM, Kuritzkes DR, Wilson CC, et al. Efficacy of a Nucleoside-sparing Regimen of Darunavir/Ritonavir Plus Raltegravir in Treatment-Naïve HIV-1-infected Patients (ACTG A5262). *AIDS.* 2011. doi: 10.1097/QAD.0b013e32834bbaa9. PubMed PMID: 21857490.

339. Métifiot M, Vandegraaff N, Maddali K, Naumova A, Zhang X, Rhodes D, et al. Elvitegravir overcomes resistance to raltegravir induced by integrase mutation Y143. *AIDS.* 2011;25(9):1175-8. doi: 10.1097/QAD.0b013e3283473599. PubMed PMID: 21505303.

340. Shimura K, Kodama E, Sakagami Y, Matsuzaki Y, Watanabe W, Yamataka K, et al. Broad antiretroviral activity and resistance profile of the novel

- human immunodeficiency virus integrase inhibitor elvitegravir (JTK-303/GS-9137). *J Virol.* 2008;82(2):764-74. doi: JVI.01534-07 [pii]  
10.1128/JVI.01534-07. PubMed PMID: 17977962; PubMed Central PMCID: PMC2224569.
341. Dicker IB, Terry B, Lin Z, Li Z, Bollini S, Samanta HK, et al. Biochemical analysis of HIV-1 integrase variants resistant to strand transfer inhibitors. *J Biol Chem.* 2008;283(35):23599-609. doi: M804213200 [pii]  
10.1074/jbc.M804213200. PubMed PMID: 18577511.
342. McColl DJ FS, Gupta S, et al. Basic Principles and Clinical Implications. XVI International HIV Drug Resistance Workshop2007.
343. Canducci F, Sampaolo M, Marinozzi MC, Boeri E, Spagnuolo V, Galli A, et al. Dynamic patterns of human immunodeficiency virus type 1 integrase gene evolution in patients failing raltegravir-based salvage therapies. *AIDS.* 2009;23(4):455-60. doi: 10.1097/QAD.0b013e328323da60. PubMed PMID: 19165083.
344. Margot NA, Hluhanich RM, Jones GS, Andreatta KN, Tsiang M, McColl DJ, et al. In vitro resistance selections using elvitegravir, raltegravir, and two metabolites of elvitegravir M1 and M4. *Antiviral Res.* 2012;93(2):288-96. Epub 2011/12/27. doi: 10.1016/j.antiviral.2011.12.008. PubMed PMID: 22197635.
345. Jones G, Ledford R, Yu F, Miller M, Tsiang M, McColl D, editors. Resistance profile of HIV-1 mutants in vitro selected by the HIV-1 integrase inhibitor, GS-9137 (JTK-303). . 14th Conference on Retroviruses and Opportunistic Infections; 2007; Los Angeles, CA.
346. Wainberg MA, Mesplede T, Quashie PK. The development of novel HIV integrase inhibitors and the problem of drug resistance. *Current opinion in virology.* 2012;2(5):656-62. Epub 2012/09/20. doi: 10.1016/j.coviro.2012.08.007. PubMed PMID: 22989757.
347. Al-Mawsawi LQ, Al-Safi RI, Neamati N. Anti-infectives: clinical progress of HIV-1 integrase inhibitors. *Expert Opin Emerg Drugs.* 2008;13(2):213-25. doi: 10.1517/14728214.13.2.213. PubMed PMID: 18537517.



348. Vacca J. WJ, Fisher T., Embrey M., Hazuda D., Miller M., Felock P., Witmer M., Gabryelski L., Lyle T. Discovery of MK-2048 – subtle changes confer unique resistance properties to a series of tricyclic hydroxypyrrrole integrase strand transfer inhibitor. 4th International AIDS Society's Conference on HIV Pathogenesis, Treatment and Prevention; Sydney, Australia 2007.
349. Van Wesenbeeck L, Rondelez E, Feyaerts M, Verheyen A, Van der Borght K, Smits V, et al. Cross-resistance profile determination of two second-generation HIV-1 integrase inhibitors using a panel of recombinant viruses derived from raltegravir-treated clinical isolates. *Antimicrob Agents Chemother.* 2011;55(1):321-5. doi: AAC.01733-09 [pii] 10.1128/AAC.01733-09. PubMed PMID: 20956600; PubMed Central PMCID: PMC3019647.
350. Pandey KK, Bera S, Vora AC, Grandgenett DP. Physical trapping of HIV-1 synaptic complex by different structural classes of integrase strand transfer inhibitors. *Biochemistry.* 2010;49(38):8376-87. doi: 10.1021/bi100514s. PubMed PMID: 20799722; PubMed Central PMCID: PMC2965028.
351. Goethals O, Van Ginderen M, Vos A, Cummings MD, Van Der Borght K, Van Wesenbeeck L, et al. Resistance to raltegravir highlights integrase mutations at codon 148 in conferring cross-resistance to a second-generation HIV-1 integrase inhibitor. *Antiviral Res.* 2011;91(2):167-76. doi: S0166-3542(11)00320-2 [pii] 10.1016/j.antiviral.2011.05.011. PubMed PMID: 21669228.
352. Bar-Magen T, Sloan RD, Donahue DA, Kuhl BD, Zabeida A, Xu H, et al. Identification of novel mutations responsible for resistance to MK-2048, a second-generation HIV-1 integrase inhibitor. *J Virol.* 2010;84(18):9210-6. doi: JVI.01164-10 [pii] 10.1128/JVI.01164-10. PubMed PMID: 20610719; PubMed Central PMCID: PMC2937597.
353. Alcorn K. Raltegravir shows promise as a PREP drug <http://www.aidsmap.com/Raltegravir-shows-potential-for-use-as-PrEP->

drug/page/1434320/2009 [cited 2011 27/08/2011]. Available from: <http://www.aidsmap.com/Raltegravir-shows-potential-for-use-as-PrEP-drug/page/1434320/>.

354. Seegulam ME, Ratner L. Integrase inhibitors effective against human T-cell leukemia virus type 1. *Antimicrob Agents Chemother*. 2011;55(5):2011-7. doi: AAC.01413-10 [pii]

10.1128/AAC.01413-10. PubMed PMID: 21343468; PubMed Central PMCID: PMC3088187.

355. Dolutegravir (Tivicay) for HIV. *The Medical letter on drugs and therapeutics*. 2013;55(1425):77-9. Epub 2013/10/02. PubMed PMID: 24081387.

356. Triumeq--a 3-drug combination for HIV. *The Medical letter on drugs and therapeutics*. 2015;57(1459):5-7. Epub 2015/01/03. PubMed PMID: 25555073.

357. Eron J LJ, Mortal P, et al. Activity of integrase inhibitor S/GSK9572 in subjects with HIV exhibiting raltegravir resistance: week 24 results of VIKING Study. 10th International Conference on Drug Therapy in HIV Infection; Glasgow, Scotland2010.

358. Tomokazu Yoshinaga MK-K, Takahiro Seki, Kayo Ishida, Erika Akihisa, Masanori Kobayashi, Akihiko Sato, Tamio Fujiwara Shionogi. Strong Inhibition of Wild-Type and Integrase Inhibitor (INI)-Resistant HIV Integrase (IN) Strand Transfer Reaction by the Novel INI S/GSK1349572. International HIV & Hepatitis Virus Drug Resistance Workshop; Dubrovnik, Croatia2010.

359. Bar-Magen T, Sloan RD, Faltenbacher VH, Donahue DA, Kuhl BD, Oliveira M, et al. Comparative biochemical analysis of HIV-1 subtype B and C integrase enzymes. *Retrovirology*. 2009;6:103. doi: 1742-4690-6-103 [pii]

10.1186/1742-4690-6-103. PubMed PMID: 19906306; PubMed Central PMCID: PMC3088187.

360. Underwood M JB, Sato A, et al. S/GSK1349572: A Next Generation Integrase Inhibitor with Activity Against Integrase Inhibitor-Resistant Clinical Isolates from Patients Experiencing Virologic Failure while on Raltegravir

Therapy. 5th International AIDS Society's Conference on HIV Pathogenesis 2009.

361. Kobayashi M, Yoshinaga T, Seki T, Wakasa-Morimoto C, Brown KW, Ferris R, et al. In Vitro antiretroviral properties of S/GSK1349572, a next-generation HIV integrase inhibitor. *Antimicrob Agents Chemother.* 2011;55(2):813-21. doi: AAC.01209-10 [pii]

10.1128/AAC.01209-10. PubMed PMID: 21115794; PubMed Central PMCID: PMC3028777.

362. Min S, Song I, Borland J, Chen S, Lou Y, Fujiwara T, et al. Pharmacokinetics and safety of S/GSK1349572, a next-generation HIV integrase inhibitor, in healthy volunteers. *Antimicrob Agents Chemother.* 2010;54(1):254-8. doi: AAC.00842-09 [pii]

10.1128/AAC.00842-09. PubMed PMID: 19884365; PubMed Central PMCID: PMC2798521.

363. Jay Lalezari LS, Edwin DeJesus, Trevor Hawkins, Lewis McCurdy,, Ivy Song JB, Richard Stroder, Shuguang Chen, Yu Lou,, Mark Underwood TF, Stephen Piscitelli, Sherene Min. Potent Antiviral Activity of S/GSK1349572, A Next Generation Integrase Inhibitor (INI), in INI-Naïve HIV-1-Infected Patients: ING111521 Protocol. 5th International AIDS Society's Conference on HIV Pathogenesis; Cape Town, South Africa 2009.

364. Min S, Sloan L, Dejesus E, Hawkins T, McCurdy L, Song I, et al. Antiviral activity, safety, and pharmacokinetics/pharmacodynamics of dolutegravir as 10-day monotherapy in HIV-1-infected adults. *AIDS.* 2011;25(14):1737-45. doi: 10.1097/QAD.0b013e32834a1dd9. PubMed PMID: 21716073.

365. Rockstroh J, Felizarta F, Maggiolo F, Pulido F, **Stellbrink H, Tsybakova O, et al.** **Once-daily S/GSK1349572 combination** therapy in antiretroviral-naïve adults: rapid and potent 24-week antiviral responses in SPRING-1 (ING112276). 10th International Conference on Drug Therapy in HIV Infection; Glasgow, Scotland 2010.

366. Waters LJ, Barber TJ. Dolutegravir for treatment of HIV: SPRING forwards? *Lancet*. 2013;381(9868):705-6. Epub 2013/01/12. doi: 10.1016/S0140-6736(12)62004-2. PubMed PMID: 23306001.
367. Quashie PK, Mesplède T, Han YS, Oliveira M, Singhroy DN, Fujiwara T, et al. Characterization of the R263K Mutation in HIV-1 Integrase That Confers Low-Level Resistance to the Second-Generation Integrase Strand Transfer Inhibitor Dolutegravir. *J Virol*. 2012;86(5):2696-705. doi: JVI.06591-11 [pii] 10.1128/JVI.06591-11. PubMed PMID: 22205735.
368. Hightower KE, Wang R, Deanda F, Johns BA, Weaver K, Shen Y, et al. Dolutegravir (S/GSK1349572) Exhibits Significantly Slower Dissociation than Raltegravir and Elvitegravir from Wild-Type and Integrase Inhibitor-Resistant HIV-1 Integrase-DNA Complexes. *Antimicrob Agents Chemother*. 2011;55(10):4552-9. doi: AAC.00157-11 [pii] 10.1128/AAC.00157-11. PubMed PMID: 21807982.
369. Grobler JA MP, Ly S, et al, editor Functionally irreversible inhibition of integration by slowly dissociating strand transfer inhibitors. 10th International Conference on Clinical Pharmacology of HIV Therapy; 2009; Amsterdam, Netherlands.
370. Hare S, Smith SJ, Métifiot M, Jaxa-Chamiec A, Pommier Y, Hughes SH, et al. Structural and Functional Analyses of the Second-Generation Integrase Strand Transfer Inhibitor Dolutegravir (S/GSK1349572). *Mol Pharmacol*. 2011;80(4):565-72. doi: mol.111.073189 [pii] 10.1124/mol.111.073189. PubMed PMID: 21719464.
371. Garrido C, Soriano V, Geretti AM, Zahonero N, Garcia S, Booth C, et al. Resistance associated mutations to dolutegravir (S/GSK1349572) in HIV-infected patients - impact of HIV subtypes and prior raltegravir experience. *Antiviral Res*. 2011;90(3):164-7. doi: S0166-3542(11)00230-0 [pii] 10.1016/j.antiviral.2011.03.178. PubMed PMID: 21439330.
372. Malet I, Wirden M, Fourati S, Armenia D, Masquelier B, Fabeni L, et al. Prevalence of resistance mutations related to integrase inhibitor S/GSK1349572

- in HIV-1 subtype B raltegravir-naive and -treated patients. *J Antimicrob Chemother.* 2011;66(7):1481-3. doi: dkr152 [pii] 10.1093/jac/dkr152. PubMed PMID: 21474479.
373. Eron JJ, Clotet B, Durant J, Katlama C, Kumar P, Lazzarin A, et al. Safety and efficacy of dolutegravir in treatment-experienced subjects with raltegravir-resistant HIV type 1 infection: 24-week results of the VIKING Study. *J Infect Dis.* 2013;207(5):740-8. Epub 2012/12/12. doi: 10.1093/infdis/jis750. PubMed PMID: 23225901; PubMed Central PMCID: PMC3563307.
374. S Min ED, L McCurdy, et al. Early Studies Demonstrate Potent Activity and Safety of Experimental Integrase Inhibitor S/GSK1265744. 49th Interscience Conference on Antimicrobials and Chemotherapy; San Francisco, USA2009.
375. Andrews CD, Spreen WR, Mohri H, Moss L, Ford S, Gettie A, et al. Long-acting integrase inhibitor protects macaques from intrarectal simian/human immunodeficiency virus. *Science.* 2014;343(6175):1151-4. Epub 2014/03/07. doi: 10.1126/science.1248707. PubMed PMID: 24594934.
376. Jenkins TM, Hickman AB, Dyda F, Ghirlando R, Davies DR, Craigie R. Catalytic domain of human immunodeficiency virus type 1 integrase: identification of a soluble mutant by systematic replacement of hydrophobic residues. *Proc Natl Acad Sci U S A.* 1995;92(13):6057-61. PubMed PMID: 7597080; PubMed Central PMCID: PMC41641.
377. Jenkins TM, Engelman A, Ghirlando R, Craigie R. A soluble active mutant of HIV-1 integrase: involvement of both the core and carboxyl-terminal domains in multimerization. *J Biol Chem.* 1996;271(13):7712-8. PubMed PMID: 8631811.
378. Dyda F, Hickman AB, Jenkins TM, Engelman A, Craigie R, Davies DR. Crystal structure of the catalytic domain of HIV-1 integrase: similarity to other polynucleotidyl transferases. *Science.* 1994;266(5193):1981-6. PubMed PMID: 7801124.
379. Hare S, Di Nunzio F, Labeja A, Wang J, Engelman A, Cherepanov P. Structural basis for functional tetramerization of lentiviral integrase. *PLoS Pathog.*

2009;5(7):e1000515. doi: 10.1371/journal.ppat.1000515. PubMed PMID: 19609359; PubMed Central PMCID: PMCPMC2705190.

380. Hare S, Gupta SS, Valkov E, Engelman A, Cherepanov P. Retroviral intasome assembly and inhibition of DNA strand transfer. *Nature*. 2010;464(7286):232-6. doi: nature08784 [pii] 10.1038/nature08784. PubMed PMID: 20118915; PubMed Central PMCID: PMCPMC2837123.

381. Hare S, Vos AM, Clayton RF, Thuring JW, Cummings MD, Cherepanov P. Molecular mechanisms of retroviral integrase inhibition and the evolution of viral resistance. *Proc Natl Acad Sci U S A*. 2010;107(46):20057-62. doi: 1010246107 [pii] 10.1073/pnas.1010246107. PubMed PMID: 21030679; PubMed Central PMCID: PMCPMC2993412.

382. Krishnan L, Li X, Naraharisetty HL, Hare S, Cherepanov P, Engelman A. Structure-based modeling of the functional HIV-1 intasome and its inhibition. *Proc Natl Acad Sci U S A*. 2010;107(36):15910-5. doi: 1002346107 [pii] 10.1073/pnas.1002346107. PubMed PMID: 20733078; PubMed Central PMCID: PMCPMC2936642.

383. Kessl JJ, Li M, Ignatov M, Shkriabai N, Eidahl JO, Feng L, et al. FRET analysis reveals distinct conformations of IN tetramers in the presence of viral DNA or LEDGF/p75. *Nucleic Acids Res*. 2011;39(20):9009-22. doi: gkr581 [pii] 10.1093/nar/gkr581. PubMed PMID: 21771857; PubMed Central PMCID: PMCPMC3203615.

384. Hall LH. A structure-information approach to the prediction of biological activities and properties. *Chem Biodivers*. 2004;1(1):183-201. doi: 10.1002/cbdv.200490010. PubMed PMID: 17191786.

385. Liu Q, Zhou H, Liu L, Chen X, Zhu R, Cao Z. Multi-target QSAR modelling in the analysis and design of HIV-HCV co-inhibitors: an in-silico study. *BMC Bioinformatics*. 2011;12:294. doi: 1471-2105-12-294 [pii]

10.1186/1471-2105-12-294. PubMed PMID: 21774796; PubMed Central PMCID: PMC3167801.

386. Johnson BC, Métifiot M, Pommier Y, Hughes SH. Molecular dynamics approaches estimate the binding energy of HIV-1 integrase inhibitors and correlate with in vitro activity. *Antimicrob Agents Chemother.* 2012;56(1):411-9. doi: AAC.05292-11 [pii]

10.1128/AAC.05292-11. PubMed PMID: 22037850; PubMed Central PMCID: PMC3256025.

387. Liao C, Nicklaus MC. Computer tools in the discovery of HIV-1 integrase inhibitors. *Future Med Chem.* 2010;2(7):1123-40. doi: 10.4155/fmc.10.193. PubMed PMID: 21426160.

388. Egbertson MS, Wai JS, Cameron M, Hoerrner RS. Discovery of MK-0536: A Potential Second-Generation HIV-1 Integrase Strand Transfer Inhibitor with a High Genetic Barrier to Mutation. 2011. In: *Antiviral Drugs: From Basic Discovery through Clinical Trials* [Internet]. Hoboken, NJ, USA.: John Wiley & Sons, Inc.

389. Métifiot M, Johnson B, Smith S, Zhao XZ, Marchand C, Burke T, et al. MK-0536 inhibits HIV-1 integrases resistant to raltegravir. *Antimicrob Agents Chemother.* 2011. doi: AAC.05288-11 [pii]

10.1128/AAC.05288-11. PubMed PMID: 21876054.

390. LLC I, inventorTerephthalamate compounds and compositions, and their use as HIV integrase inhibitors2007.

391. Pace P, Di Francesco ME, Gardelli C, Harper S, Muraglia E, Nizi E, et al. Dihydroxypyrimidine-4-carboxamides as novel potent and selective HIV integrase inhibitors. *J Med Chem.* 2007;50(9):2225-39. doi: 10.1021/jm070027u. PubMed PMID: 17428043.

392. Muraglia E, Kinzel O, Gardelli C, Crescenzi B, Donghi M, Ferrara M, et al. Design and synthesis of bicyclic pyrimidinones as potent and orally bioavailable HIV-1 integrase inhibitors. *J Med Chem.* 2008;51(4):861-74. doi: 10.1021/jm701164t. PubMed PMID: 18217703.

393. Telvekar VN, Patel KN. Pharmacophore development and docking studies of the hiv-1 integrase inhibitors derived from N-methylpyrimidones, Dihydroxypyrimidines, and bicyclic pyrimidinones. *Chem Biol Drug Des.* 2011;78(1):150-60. doi: 10.1111/j.1747-0285.2011.01130.x. PubMed PMID: 21518263.
394. Johnson TW, Tanis SP, Butler SL, Dalvie D, Delisle DM, Dress KR, et al. Design and synthesis of novel N-hydroxy-dihydronaphthyridinones as potent and orally bioavailable HIV-1 integrase inhibitors. *J Med Chem.* 2011;54(9):3393-417. doi: 10.1021/jm200208d. PubMed PMID: 21446745.
395. Wai JS, Kim B, Fisher TE, Zhuang L, Embrey MW, Williams PD, et al. Dihydroxypyridopyrazine-1,6-dione HIV-1 integrase inhibitors. *Bioorg Med Chem Lett.* 2007;17(20):5595-9. doi: S0960-894X(07)00928-6 [pii] 10.1016/j.bmcl.2007.07.092. PubMed PMID: 17822898.
396. Toropova AP, Toropov AA, Benfenati E, Gini G. Simplified molecular input-line entry system and International Chemical Identifier in the QSAR analysis of styrylquinoline derivatives as HIV-1 integrase inhibitors. *Chem Biol Drug Des.* 2011;77(5):343-60. doi: 10.1111/j.1747-0285.2011.01109.x. PubMed PMID: 21352501.
397. Nagasawa JY, Song J, Chen H, Kim HW, Blazel J, Ouk S, et al. 6-Benzylamino 4-oxo-1,4-dihydro-1,8-naphthyridines and 4-oxo-1,4-dihydroquinolines as HIV integrase inhibitors. *Bioorg Med Chem Lett.* 2011;21(2):760-3. doi: S0960-894X(10)01733-6 [pii] 10.1016/j.bmcl.2010.11.108. PubMed PMID: 21185178.
398. Meehan AM, Saenz DT, Morrison J, Hu C, Peretz M, Poeschla EM. LEDGF dominant interference proteins demonstrate pre-nuclear exposure of HIV-1 integrase and synergize with LEDGF depletion to destroy viral infectivity. *J Virol.* 2011;85(7):3570-83. doi: JVI.01295-10 [pii] 10.1128/JVI.01295-10. PubMed PMID: 21270171; PubMed Central PMCID: PMC3067863.



399. De Luca L, Ferro S, Morreale F, Chimirri A. Inhibition of the interaction between HIV-1 integrase and its cofactor LEDGF/p75: a promising approach in anti-retroviral therapy. *Mini Rev Med Chem*. 2011;11(8):714-27. doi: BSP/MRMC/Epub/232 [pii]. PubMed PMID: 21651465.
400. Fenwick C, Amad M, Bailey MD, Bethell R, Bos M, Bonneau P, et al. Preclinical Profile of BI 224436, a Novel HIV-1 Non-Catalytic Site Integrase Inhibitor. *Antimicrob Agents Chemother*. 2014. Epub 2014/03/26. doi: 10.1128/AAC.02719-13. PubMed PMID: 24663024.
401. C. Fenwick RB, M. Cordingley, P. Edwards, A-M. Quinson, P. Robinson, B. Simoneau and C. Yoakim editor BI 224436, a Non-Catalytic Site Integrase Inhibitor, is a potent inhibitor of the replication of treatment-naïve and raltegravir-resistant clinical isolates of HIV-1. 51st Interscience Conference on Antimicrobials and Chemotherapy; 2011; Chicago, IL, USA.
402. Desimmie BA, Schrijvers R, Demeulemeester J, Borrenberghs D, Weydert C, Thys W, et al. LEDGINS inhibit late stage HIV-1 replication by modulating integrase multimerization in the virions. *Retrovirology*. 2013;10:57. Epub 2013/06/01. doi: 10.1186/1742-4690-10-57. PubMed PMID: 23721378; PubMed Central PMCID: PMC3671127.
403. Balakrishnan M, Yant SR, Tsai L, O'Sullivan C, Bam RA, Tsai A, et al. Non-catalytic site HIV-1 integrase inhibitors disrupt core maturation and induce a reverse transcription block in target cells. *PLoS One*. 2013;8(9):e74163. Epub 2013/09/17. doi: 10.1371/journal.pone.0074163. PubMed PMID: 24040198; PubMed Central PMCID: PMC3767657.
404. Tang J, Maddali K, Dreis CD, Sham YY, Vince R, Pommier Y, et al. N-3 Hydroxylation of Pyrimidine-2,4-diones Yields Dual Inhibitors of HIV Reverse Transcriptase and Integrase. *ACS Med Chem Lett*. 2011;2(1):63-7. doi: 10.1021/ml1002162. PubMed PMID: 21499541; PubMed Central PMCID: PMC3074239.
405. Wang Z, Tang J, Salomon CE, Dreis CD, Vince R. Pharmacophore and structure-activity relationships of integrase inhibition within a dual inhibitor

- scaffold of HIV reverse transcriptase and integrase. *Bioorg Med Chem.* 2010;18(12):4202-11. doi: S0968-0896(10)00419-0 [pii]  
10.1016/j.bmc.2010.05.004. PubMed PMID: 20576573.
406. Brenner BG, Lowe M, Moisi D, Hardy I, Gagnon S, Charest H, et al. Subtype diversity associated with the development of HIV-1 resistance to integrase inhibitors. *J Med Virol.* 2011;83(5):751-9. doi: 10.1002/jmv.22047. PubMed PMID: 21360548.
407. Loizidou EZ, Kousiappa I, Zeinalipour-Yazdi CD, Van de Vijver DA, Kostrikis LG. Implications of HIV-1 M group polymorphisms on integrase inhibitor efficacy and resistance: genetic and structural in silico analyses. *Biochemistry.* 2009;48(1):4-6. doi: 10.1021/bi8019349 [pii]  
10.1021/bi8019349. PubMed PMID: 19090674.
408. Malet I, Fourati S, Charpentier C, Morand-Joubert L, Armenia D, Wirden M, et al. The HIV-1 integrase G118R mutation confers raltegravir resistance to the CRF02\_AG HIV-1 subtype. *J Antimicrob Chemother.* 2011. doi: dkr389 [pii]  
10.1093/jac/dkr389. PubMed PMID: 21933786.
409. Kobayashi M, Yoshinaga T, Seki T, Wakasa-Morimoto C, Brown KW, Ferris R, et al. In Vitro antiretroviral properties of S/GSK1349572, a next-generation HIV integrase inhibitor. *Antimicrobial agents and chemotherapy.* 2011;55(2):813-21. Epub 2010/12/01. doi: 10.1128/AAC.01209-10. PubMed PMID: 21115794; PubMed Central PMCID: PMC3028777.
410. Malet I, Fourati S, Charpentier C, Morand-Joubert L, Armenia D, Wirden M, et al. The HIV-1 integrase G118R mutation confers raltegravir resistance to the CRF02\_AG HIV-1 subtype. *J Antimicrob Chemother.* 2011;66(12):2827-30. Epub 2011/09/22. doi: 10.1093/jac/dkr389. PubMed PMID: 21933786.
411. Kobayashi M, Nakahara K, Seki T, Miki S, Kawauchi S, Suyama A, et al. Selection of diverse and clinically relevant integrase inhibitor-resistant human immunodeficiency virus type 1 mutants. *Antiviral Res.* 2008;80(2):213-22. Epub 2008/07/16. doi: 10.1016/j.antiviral.2008.06.012. PubMed PMID: 18625269.

412. Wang JY, Ling H, Yang W, Craigie R. Structure of a two-domain fragment of HIV-1 integrase: implications for domain organization in the intact protein. *EMBO J.* 2001;20(24):7333-43. Epub 2001/12/18. doi: 10.1093/emboj/20.24.7333. PubMed PMID: 11743009; PubMed Central PMCID: PMC125787.
413. Li X, Krishnan L, Cherepanov P, Engelman A. Structural biology of retroviral DNA integration. *Virology.* 2011;411(2):194-205. doi: S0042-6822(10)00752-X [pii] 10.1016/j.virol.2010.12.008. PubMed PMID: 21216426.
414. Quashie PK, Sloan RD, Wainberg MA. Novel therapeutic strategies targeting HIV integrase. *BMC medicine.* 2012;10:34. Epub 2012/04/14. doi: 10.1186/1741-7015-10-34. PubMed PMID: 22498430; PubMed Central PMCID: PMC3348091.
415. Serrao E, Odde S, Ramkumar K, Neamati N. Raltegravir, elvitegravir, and metoogravir: the birth of "me-too" HIV-1 integrase inhibitors. *Retrovirology.* 2009;6:25. doi: 1742-4690-6-25 [pii] 10.1186/1742-4690-6-25. PubMed PMID: 19265512; PubMed Central PMCID: PMCPMC2660292.
416. Hare S, Maertens GN, Cherepanov P. 3'-processing and strand transfer catalysed by retroviral integrase in crystallo. *EMBO J.* 2012;31(13):3020-8. Epub 2012/05/15. doi: 10.1038/emboj.2012.118. PubMed PMID: 22580823; PubMed Central PMCID: PMC3395085.
417. Johnson BC, Metifiot M, Ferris A, Pommier Y, Hughes SH. A homology model of HIV-1 integrase and analysis of mutations designed to test the model. *J Mol Biol.* 2013;425(12):2133-46. Epub 2013/04/02. doi: 10.1016/j.jmb.2013.03.027. PubMed PMID: 23542006.
418. Quashie PK, Mesplede T, Han YS, Oliveira M, Singhroy DN, Fujiwara T, et al. Characterization of the R263K mutation in HIV-1 integrase that confers low-level resistance to the second-generation integrase strand transfer inhibitor dolutegravir. *J Virol.* 2012;86(5):2696-705. Epub 2011/12/30. doi:

10.1128/JVI.06591-11. PubMed PMID: 22205735; PubMed Central PMCID: PMC3302270.

419. Quashie PK, Mesplede T, Han YS, Veres T, Osman N, Hassounah S, et al. Biochemical analysis of the role of G118R-linked dolutegravir drug resistance substitutions in HIV-1 integrase. *Antimicrob Agents Chemother.* 2013. Epub 2013/10/02. doi: 10.1128/AAC.01835-13. PubMed PMID: 24080645.

420. Mesplede T, Osman N, Wares M, Quashie PK, Hassounah S, Anstett K, et al. Addition of E138K to R263K in HIV integrase increases resistance to dolutegravir, but fails to restore activity of the HIV integrase enzyme and viral replication capacity. *J Antimicrob Chemother.* 2014. Epub 2014/06/12. doi: 10.1093/jac/dku199. PubMed PMID: 24917583.

421. Buenavista MT, Roche DB, McGuffin LJ. Improvement of 3D protein models using multiple templates guided by single-template model quality assessment. *Bioinformatics.* 2012;28(14):1851-7. Epub 2012/05/18. doi: 10.1093/bioinformatics/bts292. PubMed PMID: 22592378.

422. Soding J, Biegert A, Lupas AN. The HHpred interactive server for protein homology detection and structure prediction. *Nucleic Acids Res.* 2005;33(Web Server issue):W244-8. Epub 2005/06/28. doi: 10.1093/nar/gki408. PubMed PMID: 15980461; PubMed Central PMCID: PMC1160169.

423. Kelley L, Sternberg M. Protein structure prediction on the Web: a case study using the Phyre server. *Nature Protocols.* 2009;4(3):363-71. doi: DOI 10.1038/nprot.2009.2. PubMed PMID: ISI:000265782000009.

424. Zhang Y. I-TASSER server for protein 3D structure prediction. *BMC Bioinformatics.* 2008;9:40. Epub 2008/01/25. doi: 10.1186/1471-2105-9-40. PubMed PMID: 18215316; PubMed Central PMCID: PMC2245901.

425. Baldi P, Chauvin Y. Protein modeling with hybrid Hidden Markov Model/neural network architectures. *Proceedings / International Conference on Intelligent Systems for Molecular Biology ; ISMB International Conference on Intelligent Systems for Molecular Biology.* 1995;3:39-47. Epub 1995/01/01. PubMed PMID: 7584463.

426. Soding J. Protein homology detection by HMM-HMM comparison. *Bioinformatics*. 2005;21(7):951-60. Epub 2004/11/09. doi: 10.1093/bioinformatics/bti125. PubMed PMID: 15531603.
427. Finn RD, Bateman A, Clements J, Coggill P, Eberhardt RY, Eddy SR, et al. Pfam: the protein families database. *Nucleic Acids Res*. 2014;42(Database issue):D222-30. Epub 2013/11/30. doi: 10.1093/nar/gkt1223. PubMed PMID: 24288371; PubMed Central PMCID: PMC3965110.
428. Letunic I, Copley RR, Schmidt S, Ciccarelli FD, Doerks T, Schultz J, et al. SMART 4.0: towards genomic data integration. *Nucleic Acids Res*. 2004;32(Database issue):D142-4. Epub 2003/12/19. doi: 10.1093/nar/gkh088. PubMed PMID: 14681379; PubMed Central PMCID: PMC308822.
429. Schultz J, Milpetz F, Bork P, Ponting CP. SMART, a simple modular architecture research tool: identification of signaling domains. *Proc Natl Acad Sci U S A*. 1998;95(11):5857-64. Epub 1998/05/30. PubMed PMID: 9600884; PubMed Central PMCID: PMC34487.
430. Murzin AG, Brenner SE, Hubbard T, Chothia C. SCOP: a structural classification of proteins database for the investigation of sequences and structures. *J Mol Biol*. 1995;247(4):536-40. Epub 1995/04/07. doi: 10.1006/jmbi.1995.0159. PubMed PMID: 7723011.
431. Sussman J, Lin D, Jiang J, Manning N, Prilusky J, Ritter O, et al. Protein Data Bank (PDB): Database of three-dimensional structural information of biological macromolecules. *Acta Crystallographica Section D-Biological Crystallography*. 1998;54:1078-84. PubMed PMID: ISI:000077511400004.
432. Roy A, Kucukural A, Zhang Y. I-TASSER: a unified platform for automated protein structure and function prediction. *Nat Protoc*. 2010;5(4):725-38. Epub 2010/04/03. doi: 10.1038/nprot.2010.5. PubMed PMID: 20360767; PubMed Central PMCID: PMC2849174.
433. Yang JY, Yan RX, Roy A, Xu D, Poisson J, Zhang Y. The I-TASSER Suite: protein structure and function prediction. *Jcr-J Clin Rheumatol*.

2015;21(1):7-8. doi: Doi 10.1038/Nmeth.3213. PubMed PMID: ISI:000346993500004.

434. Eswar N, Eramian D, Webb B, Shen MY, Sali A. Protein structure modeling with MODELLER. *Methods Mol Biol.* 2008;426:145-59. Epub 2008/06/11. doi: 10.1007/978-1-60327-058-8\_8. PubMed PMID: 18542861.

435. Chen JC, Krucinski J, Miercke LJ, Finer-Moore JS, Tang AH, Leavitt AD, et al. Crystal structure of the HIV-1 integrase catalytic core and C-terminal domains: a model for viral DNA binding. *Proc Natl Acad Sci U S A.* 2000;97(15):8233-8. Epub 2000/07/13. doi: 10.1073/pnas.150220297. PubMed PMID: 10890912; PubMed Central PMCID: PMC26930.

436. Eisenberg D, Luthy R, Bowie JU. VERIFY3D: assessment of protein models with three-dimensional profiles. *Methods in enzymology.* 1997;277:396-404. Epub 1997/01/01. PubMed PMID: 9379925.

437. Melo F, Devos D, Depiereux E, Feytmans E. ANOLEA: a www server to assess protein structures. *Proceedings / International Conference on Intelligent Systems for Molecular Biology ; ISMB International Conference on Intelligent Systems for Molecular Biology.* 1997;5:187-90. Epub 1997/01/01. PubMed PMID: 9322034.

438. Bowie JU, Luthy R, Eisenberg D. A method to identify protein sequences that fold into a known three-dimensional structure. *Science.* 1991;253(5016):164-70. Epub 1991/07/12. PubMed PMID: 1853201.

439. Melo F, Feytmans E. Assessing protein structures with a non-local atomic interaction energy. *J Mol Biol.* 1998;277(5):1141-52. Epub 1998/05/22. doi: 10.1006/jmbi.1998.1665. PubMed PMID: 9571028.

440. Ramachandran GN, Ramakrishnan C, Sasisekharan V. Stereochemistry of polypeptide chain configurations. *J Mol Biol.* 1963;7:95-9. Epub 1963/07/01. PubMed PMID: 13990617.

441. Dunbrack RL, Jr., Karplus M. Conformational analysis of the backbone-dependent rotamer preferences of protein sidechains. *Nature structural biology.* 1994;1(5):334-40. Epub 1994/05/01. PubMed PMID: 7664040.

442. Wang Q, Canutescu AA, Dunbrack RL, Jr. SCWRL and MolIDE: computer programs for side-chain conformation prediction and homology modeling. *Nat Protoc.* 2008;3(12):1832-47. Epub 2008/11/08. doi: 10.1038/nprot.2008.184. PubMed PMID: 18989261; PubMed Central PMCID: PMC2682191.
443. Prlic A, Bliven S, Rose PW, Bluhm WF, Bizon C, Godzik A, et al. Pre-calculated protein structure alignments at the RCSB PDB website. *Bioinformatics.* 2010;26(23):2983-5. Epub 2010/10/13. doi: 10.1093/bioinformatics/btq572. PubMed PMID: 20937596; PubMed Central PMCID: PMC3003546.
444. The PyMOL Molecular Graphics System, Version 1.3, Schrödinger, LLC.
445. Irwin JJ, Shoichet BK. ZINC--a free database of commercially available compounds for virtual screening. *Journal of chemical information and modeling.* 2005;45(1):177-82. Epub 2005/01/26. doi: 10.1021/ci049714+. PubMed PMID: 15667143; PubMed Central PMCID: PMC1360656.
446. Dallakyan S, Olson AJ. Small-Molecule Library Screening by Docking with PyRx. *Methods Mol Biol.* 2015;1263:243-50. Epub 2015/01/27. doi: 10.1007/978-1-4939-2269-7\_19. PubMed PMID: 25618350.
447. Trott O, Olson A. Software News and Update AutoDock Vina: Improving the Speed and Accuracy of Docking with a New Scoring Function, Efficient Optimization, and Multithreading. *Journal of Computational Chemistry.* 2010;31(2):455-61. doi: DOI 10.1002/jcc.21334. PubMed PMID: ISI:000273412900020.
448. Xu HT, Asahchop EL, Oliveira M, Quashie PK, Quan Y, Brenner BG, et al. Compensation by the E138K Mutation in HIV-1 Reverse Transcriptase of Deficits in Viral Replication Capacity and Enzyme Processivity Associated with the M184I/V Mutations. *J Virol.* 2011. doi: JVI.05584-11 [pii] 10.1128/JVI.05584-11. PubMed PMID: 21849444.
449. Kramer VG, Schader SM, Oliveira M, Colby-Germinario SP, Donahue DA, Singhroy DN, et al. Maraviroc and other HIV-1 entry inhibitors exhibit a class-specific redistribution effect that results in increased extracellular viral load.

Antimicrob Agents Chemother. 2012;56(8):4154-60. Epub 2012/05/23. doi: 10.1128/AAC.00409-12. PubMed PMID: 22615275; PubMed Central PMCID: PMC3421589.

450. Han YS, Quashie P, Mesplede T, Xu H, Mekhssian K, Fenwick C, et al. A high-throughput assay for HIV-1 integrase 3'-processing activity using time-resolved fluorescence. *Journal of virological methods*. 2012;184(1-2):34-40. Epub 2012/05/16. doi: 10.1016/j.jviromet.2012.05.003. PubMed PMID: 22584270.

451. Han YS, Xiao WL, Quashie PK, Mesplede T, Xu H, Deprez E, et al. Development of a fluorescence-based HIV-1 integrase DNA binding assay for identification of novel HIV-1 integrase inhibitors. *Antiviral Res*. 2013;98(3):441-8. Epub 2013/04/16. doi: 10.1016/j.antiviral.2013.04.001. PubMed PMID: 23583286.

452. Yan H, Mizutani TC, Nomura N, Takakura T, Kitamura Y, Miura H, et al. A novel small molecular weight compound with a carbazole structure that demonstrates potent human immunodeficiency virus type-1 integrase inhibitory activity. *Antiviral chemistry & chemotherapy*. 2005;16(6):363-73. Epub 2005/12/07. PubMed PMID: 16329284.

453. Zhang Y. I-TASSER: fully automated protein structure prediction in CASP8. *Proteins*. 2009;77 Suppl 9:100-13. doi: 10.1002/prot.22588. PubMed PMID: 19768687; PubMed Central PMCID: PMC2782770.

454. Koltun WL. Precision space-filling atomic models. *Biopolymers*. 1965;3(6):665-79. Epub 1965/12/01. doi: 10.1002/bip.360030606. PubMed PMID: 4158989.

455. Seeliger D, de Groot B. Ligand docking and binding site analysis with PyMOL and Autodock/Vina. *Journal of Computer-Aided Molecular Design*. 2010;24(5):417-22. doi: DOI 10.1007/s10822-010-9352-6. PubMed PMID: ISI:000278469700004.

456. Bonnenfant S, Thomas CM, Vita C, Subra F, Deprez E, Zouhiri F, et al. Styrylquinolines, integrase inhibitors acting prior to integration: a new mechanism



of action for anti-integrase agents. *J Virol.* 2004;78(11):5728-36. Epub 2004/05/14. doi: 10.1128/JVI.78.11.5728-5736.2004. PubMed PMID: 15140970; PubMed Central PMCID: PMC415813.

457. Ceccherini-Silberstein F, Malet I, D'Arrigo R, Antinori A, Marcelin AG, Perno CF. Characterization and structural analysis of HIV-1 integrase conservation. *AIDS reviews.* 2009;11(1):17-29. Epub 2009/03/18. PubMed PMID: 19290031.

458. Kessl JJ, McKee CJ, Eidahl JO, Shkriabai N, Katz A, Kvaratskhelia M. HIV-1 Integrase-DNA Recognition Mechanisms. *Viruses.* 2009;1(3):713-36. Epub 2009/12/01. doi: 10.3390/v1030713. PubMed PMID: 21994566; PubMed Central PMCID: PMC3185514.

459. Mousnier A, Leh H, Mouscadet JF, Dargemont C. Nuclear import of HIV-1 integrase is inhibited in vitro by styrylquinoline derivatives. *Mol Pharmacol.* 2004;66(4):783-8. Epub 2004/07/13. doi: 10.1124/mol.104.001735. PubMed PMID: 15247318.

460. Rhodes DI, Peat TS, Vandegraaff N, Jeevarajah D, Le G, Jones ED, et al. Structural basis for a new mechanism of inhibition of HIV-1 integrase identified by fragment screening and structure-based design. *Antiviral chemistry & chemotherapy.* 2011;21(4):155-68. Epub 2011/05/24. doi: 10.3851/IMP1716. PubMed PMID: 21602613.

461. Sun R, Song HC, Wang CR, Shen KZ, Xu YB, Gao YX, et al. Compounds from *Kadsura angustifolia* with anti-HIV activity. *Bioorg Med Chem Lett.* 2011;21(3):961-5. Epub 2011/01/15. doi: 10.1016/j.bmcl.2010.12.055. PubMed PMID: 21232955.

462. Quashie PK, Oliviera M, Veres T, Osman N, Han YS, Hassounah S, et al. Differential effects of the G118R, H51Y and E138K resistance substitutions in HIV integrase of different subtypes. *J Virol.* 2014. Epub 2015/01/02. doi: 10.1128/JVI.03353-14. PubMed PMID: 25552724.

463. De Luca L, Ferro S, Morreale F, De Grazia S, Chimirri A. Inhibitors of the interactions between HIV-1 IN and the cofactor LEDGF/p75. *ChemMedChem*. 2011;6(7):1184-91. doi: 10.1002/cmdc.201100071. PubMed PMID: 21506277.
464. Schrijvers R, De Rijck J, Demeulemeester J, Adachi N, Vets S, Ronen K, et al. LEDGF/p75-independent HIV-1 replication demonstrates a role for HRP-2 and remains sensitive to inhibition by LEDGINs. *PLoS Pathog*. 2012;8(3):e1002558. Epub 2012/03/08. doi: 10.1371/journal.ppat.1002558. PubMed PMID: 22396646; PubMed Central PMCID: PMC3291655.
465. Di Tommaso P, Moretti S, Xenarios I, Orobitz M, Montanyola A, Chang JM, et al. T-Coffee: a web server for the multiple sequence alignment of protein and RNA sequences using structural information and homology extension. *Nucleic Acids Res*. 2011;39(Web Server issue):W13-7. Epub 2011/05/12. doi: 10.1093/nar/gkr245. PubMed PMID: 21558174; PubMed Central PMCID: PMC3125728.
466. Blanco JL, Varghese V, Rhee SY, Gatell JM, Shafer RW. HIV-1 integrase inhibitor resistance and its clinical implications. *J Infect Dis*. 2011;203(9):1204-14. PubMed PMID: 21459813.
467. Johnson VA, Brun-Vezinet F, Clotet B, Gunthard HF, Kuritzkes DR, Pillay D, et al. Update of the drug resistance mutations in HIV-1: December 2010. *Top HIV Med*. 2010;18(5):156-63. PubMed PMID: 21245516.
468. Turner D, Wainberg MA. HIV transmission and primary drug resistance. *AIDS Rev*. 2006;8(1):17-23. PubMed PMID: 16736948.
469. Wainberg MA. HIV-1 subtype distribution and the problem of drug resistance. *Aids*. 2004;18 Suppl 3:S63-8. PubMed PMID: 15322487.
470. Wainberg MA, Zaharatos GJ, Brenner BG. Development of antiretroviral drug resistance. *N Engl J Med*. 2011;365(7):637-46. PubMed PMID: 21848464.
471. Nguyen BY, Isaacs RD, Teppler H, Leavitt RY, Sklar P, Iwamoto M, et al. Raltegravir: the first HIV-1 integrase strand transfer inhibitor in the HIV armamentarium. *Ann N Y Acad Sci*. 2011;1222:83-9. PubMed PMID: 21434946.

472. Steigbigel RT, Cooper DA, Teppler H, Eron JJ, Gatell JM, Kumar PN, et al. Long-term efficacy and safety of Raltegravir combined with optimized background therapy in treatment-experienced patients with drug-resistant HIV infection: week 96 results of the BENCHMRK 1 and 2 Phase III trials. *Clin Infect Dis*. 2010;50(4):605-12. PubMed PMID: 20085491.
473. Donahue DA, Sloan RD, Kuhl BD, Bar-Magen T, Schader SM, Wainberg MA. Stage-dependent inhibition of HIV-1 replication by antiretroviral drugs in cell culture. *Antimicrob Agents Chemother*. 2010;54(3):1047-54. PubMed PMID: 20038621.
474. Mouscadet JF, Delelis O, Marcelin AG, Tchertanov L. Resistance to HIV-1 integrase inhibitors: A structural perspective. *Drug Resist Updat*. 2010;13(4-5):139-50. PubMed PMID: 20570551.
475. Cooper DA, Steigbigel RT, Gatell JM, Rockstroh JK, Katlama C, Yeni P, et al. Subgroup and resistance analyses of raltegravir for resistant HIV-1 infection. *N Engl J Med*. 2008;359(4):355-65. PubMed PMID: 18650513.
476. Goethals O, Clayton R, Van Ginderen M, Vereycken I, Wagemans E, Geluykens P, et al. Resistance mutations in human immunodeficiency virus type 1 integrase selected with elvitegravir confer reduced susceptibility to a wide range of integrase inhibitors. *J Virol*. 2008;82(21):10366-74. PubMed PMID: 18715920.
477. Marinello J, Marchand C, Mott BT, Bain A, Thomas CJ, Pommier Y. Comparison of raltegravir and elvitegravir on HIV-1 integrase catalytic reactions and on a series of drug-resistant integrase mutants. *Biochemistry*. 2008;47(36):9345-54. PubMed PMID: 18702518.
478. Van Wesenbeeck L, Rondelez E, Feyaerts M, Verheyen A, Van der Borght K, Smits V, et al. Cross-resistance profile determination of two second-generation HIV-1 integrase inhibitors using a panel of recombinant viruses derived from raltegravir-treated clinical isolates. *Antimicrob Agents Chemother*. 2011;55(1):321-5. PubMed PMID: 20956600.

479. Metifiot M, Vandegraaff N, Maddali K, Naumova A, Zhang X, Rhodes D, et al. Elvitegravir overcomes resistance to raltegravir induced by integrase mutation Y143. *Aids*. 2011;25(9):1175-8. PubMed PMID: 21505303.
480. Goethals O, Vos A, Van Ginderen M, Geluykens P, Smits V, Schols D, et al. Primary mutations selected in vitro with raltegravir confer large fold changes in susceptibility to first-generation integrase inhibitors, but minor fold changes to inhibitors with second-generation resistance profiles. *Virology*. 2010;402(2):338-46. PubMed PMID: 20421122.
481. Bar-Magen T, Sloan RD, Donahue DA, Kuhl BD, Zabeida A, Xu H, et al. Identification of novel mutations responsible for resistance to MK-2048, a second-generation HIV-1 integrase inhibitor. *J Virol*. 2010;84(18):9210-6. PubMed PMID: 20610719.
482. Goethals O, Van Ginderen M, Vos A, Cummings MD, Van Der Borght K, Van Wesenbeeck L, et al. Resistance to raltegravir highlights integrase mutations at codon 148 in conferring cross-resistance to a second-generation HIV-1 integrase inhibitor. *Antiviral Res*. 2011;91(2):167-76. PubMed PMID: 21669228.
483. Bar-Magen T, Sloan RD, Faltenbacher VH, Donahue DA, Kuhl BD, Oliveira M, et al. Comparative biochemical analysis of HIV-1 subtype B and C integrase enzymes. *Retrovirology*. 2009;6:103. PubMed PMID: 19906306.
484. Song I, Borland J, Min S, Lou Y, Chen S, Patel P, et al. Effects of etravirine alone and with ritonavir-boosted protease inhibitors on the pharmacokinetics of dolutegravir. *Antimicrob Agents Chemother*. 2011;55(7):3517-21. PubMed PMID: 21555764.
485. Min S, Song I, Borland J, Chen S, Lou Y, Fujiwara T, et al. Pharmacokinetics and safety of S/GSK1349572, a next-generation HIV integrase inhibitor, in healthy volunteers. *Antimicrob Agents Chemother*. 2010;54(1):254-8. PubMed PMID: 19884365.
486. Min S, Sloan L, Dejesus E, Hawkins T, McCurdy L, Song I, et al. Antiviral activity, safety, and pharmacokinetics/pharmacodynamics of dolutegravir as 10-

day monotherapy in HIV-1-infected adults. *Aids*. 2011. PubMed PMID: 21716073.

487. Sato A, Seki T, Kobayashi M, Yoshinaga T, Fujiwara T, Underwood M, et al. In vitro passage of drug resistant HIV-1 against a next generation integrase inhibitor (INI), S/GSK1349572. 49th ICAAC, San Francisco, CA. 2009.

488. Seki T, Kobayashi M, Wakasa-Morimoto C, Yoshinaga T, Sato A, Fujiwara T, et al. S/GSK1349572 is a potent next generation HIV integrase inhibitor and demonstrates a superior resistance profile substantiated with 60 integrase mutant molecular clones. 17th CROI, Conference on retroviruses and opportunistic infections, San Francisco, CA. 2010.

489. Xu HT, Asahchop EL, Oliveira M, Quashie PK, Quan Y, Brenner BG, et al. Compensation by the E138K Mutation in HIV-1 Reverse Transcriptase of Deficits in Viral Replication Capacity and Enzyme Processivity Associated with the M184I/V Mutations. *J Virol*. 2011. PubMed PMID: 21849444.

490. Oliveira M, Brenner BG, Wainberg MA. Isolation of drug-resistant mutant HIV variants using tissue culture drug selection. *Methods Mol Biol*. 2009;485:427-33. PubMed PMID: 19020842.

491. Brenner BG, Lowe M, Moisi D, Hardy I, Gagnon S, Charest H, et al. Subtype diversity associated with the development of HIV-1 resistance to integrase inhibitors. *J Med Virol*. 2011;83(5):751-9. PubMed PMID: 21360548.

492. Schader SM, Colby-Germinario SP, Schachter JR, Xu H, Wainberg MA. Synergy against drug-resistant HIV-1 with the microbicide antiretrovirals, dapivirine and tenofovir, in combination. *Aids*. 2011;25(13):1585-94. PubMed PMID: 21633286.

493. Bar-Magen T, Donahue DA, McDonough EI, Kuhl BD, Faltenbacher VH, Xu H, et al. HIV-1 subtype B and C integrase enzymes exhibit differential patterns of resistance to integrase inhibitors in biochemical assays. *Aids*. 2010;24(14):2171-9. PubMed PMID: 20647908.

494. Walker JM. *The proteomics protocols handbook*. Totowa, N.J.: Humana Press; 2005. xviii, 988 p. p.

495. Clinical and Laboratory Standards Institute., National Committee for Clinical Laboratory Standards., American National Standards Institute. NCCLS standard. New York, N.Y.: American National Standards Institute; 1979. v. p.
496. Hazuda DJ, Hastings JC, Wolfe AL, Emini EA. A novel assay for the DNA strand-transfer reaction of HIV-1 integrase. *Nucleic Acids Res.* 1994;22(6):1121-2. PubMed PMID: 8152918.
497. Zhang ZR, Palfrey D, Nagel DA, Lambert PA, Jessop RA, Santos AF, et al. Fluorescent microplate-based analysis of protein-DNA interactions. I: Immobilized protein. *BioTechniques.* 2003;35(5):980-2, 4, 6. Epub 2003/11/25. PubMed PMID: 14628672.
498. Maignan S, Guilloteau JP, Zhou-Liu Q, Clement-Mella C, Mikol V. Crystal structures of the catalytic domain of HIV-1 integrase free and complexed with its metal cofactor: high level of similarity of the active site with other viral integrases. *J Mol Biol.* 1998;282(2):359-68. PubMed PMID: 9735293.
499. Hare S, Di Nunzio F, Labeja A, Wang J, Engelman A, Cherepanov P. Structural basis for functional tetramerization of lentiviral integrase. *PLoS Pathog.* 2009;5(7):e1000515. PubMed PMID: 19609359.
500. Jones G, Ledford R, Yu F, Chen X, Miller MD, Tsiang M, et al. In vitro resistance profile of HIV-1 mutants selected by the HIV-1 integrase inhibitor, GS-9137 (JTK-303). 14th CROI, Conference on Retroviruses and opportunistic infections, Los Angeles, California. 2007.
501. Shimura K, Kodama E, Sakagami Y, Matsuzaki Y, Watanabe W, Yamataka K, et al. Broad antiretroviral activity and resistance profile of the novel human immunodeficiency virus integrase inhibitor elvitegravir (JTK-303/GS-9137). *J Virol.* 2008;82(2):764-74. PubMed PMID: 17977962.
502. Lutzke RA, Vink C, Plasterk RH. Characterization of the minimal DNA-binding domain of the HIV integrase protein. *Nucleic Acids Res.* 1994;22(20):4125-31. PubMed PMID: 7937137.

503. Dolan J, Chen A, Weber IT, Harrison RW, Leis J. Defining the DNA substrate binding sites on HIV-1 integrase. *J Mol Biol.* 2009;385(2):568-79. PubMed PMID: 19014951.
504. Xue W, Liu H, Yao X. Molecular mechanism of HIV-1 integrase-vDNA interactions and strand transfer inhibitor action: a molecular modeling perspective. *J Comput Chem.* 2012;33(5):527-36. Epub 2011/12/07. doi: 10.1002/jcc.22887. PubMed PMID: 22144113.
505. Jayappa KD, Ao Z, Yang M, Wang J, Yao X. Identification of critical motifs within HIV-1 integrase required for importin alpha3 interaction and viral cDNA nuclear import. *J Mol Biol.* 2011;410(5):847-62. PubMed PMID: 21763491.
506. Hazuda DJ, Anthony NJ, Gomez RP, Jolly SM, Wai JS, Zhuang L, et al. A naphthyridine carboxamide provides evidence for discordant resistance between mechanistically identical inhibitors of HIV-1 integrase. *Proc Natl Acad Sci U S A.* 2004;101(31):11233-8. PubMed PMID: 15277684.
507. Markowitz M, Nguyen BY, Gotuzzo E, Mendo F, Ratanasuwan W, Kovacs C, et al. Rapid and durable antiretroviral effect of the HIV-1 Integrase inhibitor raltegravir as part of combination therapy in treatment-naive patients with HIV-1 infection: results of a 48-week controlled study. *J Acquir Immune Defic Syndr.* 2007;46(2):125-33. PubMed PMID: 17721395.
508. McColl D, Fransen S, Gupta SS, Parkin N, Margot N, Ledford R, et al. Resistance and cross-resistance to first generation integrase inhibitors; insights from a Phase 2 study of Elvitegravir (GS-9137). 16th International HIV Drug Resistance workshop, Barbados, West Indies. 2007.
509. Low A, Prada N, Topper M, Vaida F, Castor D, Mohri H, et al. Natural polymorphisms of human immunodeficiency virus type 1 integrase and inherent susceptibilities to a panel of integrase inhibitors. *Antimicrob Agents Chemother.* 2009;53(10):4275-82. PubMed PMID: 19651917.
510. Bushman FD, Fujiwara T, Craigie R. Retroviral DNA integration directed by HIV integration protein in vitro. *Science.* 1990;249(4976):1555-8. Epub 1990/09/28. PubMed PMID: 2171144.

511. Pauza CD. Two bases are deleted from the termini of HIV-1 linear DNA during integrative recombination. *Virology*. 1990;179(2):886-9. Epub 1990/12/01. PubMed PMID: 2238479.
512. Lewinski MK, Bisgrove D, Shinn P, Chen H, Hoffmann C, Hannenhalli S, et al. Genome-wide analysis of chromosomal features repressing human immunodeficiency virus transcription. *J Virol*. 2005;79(11):6610-9. Epub 2005/05/14. doi: 10.1128/JVI.79.11.6610-6619.2005. PubMed PMID: 15890899; PubMed Central PMCID: PMC1112149.
513. Kulkosky J, Skalka AM. HIV DNA integration: observations and interferences. *J Acquir Immune Defic Syndr*. 1990;3(9):839-51. Epub 1990/01/01. PubMed PMID: 2166782.
514. Temesgen Z. Cobicistat-boosted elvitegravir-based fixed-dose combination antiretroviral therapy for HIV infection. *Drugs Today (Barc)*. 2012;48(12):765-71. Epub 2012/12/18. doi: 10.1358/dot.2012.48.12.1895682. PubMed PMID: 23243633.
515. Hazuda DJ. Resistance to inhibitors of the human immunodeficiency virus type 1 integration. *Braz J Infect Dis*. 2010;14(5):513-8. doi: S1413-86702010000500016 [pii]. PubMed PMID: 21221483.
516. Oral candidosis in HIV infection. *Lancet*. 1989;2(8678-8679):1491-2. Epub 1989/12/23. PubMed PMID: 2574773.
517. O'Neal R. Dolutegravir: A New Integrase Inhibitor in Development <http://www.sfaf.org/hiv-info/hot-topics/beta/2011-beta-winterspring-drug-watch.pdf>2011 [cited 2011 20/09/2011].
518. Dooley KE, Sayre P, Borland J, Purdy E, Chen S, Song I, et al. Safety, tolerability, and pharmacokinetics of the HIV integrase inhibitor dolutegravir given twice daily with rifampin or once daily with rifabutin: results of a phase 1 study among healthy subjects. *J Acquir Immune Defic Syndr*. 2013;62(1):21-7. Epub 2012/10/19. doi: 10.1097/QAI.0b013e318276cda9. PubMed PMID: 23075918.
519. Fantauzzi A, Turriziani O, Mezzaroma I. Potential benefit of dolutegravir once daily: efficacy and safety. *HIV AIDS (Auckl)*. 2013;5:29-40. Epub



2013/02/16. doi: 10.2147/HIV.S27765. PubMed PMID: 23413040; PubMed Central PMCID: PMC3570074.

520. Wainberg MA, Quashie PK, Mesplede T. DOLUTEGRAVIR HIV Integrase Inhibitor Treatment of HIV Infection. *Drug Future*. 2012;37(10):697-707. doi: DOI 10.1358/dof.2012.37.10.1855759. PubMed PMID: ISI:000311859800001.

521. Vavro C, Hasan S, Madsen H, Horton J, DeAnda F, Martin-Carpenter L, et al. Prevalent polymorphisms in wild-type HIV-1 integrase are unlikely to engender drug resistance to dolutegravir (S/GSK1349572). *Antimicrob Agents Chemother*. 2013;57(3):1379-84. Epub 2013/01/09. doi: 10.1128/AAC.01791-12. PubMed PMID: 23295935; PubMed Central PMCID: PMC3591886.

522. Cleland WW. The kinetics of enzyme-catalyzed reactions with two or more substrates or products. I. Nomenclature and rate equations. 1963. *Biochimica et biophysica acta*. 1989;1000:213-20. Epub 1989/01/01. PubMed PMID: 2673369.

523. Cleland WW. Enzyme kinetics revisited: a commentary on 'The Kinetics of Enzyme-Catalyzed Reactions With Two or More Substrates or Products'. *Biochimica et biophysica acta*. 1989;1000:209-12. Epub 1989/01/01. PubMed PMID: 2673368.

524. Bhuyan MS, Gao X. A protein-dependent side-chain rotamer library. *BMC Bioinformatics*. 2011;12 Suppl 14:S10. Epub 2012/03/01. doi: 10.1186/1471-2105-12-S14-S10. PubMed PMID: 22373394; PubMed Central PMCID: PMC3287466.

525. Bower MJ, Cohen FE, Dunbrack RL, Jr. Prediction of protein side-chain rotamers from a backbone-dependent rotamer library: a new homology modeling tool. *J Mol Biol*. 1997;267(5):1268-82. Epub 1997/04/18. doi: 10.1006/jmbi.1997.0926. PubMed PMID: 9150411.

526. Cleland WW. Partition analysis and the concept of net rate constants as tools in enzyme kinetics. *Biochemistry*. 1975;14(14):3220-4. Epub 1975/07/15. PubMed PMID: 1148201.

527. Smolov M, Gottikh M, Tashlitskii V, Korolev S, Demidyuk I, Brochon JC, et al. Kinetic study of the HIV-1 DNA 3'-end processing. *The FEBS journal*.

2006;273(6):1137-51. Epub 2006/03/08. doi: 10.1111/j.1742-4658.2006.05139.x. PubMed PMID: 16519680.

528. Deprez E, Barbe S, Kolaski M, Leh H, Zouhiri F, Auclair C, et al. Mechanism of HIV-1 integrase inhibition by styrylquinoline derivatives in vitro. *Mol Pharmacol*. 2004;65(1):85-98. Epub 2004/01/15. doi: 10.1124/mol.65.1.85. PubMed PMID: 14722240.

529. Parrill AL. HIV-1 integrase inhibition: binding sites, structure activity relationships and future perspectives. *Curr Med Chem*. 2003;10(18):1811-24. Epub 2003/07/23. PubMed PMID: 12871106.

530. Cleland WW. Enzyme kinetics. *Annual review of biochemistry*. 1967;36:77-112. Epub 1967/01/01. doi: 10.1146/annurev.bi.36.070167.000453. PubMed PMID: 18257716.

531. Xu D, Zhang J, Roy A, Zhang Y. Automated protein structure modeling in CASP9 by I-TASSER pipeline combined with QUARK-based ab initio folding and FG-MD-based structure refinement. *Proteins*. 2011;79 Suppl 10:147-60. doi: 10.1002/prot.23111. PubMed PMID: 22069036; PubMed Central PMCID: PMC3228277.

532. Quashie PK, Mesplede T, Wainberg MA. HIV Drug Resistance and the Advent of Integrase Inhibitors. *Current infectious disease reports*. 2013;15(1):85-100. Epub 2012/11/28. doi: 10.1007/s11908-012-0305-1. PubMed PMID: 23180144.

533. Cherepanov P, Maertens GN, Hare S. Structural insights into the retroviral DNA integration apparatus. *Curr Opin Struct Biol*. 2011;21(2):249-56. doi: S0959-440X(11)00003-0 [pii] 10.1016/j.sbi.2010.12.005. PubMed PMID: 21277766.

534. Nowotny M, Gaidamakov SA, Crouch RJ, Yang W. Crystal structures of RNase H bound to an RNA/DNA hybrid: substrate specificity and metal-dependent catalysis. *Cell*. 2005;121(7):1005-16. Epub 2005/07/02. doi: 10.1016/j.cell.2005.04.024. PubMed PMID: 15989951.

535. Williams A, Friedland G. Adherence, compliance, and HAART. *AIDS clinical care*. 1997;9(7):51-4, 8. Epub 1997/07/01. PubMed PMID: 11364415.
536. Asahchop EL, Wainberg MA, Sloan RD, Tremblay CL. Antiviral drug resistance and the need for development of new HIV-1 reverse transcriptase inhibitors. *Antimicrob Agents Chemother*. 2012;56(10):5000-8. Epub 2012/06/27. doi: 10.1128/AAC.00591-12. PubMed PMID: 22733071; PubMed Central PMCID: PMC3457356.
537. Sarafianos SG, Das K, Hughes SH, Arnold E. Taking aim at a moving target: designing drugs to inhibit drug-resistant HIV-1 reverse transcriptases. *Curr Opin Struct Biol*. 2004;14(6):716-30. Epub 2004/12/08. doi: 10.1016/j.sbi.2004.10.013. PubMed PMID: 15582396.
538. Mesplede T, Quashie PK, Zanichelli V, Wainberg MA. Integrase strand transfer inhibitors in the management of HIV-positive individuals. *Annals of medicine*. 2014;46(3):123-9. Epub 2014/03/04. doi: 10.3109/07853890.2014.883169. PubMed PMID: 24579911.
539. Cahn P, Pozniak AL, Mingrone H, Shuldyakov A, Brites C, Andrade-Villanueva JF, et al. Dolutegravir versus raltegravir in antiretroviral-experienced, integrase-inhibitor-naive adults with HIV: week 48 results from the randomised, double-blind, non-inferiority SAILING study. *Lancet*. 2013;382(9893):700-8. Epub 2013/07/09. doi: 10.1016/S0140-6736(13)61221-0. PubMed PMID: 23830355.
540. Tramontano E, Colla PL, Cheng YC. Biochemical characterization of the HIV-1 integrase 3'-processing activity and its inhibition by phosphorothioate oligonucleotides. *Biochemistry*. 1998;37(20):7237-43. doi: bi972792o [pii] 10.1021/bi972792o. PubMed PMID: 9585536.
541. Sheik SS, Sundararajan P, Hussain AS, Sekar K. Ramachandran plot on the web. *Bioinformatics*. 2002;18(11):1548-9. Epub 2002/11/09. PubMed PMID: 12424132.
542. Kolaskar AS, Sawant S. Prediction of conformational states of amino acids using a Ramachandran plot. *International journal of peptide and protein research*. 1996;47(1-2):110-6. Epub 1996/01/01. PubMed PMID: 8907507.

543. Thompson JD, Higgins DG, Gibson TJ. CLUSTAL W: improving the sensitivity of progressive multiple sequence alignment through sequence weighting, position-specific gap penalties and weight matrix choice. *Nucleic Acids Res.* 1994;22(22):4673-80. Epub 1994/11/11. PubMed PMID: 7984417; PubMed Central PMCID: PMC308517.
544. Wares M, Mesplede T, Quashie PK, Osman N, Han Y, Wainberg MA. The M50I polymorphic substitution in association with the R263K mutation in HIV-1 subtype B integrase increases drug resistance but does not restore viral replicative fitness. *Retrovirology.* 2014;11:7. Epub 2014/01/18. doi: 10.1186/1742-4690-11-7. PubMed PMID: 24433497; PubMed Central PMCID: PMC3898230.
545. Hardy I, Brenner B, Quashie P, Thomas R, Petropoulos C, Huang W, et al. Evolution of a novel pathway leading to dolutegravir resistance in a patient harbouring N155H and multiclass drug resistance. *J Antimicrob Chemother.* 2014. Epub 2014/10/05. doi: 10.1093/jac/dku387. PubMed PMID: 25281399.
546. Collins DW, Jukes TH. Rates of transition and transversion in coding sequences since the human-rodent divergence. *Genomics.* 1994;20(3):386-96. Epub 1994/04/01. doi: 10.1006/geno.1994.1192. PubMed PMID: 8034311.
547. DeAnda F, Hightower KE, Nolte RT, Hattori K, Yoshinaga T, Kawasuji T, et al. Dolutegravir interactions with HIV-1 integrase-DNA: structural rationale for drug resistance and dissociation kinetics. *PLoS One.* 2013;8(10):e77448. Epub 2013/10/23. doi: 10.1371/journal.pone.0077448. PubMed PMID: 24146996; PubMed Central PMCID: PMC3797783.
548. Oliveira M, Mesplede T, Quashie PK, Moisi D, Wainberg MA. Resistance mutations against dolutegravir in HIV integrase impair the emergence of resistance against reverse transcriptase inhibitors. *AIDS.* 2014. Epub 2014/01/28. doi: 10.1097/QAD.000000000000199. PubMed PMID: 24463394.
549. Hassounah SA, Mesplede T, Quashie PK, Oliveira M, Sandstrom PA, Wainberg MA. Effect of HIV-1 Integrase Resistance Mutations When Introduced into SIVmac239 on Susceptibility to Integrase Strand Transfer Inhibitors. *J Virol.*

2014;88(17):9683-92. Epub 2014/06/13. doi: 10.1128/JVI.00947-14. PubMed PMID: 24920794; PubMed Central PMCID: PMC4136349.

550. Cherepanov P. Integrase illuminated. *EMBO Rep.* 2010;11(5):328. doi: embor201058 [pii]

10.1038/embor.2010.58. PubMed PMID: 20428106; PubMed Central PMCID: PMCPMC2868546.

551. Metifiot M, Maddali K, Johnson BC, Hare S, Smith SJ, Zhao XZ, et al. Activities, crystal structures, and molecular dynamics of dihydro-1H-isoindole derivatives, inhibitors of HIV-1 integrase. *ACS chemical biology.* 2013;8(1):209-17. Epub 2012/10/19. doi: 10.1021/cb300471n. PubMed PMID: 23075516; PubMed Central PMCID: PMC3548936.

552. Mesplède T, Quashie PK, Han Y, Osman N, Wares M, Hassounah S, et al. HIV Resistance against the second-generation integrase inhibitor dolutegravir correlates with impaired viral replication. In: Conly JM, editor. 22nd Annual Conference on HIV/AIDS Research; 11 April 2013; Vancouver, Canada: Canadian Journal of Infectious Diseases and Medical Microbiology 2013. p. 9A.

553. Hurt CB, Sebastian J, Hicks CB, Eron JJ. Resistance to HIV integrase strand transfer inhibitors among clinical specimens in the United States, 2009-2012. *Clin Infect Dis.* 2014;58(3):423-31. Epub 2013/10/23. doi: 10.1093/cid/cit697. PubMed PMID: 24145878; PubMed Central PMCID: PMC3890334.

554. Wainberg M, Anstett K, Mesplede T, Quashie P, Han Y, Oliveira M. The R263K mutation in HIV integrase that is selected by dolutegravir may actually prevent clinically relevant resistance to this compound. *J Int Aids Soc.* 2014;17(4 Suppl 3):19518. Epub 2014/11/14. doi: 10.7448/IAS.17.4.19518. PubMed PMID: 25394027; PubMed Central PMCID: PMC4224880.

555. Anstett K, Mesplede T, Oliveira M, Cutillas V, Wainberg MA. Dolutegravir resistance mutation R263K cannot coexist in combination with many classical integrase inhibitor resistance substitutions. *J Virol.* 2015;89(8):4681-4. Epub

2015/02/06. doi: 10.1128/JVI.03485-14. PubMed PMID: 25653436; PubMed Central PMCID: PMC4442391.

556. Underwood MR, Dudas K, Horton J, Wang R, Deanda F, Griffith S, et al. Analysis and characterization of treatment-emergent resistance in ART-experienced, integrase-inhibitor-naive subjects with dolutegravir (DTG) versus raltegravir in SAILING (ING111762) Antiviral Therapy. 2013;18(Suppl1):1.

557. Guidelines for the use of antiretroviral agents in HIV-1-infected adults and adolescents. Panel on Antiretroviral Guidelines for Adults and Adolescents. Department of Health and Human Services. 2015 [01/07/2015]. Available from: <http://www.aidsinfo.nih.gov/ContentFiles/AdultandAdolescentGL.pdf>.